Role of IL-36 and the Innate Immune System in Acute Generalized Exanthematous Pustulosis

---

Dissertation

zur

Erlangung der naturwissenschaftlichen Doktorwürde
(Dr. sc. nat.)

vorgelegt der

Mathematisch-naturwissenschaftlichen Fakultät

der

Universität Zürich

von

Barbara Meier

aus

Deutschland

Promotionskommission

Prof. Dr. Onur Boyman (Vorsitz)
Prof. Dr. Lars E. French (Leitung der Dissertation)
Prof. Dr. Annette Oxenius
Prof. Dr. Maries van den Broek
Prof. Dr. Thomas Kündig

Zürich, 2017

Table of contents

Zusammenfassung

Akute generalisierte exanthematöse Pustulose (AGEP) ist eine schwere Arzneimittelreaktion der Haut. Sie zeichnet sich durch die rasche Entwicklung von sterilen, nicht-follikulären Pusteln auf der Grundlage eines ödematösen Erythems aus und wird durch die Einnahme bestimmter Medikamente ausgelöst. Obwohl über eine Beteiligung von medikamenten-spezifischen T-Zellen in AGEP berichtet wurde, sind die Pathophysiologie der AGEP und der zugrundeliegende Mechanismus der neutrophilen Hautentzündung noch nicht eindeutig geklärt.

Der Schwerpunkt dieser Dissertation lag darin, die Rolle des pro-inflammatorischen Zytokins Interleukin (IL) -36 in der Pathogenese von AGEP zu untersuchen. Darüber hinaus wurde die Beteiligung früher Immunantworten nach Medikamenten-exposition in zirkulierenden Immunzellen und Keratinozyten von AGEP-Patienten untersucht.

Eine unvoreingenommene Genexpressionsanalyse ergab eine signifikante Hochregulation der Zytokine IL-36α und -γ in läsionaler Haut von AGEP-Patienten im Vergleich zum makulo-papulösen Exanthem (MPE). IL-36γ stellt hierbei die am häufigsten vorkommende Isoform dar und wird vorwiegend von Keratinozyten und Makrophagen in AGEP produziert. *In vitro* induzierte eine Stimulation mit dem auslösenden Medikament eine spezifische IL-36γ-Freisetzung entweder direkt aus mononukleären Zellen des Blutes oder indirekt aus Keratinozyten, die in Gegenwart von autologen mononukleären Blutzellen von AGEP-Patienten kultiviert wurden. Medikamenten-induzierte IL-36γ-Freisetzung *in vitro* war spezifisch für AGEP und konnte in MPE nicht beobachtet werden.

Des Weiteren konnten wir zeigen, dass auch IL-1β eine mögliche wichtige Rolle in der Pathogenese von AGEP einnimmt. Wir konnten demonstrieren, dass IL-1β ein positiver Regulator der IL-36γ-Produktion in humanen Monozyten und Keratinozyten ist. Zudem konnte gezeigt werden, dass der IL-1β-Gehalt im Blut und in der Haut von AGEP-Patienten erhöht ist. Ähnlich der IL-36γ-Expression konnte auch die IL-1β-Expression direkt durch Stimulation mit dem auslösenden Medikament in mononukleären Blutzellen induziert werden. Dies konnte partiell durch den IL-36-Rezeptorantagonisten antagonisiert werden, was auf eine regulatorische Rolle von IL-36γ hindeutet.

Interessanterweise wurde nach Stimulation mit Lipopolysaccharid (LPS) eine gesteigerte Produktion von IL-36γ und lL-1β durch mononukleäre Zellen des Blutes von AGEP-Patienten im Vergleich zu Monozyten von MPR-Patienten und gesunden Individuen festgestellt. Diese gesteigterte Entzündungsantwort von AGEP-Monozyten auf LPS und die Tatsache, dass Monozyten direkt dazu angeregt werden konnten, IL-36γ und IL-1β zu exprimieren, liess eine gesteigerte Aktivität im *Toll-like-Rezeptor* (TLR) - *NF-κB*-Signalweg vermuten. Dies wurde unterstützt durch die Tatsache, dass zwei Nukleotidpolymorphismen (D299G und T399I) in dem für TLR4 (Rezeptor für LPS) kodierenden Gen bei AGEP-Patienten signifikant häufiger als bei gesunden Kontrollen gefunden wurden.

Zusammenfassend konnte in dieser Arbeit eine entscheidende Rolle der beiden Zytokine IL-36γ und lL-1β in der Pathogenese der AGEP demonstriert werden. Zum ersten Mal konnte eine direkte Aktivierung von Monozyten durch Medikamente gezeigt werden, was auf einen wichtigen Einfluss des angeborenen Immunsystems in der AGEP-Pathogenese hindeutet. Die Assoziation von Nukleotidpolymorphismen in dem für TLR4 kodierenden Gen mit AGEP unterstützt ferner die Annahme eines dysregulierten TLR-NF-κB-Signalweges. Diese Erkenntnisse zeigen einen interessanten neuen Aspekt bei der Entstehung von Medikamentenreaktionen der Haut auf und eröffnen neue Perspektiven in der Erforschung von Arzneimittelreaktionen der Haut.

.

Summary

Acute generalized exanthematous pustulosis (AGEP) is a severe adverse cutaneous drug reaction. It is characterized by the rapid development of sterile, non-follicular pustules on the background of edematous erythema triggered by culprit drug intake. Although previous findings reported an involvement of drug-specific T cells in AGEP, the physiopathology of AGEP and the underlying mechanism of neutrophilic skin inflammation remains incompletely understood.

The main focus of this PhD thesis was to investigate the role of the pro-inflammatory cytokine Interleukin (IL) -36 in the pathogenesis of AGEP. Moreover, it probes the involvement of early immune responses in both circulating immune cells and keratinocytes, from AGEP patients, upon culprit drug exposure.

An unbiased approach revealed significant IL-36α and γ upregulation in lesional skin of AGEP patients, when compared to macular papular rash (MPR), with IL-36γ representing the most abundant isoform. Keratinocytes and macrophages were found to be the source of IL-36γ production in AGEP patients. *In vitro*, culprit drug exposure specifically induced IL-36γ release, either directly by peripheral blood monocytes, or indirectly by keratinocytes cultured in the presence of autologous peripheral blood mononuclear cells (PBMCs) from AGEP patients. Culprit drug-induced IL-36γ secretion *in vitro* was specific for AGEP and was not observed for MPR.

Furthermore, we identified IL-1β as another key player in the pathogenesis of AGEP. IL-1β has been demonstrated to be a positive regulator of IL-36γ production in human monocytes and keratinocytes and IL-1β levels are elevated in AGEP blood and skin. Like IL-36γ, IL-1β expression is directly induced by culprit drug exposure in peripheral blood monocytes and this could be partially antagonized by IL-36Ra, suggesting a regulatory role of IL-36γ in amplifying this inflammatory loop.

Interestingly, PBMCs from AGEP patients showed an enhanced reponse to lipopolysacchardie (LPS) stimulation compared to PBMCs from MPR patients and healthy controls. This exaggerated response of AGEP PBMCs in response to LPS and the fact that monocytes could be directly stimulated to express IL-36γ and IL-1β, was suggestive of exacerbated Toll-like receptor (TLR) - NF-κB activity. Indeed, using whole exome sequencing, the presence of two single nucleotide

polymorphisms (D299G and T399I) in the gene encoding TLR4 (the receptor for LPS) were found significantly more frequently in AGEP patients than in healthy controls.

Collectively, the findings described in this thesis demonstrate crucial roles of IL-36γ and IL-1β in the pathogenesis of AGEP. Strikingly, a direct activation of monocytes by culprit drugs could be shown for the first time, suggesting an important impact of the innate immune system in AGEP pathogenesis. The association of single nucleotide polymorphisms in the gene encoding TLR4 with AGEP is further supportive of a dysregulated TLR-NF-κB signaling axis. Together, these findings open up new relevant research avenues to explore in the field of cutaneous adverse drug reactions.

List of abbreviations

AD	Atopic dermatitis
ADR	Adverse drug reaction
AGEP	Acute Generalied Exanthematous Pustulosis
APC	Antigen-presenting cell
BSA	Bovine Serum Albumin
CD	Cluster of Differentiation
CLP	Common lymphoid progenitor
CLR	C-type lectin receptors
CMP	Common myeloid progenitor
cDC	classical dendtitic cell
cDNA	complementary DNA
C_t	Cycle threshold
CXCL	chemokine (C-X-C motif) ligand
DAMP	Danger-associated molecular pattern
DAPI	4',6-Diamidino-2-Phenylindol
DC	Dendritic cell
DNA	Desoxyribonucleic acid
ER	Endoplasmic reticulum
G-CSF	Granulocyte colony stimulating factor
GM-CSF	Granulocyte-macrophage colony-stimulating factor
HLA	Human leukocyte antigen
IFN	Interferon
IL	Interleukin
ILC	Innate lymphoid cells
IRF3	Interferon regulatory factor
ITGA6	Integrin Subunit Alpha 6
Lin	Lineage

LBP	LPS-binding protein
LPS	Lipopolysaccharide
LTT	Lymphocyte transformation test
MAPK	Mitigen-activated protein kinases
MHC	Major histocompatibility complex
MHC-I	MHC class I
MHC-II	MHC class II
MyD88	Myeloid differentiation primary response gene 88
NF-κB	nuclear factor 'kappa-light-chain-enhancer' of activated B-cells
NLR	NOD-like recptor
NOD	Nucleotide-binding oligomerization domain-like receptors
PAMP	Pathogen-associated molecular pattern
PBMC	Peripheral blood mononuclear cell
pDC	Plasmacytoid dendritic cell
PRR	Pattern-recognition receptor
Ra	Receptor antagonist
r	Recombinant
RLR	RIG-like receptor
RNA	Ribonucleic acid
RORγt	RAR-related orphan receptor gamma t
ROS	Reactive oxygen species
SDRIFE	Symmetrical Drug-Related Intertriginous and Flexural Exanthema
SJS	Stevens-Johnson syndrome
ssRNA	Single-stranded RNA
TCR	T cell receptor
TEN	Toxic epidermal necrolysis
TF	Transcription factor
TIRAP	TIR Domain Containing Adaptor Protein
TRIF	TIR-domain-containing adapter-inducing interferon-β
Th cell	Helper T cell

TNF	Tumor necrosis factor
VLA-1	Very Late Activation Protein 1
WHO	World Health Organisation
Z-VAD	Z-Val-Ala-Asp fluoromethyl ketone
Z-VAD	Z-Val-Ala-Asp fluoromethyl ketone
SDRIFE	Symmetrical Drug-Related Intertriginous and Flexural Exanthema
SJS	Stevens-Johnson syndrome
ssRNA	Single-stranded RNA
TCR	T cell receptor
TEN	Toxic epidermal necrolysis
TF	Transcription factor
TIRAP	TIR Domain Containing Adaptor Protein
TRIF	TIR-domain-containing adapter-inducing interferon-β
Th cell	Helper T cell
TNF	Tumor necrosis factor
VLA-1	Very Late Activation Protein 1
WHO	World Health Organisation
Z-VAD	Z-Val-Ala-Asp fluoromethyl ketone

1 Introduction

1.1 The immune system

1.1.1 Overview and basic principles

The human body is constantly exposed to a variety of environmental insults including millions of pathogens but also potentially harmful chemicals or radiations such as UV light. However, not every contact with environmental stimuli leads to infection or disease as homeostasis and integrity of the body is ensured by several defense mechanisms. These include physical barriers such as the skin and mucosa, complement factors and antimicrobial peptides and the immune system. The immune system is a host defense system that can be classified in 2 subsystems, namely the innate and the adaptive immune system (Fig. 1) [1].

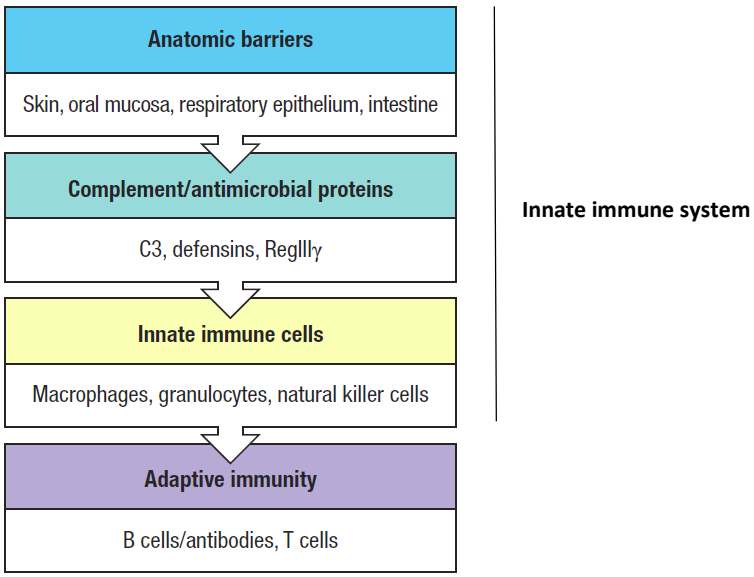

***Fig. 1: Protection against environmental insults relies on several levels of defense**. The first defense level is represented by anatomic barriers provided by the epithelia of the body's surfaces. Second, various chemical and enzymatic systems, including complement, act as an immediate antimicrobial barrier near these epithelia. As a next step of host defense, various innate immune cells can coordinate rapid immune responses. If the innate immune mechanisms are not sufficient, the slower-acting defenses of the adaptive immune system are brought to bear. Adapted from Janeways's Immunobiology [1].*

The innate immune system represents the first line of defense of the human body. It is already present from birth and provides very rapid and efficient mechanisms to prevent invasion by microbes. Innate immune responses are mediated through several mechanisms. One is the signaling through soluble proteins or small molecules such as defensins, ficolins or complement factors that are constitutively present in bio-organic fluids [2, 3]. Another is innate immune cells which can release soluble mediators upon activation, thereby directly affecting microorganisms and also amplifying the immune response by recruiting or activating other immune cell types. These include cytokines, chemokines, reactive oxygen species, lipid mediators, bioactive amines and enzymes [4]. Nonthelesss, the most efficient host defense is mediated through germ-line-encoded pattern-recognition receptors (PRRs). PRRs are able to sense conserved structures of microorganisms, the so-called pathogen-associated molecular patterns (PAMPs), as well as tissue damage by endogenous molecules released from damaged cells, the so-called danger-associated molecular patterns (DAMPs). The sensing of PAMPs and DAMPs by PRRs leads to the upregulation of genes coding for inflammatory cytokines or to the activation and release of the latter [5]. The nature of PRRs and their respective signaling mechanisms will be discussed in detail in chapter 1.1.2.2.

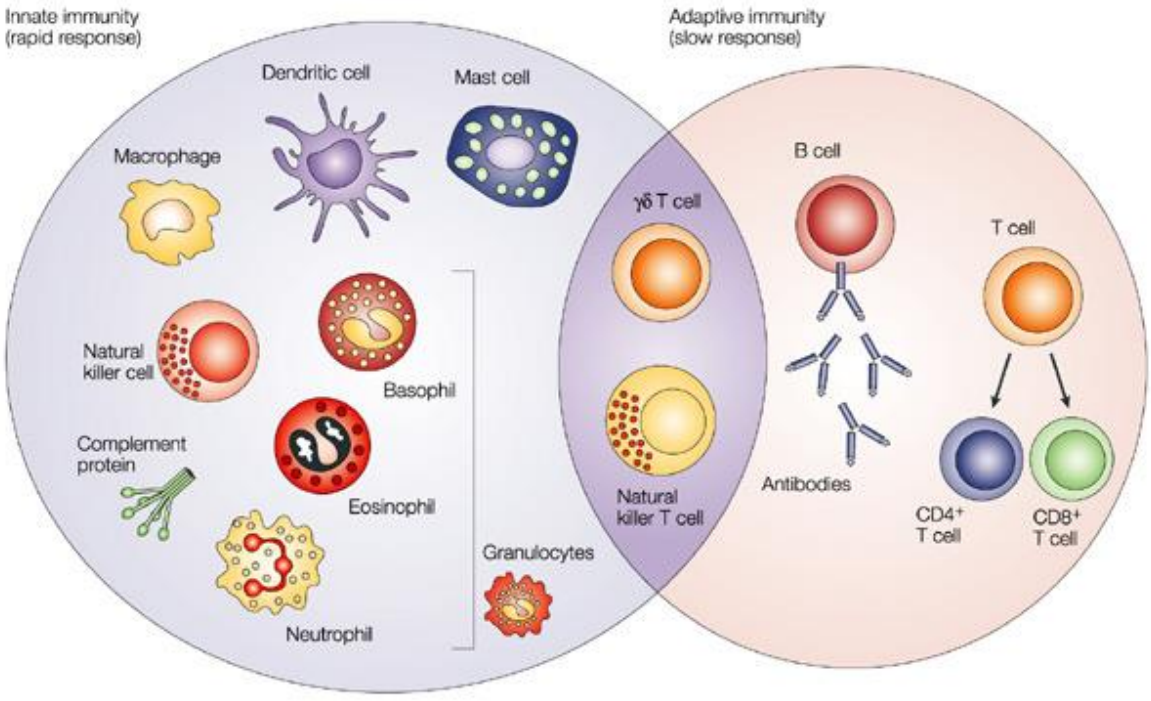

Fig. 2. Innate and adaptive immune cells. *The innate immune response functions as the first line of defence against pathogens and danger signals. It consists of soluble factors, such as complement components, and diverse cellular components including granulocytes (basophils, eosinophils and neutrophils, mast cells), macrophages, dendritic cells and natural killer cells. The adaptive immune response is a slower acting defense system, with stronger antigen-specificity and memory. It consists of antibodies, B cells, and $CD4^+$ and $CD8^+$ T lymphocytes. Natural killer T cells and γδ T cells are cytotoxic lymphocytes that straddle the interface of innate and adaptive immunity. Note: Innate lymphoid cells are missing in this figure. Adapted from Dranoff et. al [6].*

When the innate defense mechanisms are not sufficient to fight infection or inflammation, an adaptive immune response is initiated. In contrast to the innate immune system, adaptive immunity requires prior sensitization to an antigen [7]. Unlike the germ-line-encoded receptors of the innate immune system, the antigen-specific receptors of the adaptive response are encoded by genes that are assembled by somatic rearrangement of germ-line gene elements to form receptor genes [4]. The adaptive immune system is composed of antigen-specific T-cell activity (cell-mediated immunity) and specific antibody production by B cells (humoral immunity). Thus, the adaptive immune system relies on two main cell types, the T lymphocytes (T cells) and the B lymphocytes (B cells).

Both cell types show little functional activity until an antigen binds to their specific receptor. In this non-actived state, the cells are known as *naive* lymphocytes. Once an antigen binds specifically to its receptor, the lymphocyte will be activated and differentiates into a fully functional cell, the so-called *effector* lymphocytes [8].

There are three different types of effector T cells: Cytotoxic T cells are capable of destroying cells that are infected with an intracellular pathogen carrying the antigen or cells that are recognized as non-self (grafted cells, tumor cells). Helper T cells (Th cells) can help activate other immune cells by releasing soluble factors, e.g. cytokines, in order to optimally regulate an immune response. Th cells can further be distinguished in Th1, Th2, Th17 and Th9 cells, depending on the factors initiating their differentiation, the presence of specific transcription factors, and the secretion of characteristic cytokines. Interferon (IFN) γ and Interleukin- (IL-) 12 can initiate the differentiation of Th1 cells, IL-2 and IL-4 are critical for Th2 differentiation, IL-23 induces differentiation into Th17 cells and IFNβ diverts the differentiation of Th2 towards the development of Th9 cells [9]. Regulatory T cells downregulate or

suppress the activity of other lymphocytes, in particular effector T cells, in order to prevent autoimmunity or other fulminant immune reactions and to maintain tolerance to self-antigens [10].

B cells are the only cell type in our human body that are able to produce antibodies. When a naïve or memory B cell is activated by antigen (with the help of a Th cell), it proliferates and differentiates into an antibody-secreting effector cell. Each B cell produces only one type of antibody with a unique antigen-binding site. Antibodies (Immunoglobulins, Ig) consist of four polypeptide chains, two identical light chains and two identical heavy chains. In humans, there are five different types of heavy chains, namely α, δ, ε, γ, and μ. According to their heavy chain, Ig are classified as IgA, IgD, IgE, IgG or IgM. Each of these Ig classes has distinct properties [11].

Both B and T cells express distinct types of antigen receptors on their surface, resulting in different roles in the adaptive immune system. The assembly of these antigen-receptors from only a couple hundred germ-line-encoded gene elements gives rise to millions of different antigen receptors that are each specific for a particular antigen [4].

T cell receptors (TCR) recognize antigens as small peptide fragments presented on major histocompatibility complex (MHC) molecules on the cell surface of professional antigen-presenting cells (APC). Such APCs have the unique capacity to take up antigens and to process them in order to form MHC-peptide complexes which will be transported to the cell surface for antigen-presentation. [12] Dendritic cells represent the most potent APCs but monocytes, macrophages, B cells and neutrophils can also present antigens (cell types will be described in more detail in the chapter 1.1.2.1). There are two classes of MHC molecules, class I and class II. MHC class I molecules are found on the cell surface of all nucleated cells and mediate the activation of $CD8^+$ T cells. MHC class II molecules are only present on professional APCs and are responsible for the activation of CD4+ T cells.

B cells make use of antibodies in a membrane protein form as their antigen-binding receptors. The latter are capable of recognizing three-dimensional structures which allows them to bind and neutralize extracellular pathogens. They have the same unique antigen-binding site as the soluble antibodies [13].

Even though the innate and the adaptive immune system represent two distinct and separate arms of host defense, synergy between them is crucial for efficient immune responses. Indeed, besides its function as first-line defense, the innate immune system contributes to the activation of the adaptive immune system via the release of soluble mediators such as cytokines and chemokines, subsequently leading to the clonal expansion of antigen-specific B and T cells. The latter, in turn, can amplify immune responses by further recruiting innate effector cells [4].

1.1.2 Innate Immunity

1.1.2.1 Innate immune cells and their functions

Innate immune cells comprize white blood cells that arise both from common myeloid progenitor cells (CMP) and the common lymphoid progenitor (CLP). CMP are progenitors of granulocytes (neutrophils, eosinophils, basophils, mast cells), dendritic cells, monocytes and macrophages. The CLP gives rise to NK cells and to the recently defined group of innate lymphoid cells (ILCs) [14].

Granulocytes

Granulocytes include four different cell types: neutrophils, eosinophils, basophils and mast cells. Their life-span is very short (only a few days) and they are continuously produced from their precursors in the bone marrow. During immune responses, they migrate towards the site of infection and their production increases. **Neutrophils** are the most abundant type of granulocytes and play an important role in innate immune responses to pathogens. They function as phagocytes and are able to kill microorganisms by using lytic enzymes from their granules and other antimicrobial molecules like reactive oxygen species (ROS). Moreover, they can be stimulated to release complement components, chemokines and cytokines and express Fc receptors [15]. **Eosinophils** are a less abundant type of granulocytes that play an important role in the defense against infections, in particular parasite infections. Moreover, they are actively involved in the regulation of Th2-type immune responses and diseases such as asthma and skin allergy. Here, eosinophils are recruited to the inflamed tissue where they produce chemokines, cytokines and

other mediators and release highly toxic granule proteins. This leads to tissue damage but also facilitates tissue repair and regulates immune responses [16, 17]. Moreover, eosinophils have the capability to initiate antigen-specific immune responses by presenting antigens to T cells [18]. **Basophils** are the least common type of granulocytes. They have high-affinity IgE receptors that are cross-linked upon binding to specific IgE and its corresponding antigen, thereby leading to the release of a number of cytokines. Like eosinophils, they are also implicated in the control of parasite infections, and can also be involved in allergic reactions [19]. **Mast cells** are granulocytes containing a high number of granules rich in histamine and various proteases. Upon mast cell degranulation, immunomodulatory and vasoactive molecules are released and exert protective functions against parasitic and bacterial infections. Moreover, mast cells have an important role in allergy as they are also possessing high-affinity IgE receptors [20].

Dendritic cells

Dendritic cells (DCs) are professional APCs that have the unique capacity to stimulate naive T cells and thereby initiate primary adaptive immune responses. DCs are the most effective APCs, in part due to their constitutive expression of MHC class II (MHC-II) molecules, and their ability to express a number of costimulatory molecules, such as CD80/86 and CD40. DCs are grouped in several subtypes but there is no consensus regarding the way they are classified [21]. A very common classification consists in the differentiation between monocyte-derived DCs, which are dependent on M-CSF, and monocyte-independent DCs, which require Flt-3L for their development and are mostly found in lymphoid tissues [22]. DCs reside both in lymphoid and in non-lymphoid tissues. Lymphoid tissue DCs reside in the lymph nodes, spleen, thymus and mucosal-associated tissues. Non-lymphoid tissue DCs, also called interstitial DCs, populate stratified squamous tissues like the epidermis or connective tissues, and can be found in the skin, lung, liver, kidney, pancreatic islets and the intestine [23]. Besides their origin, DCs are classified into two main subsets, namely the classical and the plasmacytoid DCs. The classical DC (cDC) subset includes $CD8^+$ and $CD8^-$ cells [24]. In the steady state, $CD8^+$ DCs are mainly found in the T cell areas of the spleen and lymph nodes. Besides presenting endogenous antigens via MHC-II, they are also capable of

crosspresenting exogenous antigens via the MHC class I (MHC-I) pathway to $CD8^+$ T cells [25]. $CD8^-$ DCs are predominantly localized in the marginal zone of the lymph nodes [26] and are specialized in the presentation of exogenous antigens via MHC-II [27]. Plasmacytoid DCs (pCDs) reside mainly in lymphoid organs and express high amounts of certain TLRs which allows them to recognize viruses and to induce a Type-I-Interferon-dominated immune response. Another important DC subset are the migratory DCs. These cells act as sentinels for pathogens and self-antigens in the periphery and subsequently migrate towards a draining lymph node [24]. These migratory DCs include Langerhans cells and dermal DCs that can migrate to skin-draining lymph nodes [28]. Langerhans cells are found within the epidermis, whereas dermal DCs belong to the interstitial DC subset [29].

Monocytes and macrophages

Monocytes are one of the largest groups of leukocytes in the blood. They originate from bone marrow progenitors and are able to differentiate into macrophages and monocyte-derived DCs. After circulating in the bloodstream for about one to three days, monocytes migrate into tissues where they differentiate into tissue-resident macrophages or DCs. This recruitment of monocytes to the tissues can be enhanced by infection and inflammation [30]. Based on the expression of the surface molecules Cluster of differentiation (CD) 14 and 16, different monocyte subsets are defined. $CD14^{++}CD16^-$ represent the classical monocytes, $CD14^{++}CD16^+$ are defined as intermediate population and $CD14^+CD16^{++}$ are the nonclassical population [31]. Classical monocytes are potent phagocytic cells and secrete IL-10 and ROS upon lipopolysaccharide (LPS) stimulation, whereas intermediate and non-classical monocytes secrete pro-inflammatory cytokines upon stimulation. During inflammation, classical and intermediate monocytes are invading tissues where they differentiate into macrophages [32]. **Macrophages** are the mature form of monocytes and are typically tissue- and niche-specific. They are a heterogenous group of cells and different macrophage subsets have been described. The most common classification consists in the distinction between M1 and M2 macrophages but recent research is suggestive of additional subtypes/phenotypes [33]. M1 are classically activated macrophages that mediate host defence against a variety of pathogens and tumors. They release pro-inflammatory cytokines such as tumor

necrosis factor (TNF) and IL-1β and show strongly expressed MHC-II molecules. They have a key role in the initiation of T cells responses and proteolysis. In contrast, M2 macrophages are alternatively activated macrophages that possess anti-inflammatory properties. In reponse to Fcγ ligation, they secrete large amounts of IL-10. They have been shown to be involved in processes like wound healing, tissue fibrosis, angiogenesis and tumorigenesis [32].

Innate lymphoid cells

ILCs represent a recently-defined group of innate immune cells that morphologically appear as lymphoid cells but do not express rearranged antigen-specific receptors and lineage (Lin-) specific markers of other leukocyte populations [34, 35]. The first two members of the ILC family were already discovered in the 1970s and 1980s, namely NK and lymphoid tissue inducer (LTi) and NK cells [36]. **NK cells** are cells that express a variety of innate receptors and can induce immediate immune responses to specific viral infections and cellular stress. NK cells are able to kill certain cells without prior antigen-specific priming. **LTi cells** are cells that have a critical role in the development of lymphoid tissues during embryogenesis and in the formation of the gut-associated lymphoid tissue in the adult [37, 38]. More recently, new non-cytotoxic ILCs have been discovered [39-41]. They are characterized by their similarities with Th cell subsets regarding their cytokine and transcription factor (TF) profiles [42]. Based on these profiles, different ILC subsets can be defined: Group 1 ILCs express the TF T-bet and are able to produce IFNγ and TNFα; group 2 ILCs express the TF GATA3 and produce the typical Th2 cytokines IL-4, IL-5 and IL-13; group 3 ILCs express the three TFs T-bet, aryl hydrocarbon receptor and the RAR-related orphan receptor gamma t (RORγt). The latter produce IFNγ, TNF, IL-17 and IL-22 [43, 44]. Functions of ILCs include the maintenance of epithelial integrity as they can quickly respond to epithelial cell-derived mediators like thymic stromal lymphopoietin (TSLP) and IL-1β [45]. They are also involved in early immune responses to pathogens [39, 40] and tissue repair [46, 47].

1.1.2.2 Pattern-recognition by Toll-like receptors

The innate immune system has been long considered to consist only of unspecific defense mechanisms to pathogens, antigen-specificity being thought to be an exclusive characteristic of the adaptive immune system. However, since the discovery of Toll-like receptors (TLR) in the mid-1990s and the more recent description of other PRRs, the innate immune system is not considered to be unspecific anymore. Indeed, it is now known that PRRs exhibit some specificity in terms of stimuli sensing and subsequent intracellular signaling. PRRs include Nucleotide-binding oligomerization domain-like receptors (NOD)-like receptors (NLRs), RIG-I-like receptors (RLRs), C-type lectin receptors (CLRs) and TLRs [48].

TLRs belong to the group of germline-encoded PRRs which can detect PAMPs and DAMPs. They are type I transmembrane proteins containing leucin-rich repeat regions and play a crucial role in the early immune response to pathogens.

The TLR family is one of the best characterized PRR families. In humans, ten different TLRs have been identified of which each recognizes different molecular patterns (Table 1). TLR2 is localized in the plasma membrane and is able to sense various components from bacteria, fungi, and viruses on the cell surface. These components include lipoproteins of bacteria and mycoplasma. TLR2 is expressed on monocytes, neutrophils, DCs as well as ectodermic cells like keratinocytes, and recognizes its ligands by forming heterodimers with either TLR1 or TLR6 [49]. All other TLRs exist as homodimers. TLR3, 7, 8 and 9 are mainly present on the endoplasmic reticulum (ER) membrane and can sense both exogenous and endogenous nucleic acids [50]: TLR3 senses double-strand ribonucleotide acid (dsRNA), TLR7 and 8 sense single-strand ribonucleotide acid (ssRNA) and TLR9 senses CpG-DNA. Nucleic acid-sensing TLRs are recruited from the ER to endolysosomes following stimulation by their respective ligands. As they are not localized on the cell membrane, the access is restricted, which can prevent the constitutive activation of the TLRs by self-antigens and the resulting excessive immune response [51, 52]. TLR3 expression has been observed in keratinocytes, macrophages, mast cells [53], T lymphocytes [54] and NK cells, further in myeloid-derived DCs but not in pDCs [55]. TLR7 and 9 are primarily expressed in pDCs and to some extent in monocytes/macrophages and B cells. In contrast, TLR8 is predominantly expressed in monocytes/macrophages and myeloid DCs [56-58].

TLR5 is not highly expressed in skin cells but has been shown to play an important role in the gut immune system as it is expressed at high levels on DCs of the lamina propria in the small intestine, where it recognizes flagellin from flagellated bacteria of the intestinal flora [59].

***Table 1. Toll-like receptors and their ligands. Adapted from Takeuchi et. al** [48]*

	Localization	Ligand	Origin of the Ligand
TLR1	Plasma membrane	Triacyl lipoprotein	Bacteria
TLR2	Plasma membrane	Lipoprotein	Bacteria, viruses, parasites, self-antigen
TLR3	Intracellular membranes	dsRNA	Virus
TLR4	Plasma membrane	LPS	Bacteria, viruses, self-antigen
TLR5	Plasma membrane	Flagellin	Bacteria
TLR6	Plasma membrane	Diacyl lipoprotein	Bacteria, viruses
TLR7	Intracellular membranes	ssRNA	Virus, bacteria, self-antigen
TLR8	Intracellular membranes	ssRNA	Virus, bacteria, protozoa, self-antigen
TLR9	Intracellular membranes	CpG-DNA	Bacteria, Self-antigen
TLR10	Intracellular membranes	Unknown	Unknown

TLR4 is the first TLR to be discovered, and was done so by Jules Hoffmann [60] who was awarded the 2011 Nobel Prize together with Bruce Beutler [61] in Physiology or Medicine. TLR4 is highly expressed in myeloid cells like monocytes, macrophages and granulocytes [62]. Less expression has been shown in T cells [63]. It is also expressed in immature DCs but its expression gets lost during maturation. No TLR4 expression has been reported in pDCs [62]. In the skin, functional TLR4 was found to be expressed by keratinocytes and fibroblasts [64-66]. However, compared to myeloid cells, the level of expression is rather low. TLR4 is able to sense LPS alone, a component of the outer membrane of gram-negative bacteria. TLR4 can not recognize LPS alone but needs to form a complex on the cell surface with several other proteins. In the serum, LPS is released by LPS-binding protein (LBP) which transfers LPS to CD14. The latter presents LPS in form of monomeric molecules to the TLR4-MD-2 complex. The aggregation of this

complex results in the activation of the signaling pathways leading to nuclear factor 'kappa-light-chain-enhancer' of activated B-cells (NF-κB) and Interferon Regulatory Factor 3 (IRF3) activation [62, 67].

Upon recognition of their ligands, TLRs change their conformation and recruit adaptor proteins to iniate a signaling cascade. The cell surface TLR homo- and heterodimers recruit Myeloid differentiation primary response gene 88 (MyD88) and TIR Domain Containing Adaptor Protein (TIRAP) and subsequently activate the NF-κB signaling pathway. In addition, TLR4 recruits the the adaptor proteins TRIF and TRAM that initiate the IRF3 pathway, leading to IFNβ production. MyD88 and TIRAP also get recruited by the endolysosomal TLRs TLR7, 8 and 9. TLR3 is able to induce both NF-κB and IRF3 through its adaptor protein TIR-domain-containing adapter-inducing interferon-β (TRIF) [52] (Fig. 3).

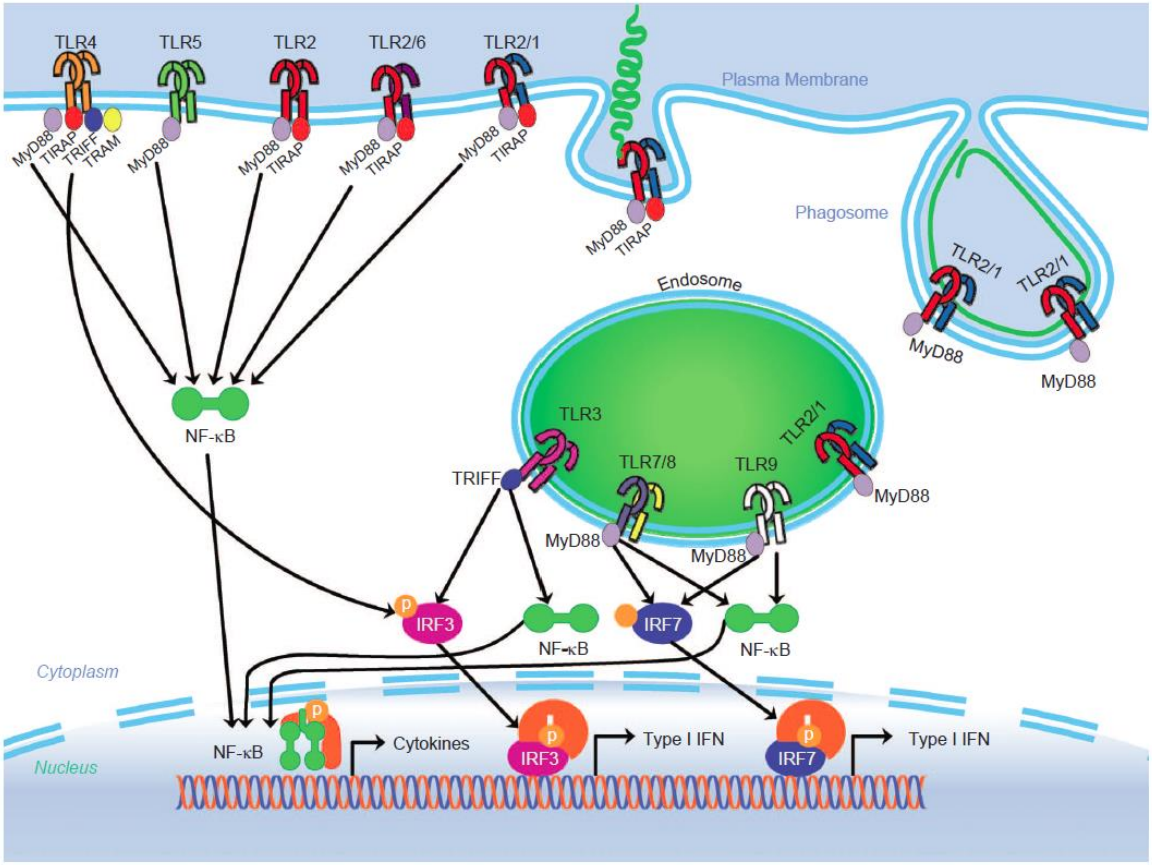

Fig 3. Overview of TLR signaling. *The TLR family can be categorized into two subgroups. TLR1, TLR2, TLR4, TLR5 and TLR6 are located primarily on the plasma membrane. Conversely, TLR3, TLR7, TLR8 and TLR9 are located within intracellular vesicles, the endolysosomes. Most TLRs are*

found as homodimers but TLR2 is able to form heterodimers with TLR1 and TLR6 (TLR1/2 and TLR2/6). Upon PAMP recognition, the TLR changes its conformation and recruits adapter proteins such as TRIF, TRAM, MyD88 and TIRAP. IFN, interferon; IRF, IFN regulatory factor; PAMP, pathogen-associated molecular pattern; NF, nuclear factor; TLR, Toll-like receptor. Adapted from Cervantes et. al [52].

1.2 Interleukin-36

1.2.1 Biology and function of Interleukin-36

Interleukin-36 (IL-36) is a member of the IL-1 family of cytokines. The latter consists of eleven members of which seven are agonists and four are antagonists. The agonists, namely IL-1α, IL-1β, IL-18, IL-33, IL-36α, IL-36β and IL-36γ, show pro-inflammatory properties whereas the receptor antagonists (Ra), namely IL-1Ra, IL-36Ra, IL-37, and IL-38, have anti-inflammatory effects [68]. IL-1 cytokines bind to their specific receptor. The three IL-36 agonists IL-36α, IL-36β and IL-36γ signal specifically through their common receptor IL-36R and its co-receptor IL-1R/AcP which leads to the activation of NF-κB and mitogen-activated protein kinases (MAPK) [69]. The IL-36R is expressed on many different cell types. Interestingly, keratinocytes and mDCs show the highest expression of IL-36R, but monocytes, macrophages and granulocytes also express IL-36R. In contrast, human B cells, T cells and NK cells do not express this receptor [70, 71].

Like other members of the IL-1 family, IL-36 cytokines are expressed as inactive proforms and require proteolytic processing for full activation. Indeed, the biological activity of the three agonists IL-36α, IL-36β and IL-36γ is increased 500-1000-fold upon cleavage at their N-terminal sites [72]. Recently, it has been demonstrated that neutrophil-derived proteases differentially process and activate all three agonists of the IL-36 family. IL-36α is activated by cathepsin G and elastase, IL-36β by cathepsin G and IL-36γ by elastase and proteinase-3 [73] (Fig. 4). Unpublished data further suggests a crucial role of cathepsin S in the activation of IL-36γ [74].

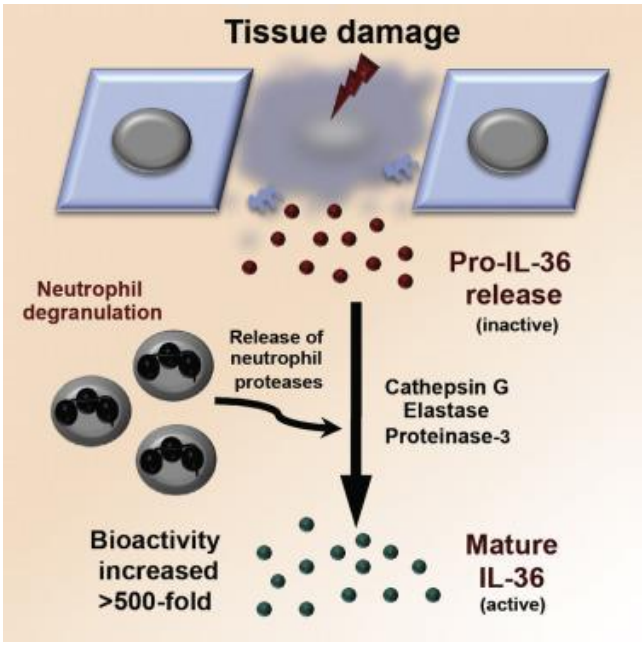

Fig. 4. IL-36 cytokines require proteolytic processing for full activation. *IL-36α, IL-36β, and IL-36γ are activated differentially by the neutrophil granule-derived proteases cathepsin G, elastase, and proteinase-3, increasing their biological activity ~500-fold. [73]*

IL-36 cytokines lack a signal sequence and therefore they are not directed to the ER for secretion [75, 76]. Their mechanism of secretion still remains unclear but a nonclassical mechanism has been suggested since IL-36γ secretion by skin epithelial cells requires adenosine 5'-triphosphate. As IL-36γ is realeased during pyroptosis, it was further sugessted that IL-36γ also acts as an alarmin [77].

1.2.2 Interleukin-36 in skin inflammation

In the last decade, IL-36 cytokines have emerged as important cytokines mediating inflammatory responses in the skin. Several reports have shown that all IL-36 isoforms are overexpressed in psoriatic skin [75, 78-80]. In keratinocytes, production of IL-36 family members can be induced by TNF, IL-17 and IL-22, cytokines known to be involved in psoriasis which further supports an important role for IL-36 in this disease [81]. The role of IL-36 in psoriasis has also been demonstrated in animal models. Transgenic expression of IL-36α leads to the development of psoriasiform skin lesions in mice [82]. Moreover, the psoriasis-like phenotype induced by the TLR7 agonist Imiquimod is dramatically increased in *IL-36RN*$^{-/-}$ mice [83]. In another mouse model where human psoriatic lesional skin is

transplanted onto mice lacking a functional adaptive immune system (SCID-mice), the blockade of IL-36R greatly improves the psoriatic changes [84].

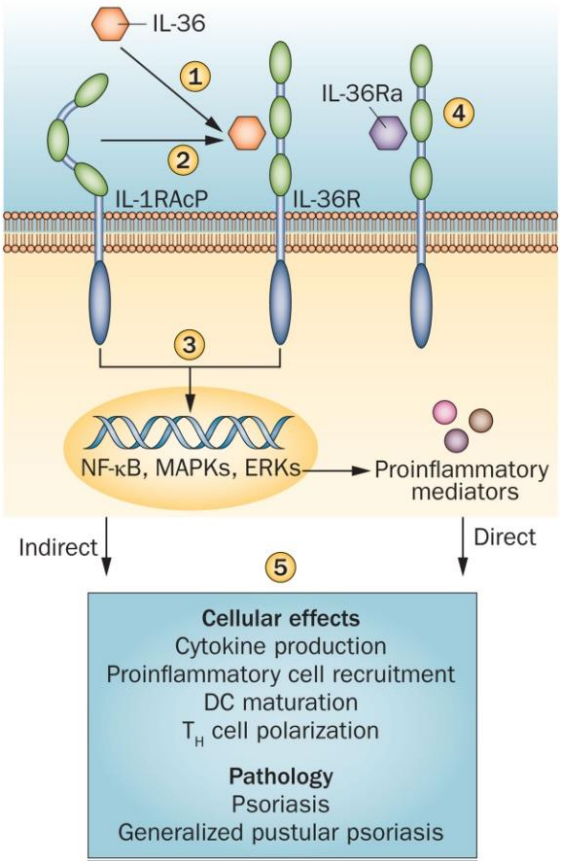

Fig. 5. IL-36 signaling. *IL-36α, IL-36β and IL-36γ are released by activated immune cells or keratinocytes and bind to IL-36R (1). IL-1RAcP is recruited (2) and an intracellular signalling cascade is initiated, thereby leading to gene transcription of proinflammatory mediators (3). IL-36Ra is acting as competitive inhibor of IL-36 cytokines by its binding to IL-36R (4). IL-36 can stimulate various cellular immune responses and is involved in diseases like psoriasis and generalized pustular psoriasis (5). DC: dendritic cell; ERKs: extracellular signal regulated kinases; IL-1RAcP: IL-1 receptor accessory protein; IL-36R: IL-36 receptor; NF-κB: nuclear factor κB, MAPKs: mitogen-activated protein kinases. Adapted from Dietrich et. al [85].*

A fulminant IL-36-mediated immune response seems to further play a crucial role in generalized pustular psoriasis (GPP). Marrakchi *et al*. identified homozygous missense mutations in *IL36RN*, the gene encoding for the IL-36RA in GPP. They demonstrated that the L27P variant of *IL36RN* has less potency to antagonize the effects of IL-36, thereby leading to an excessive immune response, in particular via

IL-8, a downstream target of IL-36. [86] This connection between mutations in *IL36RN* and GPP has been confirmed in several other reports [87-92]. Interestingly, 4 out of 96 patients with the adverse cutaneous drug eruption acute generalized exanthematous pustulosis (AGEP), which clinically resembles GPP, also carried a mutation in *IL36RN* [87]. Upregulation of IL-36 expression has been further observed in cells carrying a deficient adaptor protein complex subunit σ1C gene AP1S3 gene [93], a mutation that has been found in 10% of pustular psoriasis patients [94].

Further support for a role of IL-36 in skin inflammation was provided by the study of Foster et al., showing that exposure of human keratinocytes to all three isoforms of IL-36 significantly increased the expression of the potent chemotactic agents CXCL1, CXCL8, CCL3, CCL5, and CCL20 in human keratinocytes [71]. In the same study, it has been shown that IL-36 was able to induce high expression of of IL-1α, IL-1β and IL-6 in human blood monocytes. Also, mDCs and Langerhans cells showed a strong response to IL-36, as shown by the upregulation of CD83, CD86, HLA-DR, and the secretion of IL-1β and IL-6, thereby driving T cell proliferation. In contrast, no direct effect of IL-36 on human neutrophils and T cells could be demonstrated [70, 71].

1.3 The skin

1.3.1 Skin structure

The skin is one of the largest organs of the human body and functions as a protective interface between internal organs and the environment. It consists of three layers: the epidermis, the dermis and the subcutis.

The epidermis is a stratified epithelium which consists mainly of keratinocytes and is divided into the four sublayers *Stratum basale* (basal layer), *Stratum spinosum* (spinous layer), *Stratum granulosum* (granular layer) and *Stratum corneum* (corneal layer). Depending on their differentiation status, keratinocytes reside in different sublayers of the epidermis. The basal layer is composed of undifferentiated stem and progenitor cells of which the latter have a very strong proliferative capacity. Upon migration into the suprabasal layers, they undergo a controlled differentiation program [95-97]. The corneal layer consists of terminally differentiated

keratinocytes, so-called corneocytes, which have lost their transcriptional activity, nuclei and intracellular organelles. These cells consist mainly of keratin filaments that are surrounded by a complex series of proteins (filaggrins, involucrin, loricrin and others) forming the cornified envelope. They are held together by corneodesmosomes, and the intercellular space is filled with hydrophobic lipids in order to build a lipid bilayer [97]. Both the cornified envelope proteins and the lipid bilayer are indispensable for the integrity of epidermal barrier function and defects in these structures result in water loss, entry of pathogens, chemicals and other harmful stimuli that can contribute to a disease like atopic dermatitis [98]. Upon degradation of the corneodesmosomes by proteases in a last step, the corneocytes scale off in a process called desquamation [99, 100].

In addition to keratinocytes that represent the majority of the cells, the epidermis also contains other cell types. The pigment-building cells or melanocytes, are located in the basal layer of the epidermis where they produce melanin which is delivered to their surrounding keratinocytes in melanosomes and are responsible for skin pigmentation [101]. Furthermore, immune cells like Langerhans cells, skin-specific DCs, and tissue-resident $CD8^+$ T cells reside within the epidermis [102, 103].

The dermis is mainly composed of the extracellular matrix and a variety of immune and non-immune cells. Fibroblasts are producers of the extracellular matrix and collagen, and they interact closely with epidermal cells during hair development. Moreover, they play an important role in skin tissue-repair and wound healing [104]. The dermis is full of small blood and lymphatic vessels, through which migrating cells can traffic. They consist of endothelial cells and a basal lamina. Contractile cells, so-called pericytes, wrap around these endothelial cells. They are important in regulating stability and morphogenesis of small vessels [105], but are also thought to play a role in tissue regeneration because of their pluripotent differentiation capacity [106]. The immune cells of the skin reside mainly within the dermis and include macrophages, pDCs, dermal DCs, $CD4^+$ Th1 cells, $CD4^+$ Th2 cells, $CD4^+$ Th17 cells, γδT cells, NK cells and granulocytes including neutrophils, eosinophils, basophils and mast cells. The functions of these immune cells will be discussed in the next chapter.

The subcutis is a loose connective tissue layer localized between dermis and the muscle compartment. It is attached to the neighboring dermis by collagen and elastin fibers, moreover connecting the skin to the deep fascia by fibrous bands. It contains blood and lymphatic vessels, as well as cutaneous nerves. There is only a low number of cells residing within the subcutis, including mast cells and adipose-derived mesenchymal stem cells. However, the subcutaneous layer is mainly composed of fat cells (adipocytes) which can act as energy reservoir and minor thermoregulator [107].

1.3.2 The skin and the immune system

In addition to their physical barrier function, keratinocytes are also immunologically active cells that can initiate immediate immune reactions to pathogens and danger signals. One important mechanism is the release of antimicrobial peptides, such as LL-37, cathelicidin or β-defensins, [108-110]. These peptides are able to enter lipid-rich membranes of microbes and kill target cells by causing membrane instability [111-113] or by inhibiting important pathways inside the cell such as DNA replication and protein synthesis [114]. Another important immune tool of keratinocytes is the expression of PRRs that are able to initiate early and rapid immune responses in the skin. Various studies have reported that keratinocytes express TLRs 1–10 [64, 115-122]. Additionally, keratinocytes express the TLR4-associated CD14 and MD-2 proteins that enables TLR4 to respond to LPS [123]. Other important PRRs are the NLRs that can sense various intracellular PAMPs and DAMPs, thereby initiating the assembly of intracellular immune complexes, the so-called inflammasomes. Inflammasome assembly leads to the activation of caspase-1 which in turn cleaves pro-IL-1β and pro-IL-18 to generate the active forms of these pro-inflammatory cytokines [124]. Besides NLRs, the inflammasome in keratinocytes can also be activated by the DNA sensor protein AIM2 [125]. Moreover, keratinocytes express RIG-I-like receptors (RLRs) that allow the recognition of RNA virus infection to initiate and modulate antiviral immunity [126]. PRRs are not only expressed by keratinocytes but also by other cells in the skin including Langerhans cells, dermal DCs, macrophages, B and T cells, γδ T-cells, NK cells, granulocytes and fibroblasts [102, 127].

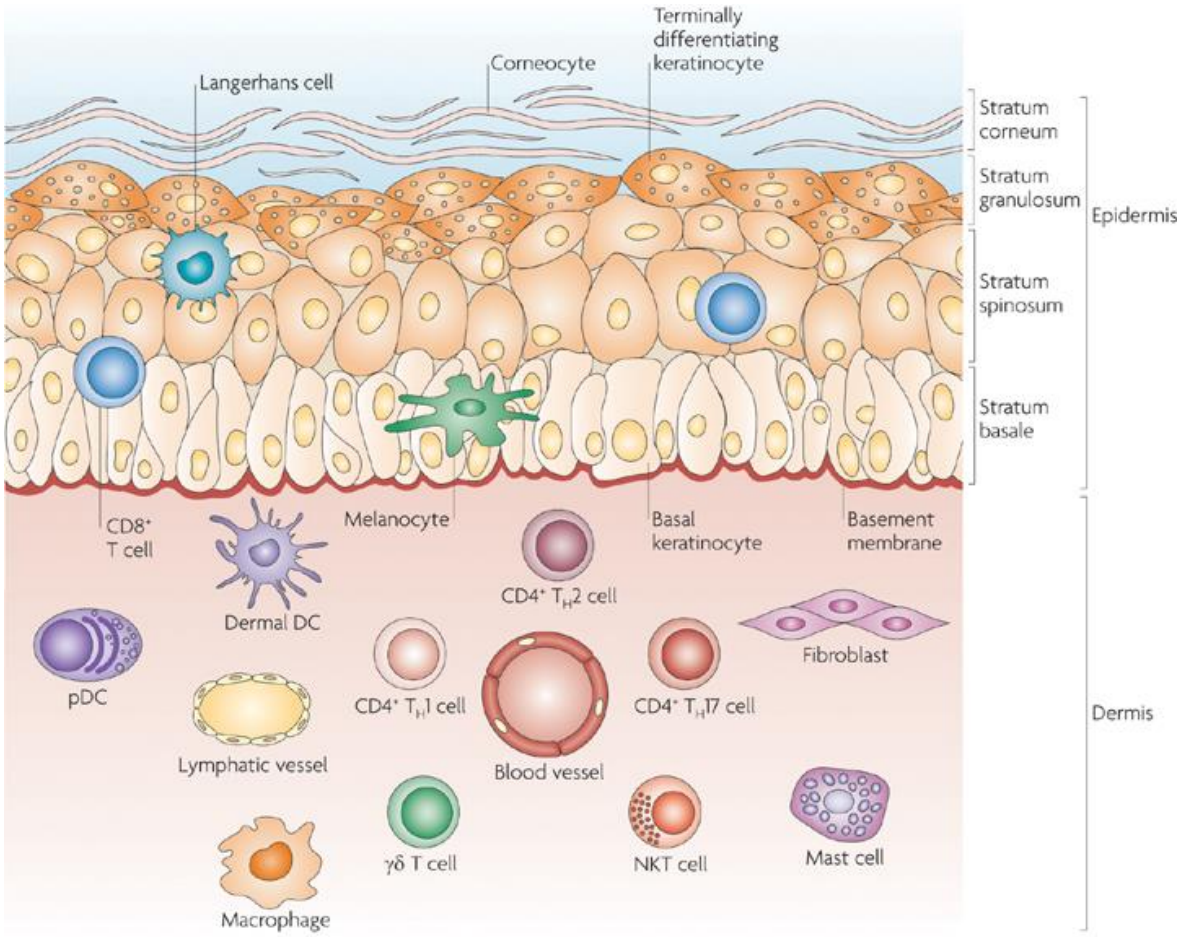

Figure 6. Skin anatomy and cellular effectors. *The skin has multiple functions in host defense including acting as protective barrier and in having an active immunological role. The epidermis is composed the stratum basale, the stratum spinosum, the stratum granulosum and the stratum corneum. Specialized cells in the epidermis include melanocytes (pigment-producing cells) and Langerhans cells, a subtype of skin DCs. Few CD8⁺ cytotoxic T cells can be found in the stratum basale and stratum spinosum. The dermis is composed of collagen, reticular fibres, elastic tissue, and many specialized immune cells, such as dermal DCs and pDCs, and CD4⁺ Th1, Th2 and Th17 cells, γδ T cells and NKT cells. Other important dermal cells are macrophages, fibroblasts and mast cells. Blood and lymphatic vessels and nerves (not shown) are also present throughout the dermis. DC = dendritic cell; pDCs = plasmacytoid DCs; Th1 = T helper 1; NKT = natural killer T. Adapted from Nestle et. al [102].*

However, pattern-recognition is not the only function of skin immune cells. DCs are professional antigen-presenting cells that have the ability to initiate adaptive immune responses by presenting antigens in a processed form via MHC-molecules.

In addition, the interaction of DCs with naive $CD4^+$ and $CD8^+$ T cells is further increased by the co-stimulatory molecules CD40, CD80 and CD86 present on DCs. The expression of these molecules can be augmented by type I interferons. Therefore they represent key molecules in the augmentation and maintanance of T cell responses [128, 129].

Another important group of innate immune cells in the skin are macrophages. Even though they also belong to the group of professional APCs, their main mechanisms of host defense are phagocytosis and the release of cytokines and chemokines. Due to the high levels of PRRs on their cell surface and intracellularly, macrophages represent excellent sensors of pathogen-derived or danger signals in the skin. Resident skin macrophages are responsible for tissue homeostasis, whilst the recruitment of monocytes from the bone marrow and the peripheral blood and differentiation into mature macrophages occurs upon skin infection, inflammation, and skin repair [130].

A key event in the early inflammatory response against pathogens and tissue damage is the migration of neutrophils to the skin. Whilst there are only a very limited number of neutrophils in the epidermis at steady state, millions of neutrophils can be recruited to the skin upon skin infection and inflammation. The most potent neutrophil attractants in the skin are chemokine (C-X-C motif) ligand (CXCL)-1, CXCL-2, IL-8 (also known as CXCL8), IL-1β and granulocyte colony-stimulating factor (G-CSF) that all can be produced by macrophages, keratinocytes and T cells [131-135].

T cells are the key cells of the adaptive immune system in the skin. Already in a healthy state, T cells are found in high numbers in the skin: healthy skin contains twice as many T cells as the blood and it has even been shown that 98% of CLA^+ effector memory T cells in the body reside within the skin [136]. Skin-resident T cells are characterized by the expression of CD103 and Very Late Activation Protein 1 (VLA-1) and play a key role in skin inflammation and inflammatory skin diseases such as psoriasis [137, 138]. $CD4^+$ and $CD8^+$ T cells are present in equal numbers in the skin [139]. In the context of inflammation, T cells from the periphery expand clonally and migrate towards the skin. In distinct pathological situations, different types of $CD4^+$ responses can be observed. During infection with intracellular microorganisms, Th1 cells predominate [140]. Th1 have also been found in high numbers in psoriasis skin [141]. In contrast, Th2 cells are associated with allergic

skin diseases and atopic dermatitis (AD) [142]. Another very important T cell subgroup in the skin are the IL-17 and IL-22 producing Th17 cells that have been shown to play a role in both AD [143] and psoriasis [144], moreover it has been shown that Propionibacterium acnes promotes Th17 responses in acne patients [145]. These Th17 cells are furthermore important in defense against acute and chronic bacterial and fungal infections [146-148]. Recently, another IL-22 producing circulatory T cell subset with skin-homing properties has been described. These so-called Th22 cells are not able to produce IL-17 or IFNγ but they seem to be involved in AD [149-151].

The TCR of the above described Th cell populations consists of an α and a β chain, and are therefore called αβ T cells and represent 95% of all T cells in humans. The other 5% of T cells are γδ T cells that also reside within the skin. γδ T cells express heterodimers consisting of the γ- and δ-chains of the TCR and represent only 2-9% of dermal T cells and 1-10% in the epidermis [102]. They enter the skin without priming in lymphoid tissues and are able to respond rapidly to antigen challenge. They have been shown to play an important role in tissue homeostasis and wound healing due to the release of particular growth factors, including connective tissue growth factor, keratinocyte growth factor, fibroblast growth factor 9, and insulin-like growth factor 1 [152]. Moreover it has been shown that the number of γδ T cells is increased in several skin diseases including psoriasis, chronic cutaneous lupus erythamtosus, Langerhans cell histiocytosis and melanoma [153-156].

1.4 Adverse cutaneous drug reactions

1.4.1 Definition

According to the World Health Organisation (WHO), an adverse drug reaction (ADR) is defined as a noxious and unintended response to a drug that occurs at a usual dose [157]. ADR represent a major health problem worldwide and approximately 5-8% of all hospitalisations are due to ADRs. Among all diseases, ADRs are rated as fifth leading cause of death. Within this group, ADRs with cutaneous manifestations represent 30-45% of all cases, and are therefore the most common ADRs. Approximately 2% of patients with a cutaneous ADR (CADR) have to be hospitalised [158].

1.4.2 Classification

Drug reactions can have both by immunologic and non-immunologic causes. Interestingly, the immune-mediated hypersensitivity reactions represent the minority of all ADRs, most of the ADRs are non-immune-mediated, and usually due to dose-dependent toxic effects of a drug.

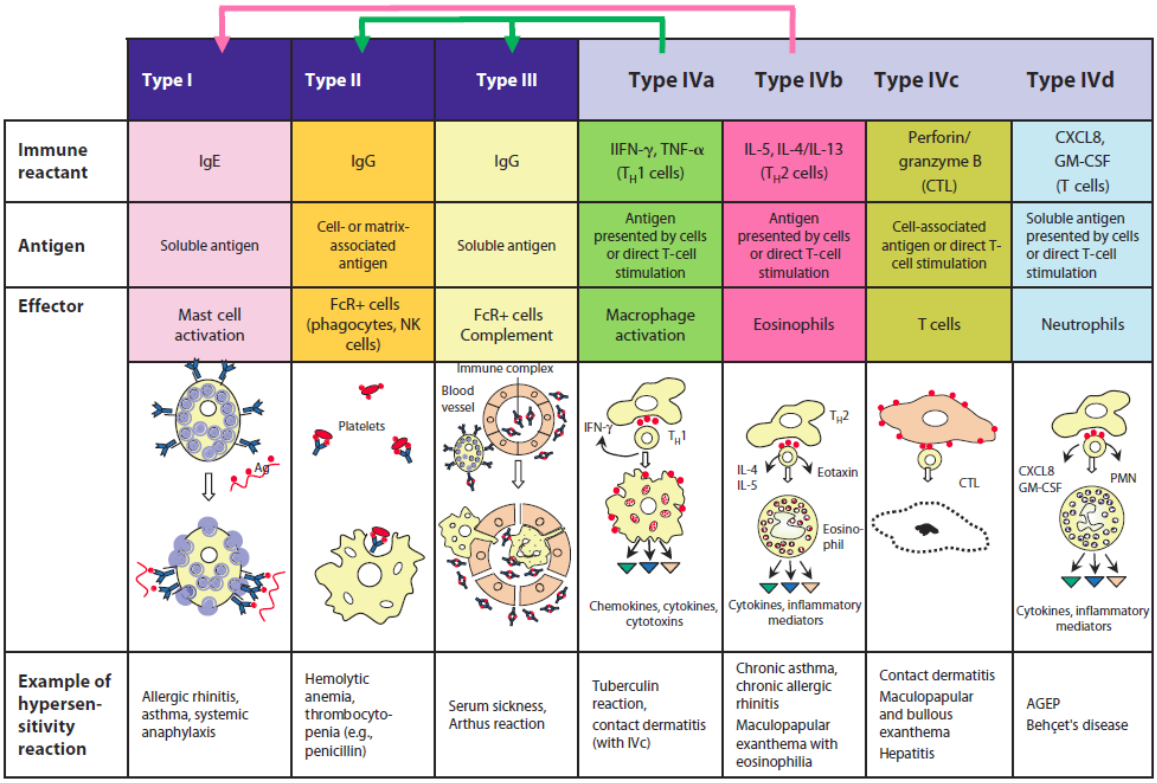

Figure 7. Revised Gell and Coombs classification of drug reactions. *Drug-induced immune reactions can be classified into different subtypes. Depending on the involved cell types and effector functions, drug reactions can result in distinct clinical reaction patterns. AGEP = Acute Generalized Exanthematous Pustulosis; PMN = polymorphonuclear leukocyte; CTL = cytotoxic T lymphocytes; GM-CSF = granulocyte-macrophage colony-stimulating factor. Adapted from Hausmann et. al [159].*

The most commonly used classification of ADRs has been proposed by Rawlins and Thompson [160]. They propose two major subtyes of ADRs, type A and type B reactions. A type A reaction represents a non-immune-mediated ADR that is caused by the pharmacological property of a drug. They are also considered as side effects. A type B reaction can be both immune-mediated and non-immune-mediated and occur only in predisposed individuals. Non-immunological type B reactions include

nonspecific mast cell degranulation, nonspecific cytokine dysbalances and enzymopathies [159]. Immune-mediated ADRs include IgE-mediated reactions (type I, according to Gell and Coombs, see Fig. 7), IgG-mediated cytotoxicity (type II), immune complex deposition (type III) and delayed drug hypersensitivity reactions (type IV). The latter can be further divided into the subtypes a-d. Type IVa reactions are characterized by the predominance of Th1 cells that activate and recruit monocytes/macrophages by the secretion of cytokines like IFNγ and TNF. Such reactions can be seen in contact dermatitis. In type IVb reactions, Th2 cells secrete IL-4, IL-5 and IL-13, leading to a strong eosinophilic inflammation. Clinical examples for a type IVb reaction is maculopapular exanthema with eosinophilia. In type IVc hypersensitivity reactions, cytotoxic T cells are the predominant cell type, leading to cell death of keratinocytes via the release of perforin and granzyme B and/or in a FasL-dependent manner. A typical example for a type IVc reaction are bullous skin reactions, toxic epidermal necrolysis (TEN) and Stevens-Johnson syndrome (SJS). Type IVd reactions are characterized by the predominance of CXCL-8 and Granulocyte-macrophage colony-stimulating factor (GM-CSF) that recruit neutrophils and thereby cause neutrophil-rich inflammation of the skin, such as in AGEP [159].

1.4.3 Uncomplicated cutaneous drug eruptions

The clinical manifestations of CADR range from mild to very severe. The majority of CADRs are mild and resolve with the termination of the medication. The most frequent (>90%) CADRs are the uncomplicated drug-induced disseminated exanthemas [161]. They manifest as different forms of drug-induced exanthemas that do not share a unique pathophysiology. Macular papular exanthemas (MPE) are the most common drug-induced exanthemas and are type IV hypersensitivitiy reactions. MPE manifest as polymorphic exanthemas with macules, papules and single pustules without systemic symptoms. The skin eruption appears after a sensitization phase of 5 to 7 days following first drug intake. Other uncomplicated CADRs include SDRIFE (Symmetrical Drug-Related Intertriginous and Flexural Exanthema, Baboon Syndrome), drug-induced urticaria, drug-induced leukocytoclastic vasculitis and fixed drug eruptions [162].

1.4.4 Severe cutaneous drug eruptions

Severe cutaneous drug eruptions represent about 2% of all CADRs. However, while being rare, they are potentially life-threatening and therefore a rapid diagnosis, identification and interruption of the culprit drug and intensive supportive care are crucial. Severe ADRs include Stevens-Johnson Syndrome (SJS), Toxic epidermal necrolysis (TEN, also known as Lyell syndrome), Drug Reaction with Eosinophilia and Systemic Symptoms (DRESS) and AGEP.

The most severe of all CADRs is TEN. It is considered to belong to the same spectrum of diseases as SJS, differing only by the extent of epidermal detachment (<10% in SJS, 10-30% in TEN-SJS-Overlap, >30% in TEN). Both diseases are rare with an incidence of 1-2/million per year. The mortality of TEN is 25-35% on average, whereas it is only of 1-5% in SJS. Clinical signs are involvement of mucosa and conjunctiva, grey skin lesions, and epidermal detachment. To date, the pathogenesis of SJS/TEN is incompletely understood. However, $CD8^+$ cytotoxic T cells seem to play an important role in the effector phase of the disease as a multitude of $CD8^+$ T cells has been found in the blister fluid of acute stage patients and it has been shown that these cells exert a drug-specific cytotoxicity against keratinocytes in a granzyme B-mediated manner [163, 164]. Another important mechanism leading to keratinocyte apoptosis involves the cytotoxic molecule FasLigand (FasL, CD95L). It has been demonstrated that keratinocytes from TEN patients express lytically active FasL and it has been proposed that Fas (CD95)-FasL interactions are directly involved in massive keratinocyte death TEN [165, 166]. Additionally the cytotoxic molecules granulysin and Annexin A1 have been shown to play a role in the pathogenesis of SJS/TEN [165, 167]. Moreover, a strong association of HLA-B*15:02 with carbamazepine-induced SJS/TEN in Han Chinese has been demonstrated [168], suggesting that genetic factors can influence the susceptibility to SJS/TEN [165].

DRESS is a severe ADR which is characterized by a polymorphic macular popular rash (MPR) with high eosinophilia, facial edema and systemic symptoms including fever and visceral involvement. The latency period is relatively long and varies between two and eight weeks after culprit drug intake. The skin symptoms are versatile, usually appearing as a MPR, but vesicles, purpura, pustules and erythroderma have also been reported in many cases. Systemic symptoms are

fever, lymphadenopathy, cytotoxic hepatitis, pneumonitis, myocarditis, nephritis and colitis. Most cases are associated with elevated blood eosinophilia (>90%). The underlying pathomechanism is not well understood but it has been suggested that the reactivation of several herpes viruses and the expansion of activated memory $CD8^+$ T cells that can specifically recognize viral peptides in the context of Human Leukocyte Antigen (HLA) class I play an important role [169]. This theory is supported by the strong association between DRESS caused by allopurinol and HLA-B*5801 [170].

1.5 AGEP

1.5.1 Definition

AGEP is a severe cutaneous adverse drug reaction characterized by the very rapid onset of a pustular eruption on an erythematous background, accompanied by fever and neutrophilia.

1.5.2 Epidemiology

AGEP is a rare form of CADR, with a reported incidence of one to five cases per million people per year [171]. In 1968, Baker and Ryan were the first to describe such pustular eruption but it was then considered as the exanthematic subtype of pustular psoriasis [172]. The term AGEP was only introduced in 1980 by Beylot [173]. Women are preferably affected by this CADR [174]. The mortality rate of AGEP, reported between 1 and 5%, is the lowest among all severe CADRs. In >90% of cases, AGEP is caused by drugs [175]. The most frequent culprit drugs are aminopenicillins, sulphonamides, hydroxychloroquine, quinolone, terbinafin and diltiazem [176]. In rare cases, bacterial, viral or parasitic infections can also cause AGEP [177-182]. Spider bites have also been reported to induce AGEP [183, 184].

1.5.3 Clinical and histological features

AGEP is characterized by the rapid disseminated development of a multitude of non-follicular, sterile pustules on an erythematous background. Usually it is

accompanied by fever >38°C and blood neutrophilia, with 30% of patients also presenting eosinophilia. Internal organs are usually not involved [185].

Upon interruption of culprit drug intake, the disease is usually self-limiting but topical and sometimes systemic steroids are recommended. In some severe cases, intensive supportive care is needed. Patients in the healing phase show pronounced scaling of the skin [186].

Fig. 8. Clinical appearance of AGEP. *Patient with numerous non-follicular pustules on a background of edematous erythema on the chest and on the abdomen after the intake of Terbinafin. Adapted from Hoetzenecker et. al. [162]*

Histological features are intraepidermal/subcorneal pustules, an abundant monocytic and lymphocytic infiltrate and single necrotic keratinocytes [174].

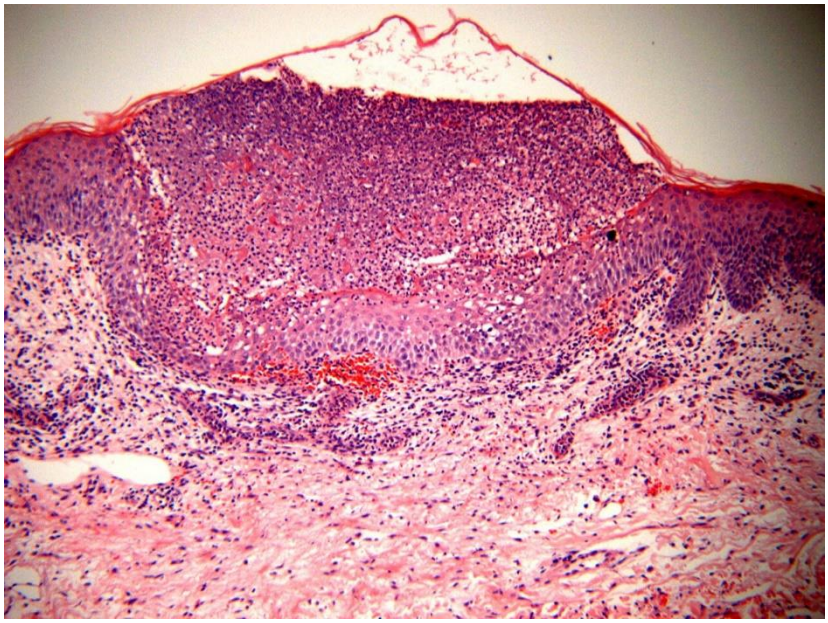

Figure 9. AGEP histology. *Hematoxylin and Eosin staining of lesional skin of an AGEP patient revealing subcorneal neutrophil infilatration, necrosis of single keratinocytes and a dermal inflammatory infiltrate. Adapted from Sulewski et. al. [187].*

1.5.4 Etiology and pathogenesis

To date, the pathophysiology of AGEP remains unclear. However, as for most other ADR, AGEP is currently considered as a T cell-mediated disease [188]. Indeed, drug-specific T cells are suspected to play a central role in AGEP as evidenced by the high levels of T cell stimulation induced selectively by causative (culprit) drugs as measured by the lymphocyte transformation test (LTT) [189]. Furthermore, drug-specific $CD4^+$ and $CD8^+$ T cells have been derived *in vitro* from AGEP patients' peripheral blood. Most of these drug-specific T cells [190] produce IL-8 [185, 191], a powerful chemoattractant for neutrophils. IL-8-producing T cells are therefore, to date, considered to be the cause of neutrophil survival and recruitment to the skin [192]. More recently, it has also been suggested that Th17 effector cytokines, namely IL-17 and IL-22, stimulate keratinocytes to produce IL-8, and that keratinocyte-derived IL-8 may also contribute to neutrophil accumulation in the skin of AGEP patients [193]. Hence, T cell- and keratinocyte-derived IL-8 has been proposed to be responsible for the recruitment of neutrophils to the intraepithelial pustules.

AGEP shares certain clinical and histological features with pustular psoriasis and these overlapping features can render the diagnosis challenging. However, signs including the rapid onset and short duration of disease as well as an association with a recently administered drug and a spontaneous healing after its discontinuation, favor the diagnosis of AGEP. Recently, genetic studies identified mutations in *IL-36RN,* the gene encoding for IL-36Ra, in patients with general pustular psoriasis [86, 194-196]. Interestingly, mutations in *IL-36RN* have also been reported in rare cases of AGEP [197], suggesting that a dysregulation in IL-36 signaling is involved in the physiopathology of both diseases. A mutation in *IL-36RN* may result in exacerbated IL-36 signaling leading to the downstream production of IL-1, IL-6 and IL-8 and subsequent neutrophilic skin infiltration with pustule formation.

1.6 Aim of the project

AGEP is a rare and severe cutaneous drug eruption whose pathophysiology is largely unknown. Like all medication-induced side effects, AGEP is an important limitation to the use of certain important drugs in some patients. Thus, it is of high importance to understand the early mechanisms leading to this adverse reaction in order to be able to envisage means of prevention in patients known to present such risks.

In this PhD thesis, I aim to investigate the pathomechanisms leading to AGEP. I will provide novel evidence that drugs causing AGEP can specifically trigger IL-36 cytokine production by peripheral blood monocytes and keratinocytes from AGEP patients and subsequently induce IL-8 by peripheral blood mononuclear cells in an IL-36-dependent manner. These observations are supportive of a drug-specific dysregulation of IL-36 signaling as an important potential driver of the immunopathogenesis of AGEP, and identify myeloid cells and keratinocytes as new important players in AGEP. Furthermore, I will provide mechanistic insights into the disease development by showing an abnormal regulation of the NF-κB pathway in cells of certain AGEP patients.

2 Materials and Methods

2.1 Materials

2.1.1 Skin biopsy and blood sampling

Skin biopsies were taken from lesional skin of patients in the acute phase of the ADR (2x 6mm punch biopsies). Healthy skin samples were obtained from the Department of Plastic Surgery, University Hospital of Zurich. For paraffinization, skin samples were fixed in formalin 5% overnight. For RNA isolation, samples were snap-frozen in liquid nitrogen and stored at -80°C before use.

Peripheral blood from patients were taken both in the acute phase of the disease and under healthy conditions (at least 6 months after the ADR). Serum from AGEP and MPR patients were obtained from Switzerland (N=17, Dermatology Department, University Hospital of Zürich), and from Asia (N=32, Dermatology Department of Chang Gung Memorial Hospital in Chinese Taiwan and Department of Dermatology of the Hokkaido University Graduate School of Medicine in Sapporo, Japan). Healthy controls were obtained from the Blood Donation Center, Schlieren, Switzerland.

The characteristics of all studied AGEP patients from the Dermatology Department of the University Hospital of Zürich are presented in Supplementary Tables 1 and 2. All human samples were collected after informed written patient consent with approval of Local Ethics Committees and according to the Declaration of Helsinki Principals.

2.1.2 Equipment

AID ELISpot Reader (AID GmbH, Strassberg, Germany)

Aperio ScanScope slide scanner (Leica Biosystems, Wetzlar, Germany)

Axio Imager 2 Fluorescence Microscope (Zeiss, Oberkochen, Germany)

BD FACS Canto (Franklin Lakes, NJ, USA)

BD FACS Canto II (Franklin Lakes, NJ, USA)

Bioanalyzer 2100 (Agilent, Waldbronn, Germany)

Cytation 3 (BioTek, Winooski, VT, USA)

Facscanto A (Becton-Dickinson, Franklin Lakes, NJ, USA)

Facscanto II (Becton-Dickinson, Franklin Lakes, NJ, USA)

Illumina HiSeq device (Illumina, San Diego, CA, USA)

Light Cycler 96 (Roche, Basel, Schweiz)

Light Cycler 480 II (Roche, Basel, Schweiz)

QuadroMACS™ Separator (Miltenyi Biotec, Bergisch Gladbach, Germany)

Mastercycler gradient PCR machine (Eppendorf, Hamburg, Germany)

Tissue Rupter (Polytron, Kinematica AG, Luzern, Switzerland)

Qubit® (1.0) Fluorometer (Life Technologies, Carlsbad, CA, USA)

Zeiss Axio Imager M2 Fluorescence Mikroskop (Zeiss, Oberkochen, Germany)

Widefield BX61 fluorescence microscope (Olympus, Tokyo, Japan)

2.1.3 Primary antibodies

Target	Company	Catalog number	Dilution	Assay
CD3	Dako	M7254	1:50	IF
CD3-APC	Biolegend	300312	1:20	FACS
CD14-FITC	BD	555397	1:5	FACS
CD45-PE-Cy7	BD	560915	1:20	FACS
CD68	Dako	M0876	1:100	IF
HLA-ABC	Biolegend	311412	1:200	Neutralization
HLA-DR	Biolegend	307612	1:200	Neutralization
IgG1	Biolegend	403102	Assay-dependent	Neutralization
IL-36α	R&D	MAB2297	1:400	ICH/IF
IL-36γ	R&D	AF2320	1:400	ICH/IF

IL-36γ	Peprotech	500-P316	1:100	ELISpot
IL-36γ biotinylated	Peprotech	500-P316Bt	1:100	ELISpot
IL-8	LSBio	LS-C165213	1:100	IHC
IL-1β	Abcam	ab53175	1:100	IHC
TLR2	Invivogen	maba2-htlr2	Assay-dependent	Neutralization
TLR4	Invivogen	mabg-htlr4	Assay-dependent	Neutralization

2.1.4 Secondary antibodies

Target	Company	Catalog number	Dilution
anti-rabbit IgG biotinylated	Abcam	ab6720	1:200
anti-mouse IgG biotinylated	Abcam	ab6788	1:200
anti-goat IgG biotinylated	Santa Cruz	sc-2042	1:200
Alexa Fluor® 488 Goat Anti-Mouse IgG	Life technologies	A11001	1:200
Alexa Fluor® 647 Donkey Anti-Goat IgG	Abcam	ab150131	1:100

2.1.5 Kits and reagents

Agilent SureSelectXT All exons V5 kit	Agilent Technologies, Santa Clara, CA, USA
Agilent Sure SelectXT kit	Agilent Technologies, Santa Clara, CA, USA

CD14 MicroBeads, human	Miltenyi Biotech, Bergisch Gladbach, Germany
ELISA development kit for human IFNγ	R&D Systems, Minneapolis, MN, USA
ELISA development kit for human IL-1β	R&D Systems, Minneapolis, MN, USA
ELISA development kit for human IL-6	R&D Systems, Minneapolis, MN, USA
ELISA development kit for human IL-8	Biolegend, San Diego, CA, USA
ELISA development kit for human IL-17A	Biolegend, San Diego, CA, USA
Human Exon 1.0 ST Affymetrix chips	Affymetrix, Santa Clara, CA, USA
LEGENDplex Kit	Biolegend, San Diego, CA, USA
MACS Separator	Miltenyi Biotech, Bergisch Gladbach, Germany
NBT/BCIP substrate kit	Promega, Madison, WC, USA
Pan T Cell Isolation Kit, human	Miltenyi Biotech, Bergisch Gladbach, Germany
QIAamp DNA mini kit	Qiagen, Hilden Deutschland
RevertAid First Strand cDNA Synthesis Kit	Thermo Fisher Scientific, Carlsbad, CA, USA
RNeasy® Fibrous Mini Kit	Qiagen, Hilden Deutschland
RNeasy® Micro Kit	Qiagen, Hilden Deutschland
TruSeq PE Cluster Kit v3-cBot-HS	Illumina, Inc., San Diego, CA, USA
TruSeq SBS Kit v3-	Illumina, Inc., San Diego, CA, USA
Vectastain ABC kit	Vector Laboratories, Burlingame, CA, USA

2.1.6 Chemicals and other consumables

Albumin from human serum	Sigma, Munich, Germany
Amoxicillin	Sigma, Munich, Germany
Antibody Diluent	Dako, Glostrup, Denmark
Bovine serum albumin (BSA)	Sigma, Munich, Germany

Carbamazepine	Sigma, Munich, Germany
DAPI (4',6-Diamidino-2-phenylindole)	Thermo Fisher Scientific, Carlsbad, CA, USA
Deoxynucleotide triphosphates (dNTPs)	Roche, Basel, Switzerland
Dulbecco's Phosphate buffered saline (PBS) (w/o Ca2+, Mg2+)	Biochrom, Berlin, Deutschland
Ethanol (EtOH)	Fluka Chemie, Buchs, Switzerland
Ethanol 70 % V/V	Kantonsapotheke, Zurich, Switzerland
Ethanol 80 % V/V KA PhEur	Kantonsapotheke, Zurich, Switzerland
Ethanol 96 % V/V KA PhEur	Kantonsapotheke, Zurich, Switzerland
Ethanol absolut KA PhEur	Kantonsapotheke, Zurich, Switzerland
Faramount Mounting Medium, Aqueous	Dako, Glostrup, Denmark
FastStart Universal SYBR Green Master	Roche, Basel, Switzerland
Ficoll-Paque PLUS	GE Healthcare, Little Chalfont, UK
Flasks and (multiwell) dishes for cell culture	Nunc, Roskilde, Denmark
Fluconazol	Sigma, Munich, Germany
Fluorescence Mounting Medium	Dako, Glostrup, Denmark
Haematoxylin solution	J.T.Baker, Phillipsburg, US-NJ
Peroxidase-Blocking solution	Dako, Glostrup, Denmark
Letrozole	Sigma, Munich, Germany
Metamizole sodium hydrate	Sigma, Munich, Germany
Pan-caspase inhibitor (z-VAD-fmk)	Alexis, Lausen, Switzerland
Pepinh-MYD (MyD88 Inhibitory Peptide)	Invivogen, San Diego, CA, USA
PepinhTRIF (TRIF Inhibitory Peptide)	Invivogen, San Diego, CA, USA
Recombinant (r) IFNα	
rIFNγ	Peprotech, Rocky Hill, NJ
rIL-1β	Peprotech, Rocky Hill, NJ
rIL-8	R&D Systems, Minneapolis, MN, USA
rIL-36Ra	R&D Systems, Minneapolis, MN, USA

rTNFα	Peprotech, Rocky Hill, NJ
RNA later	Qiagen, Hilden, Germany
Slides Super Frost^{TM} Plus	Thermo Scientific, Watham, MA, USA
SYBR Green (FS Eessential DNA Green Master)	Roche, Basel, Switzerland
Target Retrieval Solution	Dako, Glostrup, Denmark
Terbinafin hydrochloride	Sigma, Munich, Germany
Tetradecanoyl-Phorbolacetate (TPA)	Sigma, Munich, Germany
Tetramethylethylenediamide (TEMED)	Sigma, Munich, Germany
TIRAP Inhibitor Peptide	Millipore, Billerica, MA, USA
Transwell polycarbonate membrane cell culture inserts, 12 mm Transwell with 0.4 µm pore polycarbonate membrane insert	Corning, Corning, NY, USA
Triton-X 100	Sigma, Munich, Germany
Trypsin	Gibco BRL, Paisley, Scotland
Ultrapure LPS (upLPS)	Invivogen, Toulouse, France
Vancomycin	Sigma, Munich, Germany
Xylene	Synopharm, Ofingen, Switzerland
β-mercaptoethanol	Sigma, Munich, Germany

2.1.7 Buffers and solutions

AP (Alkaline phosphatase) buffer	100 mM NaCl 5 mM $MgCl_2$ 100 mM TRIS/HCl (pH 9.5)
PBS (Phosphate buffered saline)	137 mM NaCl 2,7 mM KCl 8,4 mM Na_2HPO_4
PBS-Tween20 (PBS-T)	PBS Tween20 0.1 % (v/v)
Reagent Diluent	PBS 1% BSA
2N H_2SO_4	5.5ml H_2SO_4 ad 100ml ddH20

2.1.8 Cell culture media and additives

Anti-anti antibiotic-antimycotic (A/A)	Gibco BRL, Paisley, Scotland
DMEM	Gibco BRL, Paisley, Scotland
Fetal bovine serum (FBS), heat inactivated	Gibco BRL, Paisley, Scotland
Keratinocyte-SFM, EGF, BPE	Gibco BRL, Paisley, Scotland
RPMI 1640	Gibco BRL, Paisley, Scotland
Complete Keratinocyte medium for keratinocyte isolation from hair follicles	¾ DMEM + 1% Pyruvate + ¼ HAM's F12 10% FCS 102 U/ml penicillin 0.1 mg/ml streptomycin 2 mM glutamin 0.4 µg/ml hydrocortison 10^{-10} M choleratoxin 5 µg/ml insulin 20 µg/ml adenin 5 µg/ml transferrin 2 x 10^{-9} M trijodthyronin 10 ng/ml EGF

2.2 Methods

2.2.1 Gene expression array

2.2.1.1 General remark

Experiments have been performed by the staff of the Functional Genomics Center of Zurich.

2.2.1.2 Sample processing and data analysis

Gene expression profiling was performed using arrays of Human Exon 1.0 ST Affymetrix chips. The Raw fluorescence intensity values were analyzed using the R packages Affy [198] and Limma of Bioconductor [199].

The gene expression data analysis consists of the following steps: 1. between-array normalization, 2. probe summary with the rma algorithm, 3. fitting the data to a linear model and 4. detection of differential gene expression. Quantile-normalization was applied to the log2-transformed intensity values as a method for between-array normalization, to ensure that the intensities had similar distributions across arrays [200]. To find genes with significant expression changes between groups, empirical Bayes statistics were applied to the data by moderating the standard errors of the estimated values. P-values were obtained from the moderated t-statistic and corrected for multiple testing with the Benjamini–Hochberg method [201]. The P-value adjustment guarantees a smaller number of false positive findings by controlling the false discovery rate (FDR).

Quality control and gene expression microarray data analysis was done using R/Bioconductor software (Fred Hutchinson Cancer Research Center, Seattle, WA) [199]; signal intensity files were summarized using the robust multi array average (RMA) [200] for processing and quantile normalization. A modified t-test using *limma* software (part of the Bioconductor project) [202] was performed for comparison of the experimental conditions. Both the p-values and the Benjamini-Hochberg False Discovery Rate (FDR) are reported.

2.2.2 RNA-sequencing

2.2.2.1 General remark

Experiments have been performed by the staff of the Functional Genomics Center of Zurich.

2.2.2.2 Library preparation

The quantity and quality of the isolated RNA was determined with a Qubit® (1.0) Fluorometer (Life Technologies, California, USA) and a Bioanalyzer 2100 (Agilent, Waldbronn, Germany). The TruSeq Stranded mRNA Sample Prep Kit (Illumina, Inc, California, USA) was used in the subsequent steps. Total RNA samples (500ng to 1 µg) were ribosome depleted and then reverse-transcribed into double-stranded cDNA with Actinomycin added during first-strand synthesis. The cDNA samples were fragmented, end-repaired and polyadenylated before ligation of TruSeq adapters. The adapters contain the index for multiplexing. Fragments containing TruSeq adapters on both ends were selectively enriched by PCR. The quality and quantity of the enriched libraries were validated using a Qubit® (1.0) Fluorometer and the Bioanalyzer 2100 (Agilent). The product is a smear with an average fragment size of approximately 360 bp. The libraries were normalized to 10nM in Tris-Cl 10mM, pH8.5 with 0.1% Tween 20.

2.2.2.3 Cluster Generation and RNA Sequencing

The TruSeq PE Cluster Kit v3-cBot-HS (Illumina, Inc., CA) was used for cluster generation using 8pM of pooled normalized libraries on the cBOT. RNA sequencing was performed on an Illumina HiSeq with a 2500 paired end approach at 2 X126 bp using the TruSeq SBS Kit v3-HS (Illumina, Inc.).

2.2.2.4 Data analysis

Bioinformatic analysis was performed using SUSHI [203]. In detail, the raw reads were quality checked using Fastqc (http://www.bioinformatics.babraham.ac.uk/projects/fastqc/) and FastQ Screen (http://www.bioinformatics.babraham.ac.uk/projects/fastq_screen/). Quality controlled reads (first five bases trimmed, minimum average quality Q20, minimum

tail quality Q10) were aligned to the reference transcriptome (Ensembl GRCh38, not patched) for transcript abundance estimation using RSEM [204]. Differential expression analysis was performed using edgeR [205]. Gene ontology (GO) enrichment analysis was performed using the Bioconductor packages goseq [206] and GOStats [207], and visualized using ReViGo [208]. Enrichment analysis of other gene sets was performed using Enrichr [209].

2.2.3 Serum preparation

Blood was taken from AGEP, MPR and healthy donors in serum tubes (BD Vacutainer, BD, Franklin Lakes, NJ) and left untouched for 30-60 minutes to allow the cells and clotting factors to clot to form. Serum was prepared by centrifugation of whole blood at 1'300 rpm for 10 minutes in a 50 ml Falcon. The supernatant (representing the serum) was taken, aliquoted and stored at -20°C until use in experiment.

2.2.4 PBMC isolation

PBMCs were isolated using a density gradient. For this purpose EDTA blood from AGEP, MPR and healthy donors was diluted 1:1 with PBS. 50 ml Falcon tubes were filled with 15 ml Ficoll-Paque Plus® (GE Healthcare, Little Chalfont, UK) and 35ml of the diluted blood was slowly applied on the Ficoll layer, followed by centrifugation at 2000rpm with slow acceleration and breaking rate for 20 minutes at room temperature (RT). PBMC were then collected from the interphase and transfered to a fresh 50ml Falcon tube. The tube was filled up with PBS and centrifuged at 1200rpm for 10 minutes to wash the cells. The supernatant was discarded and the washing step was repeated. Cells were then resuspended in medium for use in experiment or frozen down in FBS containing 10% DMSO using a cryo-box.

2.2.5 $CD14^+$ monocytes isolation

$CD14^+$ monocytes were isolated using magnetic-activated cell sorting (MACS). Freshly isolated PBMC from human AGEP, MPR and healthy blood were counted and resuspended in cold MACS buffer. Cells were centrifuges at 1200 rpm for ten

minutes, then the supernatant was discarded. Cells were resuspended in 80µl of MACS buffer per 10^7 total cells and 20µl of CD14 beads were added. The suspension was mixed and incubated for 15 minutes at 4-8°C in the dark. Cells were washed by adding 30 ml of cold MACS buffer, followed by centrifugation at 1200 rpm for 10 minutes. The supernatant was discarded and the cells were resuspended in 500µl of MACS buffer. Magnetic separation was then performed using MACS columns LS. For this purpose the LS columns were placed in the magnetic field of the QuadroMACS™ Separator (Miltenyi Biotec, Bergisch Gladbach, Germany) and 50ml Falcon tubes were placed under each column to collect the flow-through. The columns were prepared by rinsing with 3ml of MACS buffer. The cell suspension was added onto the column, followed by 3x 3ml of MACS buffer. The unlabeled cells were collected in the Falcon tube. To elute the $CD14^+$ cell fraction, the column was placed on a new 10ml falcon tube and 5ml of MACS buffer were added to the column. The plunger was then pushed into the column, thereby eluting the magnetically labeled $CD14^+$ cells.

2.2.6 $CD3^+$ T cell isolation

The flow-through from step 1.8.5 was centrifuged at 1300 rpm for 10 minutes and the supernatant was discarded. The cells were resuspended in 40µl of MACS buffer per 10^7 total cells and 10µl of Pan T cell Biotin-Antibody was added. The cell suspension was mixed well and incubated for 5 minutes at 4-8°C. As a next step, 30µl of MACS buffer were added, followed by 20µl of Pan T Cel MicroBead Cocktail. The suspension was mixed well and incubated for 10 minutes at 4-8°C in the dark. Magnetic separation was then performed using MACS columns LS. For this purpose the LS columns were placed in the magnetic field of the QuadroMACS™ Separator (Miltenyi Biotec) and 50ml Falcon tubes were placed under each column to collect the flow-through. The columns were prepared by rinsing with 3ml of MACS buffer. The cell suspension was applied onto the column and the flow-through was collected, and the columns were washed with 3x 3ml of MACS buffer. The flow-through was collected in a 50ml Falcon tube and represents the enriched T cells.

2.2.7 Flow cytometry

Cells in a pellet were washed 3 times with PBS and transferred to 96-well U-bottom plates. After washing the cells 3 times with FACS buffer (2 % FCS in PBS), 5µl of PE-Cy7-labeled anti-CD45, 20µl of FITC-labeled anti-CD14 or 5µl of APC-labeled anti-CD3 (single stainings and triple-stainings) were added to the cell suspensions in a total volume of 100µl and incubated for 30 minutes at 4°C in the dark. The cells were washed 3 times with FACS buffer, taken up in 200 µl FACS buffer and analyzed directly using a FACSCanto (BD, Franklin Lakes, US-NJ) with FACS DIVA software (BD, Franklin Lakes, US-NJ). Data were compiled using FlowJo analysis software (TreeStar Inc.).

2.2.8 Keratinocyte isolation from hair follicles

Hair including follicles were collected from patients and the extremities containing outer root sheath were cut. After washing the hair in complete keratinocyte medium [210] containing 100µg/ml kanamycin, it was incubated for 3 minutes in 1mg/ml Dispase II, followed by three washing steps in keratinocyte medium. The hair was then plated on Mitomycin-treated J2 feeder cells in complete keratinocyte medium and cultured until small colonies of keratinocytes become visible. Cells were splitted at 80% confluence and passaged three times before being used for experiments.

2.2.9 Preparation of drug solutions for cell stimulation

Drug solutions were prepared by dissolving the drugs in powder form in RPMI + 10%FBS, in Opti-MEM or PBS. Concentrations were administered by testing cell viability upon 24 hours of drug stimulation and the highest possible concentration was used for experiment.

2.2.10 Co-culture experiments

70.000 AGEP hair follicle keratinocytes were plated in Gibco keratinocyte medium (Thermo Scientific) on a 12mm transwell plate with 0.4µm pore polycarbonate membrane inserts (Corning, Corning, NY, USA) overnight to allow them to adhere.

The following day, keratinocyte medium was replaced by Gibco Opti-MEM medium (Thermo Scientific) and $1x10^6$ PBMC from patients having experienced AGEP, but in remission at the time of blood and hair collection (blood and hair collection at least 6 months after remission), added inside the polycarbonate membrane inserts, followed by addition of stimuli in both compartments at the same concentration. After 6 hours of incubation, cells were harvested and RNA was isolated for Real-Time quantitative PCR analysis.

2.2.11 RNA isolation

2.2.11.1 RNA isolation from fresh-frozen skin

Total RNA was isolated from AGEP, MPR and healthy skin biopsies using the Fibrous Tissue Kit (Qiagen, Hilden, Germany). All mentioned chemicals were provided with the kit.

Fresh-frozen skin was thawed in 300µl of RLT buffer containing β-Mercaptoethanol (β-ME) in a 14ml Falcon round-bottom tube. The tissue was then disrupted and the lysate was homogenized using a Tissue Rupter (Polytron, Kinematica AG, Luzern, Switzerland). The homogenized tissue was transferred into a 2ml Eppendorf tube and 590µl of RNase-free water was added, followed by 10µl of proteinase K. The solution was mixed well and incubated at 55°C for 10 minutes. The samples were centrifuged at 10.000 rpm for 3 minutes at RT and the supernatant was then transferred into a new 2ml Eppendorf tube. 450µl of 100% ethanol were added and mixed well by pipetting. 700µl of the sample were transferred to an RNeasy Mini Spin Column and centrifuged at 10.000 rpm for 15 seconds. The flow-through was discarded and the last step was repeated until no sample was left. To wash the membrane, 350µl of buffer RW1 was added to the RNeasy Spin Column, centrifuged for 15 seconds and the flow-through was discarded. DNase I treatment was performed by preparing a mix of DNase I and buffer RDD (10µl DNase I + 70µl buffer RDD per sample). This mix was added onto the membrane of the RNeasy Mini Spin Column and incubated for 15 minutes at RT. The column was washed with 350µl buffer RW1 and centrifuged at 10.000 rpm for 15 seconds. The flow-through was discarded and 500µl of buffer RPE was added to the spin column, followed by centrifugation at 10.000 rpm for 15 seconds. The flow-through was

discarded and another 500µl of buffer RPE was added to the spin column, followed by centrifugation at 10.000 rpm for 2 minutes. The spin column was then placed into a new 2ml collection tube and centrifuged at full speed for 5 minutes to remove residual liquid and dry out the membrane. The spin column was then placed into a new 1.5ml collection tube and 15-20µl of RNase-free water were added directly onto the membrane. The columns were centrifuged at full speed for 1 minute at RT to elute the RNA. The isolated RNA was kept on ice for further processing or stored at -80°C.

2.2.11.2 RNA isolation from cells

Total RNA was isolated from PBMC and keratinocytes using the RNeasy Micro Kit (Qiagen, Hilden, Germany). All mentioned chemicals were provided with the kit.

Cells were harvested and collected as a pellet in a 2ml Eppendorf tube and 350µl of RLT buffer containing β-ME was added. The same volume of 70% ethanol was added. The solution was mixed well and 700µl was transferred to an RNeasy MinElute spin column in a 2ml collection tube, centrifuged at 10.000 rpm for 15 seconds and the flow-through was discarded. This step was repeated until no sample was left. 350µl of buffer RW1 was added to the spin column and centrifuged for 15 seconds at 10.000 rpm. The flow-through was discarded. DNase I treatment was performed by preparing a mix of DNase I and buffer RDD (10µl DNase I + 70µl buffer RDD per sample). This mix was added onto the membrane of the spin column and incubated for 15 minutes at RT. The column was washed with 350µl of RW1 and the flow-through was discarded. 500µl of buffer RPE was added, centrifuged for 15 seconds at 10.000 rpm and the flow-through was discarded. Then 500µl of 80% ethanol was added and centrifuged for 2 minutes at 10.000 rpm. The spin column was placed in a new 2ml collection tube. The lid of the spin column was opened and the samples were centrifuged at full speed for 5 minutes to dry out the membrane. The spin column was then placed in a new 1.5ml collection tube and 14µl of RNase-free water was added and centrifuged for 1 minute at full speed to elute the RNA. The isolated RNA was kept on ice for further processing or stored at -80°C.

2.2.12 cDNA synthesis

cDNA synthesis was performed by reverse transcription using the Revert Aid First Strand cDNA Kit (Thermo Scientific, Watham, MA). Mix 1 was prepared in a 0.2ml Eppendorf tube on ice according to the RNA concentration and incubated for 5 minutes at 65°C. The tubes were then stored on ice and mix 2 was prepared of which 8µl was added to each reaction. The PCR program included 5 minutes incubation at 25 °C, 60 minutes at 42°C and 5 minutes at 70°C. The PCR reaction was carried out in a Mastercycler gradient PCR machine (Eppendorf, Hamburg, Germany).

mix 1

RNA	1µg (max volume 11µl)
Random Primer	1µl
H_2O (from kit)	up to 12µl

mix 2

5x Reaction buffer	4 µl
RiboLock RNase inhibitor	1 µl
10mM dNTP Mix	2 µl
Revert Aid Transcriptase	1 µl

2.2.13 Real-Time quantitative PCR

Primer sequences were obtained from http://pga.mgh.harvard.edu/primerbank/:

hRPL27 F	5`-ATC GCC AAG AGA TCA AAG ATA A-3'
hRPL27 R	5`-TCT GAA GAC ATC CTT ATT GAC G-3'
hIL36a F	5`-CCA GAC GCT CAT AGC AGT CC-3'
hIL36a R	5`-AGA TGG GGT TCC CTC TGT CTT-3'
hIL36b F	5`-ATG AAC CCA CAA CGG GAG G-3`
hIL36b R	5`-TAA TGC TGC GGC TAA GAG GAG-3`
hIL-36g F	5`-AGG AAG GGC CGT CTA TCA ATC-3'
hIL-36g R	5`-CAC TGT CAC TTC GTG GAA CTG-3'
hIL-36R F	5`-CCG AGG TGT TGG AGA GAC AAT G-3'
hIL-36R R	5`-GGA CCA CAA TGA CAA TCA GCC TC-3'
hIL36RN F	5`-ACT CGG CAT TGA AGG TGC TTT-3'
hIL36RN R	5`-GGG ACC ACG CTG ATC TCT T-3'
hIL-8 F	5`-TTT TGC CAA GGA GTG CTA AAG A-3'
hIL-8 R	5`-AAC CCT CTG CAC CCA GTT TTC-3'
hIL-1β F	5`-CAC GAT GCA CCT GTA CGA TCA-3'
hIL-1β R	5`-GTT GCT CCA TAT CCT GTC CCT-3'
ITGA6 F	5'-TCA TGG ATC TGC AAA TGG AA-3'
ITGA6 R	5'-AGG GAA CCA ACA GCA ACA TC-3'
CD45 F	5'-ACA GCC AGC ACC TTT CCT AC-3'
CD45 R	5'-GTG CAG GTA AGG CAG CAG A-3'

The real-time PCR was performed with cDNA from total cellular RNA or from tissue RNA and a primer pair designed to a fragment of ~150 bp in length flanking an intron-exon border of the desired gene. To quantify the relative expression level of a certain gene, two reaction mixes were prepared. One contained the primer pair targeting the gene of interest, the other contained a primer pair targeting an internal reference gene (RPL27).

The following mixture was prepared on ice in LightCycler 96 or 480 Multiwell detection plates:

qPCR reaction mix	
cDNA	1µl
Primer mix	0.5µl
SYBR Green	5µl
RNase-free H_2O	3.5µl

The primer mix was prepared by adding 7.5µl of 3'-Primer solution (100 □M) and 7.5µl of 5'-Primer solution (100µM) to 185µl RNase-free water.

Real-time quantitative PCR was performed using a Light Cycler 96 and a Light Cycler 480 II (Roche, Basel, Switzerland) and included an initial denaturation at 95°C for 10 min, followed by 40 cycles at 95°C for 30 s, 55°C for 1 min, 72°C for 1 min, and one cycle at 95°C for 1 min, 55°C for 30 s, 95°C for 30 s.
Specificity of the reaction was ensured by surveying the dissociation curve of a given primer pair. Data processing was performed using the LightCycler 480 software provided by the manufacturers according to the guidelines. Data evaluation and statistical analysis followed the rules of the ∧CT method described by the system manufacturer.

2.2.14 Immunohistochemical stainings

To analyze IL-36, IL-8 and IL-1β expression on tissue, 5µm paraffin-embedded AGEP, MPR and healthy control skin sections were deparaffinized and rehydrated. Antigen demasking was performed using pressure cooker heating of the slides for 25 minutes in Target Retrieval solution (DAKO, Glostrup, Denmark). After permeabilization using 0.03% Triton X in PBS for 10 minutes, sections were blocked using 5% BSA in PBS for one hour at room temperature. After washing with PBS, sections were stained overnight at 4°C with 0.5µg/ml goat anti-human IL-36α or 0.5µg/ml goat anti-human IL-36γ (both from R&D, Minneapolis, MN), or 2µg/ml rabbit anti-human IL-8 (LSBio, Seattle, WA) or 10µg/ml rabbit anti-human IL-1β

(Abcam, Cambridge, UK). A goat IgG isotype antibody (R&D, Minneapolis, MN) and a rabbit IgG isotype antibody (Abcam) at corresponding concentrations were used as controls. Slides were washed with PBS and a goat-anti-rabbit secondary antibody (Southern Biotech, Birmingham, USA) was added and incubated for 1 hour at room temperature. Slides were washed with PBS and mounted with an Avidin-Biotin-complex (Vector Laboratories, Peterborough, UK). After 45 minutes of incubation, slides were washed with PBS, and AEC (3-amino-9-ethylcarbazole) HRP substrate (Vector Laboratories) was added to produce a red reaction product. After washing, a counterstain with hematoxylin was performed. The sections were mounted in Faramount mounting medium (DAKO) and imaged by using an Aperio ScanScope (Leica Biosystems, Wetzlar, Germany).

2.2.15 Immunofluorescence stainings

To analyze the cellular source of IL-36 expression cells in tissue, 5µm paraffin-embedded AGEP sections were deparaffinized and rehydrated. Antigen demasking was performed using pressure cooker heating of the slides for 25 minutes in Target Retrieval solution (Dako). After permeabilization using 0.03% Triton X in PBS for 10 minutes, sections were blocked using 5% BSA in PBS for one hour at room temperature. Sections were then stained overnight at 4 °C with a) 0.5µg/ml goat anti-human IL-36α (R&D), together with either 20µg/ml mouse anti-human CD3 (Dako) or 20µg/ml mouse anti-human CD68 (Dako), or b) with 0.5µg/ml goat anti-human IL-36γ (R&D), together with either 20µg/ml mouse anti-human CD3 (Dako) or 20µg/ml mouse anti-human CD68 (Dako) or 20 µg/ml mouse anti-human Myeloperoxidase (Dako). Goat IgG isotype (R&D, Minneapolis, MN) and mouse IgG isotype (Abcam) antibodies at corresponding concentrations was used as isotype-specific controls. After washing with PBS, samples were incubated for 60 min at room temperature with conjugated secondary antibodies as follows: Alexa Fluor® 488 Goat Anti-Mouse IgG (Life Technologies, Carlsbad, CA) and Alexa Fluor® 647 Donkey Anti-Goat IgG (Abcam). Nuclear staining was performed at the same time using 4',6-diamidino-2-phenylindole (DAPI, Thermo Fisher Scientific, Carlsbad, CA). Slides were mounted with Fluorescence Mounting Medium (Dako) and analyzed with a Widefield BX61 fluorescence microscope (Olympus, Tokyo, Japan) using the Analysis Pro software (Soft Imaging Systems, Münster, Germany) and the

Axio Imager 2 Fluorescence Microscope (Zeiss, Oberkochen, Germany) using the ZEN software (Zeiss).

2.2.16 Enzyme Linked Immunosorbent Assay (ELISA)

AGEP, MPR and healthy control serum samples were analyzed for the presence of cytokines by ELISA. Human IL-6, IL-17A and IFN-γ were determined using ELISA kits from R&D Systems, and human TNF and IL-8 using ELISA kits from Biolegend (San Diego, CA, USA).

ELISA plates were coated with 70µl of capture antibodies diluted in PBS and incubated overnight at RT. The next day, the plate was washed 2x with PBS+Tween-20 and 100 µl of reagent diluent (PBS + 5% BSA) were added to each well. After one hour of incubation the wells were washed 2x with PBS-T and 70µl of samples, standard, blank and negative control were added to the according wells and incubated for two hours at RT. The samples were discarded and the wells were washed 3x with PBS-T. As a next step, 70µl of the detection antibodies, diluted in reagent diluent, were added to the wells and incubated for two hours at RT. After washing the wells 3x with PBS-T, 70µl of Strepatavidin-HRP, diluted in reagent diluent, were added to each well and incubated for 30 minutes at RT. The wells were then washed 5x with PBS-T and 70µl of substrate was added to each well and incubated at RT in the dark until blue colour emerged. The reaction was then stopped by adding 35µl of 2N H_2SO_4 to each well. Optical densities were measured by the the Cytation 3 ELISA reader at a wavelength of 450 nm.

Human IL-36α and IL-36γ were detected using ELISA kits from Cusabio (Hubei, China). The ELISA assays were performed according to the manufacturer's instructions. Optical densities were measured by the the Cytation 3 ELISA reader at a wavelength of 450 nm.

2.2.17 Enzyme Linked Immuno Spot Assay (ELISpot)

To perform ELIspot analysis, PVDF-plates (Merck Millipore, Billerica, MA) were pre-wetted by 50µl 70% ethanol per well for 2 minutes. After washing with PBS, plates were coated with 2µg/ml anti-human IL-36γ (Peprotech, Rocky Hill, NJ) or 15µg/ml

anti-human IL-1β (Mabtech, Nacka Strand, Sweden) per well overnight. After removing excess antibody and washing with PBS, a blocking step was performed using RPMI medium containing 10% FBS. After one hour of incubation, the medium was removed and the cell suspensions ± stimuli were added and incubated at 37°C for the indicated time (Fig. 5). After washing with PBS, 2µg/ml biotinylated anti-IL-36γ (Peprotech) or 1µg/ml biotinylated anti-IL-1β antibody was added to the wells and incubated for 2 hours at room temperature, followed by one-hour incubation with Streptavidin-ALP (Mabtech). For detection of the protein, BCIP/NBT substrate mix (Promega, Dübendorf, Switzerland) in AP buffer was added and developed until distinct spots emerged. Data was analyzed using the AID ELISpot Reader (AID GmbH, Strassberg, Germany).

2.2.18 Cytometric bead assay

The experiment has been performed by Alaz Özcan Özge from the research group of Prof. Dr. Onur Boyman.

Cytometric bead assay (CBA) was performed using the LEGENDplex Kit (Biolegend, San Diego, CA) and experiments were performed in a V bottom plate. As a first step, 25µL of Matrix B were added to the standard wells and 25 µL of Assay Buffer to sample wells. The standards were prepared and 25 µL of each standard was added to the according wells. Then 25µL of each serum sample (undiluted) was added form to the according wells. Finally, 25µL of mixed beads to were added to all wells, followed by 25µL detection antibodies. The entire plate was covered with aluminum foil to protect the plate from light and shaked at 600 rpm on a plate shaker for 2 hours at room temperature. Without washing the plate, 25µL of SA-PE were added to each well. The entire plate was packed again with aluminum foil and shaked at 600rpm on a plate shaker for 30 minutes at room temperature. The plate was then centrifuged at 1,000 x g for 5 minutes, using a swinging bucket rotor with microplate adaptor. The supernatant was removed using a multichannel pipette and 200µL of 1x Wash Buffer were added to all wells. The beads were resuspended by shaking on a plate shaker for 1 minute. The plate was then centrifuged again at 1,000 x g for 5 minutes, using a swinging bucket rotor with microplate adaptor and the supernatant was removed. 200µL of 1x Wash Buffer were then added to each well and the beads were resuspended by pippeting. The

samples were read on a FACS Canto II flow cytometer (BD) with FACS DIVA software (BD). Data were compiled using LEGENDplexTM Data Analysis Software.

2.2.19 Whole Exome Sequencing

Experiments Experiments have been performed by Alexander Navarini and colleagues in London, UK.

DNA was extracted from AGEP and healthy control PBMC using the QIAamp DNA mini kit (Qiagen, Hilden Deutschland) according to manufacturer's instructions. Genomic DNA was fragmented with ultrasonic shearing to fragments of about 150-200bp. End repair, adenylation of the 3' end and adaptor ligation was performed using the Agilent Sure SelectXT kit according to manufacturer's instructions. Biotinylated RNA (ribonucleic acid) oligos were hybridized in order to select the exomic sequences using the Agilent SureSelectXT All exons V5 kit according to manufacturer's instructions. Sequencing was carried out on an Illumina HiSeq device using 125bp paired-end sequencing. The sequence reads obtained were aligned to the reference human genome (hg19) using BWA sequence aligner. Capture efficiency coverage and quality score were determined with R and sequence recalibration was performed as per GATK (Genomic Analysis Tool Kit https://www.broadinstitute.org/gatk/) guidelines.

2.2.20 Statistical analysis

Differences between groups were assessed using one-way Anova followed by Turkey's post-test. Differences were considered significant when: *$p \leq 0.05$, ** $p \leq 0.01$, *** $p \leq 0.001$ and **** $p \leq 0.0001$.

3 Results

Culprit drug specific IL-36 overexpression in Acute Generalized Exanthematous Pustulosis

Barbara Meier, MD [a], Laurence Feldmeyer, MD, PhD [b], Dragana Jankovic, PhD [a], Takashi K. Satoh, MD, PhD [a], Mark Mellett, PhD [a], Daniel Yerly, PhD [c], Alexander Navarini, MD, PhD [a], Riichiro Abe, MD, PhD [d], Nikhil Yawalkar, MD [b], Chung Wen-Hung [e], Emmanuel Contassot, PhD [a,#], Lars E. French, MD [a,#]

[a] Department of Dermatology, University Hospital, Zürich, Switzerland

[b] Department of Dermatology, Inselspital, Bern University Hospital, University of Bern, Switzerland

[c] Department of Rheumatology, Clinical Immunology and Allergology, Inselspital, Bern University Hospital, University of Bern, Switzerland

[d] Division of Dermatology, Niigata University Graduate School of Medical and Dental Sciences, Niigata, Japan

[e] Department of Dermatology, Drug Hypersensitivity Clinical and Research Center, Chang Gung Memorial Hospital, Taipei and Linkou, Taiwan

[#] Co-senior authors

This manuscript in preparation will be shortly submitted for publication. Barbara Meier has performed 90% of all experiments in this manuscript including the experimental design and has been actively involved in the design and the writing of the manuscript.

3.1 Enhanced IL36 and IL-8 gene expression in lesional skin of AGEP patients

In a first unbiased approach, we performed gene expression profiling using Affymetrix Human Exon 1.0 ST chips. Total RNAs were extracted from lesional skin from patients suffering from AGEP (n=8), from patients with maculo-papular rash (MPR, n=6), and from healthy skin from individuals undergoing plastic surgery (n=7). The hierarchical clustering of genes differentially expressed in AGEP, MPR and healthy skin biopsies revealed a perfect segregation of these three conditions based on the gene expression profile of individual samples and the magnitude of change in gene expression (Fig.10A and Suppl. Table 3). IL-8 has been previously reported to be produced by drug-specific T cells in the skin of AGEP patients [185] and in accordance with this, *IL-8* expression was significantly upregulated in AGEP skin biopsies analyzed here when compared to healthy skin (ratio=2.25, p=0.01; Suppl. Table 4) but also when compared to MPR (ratio=2.24, p=0.008; Suppl. Table 6). Interestingly, the IL-36γ gene (*IL1F9*) was also found to be significantly overexpressed in AGEP skin biopsies when compared to healthy skin (ratio=3.06, p=0.0006; Suppl. Table 4) and MPR (ratio=2.54, p=0.005; Suppl. Table 5). RNAseq analysis of a second, independent series of AGEP (n=9) and MPR (n=8) patient lesional skin biopsies confirmed the overexpression of the *IL-36γ* gene (ratio=3.12; p=0.02) in AGEP (Fig.10B). Although not reaching statistical significance (p=0.12), RNAseq analysis also revealed an overexpression of IL-8 (ratio=2.31) in AGEP skin. We then confirmed the observed upregulation of *IL-36γ* and *IL-8* by quantitative PCR in AGEP (n=16) and MPR (n=16) skin biopsies. In accordance with the gene expression array and RNAseq data, expression of *IL-36γ* was found to be significantly upregulated (32-fold, p<0.0001) in AGEP skin biopsies when compared to MPR (Fig. 1C). In addition to *IL-36γ*, *IL-36α* (15-fold, p<0.0001) and *IL-36β* (28-fold, p<0.0001) expression were also upregulated in AGEP skin when compared to MPR. The expression of *IL-36RN* was also found to be higher (4.5-fold, p<0.0001) in AGEP skin as compared to MPR, whereas *IL-36R* expression was similarly expressed in both diseases. As previously reported, levels of IL-8 mRNA were higher in the lesional skin of AGEP patients than in MPR patients (127-fold, p<0.0001).

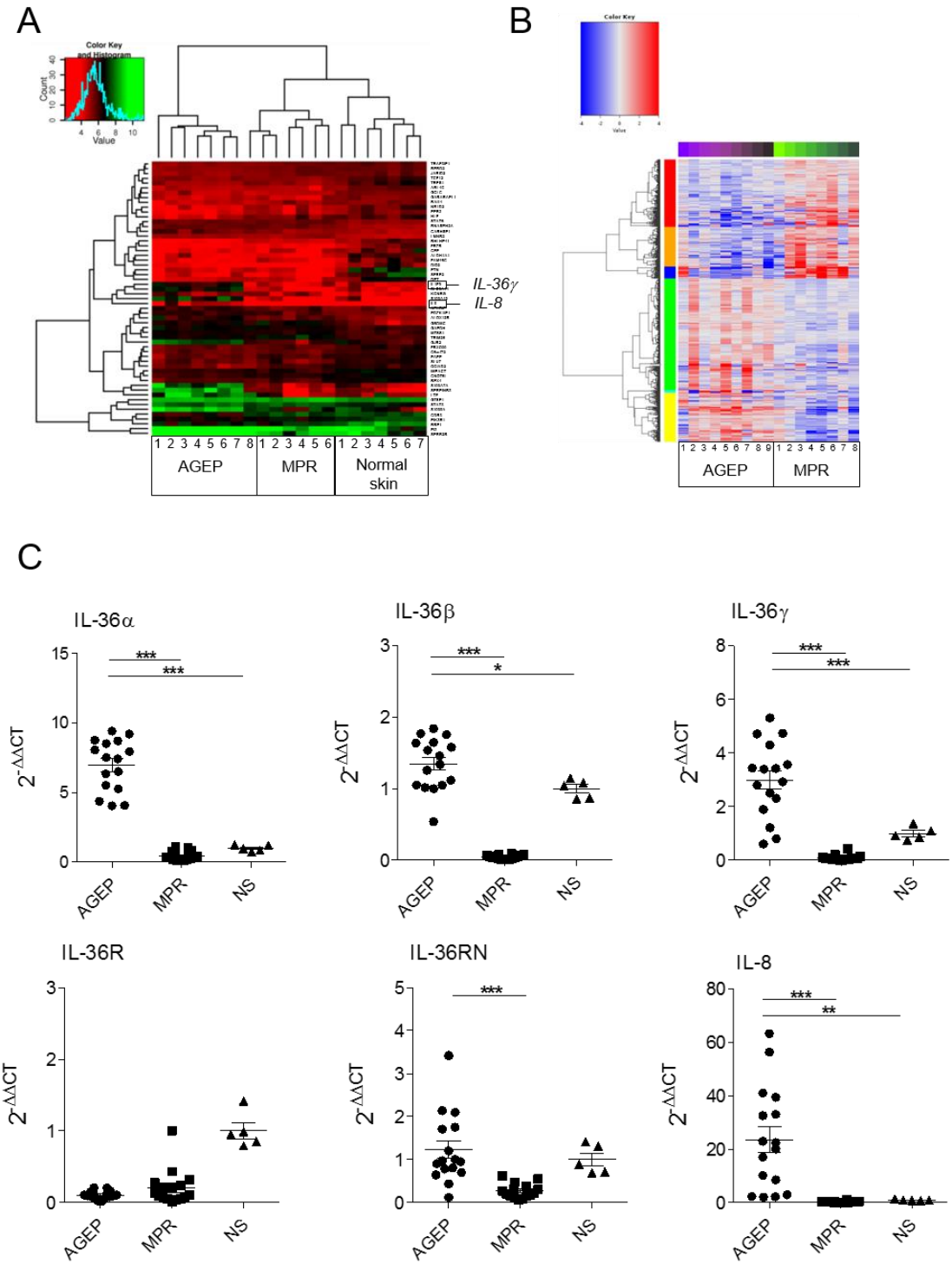

Fig. 10. IL-36 and IL-8 gene overexpression in AGEP lesional skin. *Gene expression hierarchical clustering in lesional skin biopsies from patients suffering from AGEP and MPR analyzed using (A) Affymetrix Human Exon 1.0 ST chips or (B) RNAseq technology. (C) Quantitative RT-PCR analysis of IL-36α, IL-36β, IL-36γ, IL-36R, IL-36RN and IL-8 in lesional skin biopsies of patients suffering from AGEP (n=16), MPR (n=16) and normal skin (NS; n=5). **** p<0.0001. The patient cohorts studied in (A), (B) and (C) were independent and all recruited in the Dermatology Department of the University Hospital of Zürich (patients no. 1-19).*

3.2 IL-36α and IL-36γ cytokines are highly expressed in the lesional skin of AGEP patients

Unlike IL-36β, IL-36α and γ were found to be unique for AGEP compared to MPR and healthy skin (Suppl. Table 3). Therefore, we further analyzed their expression and tissue distribution. To this end, we labeled AGEP and MPR lesional skin biopsies with antibodies to both cytokines. IL-36α and γ were found to be highly expressed in pustular and peri-pustular regions of AGEP skin biopsies (Fig 11A). Both keratinocytes and dermal immune cells infiltrating pustular areas of the epidermis were found to produce IL-36α and γ (Fig. 11B). In contrast, IL-36γ was weakly expressed in MPR skin biopsies and IL-36α was barely detectable (Fig. 11A). In AGEP lesional skin biopsies, IL-36γ was found to be predominantly expressed by keratinocytes in the epidermis and by immune cells infiltrating the dermis in pustular areas (Fig. 11B). Also, IL-36γ staining intensity was particularly important in non-pustular areas of the epidermis surrounding the pustules in AGEP. As previously reported [211], IL-36γ was expressed in pustules from patients suffering from generalized pustular psoriasis (GPP) and, like in AGEP biopsies, IL-36γ was the predominant form in the epidermis (Fig. 11B).

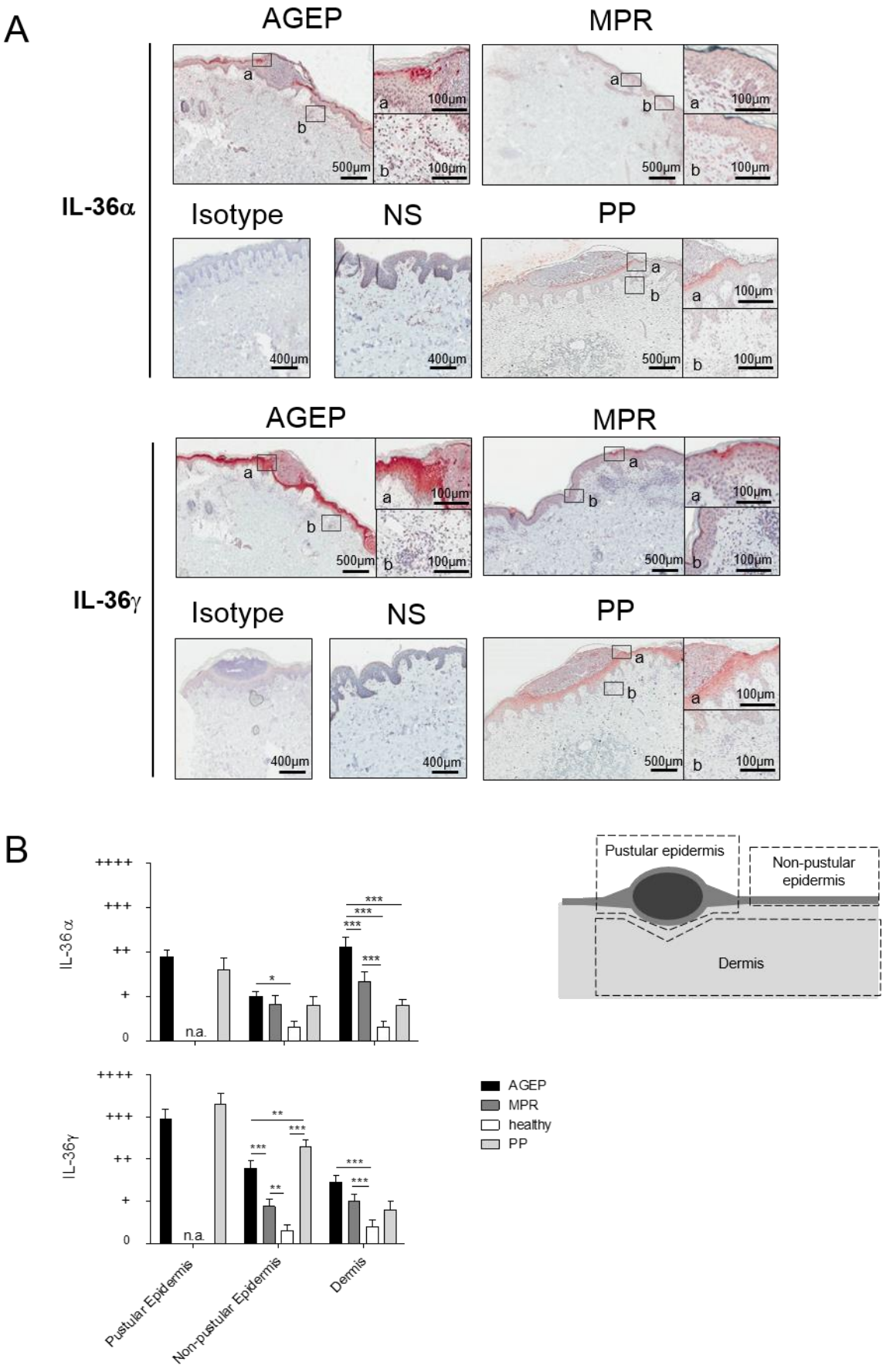
A
AGEP
MPR
IL-36α
Isotype
NS
PP
AGEP
MPR
IL-36γ
Isotype
NS
PP
a
b
100µm
500µm
400µm
B
IL-36α
IL-36γ
++++
+++
++
+
0
n.a.
*
**
***
Pustular Epidermis
Non-pustular Epidermis
Dermis
AGEP
MPR
healthy
PP
Pustular epidermis
Non-pustular epidermis
Dermis

Fig. 11. IL-36α and IL-36γ are overexpressed in pustular regions of AGEP lesional skin biopsies. *(A) Immunohistochemical analysis of lesional skin biopsies revealed that IL-36α and IL-36γ are overexpressed at the site of pustules in AGEP and PP controls while, in MPR, IL-36α and IL-36γ were weakly expressed. Representative pictures of 18 AGEP, 10 PP and 18 MPR cases are shown. Neither IL-36α, nor IL-36γ were detectable in normal skin (NS) from healthy donors. (B) Semi-quantitative evaluation of IL-36α and IL-36γ labeling by immunohistochemistry in the pustular epidermis, non-pustular epidermis, and dermis of lesional skin biopsies from patients with AGEP (n=18; patients no. 5, 6, 8, 10, 11, 13-17, and 21-28), PP (n=10), MPR (n=18) and normal skin (NS) from healthy donors (n=5). Expression levels were qualified as very strong (++++), strong (+++), moderate (++), weak (+) or absent (0). *p<0.05; **p<0.01; *** p<0.001; **** p<0.0001.*

To identify which cell types release IL-36α and γ in AGEP patients' skin, we co-labeled AGEP biopsy sections with antibodies to IL-36α and γ and antibodies against CD68 to identify macrophages, and against CD3 to identify T-cells (Fig. 12). IL-36α was predominantly expressed by $CD68^+$ macrophages (41.17%±4.71 of positively labeled cells) and to a lesser extent by epidermal cells (keratinocytes) and $CD3^+$ T cells (27.33%±2.17 and 22.33%±2.39 of positively labeled cells respectively). IL-36γ was predominantly expressed by epidermal cells (keratinocytes) and $CD68^+$ macrophages (44.08%±4.47 and 43.17%±3.31 of positively labeled cells, respectively) and to a lesser extent by $CD3^+$ T cells (15.17%±1.26 of positively labeled cells). In contrast, IL-36α and IL-36γ were not expressed by neutrophils present in the pustular area (Suppl. Fig. 1).

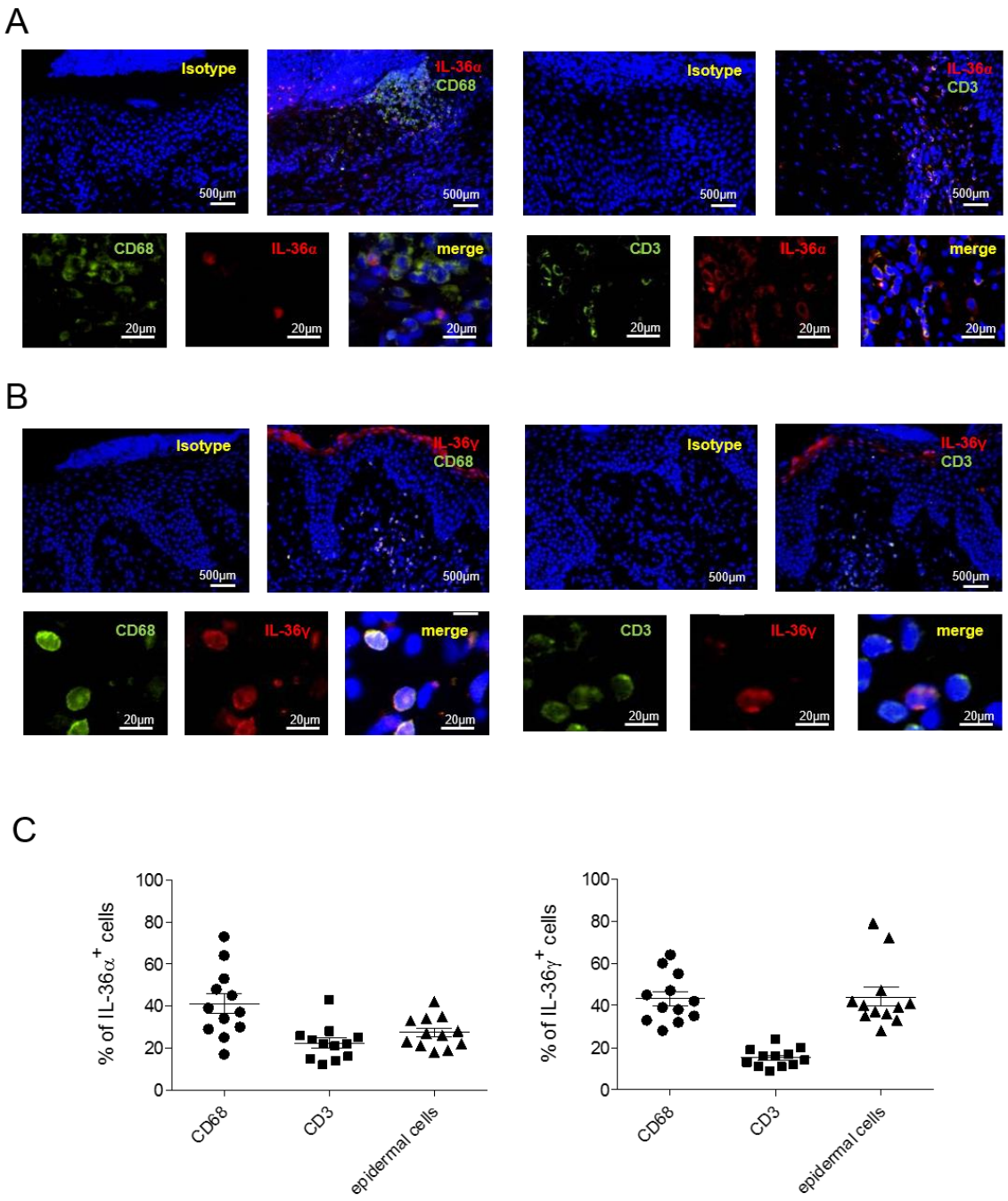

Fig. 12. IL-36 is expressed by keratinocytes and immune cells in AGEP skin. *Pustule-containing sections of AGEP skin samples were co-labeled with antibodies to CD68 (green), CD3 (green) and IL-36α (red) (A) or IL-36γ (red) (B). The percentage of epidermal cells (keratinocytes), CD68 and CD3-labeled cells among the IL-36α or IL-36γ-labeled cells was determined (C). Cell nuclei appear in blue (DAPI). The mean±SD of 12 examined patients is shown (patients no. 8-10 and 20-28).*

3.3 Culprit drugs specifically induce rapid monocyte IL-36γ secretion in AGEP

Since our immunofluorescence analyses of AGEP biopsies suggested that, in addition to keratinocytes, immune cells may also represent an important source of local IL-36γ in the skin, we assessed whether PBMC taken from AGEP patients number 8, 9 and 20 at more than 6 months after the CADR – i.e. when in complete remission - were still able to respond directly to the causative drug. To this end, PBMC from patients having experienced AGEP or MPR were exposed in ELISpot plates to the culprit drug or an irrelevant control drug. The number of IL-36γ$^+$ spots - indicative of PBMC producing IL-36γ - were then counted after 1, 2, 4, 6 and 8 hrs. IL-36γ release was detected in PBMC from AGEP patients already after 1 hr (1.7-fold more spots than control drug, $p<0.001$) of culprit drug exposure and reached a plateau after 4 hrs (2.7-fold more spots than control drug, $p<0.001$; Fig. 13A, left panel), whereas no increase in IL-36γ production was observed with an irrelevant control drug (Fig. 13A, right panel). Furthermore, and in contrast, the culprit drug did not induce IL-36γ secretion in MPR as revealed by comparable IL-36γ levels upon culprit-, control-drug and vehicle exposure. Similarly, none of the drugs used were able to induce IL-36γ secretion in PBMC from healthy blood donors when compared to vehicle (Fig 13A). Since immunofluorescence analyses of AGEP skin lesions revealed that macrophages and, to a lesser extent, T cells are possible sources of IL-36, we sorted CD14$^+$ (monocytes) and CD3$^+$ cells (T cells) from patients' PBMC and exposed them to culprit or control drug to evaluate IL-36γ secretion by ELISpot (Fig. 13B). Whereas the control drug did not induce Il-36γ secretion in PBMC or in sorted CD14$^+$ and CD3$^+$ cells, the culprit drug was able to induce IL-36γ secretion in sorted CD14$^+$ cells at levels similar to those observed with total PBMC. In contrast, the culprit drug was not able to induce IL-36γ secretion in CD3$^+$ PBMC. Two out of the three tested patients were also analysed for the presence of a mutation in the IL-36RN gene (Suppl. Table 2). In both cases, no mutation could be determined. These results suggest that PBMC from patients having experienced AGEP are able to respond directly and specifically to the causative drug and that monocytes/macrophages are an important source of IL-36γ production in response to culprit drug exposure, independently of an IL36RN mutation.

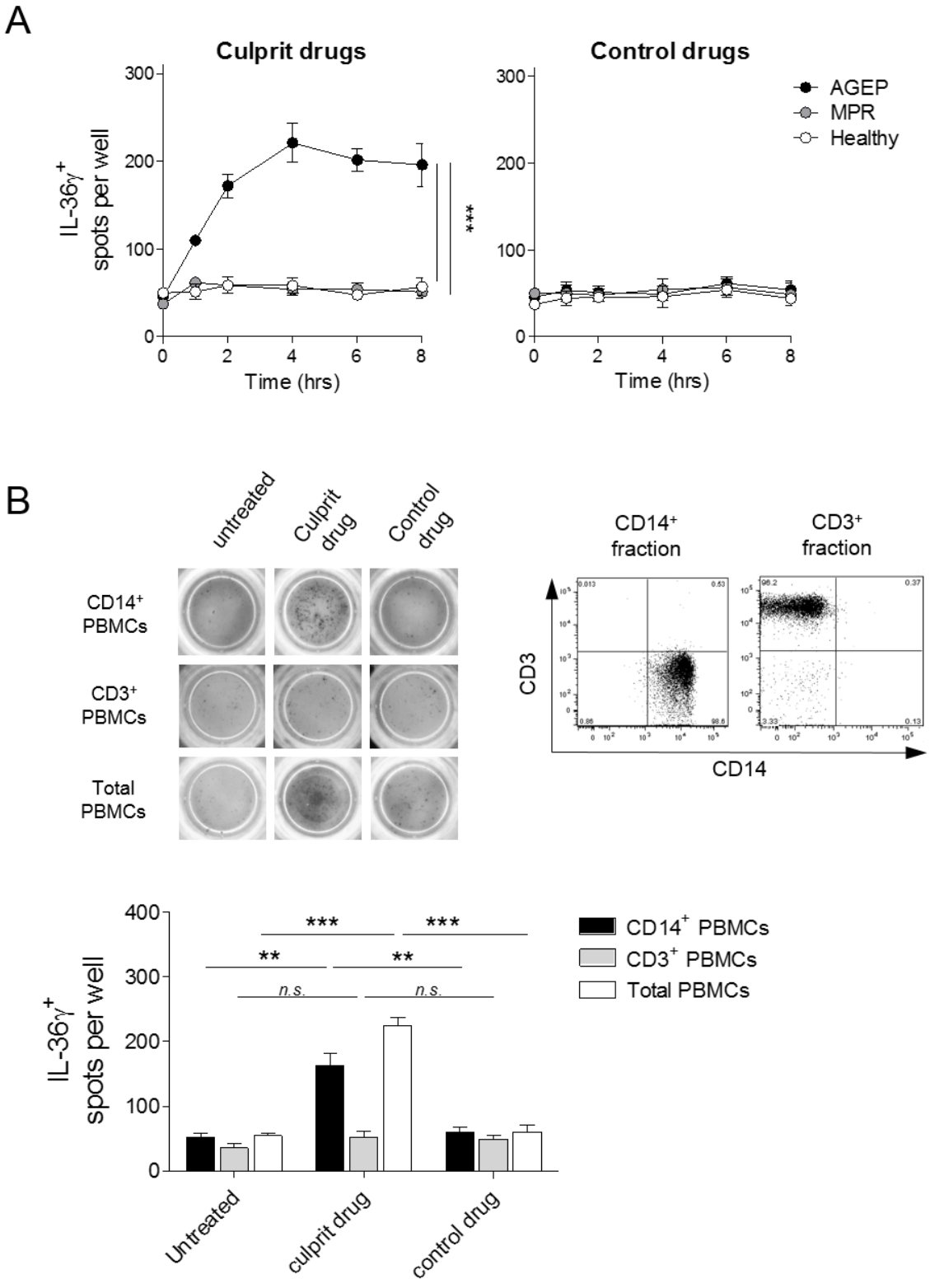

Fig. 13. PBMC and monocytes taken from AGEP patients more than 6 months after the ADR selectively secrete IL-36γ in response to culprit drug exposure. *(A) PBMC from AGEP or MPR patients as well as healthy donors were cultured in IL-36γ ELISpot plates for 8 hrs in presence of the culprit drug (left panel) or a control drug (right panel). The number of spots was counted 1, 2, 4, 6*

*and 8 hrs after drug exposure. The means±SD of 3 different AGEP patients (no. 8, 10 and 21), 3 MPR patients and 3 healthy blood donors are shown. ***p<0.001. (B) CD14^{+} monocytes and CD3^{+} T cells were isolated from AGEP blood with a purity of >96% and were cultured in IL-36γ ELISpot plates in presence of the culprit drug or a control drug and compared to total PBMC. The number of spots was counted 8 hrs after drug exposure. The mean±SD of 3 different patients (patient no. 8, 9 and 10) is shown. *p<0.05.*

3.4 IL-36 can be induced by culprit drugs in both keratinocytes and PBMC from patients having experienced AGEP

By immunolabeling both keratinocytes and macrophages were shown to be positively labeled for IL-36α and γ in pustular areas of AGEP biopsies. To assess a possible cross-talk between macrophages and keratinocytes, and the relative contribution of each cell type to drug-induced IL-36 secretion, we performed co-culture experiments using autologous hair follicle-derived keratinocytes and PBMC from three patients having experienced AGEP but in remission at the time of blood and hair collection (at least 6 months after disappearance of symptoms, patients 8, 9 and 20). Keratinocytes and PBMC were cultured either alone or together using a transwell culture system (Suppl. Fig. 2A). To formally exclude the contamination of one cell type by the other, we performed qPCR using primers to CD45 (PBMC marker) and Integrin Subunit Alpha 6 (ITGA6, keratinocyte marker) on both PBMC and keratinocytes after a 6hr-co-culture (Suppl. Fig. 3). When keratinocytes and PBMC were each cultured alone, only PBMC showed elevated IL-36γ mRNA levels after exposure to the culprit drug. Interestingly, both keratinocytes and PBMC showed culprit drug-specific IL-36γ gene expression when cultured together. In contrast, keratinocytes exposed alone to the culprit drug exhibited increased IL-36α gene expression (Suppl. Fig. 2B). This increase in gene expression was further augmented in keratinocytes co-cultured with PBMC but, nonetheless, remained modest when compared to IL-36γ. Indeed, the highest levels of IL-36α mRNA measured in keratinocytes corresponded to the lowest gene expression levels measured in PBMC (about 10-fold less when compared to IL-36γ). In this *in vitro* co-culture model, the addition of soluble IL-36Ra did not reduce IL-36 expression, suggesting that, at the analyzed time point, there is no auto- or paracrine amplification and/or induction of IL-36 gene expression by IL-36 released by PBMC

or keratinocytes. Taken together, these results indicate that, in culprit drug-induced responses of patient-derived keratinocytes and monocytes, IL-36γ is the predominant form of IL-36 induced. Furthermore, in response to culprit drug exposure, IL-36 is expressed directly by PBMC and indirectly by keratinocytes.

A

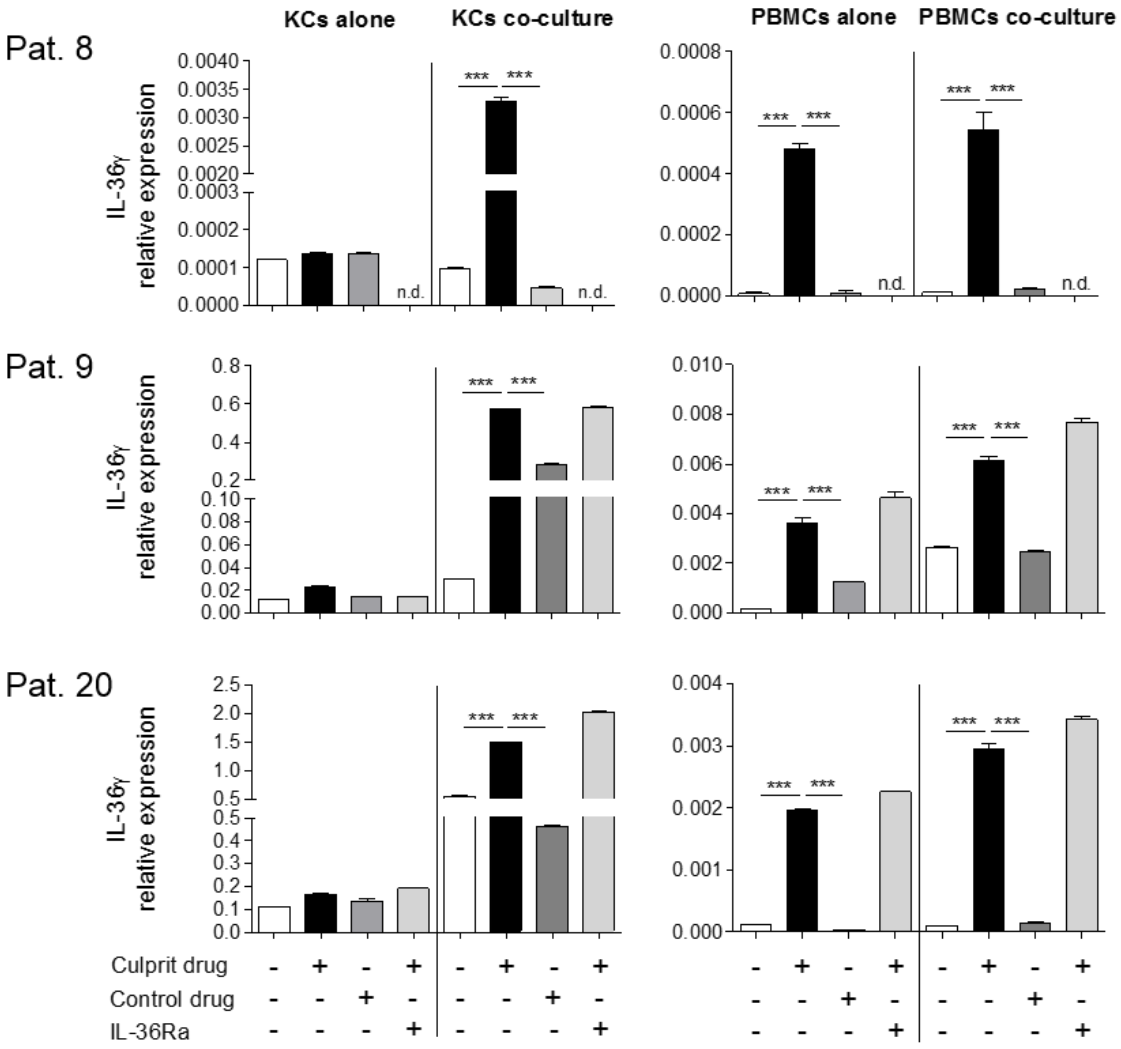
KCs alone
KCs co-culture
PBMCs alone
PBMCs co-culture
Pat. 8
Pat. 9
Pat. 20
IL-36γ
relative expression
***
n.d.
Culprit drug
Control drug
IL-36Ra

B

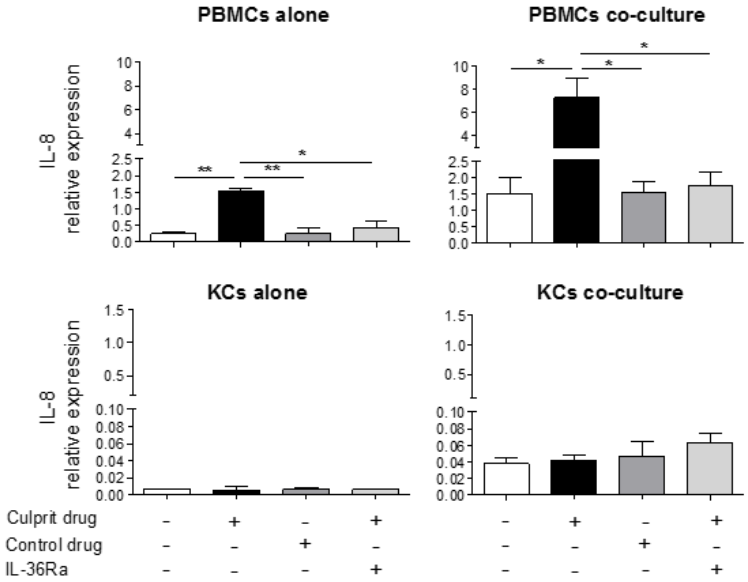
PBMCs alone
PBMCs co-culture
KCs alone
KCs co-culture
IL-8
relative expression
**
*
Culprit drug
Control drug
IL-36Ra

Fig. 14. Culprit drugs specifically induce IL-36 in PBMC and keratinocytes and IL-8 in PBMC in a co-culture system. *Autologous PBMC and keratinocytes (KC) from patients having experienced AGEP but in remission at the time of blood and hair collection were cultured either alone or together in a transwell system allowing for soluble factor-mediated interactions. Patients' cells were exposed to the culprit drug (Amoxicillin 1mg/ml, patient 8; Letrozole 100nM, patient 9; Vancomycin 500µg/ml, patient 20) or a control drug (Metamizole 100µg/ml, patient 8; Carbamazepine 10□g/ml, patient 9; Amoxicillin 1mg/ml, patient 20) in presence or absence of IL-36RA (1µg/ml). After 6 hrs of culture, RNA was extracted from KC (left panels) and PBMC (right panels) to measure IL-36γ mRNA levels (A). Relative IL-36γ expression in KC and PBMC cultured either alone or in co-culture as indicated and exposed to the culprit drug or a control drug in presence or absence of IL-36Ra are shown for each tested patient. Means±SD of 3 replicates are shown. (B) Quantitative PCR analysis of IL-8 gene expression in PBMC (upper panels) and KC (lower panels) cultured either alone or in co-culture as indicated and exposed to the culprit drug or a control drug in the presence or absence of IL-36Ra. Gene expression reported as $2^{-\Delta CT}$, which represents the target gene expression relative to the reference gene (RPL27). Mean±SD of the 3 tested patients is shown. The figure illustrates a representative experiment that was repeated 3 times for each patient. *p<0.05; **p<0.01; ***p<0.001.*

3.5 IL-8 is selectively produced by patients' PBMC and induced by IL-36

IL-8 has previously been reported to be a key chemokine in AGEP physiopathology and has been shown to be inducible by IL-36 [70, 212]. Immunohistochemistry analysis confirmed that IL-8 was expressed by cells of the infiltrate in pustular regions of AGEP skin (Suppl. Fig. 4). Herein, using the keratinocyte/PBMC co-culture model described above, we assessed whether IL-36 could promote IL-8 gene expression, and if so, which cell type could produce IL-8 in response to IL-36. We observed that high levels of IL-8 gene expression (4.6-fold increase over control-drug exposure, $p<0.05$) occurred exclusively in patients' PBMC co-cultured with autologous keratinocytes selectively in response to culprit drug exposure (Fig. 14B). Interestingly, upregulation of IL-8 gene expression in AGEP patients PBMC was abrogated by IL-36Ra. IL-8 gene expression was only weakly induced by culprit drugs in isolated PBMC cultures, and barely detectable in isolated keratinocyte cultures. Taken together, these results indicate that PBMC are the main source of culprit drug induced IL-8 production, and that IL-8 gene expression in PBMC is dependent on PBMC- and/or keratinocyte-derived IL-36.

3.6 IL-1β induces IL-36γ expression in human monocytes and keratinocytes

To determine whether other inflammatory cytokines could regulate IL-36γ expression, human keratinocytes and peripheral blood monocytes were treated with recombinant cytokines for 6 hours before cells were harvested for RNA isolation. As already shown by others [81], recombinant TNF induced a 5.8-fold increase of IL-36γ expression in keratinocytes as compared to untreated keratinocytes ($p<0.001$) (Fig 15A) and a 3.4-fold increase in monocytes as compared to untreated monocytes ($p>0.05$) (Fig 15B), however not statistically significant. Recombinant IFNγ and IL-8 had no impact on IL-36γ expression in both cell types. Intriguingly, IL-1β induced a dramatic increase in IL-36γ expression in both keratinocytes and monocytes with, respectively, a 12-fold ($p<0.001$) and 57-fold ($p<0.001$) upregulation when compared to untreated cells (Fig 15A and 15B).

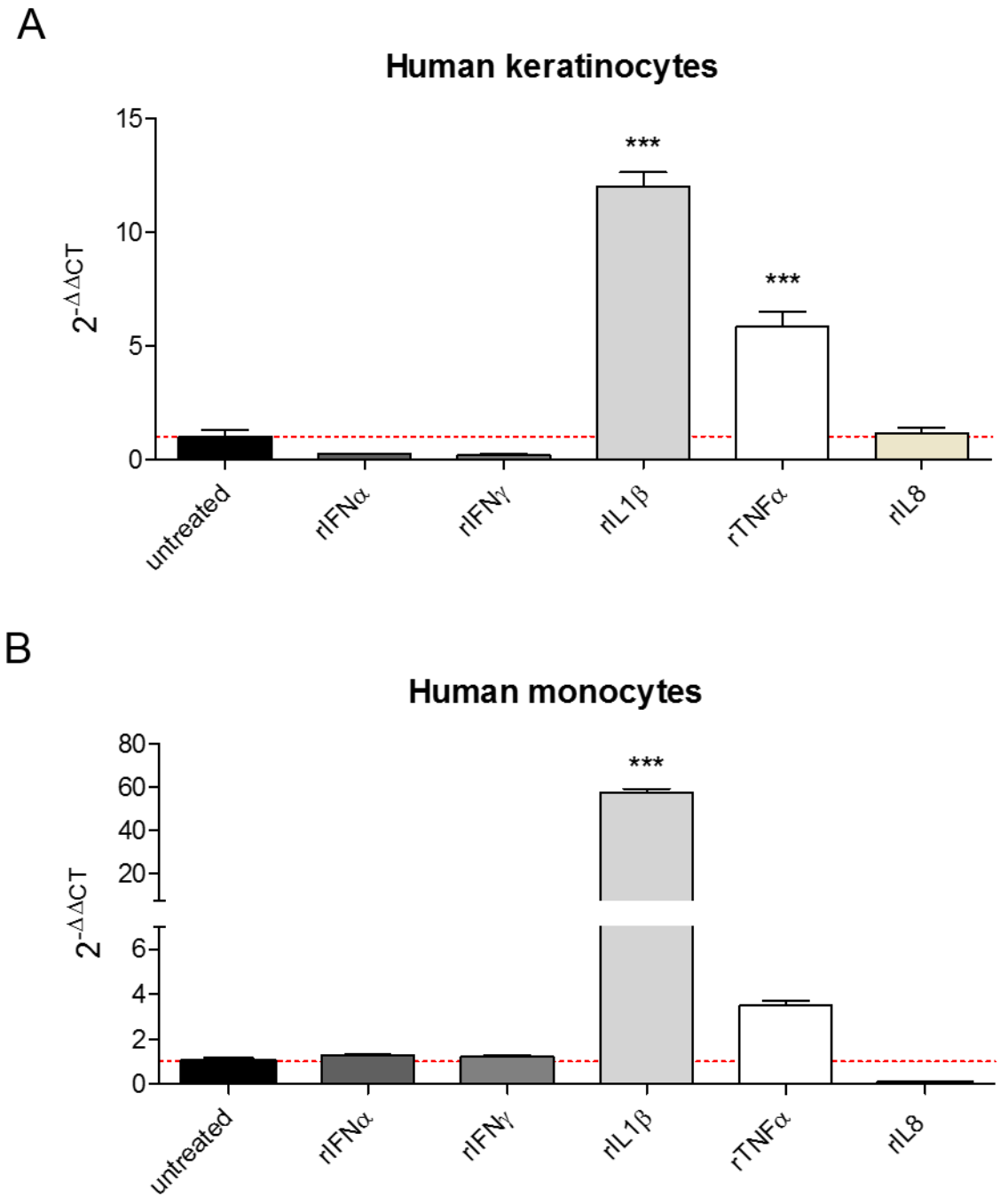

Fig. 15. Regulation of IL-36γ in human cells by inflammatory cytokines. *Healthy human keratinocytes (A) and human monocytes from peripheral blood (B) were treated with 100g/ml recombinant Interferon α (rIFNα), 100ng/ml recombinant Interferon (rIFNγ), 100ng/ml recombinant Interleukin-1β (rIL-1β,) 100ng/ml recombinant tumor necrosis factor α (rTNF) 100ng/ml recombinant Interleukin-8 (rIL-8). Cells were harvested after 6h inculation at 37°C and RNA was isolated, followed by cDNA synthesis and qPCR with primers to the IL-36γ gene. RPL27 served as housekeeping gene. Results are normalized to untreated cells ($2^{-\Delta\Delta CT}$). *** p≤0.0001.*

3.7 IL-36γ, IL-8, IL-6 and IL-1β can be found at high levels in the blood of AGEP patients during acute reaction.

We next measured cytokines in the serum of AGEP and MPR patients as well as healthy blood donors by ELISA and by CBA. While IFNγ, TNF and IL-17A did not reveal any difference between all three conditions, IL-6 and IL-8 levels were significantly higher in the serum of AGEP patients when compared to MPR and healthy donors (Fig. 16). In Swiss, Taiwanese and Japanese patient cohorts, IL-36γ was found to be higher in the serum of AGEP and MPR patients when compared to healthy donors whereas IL-36α levels were not different. Surprisingly, IL-36γ serum levels were not statistically different in AGEP and MPR (Fig. 16A). Additionally, as we could show that IL-1β is a positive regulator of IL-36γ, we measured IL-1β levels in the serum of AGEP, MPR and healthy donors using cytometric bead assay (CBA). Strikingly, we found elevated levels of IL-1β in AGEP when compared to MPR and healthy serum, even though not statistically significant ($p>0.05$). Moreover, when comparing IL-23 levels in AGEP serum to serum of MPR or healthy individuals, we found elevated levels of the cytokine but without statistical significance (Fig. 16B).

A

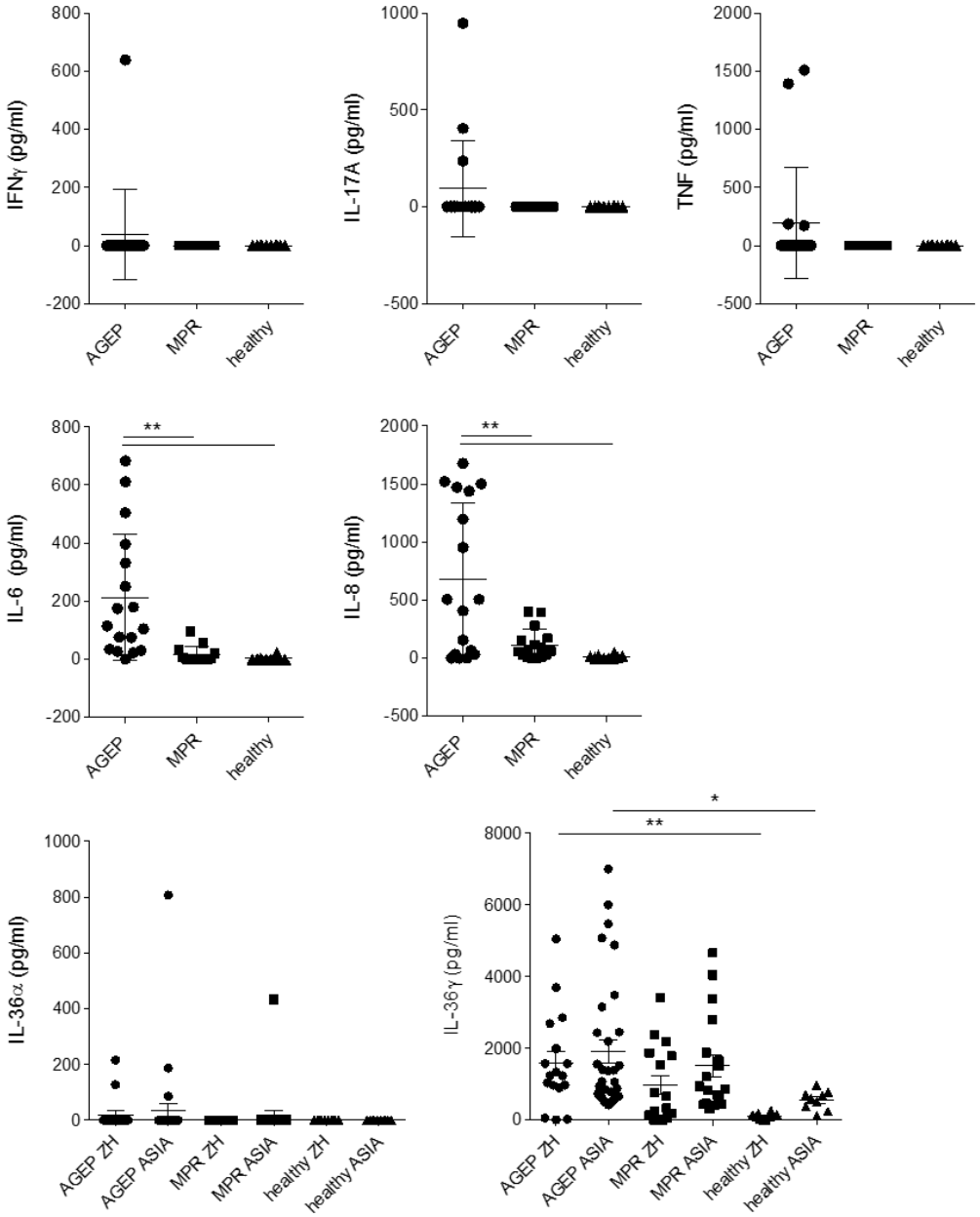
IFNγ (pg/ml)
IL-17A (pg/ml)
TNF (pg/ml)
IL-6 (pg/ml)
IL-8 (pg/ml)
AGEP
MPR
healthy
**
IL-36α (pg/ml)
IL-36γ (pg/ml)
*
AGEP ZH
AGEP ASIA
MPR ZH
MPR ASIA
healthy ZH
healthy ASIA

B

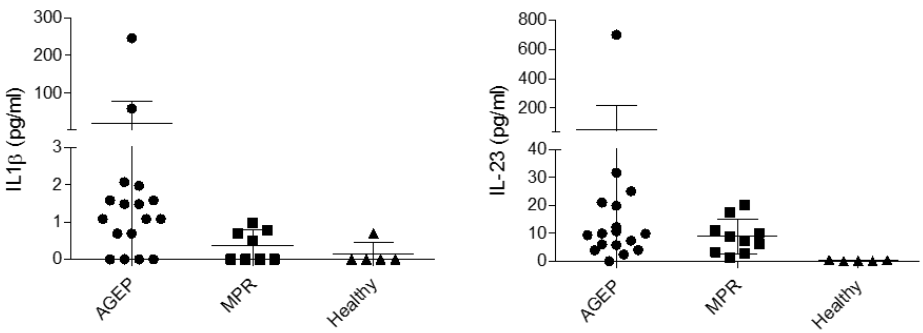
IL1β (pg/ml)
IL-23 (pg/ml)
AGEP
MPR
Healthy

Fig. 16. IL-36γ, IL-8 and IL-6 are elevated in the serum of AGEP patients. *(A) Serum was collected from patients with AGEP (n=17) or MPR (n=16) from the Dermatology Department of the University Hospital of Zürich and from healthy donors (n=10) and IFNγ, IL-17A, TNF, IL-6, and IL-8 were measured by ELISA. IL-36α and IL-36γ were measured in patients from the Dermatology Department of the University Hospital of Zürich (ZH, n=17; patients no. 6, 8-11, 13-19, 21 and 26-29) and from the Dermatology Department of Chang Gung Memorial Hospital in Taiwan and the Dermatology Department of the Hokkaido University in Japan (ASIA, n=32). *p<0.05; **p<0.01. (B) Serum from 17 AGEP, 9 MPR and 5 healthy donors from the Dermatology Department of the University Hospital of Zürich was collected and IL-1β and IL-23 were measured using cytometric bead assay.*

3.8 IL-1β is highly expressed in the lesional skin of AGEP patients

Since we found high levels of IL-1β in the serum of AGEP patients in the acute phase of disease, we further investigated whether it is also present in lesional skin. When comparing IL-1β expression in AGEP and MPR using RNA sequencing, IL-1β was upregulated in AGEP compared to MPR with a ratio of 1.94 (FDR 0.51), even though not statistically significant (p=0.098) (Fig. 10B). qPCR analysis confirmed an upregulation of IL-1β in AGEP compared to MPR (3.6-fold), however not statistically significant due to high standard deviations. When comparing AGEP to healthy skin, a statistically significant upregulation could be observed (52-fold; p<0.05). To determine IL-1β protein expression in AGEP skin, immunohistochemistry was performed using an antibody against mature IL-1β. Notably, a higher amount of IL-1β positive cells could be found in the dermal infiltrate and in the pustules of AGEP lesional skin compared to MPR (Fig. 17). In both diseases, it was barely expressed in the epidermis. As the antibody used is specific for the mature form of IL-1β, an active role of the cytokine can be presumed.

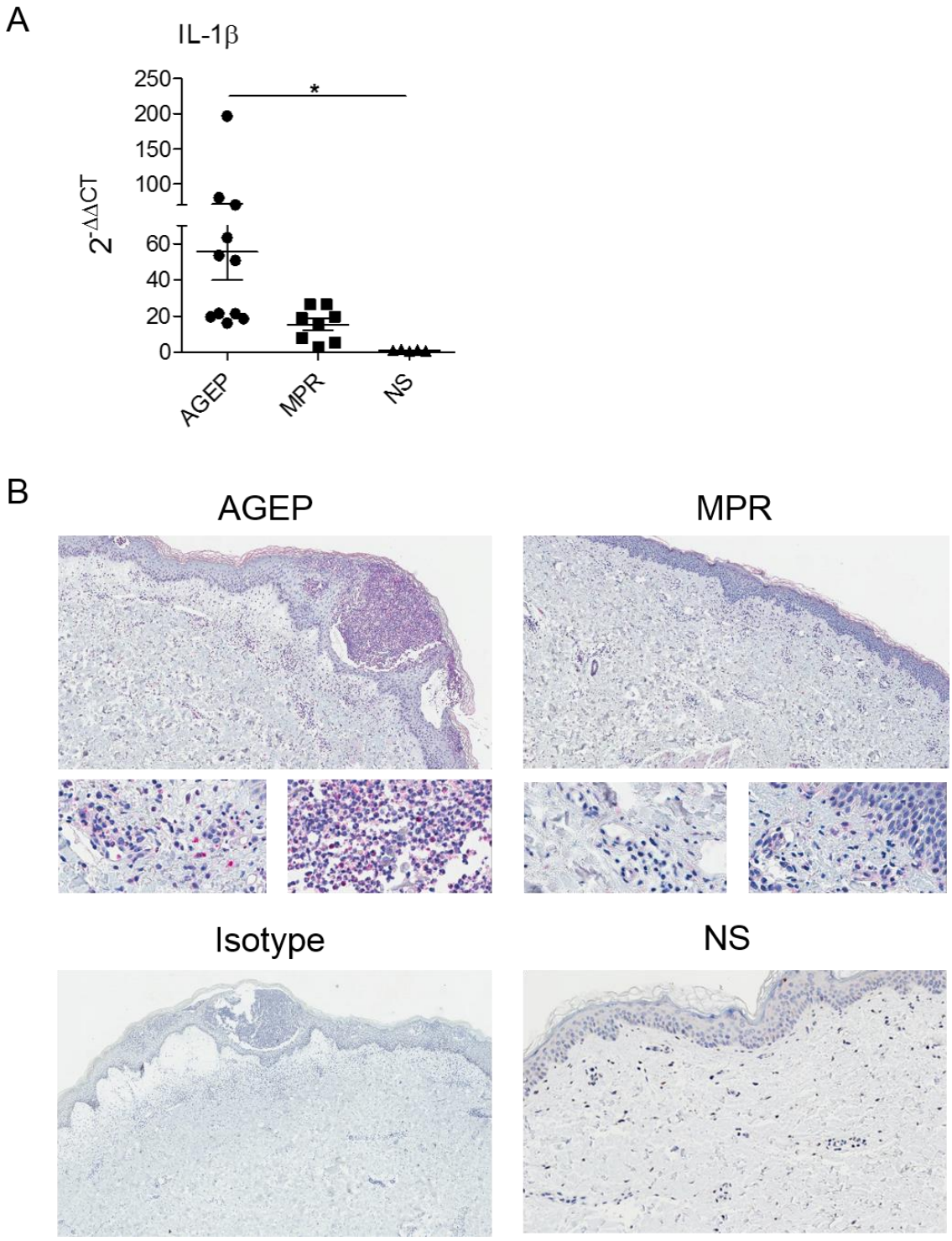

Fig. 17. IL-1β gene and protein is expressed in AGEP skin. *(A) Quantitative RT-PCR analysis of IL-1β in lesional skin biopsies of patients suffering from AGEP (n=11), MPR (n=8) and normal skin (NS; n=5). * p<0.05. (B) Immunohistochemical analysis of lesional skin biopsies from AGEP patients revealed that mature IL-1β is expressed in the dermal infiltrate and in the pustular region, while it was only weakly expressed in MPR. Representative pictures of 10 AGEP and 10 MPR cases are shown. IL-1β was not detectable in normal skin (NS) from healthy donors (n=5).*

3.9 IL-1β can be induced by culprit drugs in PBMC from patients having experienced AGEP and can be antagonized by IL-36RA

To further investigate the role of IL-1β in AGEP, we assessed whether PBMC taken from AGEP patients more than 6 months after the adverse reaction were able to secrete IL-1β upon stimulation with the causative drug. To this end, PBMC from patients having experienced AGEP or MPR were exposed to the culprit drug or an irrelevant control drug in ELISpot plates. The number of IL-1β$^+$ spots was then counted after 1, 2, 4, 6 and 8 hrs. IL-1β release was detected in PBMC from AGEP patients after 4 hrs of culprit drug exposure (3-fold more spots than control drug, $p<0.01$) and reached a plateau after 6 hrs (7-fold more spots than control drug, $p<0.0001$; Fig. 18A, left panel), whereas no increase in IL-1β production was observed with an irrelevant control drug (Fig. 18A, right panel). Furthermore and in contrast, the culprit drug did not induce IL-1β secretion in MPR PBMC as revealed by comparable IL-1β levels upon culprit-, control-drug and vehicle exposure. Similarly, none of the drugs used was able to induce IL-1β secretion in PBMC from healthy blood donors when compared to vehicle (Fig 18A).

We then sorted CD14$^+$ (monocytes) and CD3$^+$ cells (T cells) from patients' PBMC and exposed them to culprit or control drug in ELISpot plates to evaluate IL-1β secretion by both cell types (Fig. 18B). The culprit drug was able to induce IL-1β secretion in sorted CD14$^+$ cells from AGEP patients at levels similar to those observed with total PBMC. In contrast, the culprit drug was not able to induce IL-1β secretion in CD3$^+$ PBMC.

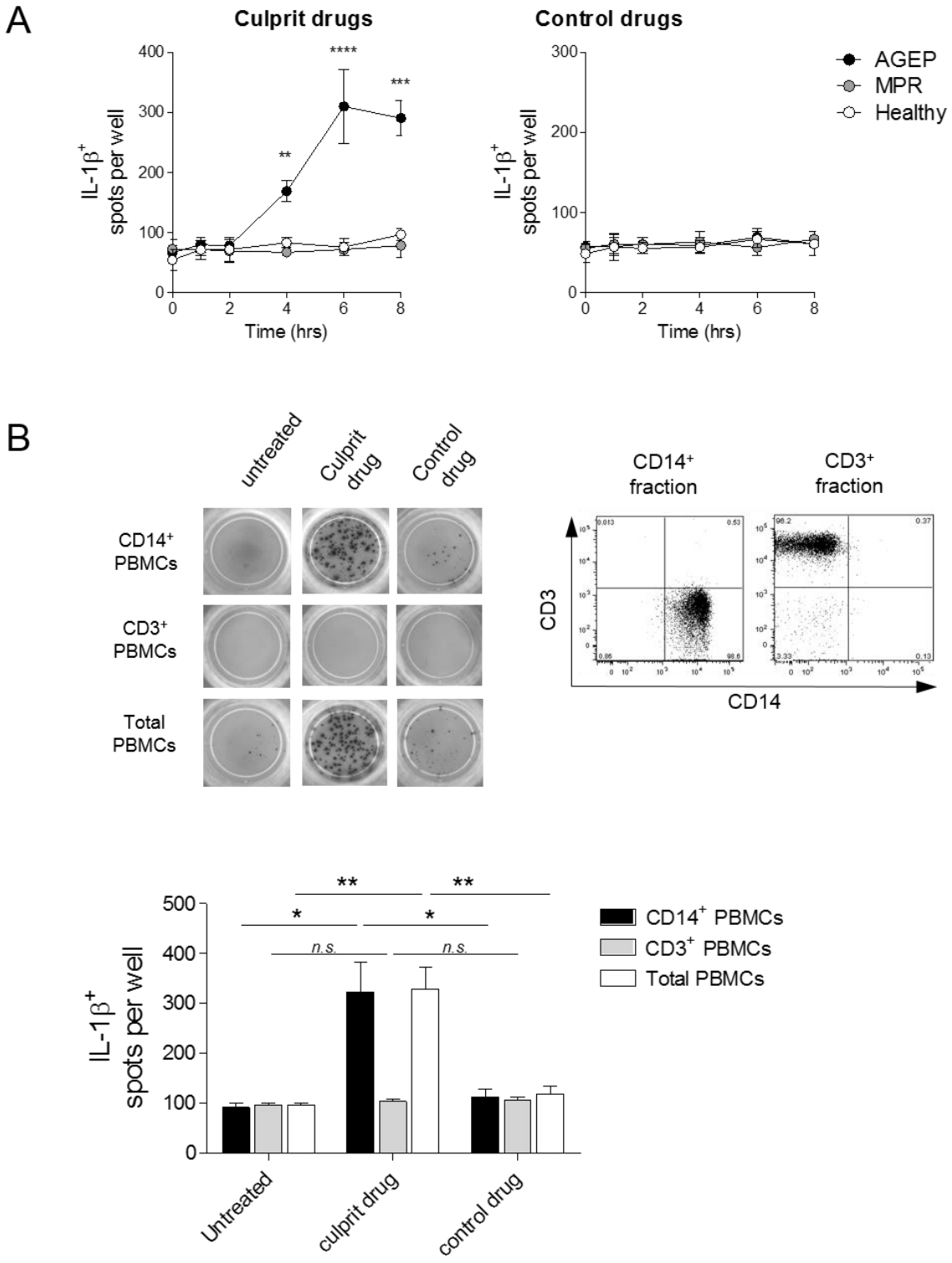

Fig. 18. PBMC and monocytes taken from AGEP patients more than 6 months after the ADR selectively secrete IL-1β in response to culprit drug exposure. *(A) PBMC from AGEP or MPR patients as well as healthy donors were cultured in IL-1β ELISpot plates for 8 hrs in presence of the culprit drug (left panel) or a control drug (right panel). The number of spots was counted 1, 2, 4, 6 and 8 hrs after drug exposure. The means±SD of 3 AGEP patients (no. 8, 10 and 21), 3 MPR patients and 3 healthy blood donors are shown. **p<0.01, ***p<0.001, ****p<0.0001. (B) CD14⁺ monocytes*

*and CD3⁺ T cells were isolated from AGEP blood with a purity of >96% and were cultured in IL-1β ELISpot plates in presence of the culprit drug or a control drug and compared to total PBMC. The number of spots was counted 8 hrs after drug exposure. The mean±SD of 3 patients (patient no. 8, 9 and 10) is shown. *p<0.05, **p<0.01.*

IL-1β is produced as a proform and needs to be cleaved by caspase-1 to become biologically active. To determine whether the secreted IL-1β in our drug stimulation experiments is the pro- or mature form, AGEP PBMC were incubated with the caspase inhibitor Z-Val-Ala-Asp fluoromethyl ketone (Z-VAD, 10 µM) for 2 hours before and during drug stimulation. Z-VAD was able to abrogate IL-1β secretion in PBMC exposed to the culprit drug (p=ns when compared to PBMC exposed to vehicle or a control drug), demonstrating that the released IL-1β upon drug stimulation represents the active cleaved form of IL-1β. To further investigate whether IL-36γ has an effect on IL-1β expression, cells were treated with IL-36RA two hours before and during drug stimulation of AGEP PBMC. Interestingly, a partial decrease of IL-1β could be observed, suggesting that IL-36γ acts as upstream target of IL-1β.

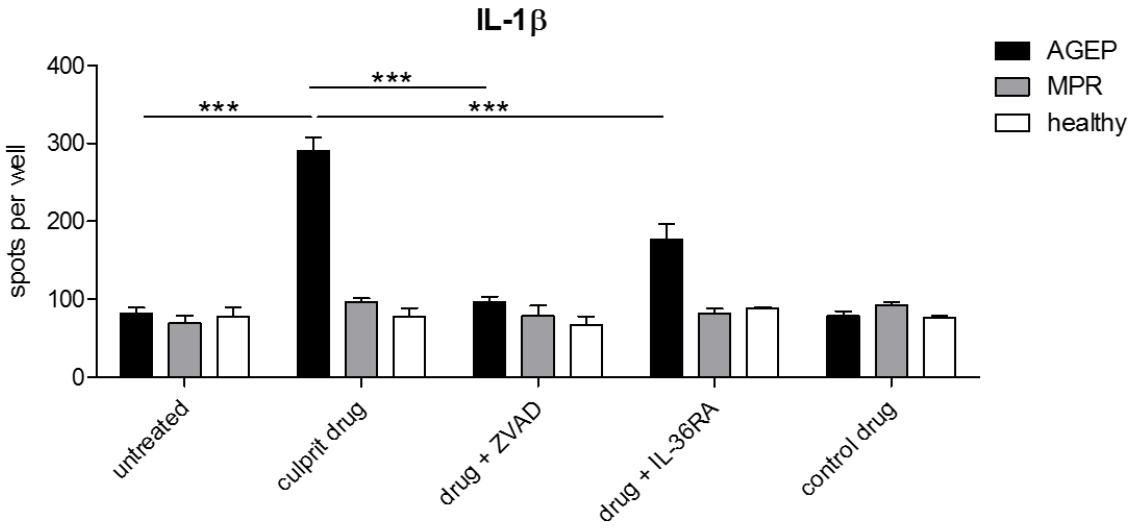

Fig 19. IL-1β secretion can be abrogated by the caspase-inhibitor ZVAD and partially abrogated by IL-36RA. *PBMC from AGEP or MPR patients as well as healthy donors were cultured in IL-1β ELISpot plates for 6 hrs in presence of the culprit drug +/- ZVAD, +/- IL36RA and a control drug. The number of spots was counted 6 hrs after drug exposure. The means±SD of 3 different AGEP patients (no. 8, 10 and 21), 3 MPR patients and 3 healthy blood donors are shown. *** p<0.001.*

Taken together, we could show that IL-1β is present in high amounts in AGEP blood and skin. Intriguingly, when stimulated with the culprit drug, monocytes secreted high amounts of IL-1β, suggesting that it is involved in the early phase of AGEP pathogenesis. Blockade of IL-1β secretion by IL36RA further suggests a regulatory role of IL-36γ.

3.10 Myeloid cells from AGEP patients exhibit an exacerbated response to TLR4 stimulation

LPS is an agonist of TLR4 and thereby initiates a signaling cascade that leads to NF-κB activation and subsequent production and secretion of proinflammatory cytokines, including IL-36γ and IL-1β [213]. In *in vitro* experiments with cytokine measurements as experimental output, it is very often used as positive control. For this purpose, LPS has also been used in our experimental settings. Strikingly, we observed significantly higher responses to LPS in AGEP patients' PBMC than in MPR and healthy control PBMC, which turned out to be statistically significant for both IL-36γ ($p<0.01$) and IL-1β ($p<0.001$). This observation is suggestive of an exacerbated response of AGEP myeloid cells to TLR4 stimulation (Fig. 20).

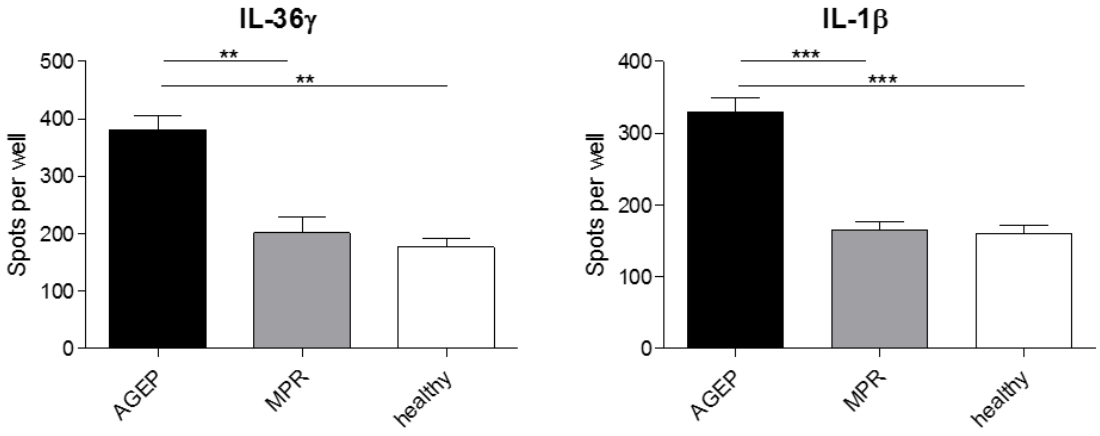

Fig. 20. Higher IL-36γ and IL-1β secretion upon LPS stimulation. *PBMC from AGEP or MPR patients as well as healthy donors were cultured in IL-36γ and L-1β ELISpot plates for 24 hrs. The number of spots was counted 24 hrs after LPS exposure. The mean±SD of 3 different patients (patient no. 8, 9 and 10) is shown. **p<0.01, ***p<0.001.*

3.11 AGEP patients do not express higher amounts of TLRs but carry polymorphisms in the TLR4 gene

Given the fact that pure monocyte populations of AGEP patients respond directly to the culprit drug and that a strong response to LPS has been observed in AGEP PBMC, we hypothesized that AGEP cells show exacerbated TLR-NF-κB activity. To investigate whether TLR4 and possibly other TLRs are overexpressed in AGEP compared to healthy PBMC, RNA was isolated and qPCR was performed with primers to all 10 TLRs. No overexpression of TLRs could be detected in AGEP PBMC when compared to MPR and healthy PBMC (Fig. 21). When comparing the expression levels of TLRs in AGEP skin compared to MPR skin using RNA sequencing, a significant increase of TLR2 (log2-ratio 0.8492 and $p<0.05$) only was detectable in AGEP skin, while the other TLRs were equally expressed (Table 6).

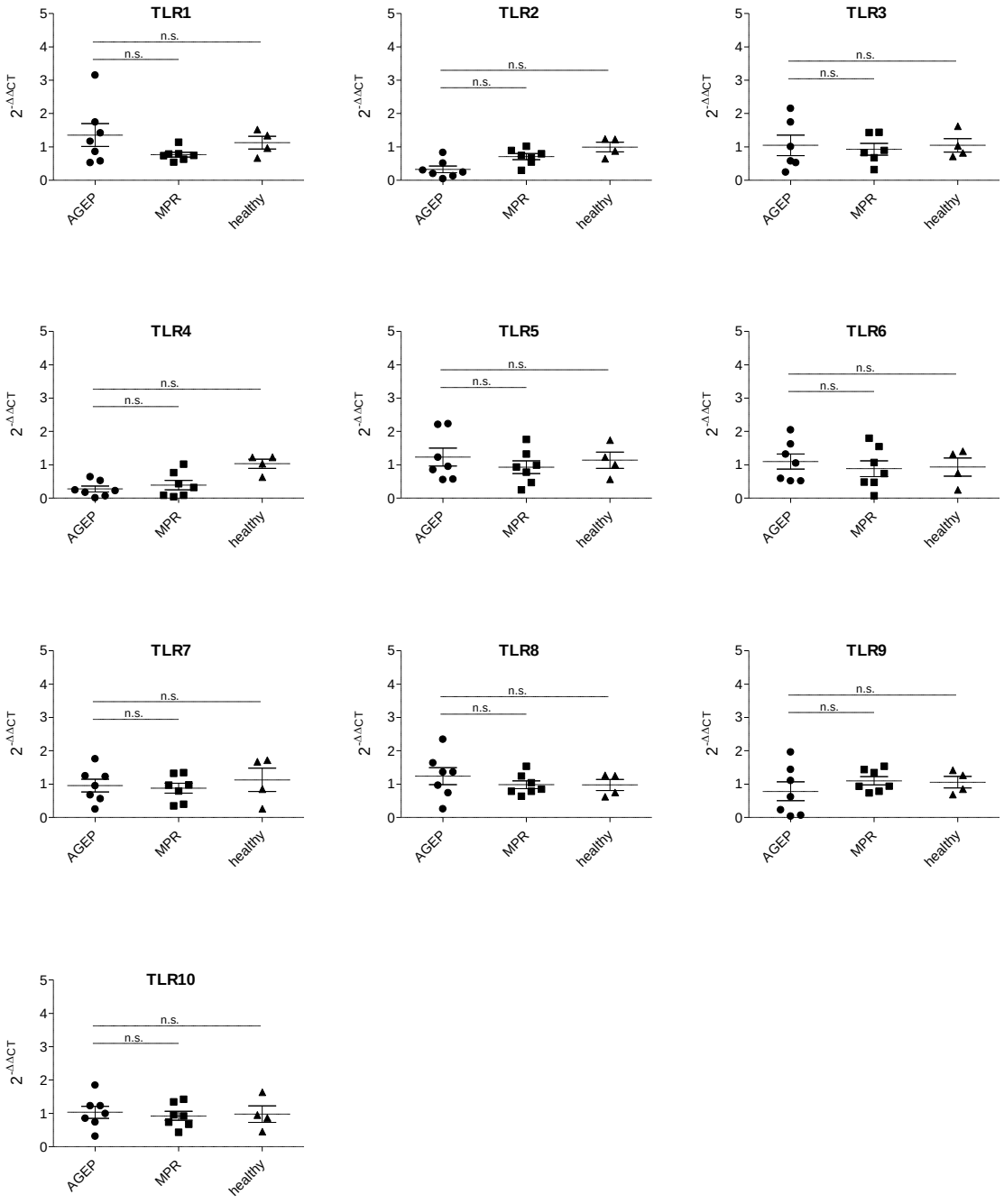

Fig. 21. No upregulation of Toll-like receptors in PBMC from AGEPpatients. *RNA was extracted from AGEP, MPR and healthy PBMC and mRNA expression levels of TLR 1-10 were measured using qPCR. n.s. = not significant*.

Table 6. Expression levels of Toll-like receptors 1-10 measured by RNAseq in AGEP compared to MPR skin:

	Log2 ratio	P-value
TLR1	-0.02439	0.9502
TLR2	0.8492	0.01834
TLR3	0.1072	0.7914
TLR4	-0.1277	0.7527
TLR5	0.4328	0.1424
TLR6	0.1523	0.7109
TLR7	0.3521	0.5187
TLR8	0.8132	0.1712
TLR9	-0.8119	0.424
TLR10	-0.2039	0.73

As no relevant increase in TLR expression was detectable, we analyzed 96 AGEP patients from RegiSCAR [197] for possible genetic changes in genes involved in TLR-NF-κB signaling using whole exome sequencing. Interestingly, we found a single nucleotide polymorphism (SNP) in *TLR4* in a high proportion of AGEP patients (Table 7). Indeed, 17/96 AGEP cases (18%) carry one of these polymorphisms and 14 out of 17 (14.6%) simultaneously carry two polymorphisms.

Table 7. Polymorphisms in the TLR4 gene in AGEP patients.

Gene	MARKER_ID	PVALUE	N.CASE	N.CTRL	AF.CASE	AF.CTRL
TLR4	9:120475302_A/G	0.067	96	480	0.083	0.050
TLR4	9:120475602_C/T	0.090	96	480	0.078	0.048
Combined burden test:		**0.014**				

The SNP 9:120475302_A/G replaces Asp on the position 299 with Gly (D299G) and the SNP 9:120475602_C/T replaces Thr at the position 399 with Ile (T339I). The presence of those two SNPs is connected in many cases [214].

3.12 Blockade of TLR pathway signaling molecules prevents IL-36γ and IL-1β production by AGEP PBMC

As we suspected an abnormal regulation of the NF-κB pathway in the PBMC of AGEP patients, we tested if the blockade of TLR signaling molecules has a functional inhibitory effect on the signaling response to culprit drugs in AGEP PBMC. To this end, we stimulated AGEP patients' PBMC with the culprit drug or LPS in the presence of inhibitors of the TLR adaptor proteins MyD88, TRIF and TIRAP and antagonist antibodies to TLR2 and 4 and to HLA-ABC (MHC-I) and HLA-DR (MHC-II). Notably, the blockade of MyD88 and TIRAP led to the abrogation of IL-36γ and IL-1β production by AGEP patients' PBMC upon exposure to culprit drugs, further supporting an NF-κB-mediated pathogenic reaction to culprit drugs in AGEP patients. The blockade of TRIF also decreased the immune response although to a lesser extent. On the contrary, blockade of the HLA-molecules did not lead to an abrogation of IL-36γ and IL-1β expression, suggesting that the drugs do not bind directly to HLA-molecules. When blocking TLR4, we could also inhibit IL-36γ and IL-1β production, whereas the inhibition of TLR2 had no effect on culprit drug-induced IL-36γ and IL-1β (Fig. 22 A and B). However, in one of the four tested patients no effect TLR4 blockade could be seen (Fig. 22 C), suggesting that the pathomechanism leading to AGEP is not unique in all patients.

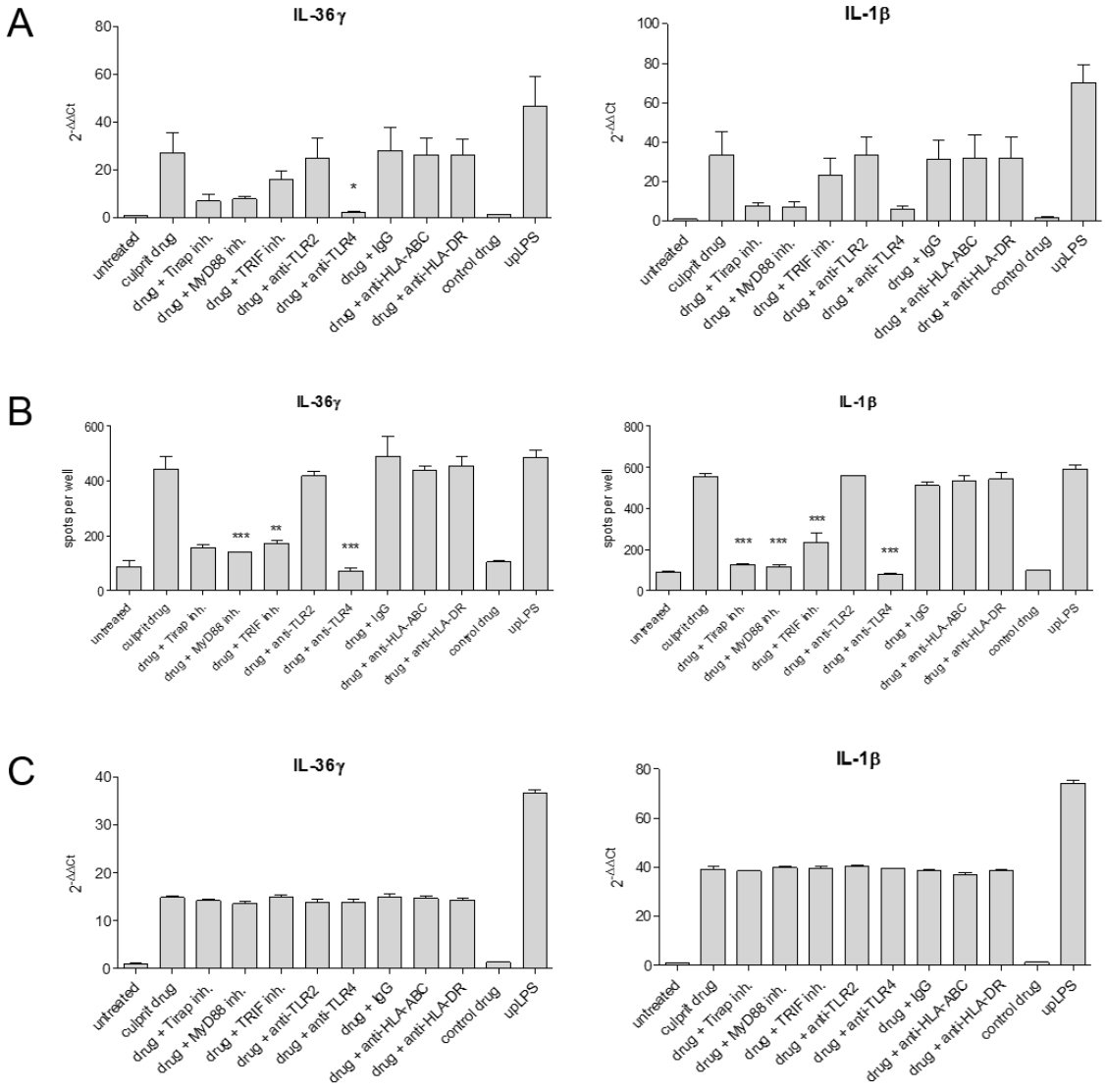

Fig. 22. Blockade of TLR signaling molecules abrogates IL-36γ and IL-1β production by AGEP PBMC. *PBMC were isolated from AGEP patients and cultured in cell culture (A + C) or ELISpot plates (B). Cells were stimulated with the culprit drug in the presence or absence of Tirap-inhibitor (25mM), MyD88 inhibitor (25mM), TRIF-inhibitor (25mM), anti-TLR2 antibody (5µg/ml), anti-TLR4 antibody (5µg/ml), control IgG antibody (5µg/ml), anti-HLA-ABC-antibody (5µg/ml), and anti-HLA-DR-antibody (5µg/ml). Untreated cells, control drug and upLPS served as controls. (A + C) Cells were harvested after 6 hrs incubation at 37°C and RNA was isolated, followed by cDNA synthesis and qPCR using primers to IL-36γ and IL-1β gene. RPL27 served as housekeeping gene. Presented results are normalized to untreated cells ($2^{-\Delta\Delta CT}$). (B) Cells were removed from ELISpot plate after 6 hrs of incubation at 37°C and the number of spots was counted. The means±SD of 3 AGEP patients, 3 MPR patients and 3 healthy blood donors are shown. n=3 in (A + B); n= 1 in (C). * p≤0.05, ** p≤0.01, *** p≤0.001.*

3.13 In certain cases, IL-36γ and IL-1β production by AGEP PBMC is dependent on albumin

When administered *in vivo*, certain drugs are known to bind to proteins present in the serum [215]. Such a drug-protein binding has a direct impact on drug distribution and efficacy [216]. Human serum albumin (HSA) is the most abundant plasma protein with a concentration of 35-50g/l and many drugs have a high binding affinity to HSA [217]. As TLR4 agonists are usually large molecules (e.g. LPS, [218]), we hypothesized that small molecules like drugs rather act as drug-protein complex in AGEP rather than alone in a free form. To assess whether HSA acts as a mandatory partner molecule in AGEP, patients' monocytes were first exposed to culprit and control drugs in the presence or absence of proteins in the culture medium. Notably, in two out of three patients, the absence of protein led to the absence of IL-1β and IL-36γ production upon culprit drug exposure while LPS stimulation still was still able to induce high amounts of both cytokines (Fig. 23). To determine whether HSA is involved in a possible hapten-protein complex in AGEP, thereby activating NF-kB via TLR4, we added HSA to the protein-free cell suspension. The cytokine production in the two patients where IL-1β and IL-36γ production was abrogated by absence of proteins, could be restored by the addition of HSA, suggesting that HSA acts as drug partner molecule in AGEP.

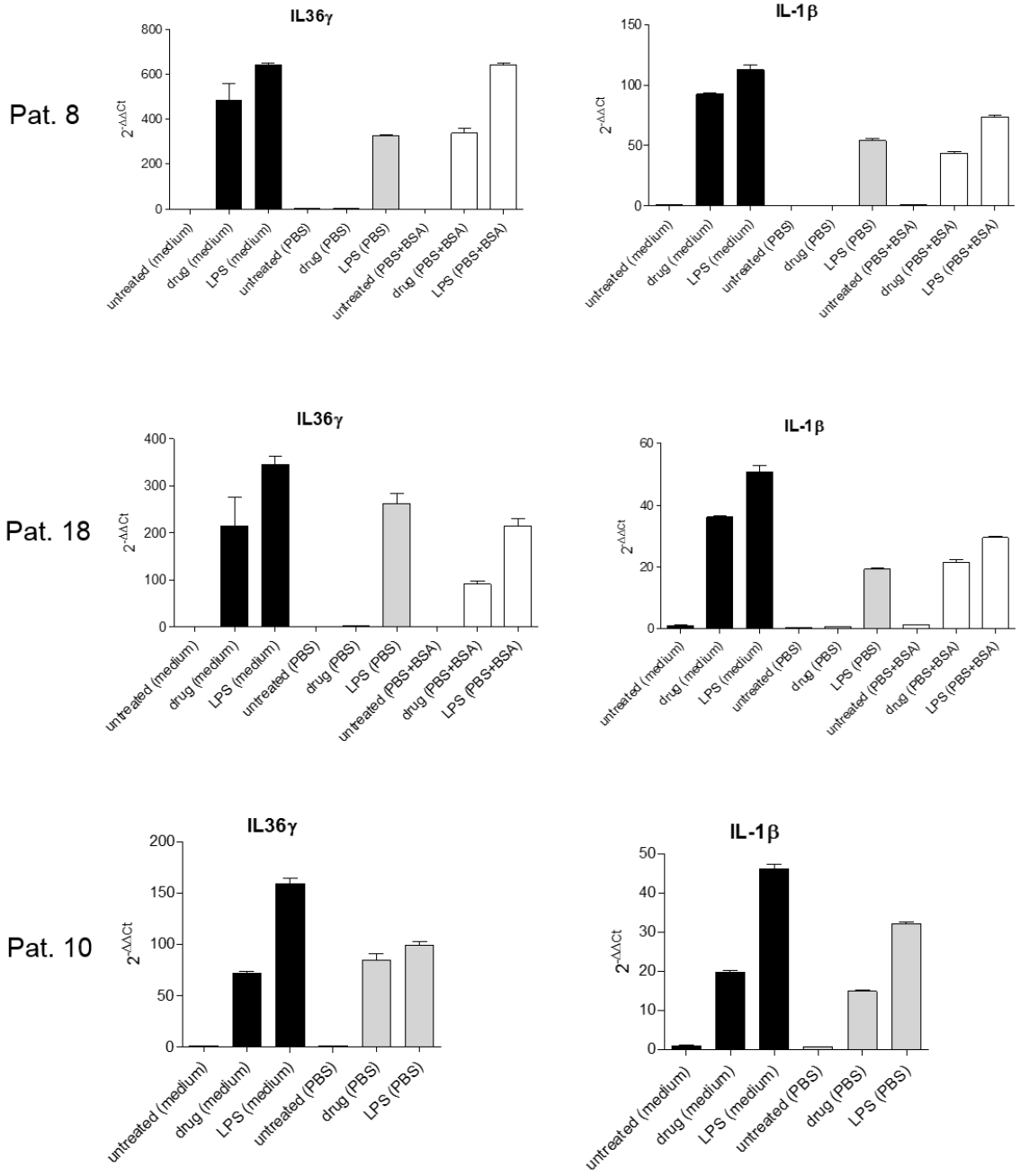

Fig. 23. In certain cases IL-36γ and IL-1β production by AGEP PBMC in response to culprit drugs is dependent on albumin. *PBMC were isolated from AGEP patients (patient 8, 10 and 20) and plated in 96-well-plates in complete medium (black histogram), PBS (grey histogram) or PBS + human 2.5mg/ml albumin (white histogram). Cells were then stimulated with the culprit drug (pat. 8: Amoxicillin 1mg/ml; pat. 18: Terbinafin 100 µg/ml; pat. 10: Amoxicillin 1mg/ml) and LPS and incubated for 3 hrs at 37°C. Cells were then harvested and RNA was isolated, followed by cDNA synthesis and qPCR using primers to IL-36γ and IL-1β gene. RPL27 served as housekeeping gene. Presented results are normalized to untreated cells ($2^{-\Delta\Delta CT}$).*

4 Discussion & Perspectives

AGEP is considered to be a severe adverse cutaneous drug eruption in which T cells and neutrophils are major players [175, 185]. It has been proposed that upon presentation, drugs responsible for causing AGEP elicit drug-specific T cell responses, and that these T cells secrete the neutrophil chemoattractant IL-8 [185]. Recently mutations in the IL-36RN gene encoding IL-36RA have been reported in rare cases of AGEP [197], suggesting that a dysregulation in IL-36 signaling may contribute to the physiopathology of AGEP. My data is supportive of this hypothesis, showing that culprit drugs can directly induce IL-36 secretion in AGEP patients' monocytes, and indirectly in patients' keratinocytes *in vitro*. Analysis of IL-36 gene and protein expression *in vivo* is also supportive of the above, revealing that macrophages and keratinocytes are the main producers of IL-36 and are located in the pustular areas of AGEP patients' skin. Among the IL-36 family members, IL-36γ was found to be the predominant form expressed in AGEP skin biopsies, and also the predominant form induced experimentally by the culprit drug in monocytes and keratinocytes *in vitro*.

Il-36γ is produced as inactive proform and requires activation by the neutrophil proteases elastase, proteinase-3 [73] or by cathespsin S [74]. As AGEP is a pustular reaction with abundant neutrophils in the blood and skin, it is very likely that neutrophil-derived proteases activate IL-36 cytokines within skin lesions.

Keratinocytes have been shown to be a major source of IL-36 cytokines in cutaneous inflammation, particularly in psoriasis [81]. Our data suggests that keratinocytes are also an important source of IL-36 in the skin in AGEP. However, co-culture experiments revealed that keratinocytes exposed to culprit drugs were only able to produce very little amounts of IL-36α and IL-36γ when cultured alone but, interestingly, produced high amounts of IL-36γ when cultured in presence of autologous monocytes and culprit drug. This observation suggests that, when exposed to the causative drug, patients' monocytes release a soluble factor that will stimulate IL-36γ production by keratinocytes. Unlike what has been reported in psoriasis [81], we could not demonstrate evidence of direct IL-36 induction by itself within a positive feed-back loop in AGEP patients' keratinocytes in our co-culture model using IL-36RA. However, as more than 6 hours incubation might be needed

for induction of its own expression, a self-amplifying effect of IL-36γ cannot be excluded and later time-points should be investigated.

Like in other inflammatory diseases such as psoriasis [219], contact hypersensitivity [220] or sunburn [221], keratinocytes may actively participate in the pathogenesis of AGEP by secreting IL-36γ, which could contribute to the herein observed and previously reported induction of IL-8 gene expression by macrophages. The latter likely contributes to the observed neutrophil recruitment to the epidermis in AGEP. Indeed, IL-8 expression was more important in culprit drug-exposed PBMC cultured with keratinocytes than in PBMC alone and could be blocked by IL-36RA, suggesting an additive effect of PBMC- and keratinocyte-derived IL-36 on IL-8 gene expression. As previously reported in AGEP patients, neutrophil-attracting IL-8 may also originate from drug-specific T cells [185]. Indeed, AGEP is currently seen as a delayed type hypersensitivity reaction with T cell involvement. However, the precise mechanisms leading to drug-specific T cell priming and recruitment to the skin in AGEP have not been elucidated to date. Unlike murine T cells, human T cells do not express IL-36R [71]. In AGEP, IL-36 may nevertheless contribute to T cell-mediated immune responses through its strong stimulatory effects on antigen-presenting cells [222]. My findings that IL-36 can be induced by a drug very early in innate immune cells do not exclude a delayed drug-specific T cell response but whether the induction of IL-36 in monocytes by culprit drugs and the activation of drug-specific T cells are interdependent events in AGEP pathogenesis or not remains to be investigated.

It has been previously reported that Th17 cells may also be involved in AGEP as revealed by their increased frequencies and elevated IL-22 levels in AGEP patients' peripheral blood [193]. Interestingly, we found high levels of IL-23 in the serum of our AGEP patients' cohort. As IL-23 induces the differentiation of naive $CD4^+$ T cells into Th17 cells [223], this finding is supportive of a role of Th17 cells in AGEP. IL-17 has been shown to increase IL-8 secretion by keratinocytes [224] in allergic contact dermatitis [225] and in psoriasis [226]. Our *in vitro* data revealed, however, that in response to IL-36, the major source of IL-8 was patients' monocytes, consistent with the elevated expression of IL-36R and potential strong responsiveness to IL-36 by dermal myeloid cells [70]. In contrast and although keratinocytes also express high levels of IL-36R [70], IL-8 production by keratinocytes was marginal as confirmed by qPCR in coculture experiments and

immunohistochemistry where IL-8 was only detected in the peri-pustular immune infiltrate.

A key question in this study was why and how a drug induces IL-36 and subsequent IL-8 production in immune and/or epidermal cells in a rare disease like AGEP. Although mutations in the IL-36RN gene have been identified in rare AGEP patients, no other marker(s) of genetic predisposition have been formally identified for AGEP to date. My data provide evidence that a dysregulation of the IL-36-IL-8 axis can occur independently of IL-36RN mutations in AGEP patients, suggesting that other factors influencing the susceptibility to an IL-36-mediated proinflammatory response to culprit drugs are at play in AGEP patients.

To determine whether other inflammatory cytokines are involved in the regulation of IL-36γ, healthy monocytes and keratinocytes were treated with several recombinant cytokines. Strikingly, IL-1β induced high IL-36γ expression in both monocytes and keratinocytes. To investigate a possible role of IL-1β in AGEP, IL-1β levels were measured in the serum of AGEP patients in the acute phase. Interestingly, when compared to MPR and healthy serum, we found higher levels of IL-1β in AGEP. This finding was associated with high amounts of IL-6 which is a known downstream target of IL-1β [227, 228]. As IL-1β and IL-6 are known to be strong inducers of fever (pyrogens) [229, 230], the elevated levels of these cytokines in AGEP blood might be responsible for the fever from which almost all AGEP patients suffer during the reaction.

Moreover, even though not statistically significant, IL-1β was found to be highly expressed in AGEP compared to MPR skin, as shown by RNA sequencing. This observation has been confirmed by Liang et. al who demonstrated in their recently published article that pustular diseases including AGEP show high expression levels of IL-1β [231]. Also, immunohistochemistry staining using an antibody against mature IL-1β revealed high amounts of IL-1β, showing that the biologically active form is present in AGEP skin.

It has been demonstrated by others that IL-36γ can induce IL-1β expression and secretion in human APCs [71]. In turn, IL-36γ can be strongly induced by IL-1β, as shown in myelofibroblasts [232]. Interestingly, I could also detect a dramatic increase of IL-36γ expression in human keratinocytes and monocytes in vitro upon treatment with recombinant IL-1β. ELISpot analysis revealed that IL-1β secretion by PBMC could be partly antagonized by IL-36RA, indicating that IL-36γ may be an

upstream driver of IL-1β in AGEP. Given that both cytokines can induce the others expression, they might act in an amplification loop. As we could not prove in our coculture experiment that IL-36 is the soluble factor initiating its own upregulation, IL-1β represents a possible candidate for IL-36γ regulation. In order to identify IL-1β as possible upstream driver of IL-36γ and amplifier, co-culture experiments should be repeated with Canakinumab, an antibody against IL-1β, or the IL-1 receptor antagonist Anakinra.

Likewise IL-36γ, rapid IL-1β release could be induced by culprit drug treatment of monocytes. Moreover, cytokine release from PBMC upon LPS stimulation was significantly elevated compared to MPR and healthy cells. The direct activation of innate immune cells by culprit drugs and the important response of AGEP PBMC to LPS stimulation are suggestive of an exacerbated NF-κB activity in these patients. Further supportive of this theory is the very rapid onset of the disease after the first intake of a drug, suggesting an early response mediated by the innate immune system.

Using whole exome sequencing of 96 AGEP DNA samples from the RegiSCAR cohort compared to 480 DNA samples of healthy individuals, we could identify two SNPs in the gene encoding TLR4 that were significantly increased in frequency in AGEP compared to healthy individuals. These D299G and T399I SNPs have been linked to several human diseases including inflammatory bowel disease, septic shock, childhood respiratory syncytial virus infection, and colon and gastric cancers [233-236]. Given our *in vitro* data and the identification of SNPs in the TLR4 gene, we hypothesized that dysregulated TLR4 signaling might be involved in the pathogenesis of AGEP.

The D299G and T399I SNPs are localized in the TLR4 ligand binding region for LPS and it has been shown that cells carrying these polymorphisms have dysregulated TLR4 signaling [214, 237, 238]. Contradicting our results, it was demonstrated that D299G and T399I SNPs lead to hyporesponsiveness to LPS stimulation through local conformational changes in the ligand binding region. However, even though Hold *et al.* found less NF-κB activity upon LPS stimulation in mutant cells, they also demonstrated a significant increase in production of IL-1β, TNF, IL-6 and IL-10 in cells from polymorphic TLR4 carriers compared to individuals with WT TLR4 [237]. As my data suggest that IL-1β and IL-36 are important players in AGEP, the finding of dysregulated cytokine production in cells from D299G and T399I SNP carriers is

supportive of our hypothesis that changes in the TLR4 protein might lead to the immune response happening in AGEP.

To functionally prove the impact of TLR4 dysregulation in AGEP, blocking experiments were performed. We could show that blockade of TLR4 and its adaptor proteins MyD88, TRIF and TIRAP led to an abrogation of IL36γ and IL1β expression in three out of four cases. These results indicate that activation of TLR4 has a functional impact on the immune activation by drugs in AGEP PBMC. However, the number of patients should be increased to emphasize the relevance of these findings. Perspectively, it would be of high importance to screen all AGEP patients of the Zurich cohort for the detected D299G and T399I SNPs and compare carriers and non-carriers in functional experiments. As a first approach, primary monocytes from patients harboring either TLR4-D299G or TLR4-T399I or both could be transfected with siRNA to TLR4 or to scramble siRNA as control. Transfected cells should then be exposed to the culprit drug, a control irrelevant drug and LPS and the secretion of IL-36γ and IL-1β could be measured by ELISpot. If a difference in cytokine secretion is seen in TLR4-knockdown cells as compared to cells transfected with scramble siRNA, the extent of inhibition should be compared between cells from patients with either TLR4-D299G, TLR4-T399I or both variants to assess a possible hyperresponsiveness due to one of the TLR4 variants.

To further assess whether the D299G T399I SNPs of TLR4 bestow the receptor with the ability to interact with the drugs known to induce AGEP, it would be of interest to generate plasmids encoding TLR4 with D299G, T399I or D299G/T399I polymorphism mutations, using site-directed mutagenesis. These could then be used in *in vitro* experiments by overexpressing mutants and wild-type TLR4 with an NF-κB luciferase reporter construct in Human embryonic kidney cells 293 (HEK293 cells). As they do not express TLR4 [239], they represent very good candidates for TLR4 mutant overexpression experiments. These can then be treated with candidate drugs to assess whether, in response to these drugs, receptor variants differentially activate NF-κB. This approach would give an indication to whether either SNP or both together affect the ability of TLR4 to interact with drugs known to cause AGEP. LPS can be used as a control and supernatants could be used to measure IL-8, IL-6 and IL-1β production, to further determine whether transcription of NF-κB-inducible genes are affected. From another approach, the THP-1 monocytic cell line stably-transfected with wild-type, D299G, T399I or D299G/T399I

TLR4 could be used. These cells could also be co-cultured with primary keratinocytes and stimulated with candidate drugs and LPS prior to IL-1β and IL-36γ expression analysis.

As SNPs in TLR4 have only been found in 20% of the analyzed AGEP patients, other mechanisms leading to the strong drug-induced innate immune response in AGEP should be taken into account. Besides genetic changes, also epigenetic factors could cause a dysregulation in the signaling pathway of TLR4 or other molecules, leading to exacerbated NF-κB activity. It has been shown that epigenetic changes in H3K4me1, H3K4me3, H2K27me, or H3K9me2 can result in trained immunity of monocytes/macrophages in response to LPS [240-242]. Even though most of these changes rather lead to tolerance to certain stimuli, e.g. in bacterial infection [243], epigenetic changes in the NF-κB pathway could cause an inadequate response to drugs in the case of AGEP and should be further investigated. To study epigenetics in AGEP patients, DNA methylation could be analysed using high resolution melt analysis (HRM). For this purpose, the DNA region of the mutation of interest (e.g. TLR4) should be amplified and the PCR product can then be subjected to decreasing temperatures. Thereby the melt temperatures and melt curve can be obtained and compared to known standard DNA samples to determine the relative levels of methylation. To study DNA/protein interactions, a technique known as chromatin immunoprecipitation (ChIP) could be used. ChIP assays allow the chromatin structure surrounding a specific DNA sequence to be analyzed. Formaldehyde can be used to crosslink DNA and protein, followed by immunoprecipitation of DNA–protein complexes. Once the crosslinks are reversed, recovered DNA can then be analyzed using PCR [244].

Another possible activation mechanism in AGEP may consist of inflammasome activation. As mentioned above, mature IL-1β could be found in AGEP lesional skin. This is further supported by the fact that the caspase-inhibitor ZVAD could suppress IL-1β secretion after culprit drug exposure in ELISpot experiments. However, how the activation of IL-1β is initiated, remains unclear to date. IL-1β activation requires its cleavage by caspase-1 which is only activated when an inflammasome assembles upon stimulation of certain NLRs or the DNA sensor AIM2 [124]. Besides IL-1β, activated caspase-1 also cleaves IL-18, another proinflammatory cytokine. Thus, to further detect inflammasome activation, it would be interesting to measure IL-18 in the AGEP patients' serum and to perform immunohistochemistry stainings

for IL-18 on AGEP lesional skin samples. Intriguingly, it has been demonstrated that IL-36 signaling facilitates the activation of the NLRP3 inflammasome [245]. Moreover, to detect a possible genetic dysregulation of the inflammasome in AGEP, it would be of high interest to screen the whole exome sequencing database of the RegiSCAR AGEP patients for SNPs or mutations in inflammasome components.
Another key question of this study was how drugs can activate TLR4 or other receptors in AGEP. We could show that the absence of protein prevented cells from AGEP patients to produce IL-36γ and IL-1β upon culprit drug treatment in two out of three analyzed cases. This suggests that the drug might act as a hapten and activate the receptor only in a drug-protein-complex. However, as the absence of protein did not abrogate the immune activation in all cases, TLR4 signaling by drug-protein complexes may not occur in all patients. As suggested in other adverse drug reactions, a direct interaction of a drug with immune receptors – usually T-cell receptors - could lead to an immune activation (the so-called pi-concept) [246]. Alternatively, other ways of TLR4 activation might be possible. It has been shown in the case of nickel, that TLR4 signaling was initiated by direct interaction with the molecule [247]. In this study, Schmidt et. al demonstrated that the non-conserved histidines 456 and 458 of the human TLR4 are required for hypersensitivity reactions by nickel.

To formally demonstrate that the culprit drug binds - as a drug-protein complex or not - to TLR4, we will use a previously published biotinylated-amoxicillin (biot-AMX) [248] (amoxicillin is associated to AGEP and has been functionally evaluated in our lab for IL-36 induction in patients' cells). Biot-AMX will be added to THP-1 cells stably expressing $TLR4^{D299G}$, $TLR4^{T399I}$ or $TLR4^{D299G/T399I}$ variants (as described in Aim 3) with or without albumin. For each condition, THP-1 cells will be collected 1, 2 and 4 four hours for protein extraction. Immuno-precipitation will then be performed using an anti-TLR4 antibody and the precipitate will be revealed using HRP-streptavidin after SDS-PAGE. Alternatively, flow cytometry will be used to quantify the binding intensity of the AMX-Biot/albumin complex to TLR4-expressing THP-1.

Overall, my work provides the first evidence to date that IL-36 is involved in the pathogenesis of the pustular cutaneous adverse drug reaction AGEP, and identifies

monocytes and keratinocytes as potential key producers of IL-36 in AGEP. Given that monocytes/PBMC of all AGEP patients tested have an enhanced propensity to produce IL-36 upon culprit drug exposure, the opportunity to identify predictive markers that would help identify patients prone to pathological IL-36 production upon exposure to certain medications may be achievable. Moreover, IL-1β potentially represents an important player in immune responses to drugs in AGEP. This observation may also be of interest for diagnosis and/or culprit drug identification together with IL-36γ.

Strikingly, the possible involvement of TLR4 in the drug-induced inflammation in AGEP could be identified in the present work. For the first time, a possible role of the innate immune sytem in the early pathogenesis of AGEP could be demonstrated, opening new research avenues in the field of cutaneous adverse drug reactions.

5 Bibliography

1. M., M., *Anatomic and chemical barriers are the first defense against pathogens*, in *Janeways's Immunobiology*. 2017, Garland Science: New York and London. p. 5.
2. Holmskov, U. and J.C. Jensenius, *Structure and function of collectins: humoral C-type lectins with collagenous regions.* Behring Inst Mitt, 1993(93): p. 224-35.
3. Sjoberg, A.P., L.A. Trouw, and A.M. Blom, *Complement activation and inhibition: a delicate balance.* Trends Immunol, 2009. **30**(2): p. 83-90.
4. Chaplin, D.D., *Overview of the immune response.* J Allergy Clin Immunol, 2010. **125**(2 Suppl 2): p. S3-23.
5. Medzhitov, R. and C. Janeway, Jr., *Innate immune recognition: mechanisms and pathways.* Immunol Rev, 2000. **173**: p. 89-97.
6. Dranoff, G., *Cytokines in cancer pathogenesis and cancer therapy.* Nat Rev Cancer, 2004. **4**(1): p. 11-22.
7. Turvey, S.E. and D.H. Broide, *Innate immunity.* J Allergy Clin Immunol, 2010. **125**(2 Suppl 2): p. S24-32.
8. Alberts B, J.A., Lewis J, et al., *Molecular Biology of the Cell.* Lymphocytes and the Cellular Basis of Adaptive Immunity. 2002, New York: Garland Sciences.
9. Luckheeram, R.V., et al., *CD4(+)T cells: differentiation and functions.* Clin Dev Immunol, 2012. **2012**: p. 925135.
10. Sakaguchi, S., et al., *Regulatory T cells and immune tolerance.* Cell, 2008. **133**(5): p. 775-87.
11. Alberts B, J.A., Lewis J, et al., *Molecular Biology of the Cell.* . 4th edition.

ed. B Cells and Antibodies. 2002.

12. Alberts B, J.A., Lewis J, et al., *Molecular Biology of the Cell.* . 4th edition. ed. T Cells and MHC Proteins. 2002, New York: Garland Science.
13. Paul, W.E., *Bridging innate and adaptive immunity.* Cell, 2011. **147**(6): p. 1212-5.
14. Kondo, M., *Lymphoid and myeloid lineage commitment in multipotent hematopoietic progenitors.* Immunol Rev, 2010. **238**(1): p. 37-46.
15. Mantovani, A., et al., *Neutrophils in the activation and regulation of innate and adaptive immunity.* Nat Rev Immunol, 2011. **11**(8): p. 519-31.
16. Rosenberg, H.F., K.D. Dyer, and P.S. Foster, *Eosinophils: changing perspectives in health and disease.* Nat Rev Immunol, 2013. **13**(1): p. 9-22.
17. Kita, H., *Eosinophils: multifaceted biological properties and roles in health and disease.* Immunol Rev, 2011. **242**(1): p. 161-77.
18. Akuthota, P., H. Wang, and P.F. Weller, *Eosinophils as antigen-presenting cells in allergic upper airway disease.* Curr Opin Allergy Clin Immunol, 2010. **10**(1): p. 14-9.

19. Falcone, F.H., H. Haas, and B.F. Gibbs, *The human basophil: a new appreciation of its role in immune responses.* Blood, 2000. **96**(13): p. 4028-38.
20. Daeron, M., et al., *Regulation of high-affinity IgE receptor-mediated mast cell activation by murine low-affinity IgG receptors.* J Clin Invest, 1995. **95**(2): p. 577-85.
21. Steinman, R.M. and J. Idoyaga, *Features of the dendritic cell lineage.* Immunological reviews, 2010. **234**(1): p. 5-17.
22. Schmid, M.A., et al., *Instructive cytokine signals in dendritic cell lineage commitment.* Immunological reviews, 2010. **234**(1): p. 32-44.
23. Helft, J., et al., *Origin and functional heterogeneity of non-lymphoid tissue dendritic cells in mice.* Immunological reviews, 2010. **234**(1): p. 55-75.
24. Naik, S.H., *Demystifying the development of dendritic cell subtypes, a little.* Immunology and Cell Biology, 2008. **86**(5): p. 439-452.
25. den Haan, J.M., S.M. Lehar, and M.J. Bevan, *CD8(+) but not CD8(-) dendritic cells cross-prime cytotoxic T cells in vivo.* The Journal of experimental medicine, 2000. **192**(12): p. 1685-96.
26. Leenen, P.J., et al., *Heterogeneity of mouse spleen dendritic cells: in vivo phagocytic activity, expression of macrophage markers, and subpopulation turnover.* Journal of immunology, 1998. **160**(5): p. 2166-73.
27. Dudziak, D., et al., *Differential Antigen Processing by Dendritic Cell Subsets in Vivo.* Science, 2007. **315**(5808): p. 107-111.
28. Merad, M. and M.G. Manz, *Dendritic cell homeostasis.* Blood, 2009. **113**(15): p. 3418-27.
29. Merad, M., F. Ginhoux, and M. Collin, *Origin, homeostasis and function of Langerhans cells and other langerin-expressing dendritic cells.* Nature reviews. Immunology, 2008. **8**(12): p. 935-47.
30. Shi, C. and E.G. Pamer, *Monocyte recruitment during infection and inflammation.* Nat Rev Immunol, 2011. **11**(11): p. 762-74.
31. Ziegler-Heitbrock, L., et al., *Nomenclature of monocytes and dendritic cells in blood.* Blood, 2010. **116**(16): p. e74-80.
32. Yang, J., et al., *Monocyte and macrophage differentiation: circulation inflammatory monocyte as biomarker for inflammatory diseases.* Biomark Res, 2014. **2**(1): p. 1.
33. Murray, P.J., et al., *Macrophage activation and polarization: nomenclature and experimental guidelines.* Immunity, 2014. **41**(1): p. 14-20.
34. Spits, H. and T. Cupedo, *Innate lymphoid cells: emerging insights in development, lineage relationships, and function.* Annu Rev Immunol, 2012. **30**: p. 647-75.
35. Hazenberg, M.D. and H. Spits, *Human innate lymphoid cells.* Blood, 2014. **124**(5): p. 700-9.
36. Kiessling, R., et al., *"Natural" killer cells in the mouse. II. Cytotoxic cells with specificity for mouse Moloney leukemia cells. Characteristics of the killer cell.* Eur J Immunol, 1975. **5**(2): p. 117-21.

37. Mebius, R.E., P. Rennert, and I.L. Weissman, *Developing lymph nodes collect CD4+CD3- LTbeta+ cells that can differentiate to APC, NK cells, and follicular cells but not T or B cells.* Immunity, 1997. **7**(4): p. 493-504.
38. Ivanov, II, G.E. Diehl, and D.R. Littman, *Lymphoid tissue inducer cells in intestinal immunity.* Curr Top Microbiol Immunol, 2006. **308**: p. 59-82.
39. Cella, M., et al., *A human natural killer cell subset provides an innate source of IL-22 for mucosal immunity.* Nature, 2009. **457**(7230): p. 722-5.
40. Moro, K., et al., *Innate production of T(H)2 cytokines by adipose tissue-associated c-Kit(+)Sca-1(+) lymphoid cells.* Nature, 2010. **463**(7280): p. 540-4.
41. Satoh-Takayama, N., et al., *Microbial flora drives interleukin 22 production in intestinal NKp46+ cells that provide innate mucosal immune defense.* Immunity, 2008. **29**(6): p. 958-70.
42. Spits, H. and J.P. Di Santo, *The expanding family of innate lymphoid cells: regulators and effectors of immunity and tissue remodeling.* Nat Immunol, 2011. **12**(1): p. 21-7.
43. Eberl, G. and D.R. Littman, *Thymic origin of intestinal alphabeta T cells revealed by fate mapping of RORgammat+ cells.* Science, 2004. **305**(5681): p. 248-51.
44. Serafini, N., C.A. Vosshenrich, and J.P. Di Santo, *Transcriptional regulation of innate lymphoid cell fate.* Nat Rev Immunol, 2015. **15**(7): p. 415-28.
45. Sonnenberg, G.F. and D. Artis, *Innate lymphoid cells in the initiation, regulation and resolution of inflammation.* Nat Med, 2015. **21**(7): p. 698-708.
46. Scandella, E., et al., *Restoration of lymphoid organ integrity through the interaction of lymphoid tissue-inducer cells with stroma of the T cell zone.* Nat Immunol, 2008. **9**(6): p. 667-75.
47. Monticelli, L.A., et al., *Innate lymphoid cells promote lung-tissue homeostasis after infection with influenza virus.* Nat Immunol, 2011. **12**(11): p. 1045-54.
48. Takeuchi, O. and S. Akira, *Pattern recognition receptors and inflammation.* Cell, 2010. **140**(6): p. 805-20.
49. Triantafilou, M., et al., *Membrane sorting of toll-like receptor (TLR)-2/6 and TLR2/1 heterodimers at the cell surface determines heterotypic associations with CD36 and intracellular targeting.* J Biol Chem, 2006. **281**(41): p. 31002-11.
50. Akira, S., S. Uematsu, and O. Takeuchi, *Pathogen recognition and innate immunity.* Cell, 2006. **124**(4): p. 783-801.
51. Barton, G.M. and J.C. Kagan, *A cell biological view of Toll-like receptor function: regulation through compartmentalization.* Nat Rev Immunol, 2009. **9**(8): p. 535-42.
52. Cervantes, J.L., et al., *TLR8: the forgotten relative revindicated.* Cell Mol Immunol, 2012. **9**(6): p. 434-8.
53. Orinska, Z., et al., *TLR3-induced activation of mast cells modulates CD8+ T-cell recruitment.* Blood, 2005. **106**(3): p. 978-87.
54. Wesch, D., et al., *Direct costimulatory effect of TLR3 ligand poly(I:C) on human gamma delta T lymphocytes.* J Immunol, 2006. **176**(3): p. 1348-54.

55. Kadowaki, N., et al., *Subsets of human dendritic cell precursors express different toll-like receptors and respond to different microbial antigens.* J Exp Med, 2001. **194**(6): p. 863-9.
56. Gantier, M.P., et al., *TLR7 is involved in sequence-specific sensing of single-stranded RNAs in human macrophages.* J Immunol, 2008. **180**(4): p. 2117-24.
57. Alexopoulou, L., B. Desnues, and O. Demaria, *[Toll-like receptor 8: the awkward TLR].* Med Sci (Paris), 2012. **28**(1): p. 96-102.
58. Hornung, V., et al., *Quantitative expression of toll-like receptor 1-10 mRNA in cellular subsets of human peripheral blood mononuclear cells and sensitivity to CpG oligodeoxynucleotides.* J Immunol, 2002. **168**(9): p. 4531-7.
59. Uematsu, S., et al., *Regulation of humoral and cellular gut immunity by lamina propria dendritic cells expressing Toll-like receptor 5.* Nat Immunol, 2008. **9**(7): p. 769-76.
60. Lemaitre, B., et al., *The dorsoventral regulatory gene cassette spatzle/Toll/cactus controls the potent antifungal response in Drosophila adults.* Cell, 1996. **86**(6): p. 973-83.
61. Poltorak, A., et al., *Defective LPS signaling in C3H/HeJ and C57BL/10ScCr mice: mutations in Tlr4 gene.* Science, 1998. **282**(5396): p. 2085-8.
62. Vaure, C. and Y. Liu, *A comparative review of toll-like receptor 4 expression and functionality in different animal species.* Front Immunol, 2014. **5**: p. 316.
63. Zanin-Zhorov, A., et al., *Cutting edge: T cells respond to lipopolysaccharide innately via TLR4 signaling.* J Immunol, 2007. **179**(1): p. 41-4.
64. Lebre, M.C., et al., *Human keratinocytes express functional Toll-like receptor 3, 4, 5, and 9.* J Invest Dermatol, 2007. **127**(2): p. 331-41.
65. Song, P.I., et al., *Human keratinocytes express functional CD14 and toll-like receptor 4.* J Invest Dermatol, 2002. **119**(2): p. 424-32.
66. Yao, C., et al., *Toll-like receptor family members in skin fibroblasts are functional and have a higher expression compared to skin keratinocytes.* Int J Mol Med, 2015. **35**(5): p. 1443-50.
67. Park, B.S. and J.O. Lee, *Recognition of lipopolysaccharide pattern by TLR4 complexes.* Exp Mol Med, 2013. **45**: p. e66.
68. Palomo, J., et al., *The interleukin (IL)-1 cytokine family--Balance between agonists and antagonists in inflammatory diseases.* Cytokine, 2015. **76**(1): p. 25-37.
69. Gunther, S. and E.J. Sundberg, *Molecular determinants of agonist and antagonist signaling through the IL-36 receptor.* J Immunol, 2014. **193**(2): p. 921-30.
70. Dietrich, D., et al., *Interleukin-36 potently stimulates human M2 macrophages, Langerhans cells and keratinocytes to produce pro-inflammatory cytokines.* Cytokine, 2016. **84**: p. 88-98.
71. Foster, A.M., et al., *IL-36 promotes myeloid cell infiltration, activation, and inflammatory activity in skin.* J Immunol, 2014. **192**(12): p. 6053-61.

72. Towne, J.E., et al., *Interleukin-36 (IL-36) ligands require processing for full agonist (IL-36alpha, IL-36beta, and IL-36gamma) or antagonist (IL-36Ra) activity.* J Biol Chem, 2011. **286**(49): p. 42594-602.
73. Henry, C.M., et al., *Neutrophil-Derived Proteases Escalate Inflammation through Activation of IL-36 Family Cytokines.* Cell Rep, 2016. **14**(4): p. 708-22.
74. al, A.J.e., *Skin and neutrophil-derived proteases regulate the activity of IL-36 family members*. 2017: ADF 2017.
75. Gresnigt, M.S. and F.L. van de Veerdonk, *Biology of IL-36 cytokines and their role in disease.* Semin Immunol, 2013. **25**(6): p. 458-65.
76. Martin, U., et al., *Externalization of the leaderless cytokine IL-1F6 occurs in response to lipopolysaccharide/ATP activation of transduced bone marrow macrophages.* J Immunol, 2009. **183**(6): p. 4021-30.
77. Lian, L.H., et al., *The double-stranded RNA analogue polyinosinic-polycytidylic acid induces keratinocyte pyroptosis and release of IL-36gamma.* J Invest Dermatol, 2012. **132**(5): p. 1346-53.
78. Johnston, A., et al., *IL-1F5, -F6, -F8, and -F9: a novel IL-1 family signaling system that is active in psoriasis and promotes keratinocyte antimicrobial peptide expression.* J Immunol, 2011. **186**(4): p. 2613-22.
79. He, Q., et al., *IL-36 cytokine expression and its relationship with p38 MAPK and NF-kappaB pathways in psoriasis vulgaris skin lesions.* J Huazhong Univ Sci Technolog Med Sci, 2013. **33**(4): p. 594-9.
80. Debets, R., et al., *Two novel IL-1 family members, IL-1 delta and IL-1 epsilon, function as an antagonist and agonist of NF-kappa B activation through the orphan IL-1 receptor-related protein 2.* J Immunol, 2001. **167**(3): p. 1440-6.
81. Carrier, Y., et al., *Inter-regulation of Th17 cytokines and the IL-36 cytokines in vitro and in vivo: implications in psoriasis pathogenesis.* J Invest Dermatol, 2011. **131**(12): p. 2428-37.
82. Blumberg, H., et al., *Opposing activities of two novel members of the IL-1 ligand family regulate skin inflammation.* J Exp Med, 2007. **204**(11): p. 2603-14.
83. Tortola, L., et al., *Psoriasiform dermatitis is driven by IL-36-mediated DC-keratinocyte crosstalk.* J Clin Invest, 2012. **122**(11): p. 3965-76.
84. Blumberg, H., et al., *IL-1RL2 and its ligands contribute to the cytokine network in psoriasis.* J Immunol, 2010. **185**(7): p. 4354-62.
85. Dietrich, D. and C. Gabay, *Inflammation: IL-36 has proinflammatory effects in skin but not in joints.* Nat Rev Rheumatol, 2014. **10**(11): p. 639-40.
86. Marrakchi, S., et al., *Interleukin-36-receptor antagonist deficiency and generalized pustular psoriasis.* N Engl J Med, 2011. **365**(7): p. 620-8.
87. Navarini, A.A., et al., *Homozygous missense mutation in IL36RN in generalized pustular dermatosis with intraoral involvement compatible with both AGEP and generalized pustular psoriasis.* JAMA Dermatol, 2015. **151**(4): p. 452-3.
88. Shiratori, T., et al., *IL36RN gene analysis of two Japanese patients with generalized pustular psoriasis.* Int J Dermatol, 2015. **54**(2): p. e60-2.

89. Renert-Yuval, Y., et al., *IL36RN mutation causing generalized pustular psoriasis in a Palestinian patient.* Int J Dermatol, 2014. **53**(7): p. 866-8.
90. Pan, J., et al., *Juvenile generalized pustular psoriasis with IL36RN mutation treated with short-term infliximab.* Dermatol Ther, 2016. **29**(3): p. 164-7.
91. Korber, A., et al., *Mutations in IL36RN in patients with generalized pustular psoriasis.* J Invest Dermatol, 2013. **133**(11): p. 2634-7.
92. Hayashi, M., et al., *Novel IL36RN gene mutation revealed by analysis of 8 Japanese patients with generalized pustular psoriasis.* J Dermatol Sci, 2014. **76**(3): p. 267-9.
93. Mahil, S.K., et al., *AP1S3 Mutations Cause Skin Autoinflammation by Disrupting Keratinocyte Autophagy and Up-Regulating IL-36 Production.* J Invest Dermatol, 2016. **136**(11): p. 2251-2259.
94. Setta-Kaffetzi, N., et al., *AP1S3 mutations are associated with pustular psoriasis and impaired Toll-like receptor 3 trafficking.* Am J Hum Genet, 2014. **94**(5): p. 790-7.
95. Fuchs, E. and S. Raghavan, *Getting under the skin of epidermal morphogenesis.* Nat Rev Genet, 2002. **3**(3): p. 199-209.
96. Hsu, Y.C., L. Li, and E. Fuchs, *Emerging interactions between skin stem cells and their niches.* Nat Med, 2014. **20**(8): p. 847-56.
97. Proksch, E., J.M. Brandner, and J.M. Jensen, *The skin: an indispensable barrier.* Exp Dermatol, 2008. **17**(12): p. 1063-72.
98. Haftek, M., *Epidermal barrier disorders and corneodesmosome defects.* Cell Tissue Res, 2015. **360**(3): p. 483-90.
99. Ovaere, P., et al., *The emerging roles of serine protease cascades in the epidermis.* Trends Biochem Sci, 2009. **34**(9): p. 453-63.
100. Eckhart, L., et al., *Cell death by cornification.* Biochim Biophys Acta, 2013. **1833**(12): p. 3471-80.
101. Lin, J.Y. and D.E. Fisher, *Melanocyte biology and skin pigmentation.* Nature, 2007. **445**(7130): p. 843-50.
102. Nestle, F.O., et al., *Skin immune sentinels in health and disease.* Nat Rev Immunol, 2009. **9**(10): p. 679-91.
103. Zaid, A., et al., *Persistence of skin-resident memory T cells within an epidermal niche.* Proc Natl Acad Sci U S A, 2014. **111**(14): p. 5307-12.
104. Sorrell, J.M. and A.I. Caplan, *Fibroblast heterogeneity: more than skin deep.* J Cell Sci, 2004. **117**(Pt 5): p. 667-75.
105. Bergers, G. and S. Song, *The role of pericytes in blood-vessel formation and maintenance.* Neuro Oncol, 2005. **7**(4): p. 452-64.
106. Paquet-Fifield, S., et al., *A role for pericytes as microenvironmental regulators of human skin tissue regeneration.* J Clin Invest, 2009. **119**(9): p. 2795-806.
107. Heinrich, S.T., *Zytologie, Histologie, Entwicklungsgeschichte, makroskopische und mikroskopische Anatomie des Menschen*. Vol. 9th edition. 2005: Springer.
108. Harder, J., J.M. Schroder, and R. Glaser, *The skin surface as antimicrobial barrier: present concepts and future outlooks.* Exp Dermatol, 2013. **22**(1): p. 1-5.

109. Afshar, M. and R.L. Gallo, *Innate immune defense system of the skin.* Vet Dermatol, 2013. **24**(1): p. 32-8 e8-9.
110. Kang, R., et al., *HMGB1 as an autophagy sensor in oxidative stress.* Autophagy, 2011. **7**(8): p. 904-6.
111. Shai, Y., *Mode of action of membrane active antimicrobial peptides.* Biopolymers, 2002. **66**(4): p. 236-48.
112. Sitaram, N. and R. Nagaraj, *Interaction of antimicrobial peptides with biological and model membranes: structural and charge requirements for activity.* Biochim Biophys Acta, 1999. **1462**(1-2): p. 29-54.
113. Zhang, L., A. Rozek, and R.E. Hancock, *Interaction of cationic antimicrobial peptides with model membranes.* J Biol Chem, 2001. **276**(38): p. 35714-22.
114. Brogden, K.A., *Antimicrobial peptides: pore formers or metabolic inhibitors in bacteria?* Nat Rev Microbiol, 2005. **3**(3): p. 238-50.
115. Baker, B.S., et al., *Normal keratinocytes express Toll-like receptors (TLRs) 1, 2 and 5: modulation of TLR expression in chronic plaque psoriasis.* Br J Dermatol, 2003. **148**(4): p. 670-9.
116. Curry, J.L., et al., *Innate immune-related receptors in normal and psoriatic skin.* Arch Pathol Lab Med, 2003. **127**(2): p. 178-86.
117. Kawai, K., *Expression of functional toll-like receptors on cultured human epidermal keratinocytes.* J Invest Dermatol, 2003. **121**(1): p. 217; author reply 217-8.
118. Miller, L.S., et al., *TGF-alpha regulates TLR expression and function on epidermal keratinocytes.* J Immunol, 2005. **174**(10): p. 6137-43.
119. Schauber, J., et al., *Injury enhances TLR2 function and antimicrobial peptide expression through a vitamin D-dependent mechanism.* J Clin Invest, 2007. **117**(3): p. 803-11.
120. de Koning, H.D., et al., *A comprehensive analysis of pattern recognition receptors in normal and inflamed human epidermis: upregulation of dectin-1 in psoriasis.* J Invest Dermatol, 2010. **130**(11): p. 2611-20.
121. Mempel, M., et al., *Toll-like receptor expression in human keratinocytes: nuclear factor kappaB controlled gene activation by Staphylococcus aureus is toll-like receptor 2 but not toll-like receptor 4 or platelet activating factor receptor dependent.* J Invest Dermatol, 2003. **121**(6): p. 1389-96.
122. Pivarcsi, A., et al., *Expression and function of Toll-like receptors 2 and 4 in human keratinocytes.* Int Immunol, 2003. **15**(6): p. 721-30.
123. Kollisch, G., et al., *Various members of the Toll-like receptor family contribute to the innate immune response of human epidermal keratinocytes.* Immunology, 2005. **114**(4): p. 531-41.
124. Schroder, K. and J. Tschopp, *The inflammasomes.* Cell, 2010. **140**(6): p. 821-32.
125. Rathinam, V.A., et al., *The AIM2 inflammasome is essential for host defense against cytosolic bacteria and DNA viruses.* Nat Immunol, 2010. **11**(5): p. 395-402.
126. Loo, Y.M. and M. Gale, Jr., *Immune signaling by RIG-I-like receptors.* Immunity, 2011. **34**(5): p. 680-92.

127. Kupper, T.S. and R.C. Fuhlbrigge, *Immune surveillance in the skin: mechanisms and clinical consequences.* Nat Rev Immunol, 2004. **4**(3): p. 211-22.
128. Honda, K., et al., *Selective contribution of IFN-alpha/beta signaling to the maturation of dendritic cells induced by double-stranded RNA or viral infection.* Proc Natl Acad Sci U S A, 2003. **100**(19): p. 10872-7.
129. Le Bon, A. and D.F. Tough, *Links between innate and adaptive immunity via type I interferon.* Curr Opin Immunol, 2002. **14**(4): p. 432-6.
130. Volkman, A. and J.L. Gowans, *The Origin of Macrophages from Bone Marrow in the Rat.* Br J Exp Pathol, 1965. **46**: p. 62-70.
131. Rot, A., *Neutrophil attractant/activation protein-1 (interleukin-8) induces in vitro neutrophil migration by haptotactic mechanism.* Eur J Immunol, 1993. **23**(1): p. 303-6.
132. Christoffersson, G., et al., *VEGF-A recruits a proangiogenic MMP-9-delivering neutrophil subset that induces angiogenesis in transplanted hypoxic tissue.* Blood, 2012. **120**(23): p. 4653-62.
133. Semerad, C.L., et al., *G-CSF is an essential regulator of neutrophil trafficking from the bone marrow to the blood.* Immunity, 2002. **17**(4): p. 413-23.
134. Miller, L.S., et al., *Inflammasome-mediated production of IL-1beta is required for neutrophil recruitment against Staphylococcus aureus in vivo.* J Immunol, 2007. **179**(10): p. 6933-42.
135. Sawant, K.V., et al., *Chemokine CXCL1 mediated neutrophil recruitment: Role of glycosaminoglycan interactions.* Sci Rep, 2016. **6**: p. 33123.
136. Clark, R.A., et al., *The vast majority of CLA+ T cells are resident in normal skin.* J Immunol, 2006. **176**(7): p. 4431-9.
137. Boyman, O., et al., *Spontaneous development of psoriasis in a new animal model shows an essential role for resident T cells and tumor necrosis factor-alpha.* J Exp Med, 2004. **199**(5): p. 731-6.
138. Conrad, C., et al., *Alpha1beta1 integrin is crucial for accumulation of epidermal T cells and the development of psoriasis.* Nat Med, 2007. **13**(7): p. 836-42.
139. Bos, J.D. and M.L. Kapsenberg, *The skin immune system: progress in cutaneous biology.* Immunol Today, 1993. **14**(2): p. 75-8.
140. Quiroga, M.F., et al., *Activation of signaling lymphocytic activation molecule triggers a signaling cascade that enhances Th1 responses in human intracellular infection.* J Immunol, 2004. **173**(6): p. 4120-9.
141. Schlaak, J.F., et al., *T cells involved in psoriasis vulgaris belong to the Th1 subset.* J Invest Dermatol, 1994. **102**(2): p. 145-9.
142. Brandt, E.B. and U. Sivaprasad, *Th2 Cytokines and Atopic Dermatitis.* J Clin Cell Immunol, 2011. **2**(3).
143. Di Cesare, A., P. Di Meglio, and F.O. Nestle, *A role for Th17 cells in the immunopathogenesis of atopic dermatitis?* J Invest Dermatol, 2008. **128**(11): p. 2569-71.
144. Di Cesare, A., P. Di Meglio, and F.O. Nestle, *The IL-23/Th17 axis in the immunopathogenesis of psoriasis.* J Invest Dermatol, 2009. **129**(6): p. 1339-50.

145. Kistowska, M., et al., *Propionibacterium acnes promotes Th17 and Th17/Th1 responses in acne patients.* J Invest Dermatol, 2015. **135**(1): p. 110-8.
146. Eyerich, K., et al., *Patients with chronic mucocutaneous candidiasis exhibit reduced production of Th17-associated cytokines IL-17 and IL-22.* J Invest Dermatol, 2008. **128**(11): p. 2640-5.
147. Milner, J.D., et al., *Impaired T(H)17 cell differentiation in subjects with autosomal dominant hyper-IgE syndrome.* Nature, 2008. **452**(7188): p. 773-6.
148. Weaver, C.T., et al., *IL-17 family cytokines and the expanding diversity of effector T cell lineages.* Annu Rev Immunol, 2007. **25**: p. 821-52.
149. Duhen, T., et al., *Production of interleukin 22 but not interleukin 17 by a subset of human skin-homing memory T cells.* Nat Immunol, 2009. **10**(8): p. 857-63.
150. Trifari, S., et al., *Identification of a human helper T cell population that has abundant production of interleukin 22 and is distinct from T(H)-17, T(H)1 and T(H)2 cells.* Nat Immunol, 2009. **10**(8): p. 864-71.
151. Nograles, K.E., et al., *IL-22-producing "T22" T cells account for upregulated IL-22 in atopic dermatitis despite reduced IL-17-producing TH17 T cells.* J Allergy Clin Immunol, 2009. **123**(6): p. 1244-52 e2.
152. Toulon, A., et al., *A role for human skin-resident T cells in wound healing.* J Exp Med, 2009. **206**(4): p. 743-50.
153. Cordova, A., et al., *Characterization of human gammadelta T lymphocytes infiltrating primary malignant melanomas.* PLoS One, 2012. **7**(11): p. e49878.
154. Yoshiki, R., et al., *IL-23 from Langerhans cells is required for the development of imiquimod-induced psoriasis-like dermatitis by induction of IL-17A-producing gammadelta T cells.* J Invest Dermatol, 2014. **134**(7): p. 1912-21.
155. Alaibac, M. and A.C. Chu, *T-Lymphocytes bearing the gamma delta T-cell receptor in cutaneous lesions of Langerhans' cell histiocytosis.* Med Pediatr Oncol, 1993. **21**(5): p. 347-9.
156. Volc-Platzer, B., et al., *Accumulation of gamma delta T cells in chronic cutaneous lupus erythematosus.* J Invest Dermatol, 1993. **100**(1): p. 84S-91S.
157. *International drug monitoring: the role of national centres. Report of a WHO meeting.* World Health Organ Tech Rep Ser, 1972. **498**: p. 1-25.
158. Valeyrie-Allanore, L., B. Sassolas, and J.C. Roujeau, *Drug-induced skin, nail and hair disorders.* Drug Saf, 2007. **30**(11): p. 1011-30.
159. Hausmann, O., B. Schnyder, and W.J. Pichler, *Etiology and pathogenesis of adverse drug reactions.* Chem Immunol Allergy, 2012. **97**: p. 32-46.
160. Rawlins, M.D., *Pathogenesis of adverse drug reactions*. Textbook of adverse drug reactions, ed. D. DM. 1977: Oxford University Press. 10-31.
161. Bircher, A.J., *Uncomplicated drug-induced disseminated exanthemas.* Chem Immunol Allergy, 2012. **97**: p. 79-97.
162. Hoetzenecker, W., et al., *Adverse cutaneous drug eruptions: current understanding.* Semin Immunopathol, 2016. **38**(1): p. 75-86.

163. Correia, O., et al., *Cutaneous T-cell recruitment in toxic epidermal necrolysis. Further evidence of CD8+ lymphocyte involvement.* Arch Dermatol, 1993. **129**(4): p. 466-8.
164. Le Cleach, L., et al., *Blister fluid T lymphocytes during toxic epidermal necrolysis are functional cytotoxic cells which express human natural killer (NK) inhibitory receptors.* Clin Exp Immunol, 2000. **119**(1): p. 225-30.
165. Chung, W.H., et al., *Granulysin is a key mediator for disseminated keratinocyte death in Stevens-Johnson syndrome and toxic epidermal necrolysis.* Nat Med, 2008. **14**(12): p. 1343-50.
166. Viard, I., et al., *Inhibition of toxic epidermal necrolysis by blockade of CD95 with human intravenous immunoglobulin.* Science, 1998. **282**(5388): p. 490-3.
167. Saito, N., et al., *An annexin A1-FPR1 interaction contributes to necroptosis of keratinocytes in severe cutaneous adverse drug reactions.* Sci Transl Med, 2014. **6**(245): p. 245ra95.
168. Chung, W.H., et al., *Medical genetics: a marker for Stevens-Johnson syndrome.* Nature, 2004. **428**(6982): p. 486.
169. Hashimoto, K., M. Yasukawa, and M. Tohyama, *Human herpesvirus 6 and drug allergy.* Curr Opin Allergy Clin Immunol, 2003. **3**(4): p. 255-60.
170. Hung, S.I., et al., *HLA-B*5801 allele as a genetic marker for severe cutaneous adverse reactions caused by allopurinol.* Proc Natl Acad Sci U S A, 2005. **102**(11): p. 4134-9.
171. Sidoroff, A., *Acute generalized exanthematous pustulosis.* Chem Immunol Allergy, 2012. **97**: p. 139-48.
172. Baker, H. and T.J. Ryan, *Generalized pustular psoriasis. A clinical and epidemiological study of 104 cases.* Br J Dermatol, 1968. **80**(12): p. 771-93.
173. Beylot, C., P. Bioulac, and M.S. Doutre, *[Acute generalized exanthematic pustuloses (four cases) (author's transl)].* Ann Dermatol Venereol, 1980. **107**(1-2): p. 37-48.
174. Sidoroff, A., et al., *Acute generalized exanthematous pustulosis (AGEP)--a clinical reaction pattern.* J Cutan Pathol, 2001. **28**(3): p. 113-9.
175. Feldmeyer, L., K. Heidemeyer, and N. Yawalkar, *Acute Generalized Exanthematous Pustulosis: Pathogenesis, Genetic Background, Clinical Variants and Therapy.* Int J Mol Sci, 2016. **17**(8).
176. Sidoroff, A., et al., *Risk factors for acute generalized exanthematous pustulosis (AGEP)-results of a multinational case-control study (EuroSCAR).* Br J Dermatol, 2007. **157**(5): p. 989-96.
177. Haro-Gabaldon, V., et al., *Acute generalized exanthematous pustulosis with cytomegalovirus infection.* Int J Dermatol, 1996. **35**(10): p. 735-7.
178. Lee, D., et al., *Acute generalized exanthematous pustulosis induced by parvovirus b19 infection.* Ann Dermatol, 2014. **26**(3): p. 399-400.
179. Lim, C.S. and S.L. Lim, *Acute generalized exanthematous pustulosis associated with asymptomatic Mycoplasma pneumoniae infection.* Arch Dermatol, 2009. **145**(7): p. 848-9.

180. Manzano, S., et al., *[Acute generalized exanthematous pustulosis: first case associated with a Chlamydia pneumoniae infection].* Arch Pediatr, 2006. **13**(9): p. 1230-2.
181. Taguchi, K., et al., *Acute generalized exanthematous pustulosis induced by Mycoplasma pneumoniae infection.* J Dermatol, 2016. **43**(1): p. 113-4.
182. Cannistraci, C., et al., *Acute generalized exanthematous pustulosis in cystic echinococcosis: immunological characterization.* Br J Dermatol, 2003. **148**(6): p. 1245-9.
183. Ben Said, Z., et al., *[Acute generalized exanthematous pustulosis following a spider bite: three cases from Tunisia].* Ann Dermatol Venereol, 2010. **137**(12): p. 813-8.
184. Pippirs, U., et al., *Acute generalized exanthematous pustulosis following a Loxosceles spider bite in Great Britain.* Br J Dermatol, 2009. **161**(1): p. 208-9.
185. Britschgi, M., et al., *T-cell involvement in drug-induced acute generalized exanthematous pustulosis.* J Clin Invest, 2001. **107**(11): p. 1433-41.
186. Szatkowski, J. and R.A. Schwartz, *Acute generalized exanthematous pustulosis (AGEP): A review and update.* J Am Acad Dermatol, 2015. **73**(5): p. 843-8.
187. Sulewski, R.J., Jr., M. Blyumin, and F.A. Kerdel, *Acute generalized exanthematous pustulosis due to clindamycin.* Dermatol Online J, 2008. **14**(7): p. 14.
188. Pichler, W.J., *Delayed drug hypersensitivity reactions.* Ann Intern Med, 2003. **139**(8): p. 683-93.
189. Anliker, M.D. and B. Wuthrich, *Acute generalized exanthematous pustulosis due to sulfamethoxazol with positive lymphocyte transformation test (LTT).* J Investig Allergol Clin Immunol, 2003. **13**(1): p. 66-8.
190. Nishio, D., et al., *T cell populations propagating in the peripheral blood of patients with drug eruptions.* J Dermatol Sci, 2007. **48**(1): p. 25-33.
191. Britschgi, M. and W.J. Pichler, *Acute generalized exanthematous pustulosis, a clue to neutrophil-mediated inflammatory processes orchestrated by T cells.* Curr Opin Allergy Clin Immunol, 2002. **2**(4): p. 325-31.
192. Schaerli, P., et al., *Characterization of human T cells that regulate neutrophilic skin inflammation.* J Immunol, 2004. **173**(3): p. 2151-8.
193. Kabashima, R., et al., *Increased circulating Th17 frequencies and serum IL-22 levels in patients with acute generalized exanthematous pustulosis.* J Eur Acad Dermatol Venereol, 2011. **25**(4): p. 485-8.
194. Sugiura, K., et al., *A novel IL36RN/IL1F5 homozygous nonsense mutation, p.Arg10X, in a Japanese patient with adult-onset generalized pustular psoriasis.* Br J Dermatol, 2012. **167**(3): p. 699-701.
195. Onoufriadis, A., et al., *Mutations in IL36RN/IL1F5 are associated with the severe episodic inflammatory skin disease known as generalized pustular psoriasis.* Am J Hum Genet, 2011. **89**(3): p. 432-7.
196. Kanazawa, N., et al., *Novel IL36RN mutation in a Japanese case of early onset generalized pustular psoriasis.* J Dermatol, 2013. **40**(9): p. 749-51.

197. Navarini, A.A., et al., *Rare variations in IL36RN in severe adverse drug reactions manifesting as acute generalized exanthematous pustulosis.* J Invest Dermatol, 2013. **133**(7): p. 1904-7.
198. Gautier, L., et al., *affy--analysis of Affymetrix GeneChip data at the probe level.* Bioinformatics, 2004. **20**(3): p. 307-15.
199. Gentleman, R.C., et al., *Bioconductor: open software development for computational biology and bioinformatics.* Genome Biol, 2004. **5**(10): p. R80.
200. Irizarry, R.A., et al., *Exploration, normalization, and summaries of high density oligonucleotide array probe level data.* Biostatistics, 2003. **4**(2): p. 249-64.
201. Klipper-Aurbach, Y., et al., *Mathematical formulae for the prediction of the residual beta cell function during the first two years of disease in children and adolescents with insulin-dependent diabetes mellitus.* Med Hypotheses, 1995. **45**(5): p. 486-90.
202. Smyth, G.K., *Linear models and empirical bayes methods for assessing differential expression in microarray experiments.* Stat Appl Genet Mol Biol, 2004. **3**: p. Article3.
203. Hatakeyama, M., et al., *SUSHI: an exquisite recipe for fully documented, reproducible and reusable NGS data analysis.* BMC Bioinformatics, 2016. **17**(1): p. 228.
204. Li, B. and C.N. Dewey, *RSEM: accurate transcript quantification from RNA-Seq data with or without a reference genome.* BMC Bioinformatics, 2011. **12**: p. 323.
205. Robinson, M.D., D.J. McCarthy, and G.K. Smyth, *edgeR: a Bioconductor package for differential expression analysis of digital gene expression data.* Bioinformatics, 2010. **26**(1): p. 139-40.
206. Young, M.D., et al., *Gene ontology analysis for RNA-seq: accounting for selection bias.* Genome Biol, 2010. **11**(2): p. R14.
207. Falcon, S. and R. Gentleman, *Using GOstats to test gene lists for GO term association.* Bioinformatics, 2007. **23**(2): p. 257-8.
208. Supek, F., et al., *REVIGO summarizes and visualizes long lists of gene ontology terms.* PLoS One, 2011. **6**(7): p. e21800.
209. Chen, E.Y., et al., *Enrichr: interactive and collaborative HTML5 gene list enrichment analysis tool.* BMC Bioinformatics, 2013. **14**: p. 128.
210. Strittmatter, G.E., et al., *Human Primary Keratinocytes as a Tool for the Analysis of Caspase-1-Dependent Unconventional Protein Secretion.* Methods Mol Biol, 2016. **1459**: p. 135-47.
211. Song, H.S., et al., *Immunohistochemical Comparison of IL-36 and the IL-23/Th17 Axis of Generalized Pustular Psoriasis and Acute Generalized Exanthematous Pustulosis.* Ann Dermatol, 2016. **28**(4): p. 451-6.
212. van de Veerdonk, F.L., et al., *IL-38 binds to the IL-36 receptor and has biological effects on immune cells similar to IL-36 receptor antagonist.* Proc Natl Acad Sci U S A, 2012. **109**(8): p. 3001-5.
213. Tak, P.P. and G.S. Firestein, *NF-kappaB: a key role in inflammatory diseases.* J Clin Invest, 2001. **107**(1): p. 7-11.

214. Ohto, U., et al., *Structural analyses of human Toll-like receptor 4 polymorphisms D299G and T399I.* J Biol Chem, 2012. **287**(48): p. 40611-7.
215. Hage, D.S., et al., *Characterization of drug interactions with serum proteins by using high-performance affinity chromatography.* Curr Drug Metab, 2011. **12**(4): p. 313-28.
216. Palleria, C., et al., *Pharmacokinetic drug-drug interaction and their implication in clinical management.* J Res Med Sci, 2013. **18**(7): p. 601-10.
217. Ghuman, J., et al., *Structural basis of the drug-binding specificity of human serum albumin.* J Mol Biol, 2005. **353**(1): p. 38-52.
218. Qiao, S., et al., *Structural basis for lipopolysaccharide insertion in the bacterial outer membrane.* Nature, 2014. **511**(7507): p. 108-11.
219. Nickoloff, B.J., *Keratinocytes regain momentum as instigators of cutaneous inflammation.* Trends Mol Med, 2006. **12**(3): p. 102-6.
220. Watanabe, H., et al., *Activation of the IL-1beta-processing inflammasome is involved in contact hypersensitivity.* J Invest Dermatol, 2007. **127**(8): p. 1956-63.
221. Feldmeyer, L., et al., *The inflammasome mediates UVB-induced activation and secretion of interleukin-1beta by keratinocytes.* Curr Biol, 2007. **17**(13): p. 1140-5.
222. Vigne, S., et al., *IL-36R ligands are potent regulators of dendritic and T cells.* Blood, 2011. **118**(22): p. 5813-23.
223. Iwakura, Y. and H. Ishigame, *The IL-23/IL-17 axis in inflammation.* J Clin Invest, 2006. **116**(5): p. 1218-22.
224. Pennino, D., et al., *IL-17 amplifies human contact hypersensitivity by licensing hapten nonspecific Th1 cells to kill autologous keratinocytes.* J Immunol, 2010. **184**(9): p. 4880-8.
225. Albanesi, C., A. Cavani, and G. Girolomoni, *IL-17 is produced by nickel-specific T lymphocytes and regulates ICAM-1 expression and chemokine production in human keratinocytes: synergistic or antagonist effects with IFN-gamma and TNF-alpha.* J Immunol, 1999. **162**(1): p. 494-502.
226. Chiricozzi, A., et al., *Integrative responses to IL-17 and TNF-alpha in human keratinocytes account for key inflammatory pathogenic circuits in psoriasis.* J Invest Dermatol, 2011. **131**(3): p. 677-87.
227. Martin, M.U. and H. Wesche, *Summary and comparison of the signaling mechanisms of the Toll/interleukin-1 receptor family.* Biochim Biophys Acta, 2002. **1592**(3): p. 265-80.
228. Cahill, C.M. and J.T. Rogers, *Interleukin (IL) 1beta induction of IL-6 is mediated by a novel phosphatidylinositol 3-kinase-dependent AKT/IkappaB kinase alpha pathway targeting activator protein-1.* J Biol Chem, 2008. **283**(38): p. 25900-12.
229. Endres, S., J.W. van der Meer, and C.A. Dinarello, *Interleukin-1 in the pathogenesis of fever.* Eur J Clin Invest, 1987. **17**(6): p. 469-74.
230. Dinarello, C.A., et al., *Interleukin-6 as an endogenous pyrogen: induction of prostaglandin E2 in brain but not in peripheral blood mononuclear cells.* Brain Res, 1991. **562**(2): p. 199-206.

231. Liang, Y., et al., *Six-transmembrane epithelial antigens of the prostate comprise a novel inflammatory nexus in patients with pustular skin disorders.* J Allergy Clin Immunol, 2016.
232. Takahashi, K., et al., *Interleukin (IL)-1beta Is a Strong Inducer of IL-36gamma Expression in Human Colonic Myofibroblasts.* PLoS One, 2015. **10**(11): p. e0138423.
233. Franchimont, D., et al., *Deficient host-bacteria interactions in inflammatory bowel disease? The toll-like receptor (TLR)-4 Asp299gly polymorphism is associated with Crohn's disease and ulcerative colitis.* Gut, 2004. **53**(7): p. 987-92.
234. Eyking, A., et al., *Toll-like receptor 4 variant D299G induces features of neoplastic progression in Caco-2 intestinal cells and is associated with advanced human colon cancer.* Gastroenterology, 2011. **141**(6): p. 2154-65.
235. Hold, G.L., et al., *A functional polymorphism of toll-like receptor 4 gene increases risk of gastric carcinoma and its precursors.* Gastroenterology, 2007. **132**(3): p. 905-12.
236. Tal, G., et al., *Association between common Toll-like receptor 4 mutations and severe respiratory syncytial virus disease.* J Infect Dis, 2004. **189**(11): p. 2057-63.
237. Hold, G.L., et al., *The TLR4 D299G and T399I SNPs are constitutively active to up-regulate expression of Trif-dependent genes.* PLoS One, 2014. **9**(11): p. e111460.
238. Yamakawa, N., et al., *Human TLR4 polymorphism D299G/T399I alters TLR4/MD-2 conformation and response to a weak ligand monophosphoryl lipid A.* Int Immunol, 2013. **25**(1): p. 45-52.
239. Zarember, K.A. and P.J. Godowski, *Tissue expression of human Toll-like receptors and differential regulation of Toll-like receptor mRNAs in leukocytes in response to microbes, their products, and cytokines.* J Immunol, 2002. **168**(2): p. 554-61.
240. Foster, S.L., D.C. Hargreaves, and R. Medzhitov, *Gene-specific control of inflammation by TLR-induced chromatin modifications.* Nature, 2007. **447**(7147): p. 972-8.
241. Ostuni, R., et al., *Latent enhancers activated by stimulation in differentiated cells.* Cell, 2013. **152**(1-2): p. 157-71.
242. Yoshida, K., et al., *The transcription factor ATF7 mediates lipopolysaccharide-induced epigenetic changes in macrophages involved in innate immunological memory.* Nat Immunol, 2015. **16**(10): p. 1034-43.
243. Netea, M.G., et al., *Innate immune memory: a paradigm shift in understanding host defense.* Nat Immunol, 2015. **16**(7): p. 675-9.
244. DeAngelis, J.T., W.J. Farrington, and T.O. Tollefsbol, *An overview of epigenetic assays.* Mol Biotechnol, 2008. **38**(2): p. 179-83.
245. Chi, H.H., et al., *IL-36 Signaling Facilitates Activation of the NLRP3 Inflammasome and IL-23/IL-17 Axis in Renal Inflammation and Fibrosis.* J Am Soc Nephrol, 2017.
246. Pichler, W.J., *The p-i Concept: Pharmacological Interaction of Drugs With Immune Receptors.* World Allergy Organ J, 2008. **1**(6): p. 96-102.

247. Schmidt, M., et al., *Crucial role for human Toll-like receptor 4 in the development of contact allergy to nickel.* Nat Immunol, 2010. **11**(9): p. 814-9.
248. Ariza, A., et al., *Study of protein haptenation by amoxicillin through the use of a biotinylated antibiotic.* PLoS One, 2014. **9**(3): p. e90891.

Supplementary material

1. Supplementary figures

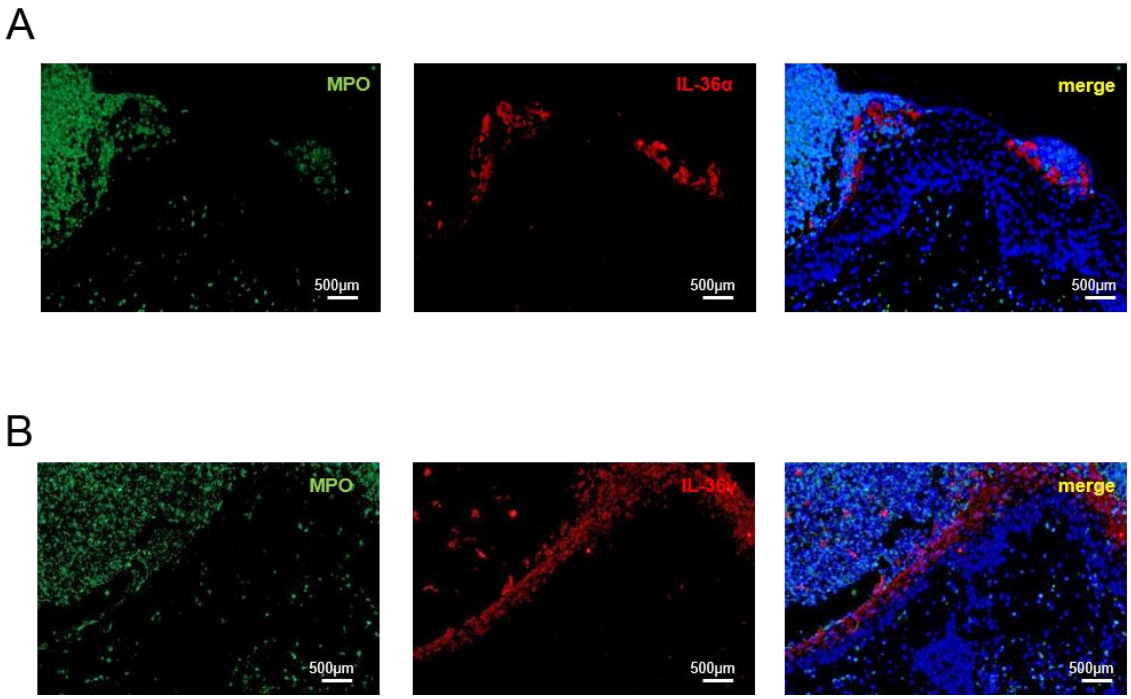

Suppl. Fig 1. IL-36 is not expressed by neutrophils in AGEP skin. *Pustule-containing sections of AGEP skin samples were co-labeled with anti-myeloperoxidase (MPO, green), and IL-36a (red) (A) or IL-36 (red) (B). Cell nuclei appear in blue (DAPI).*

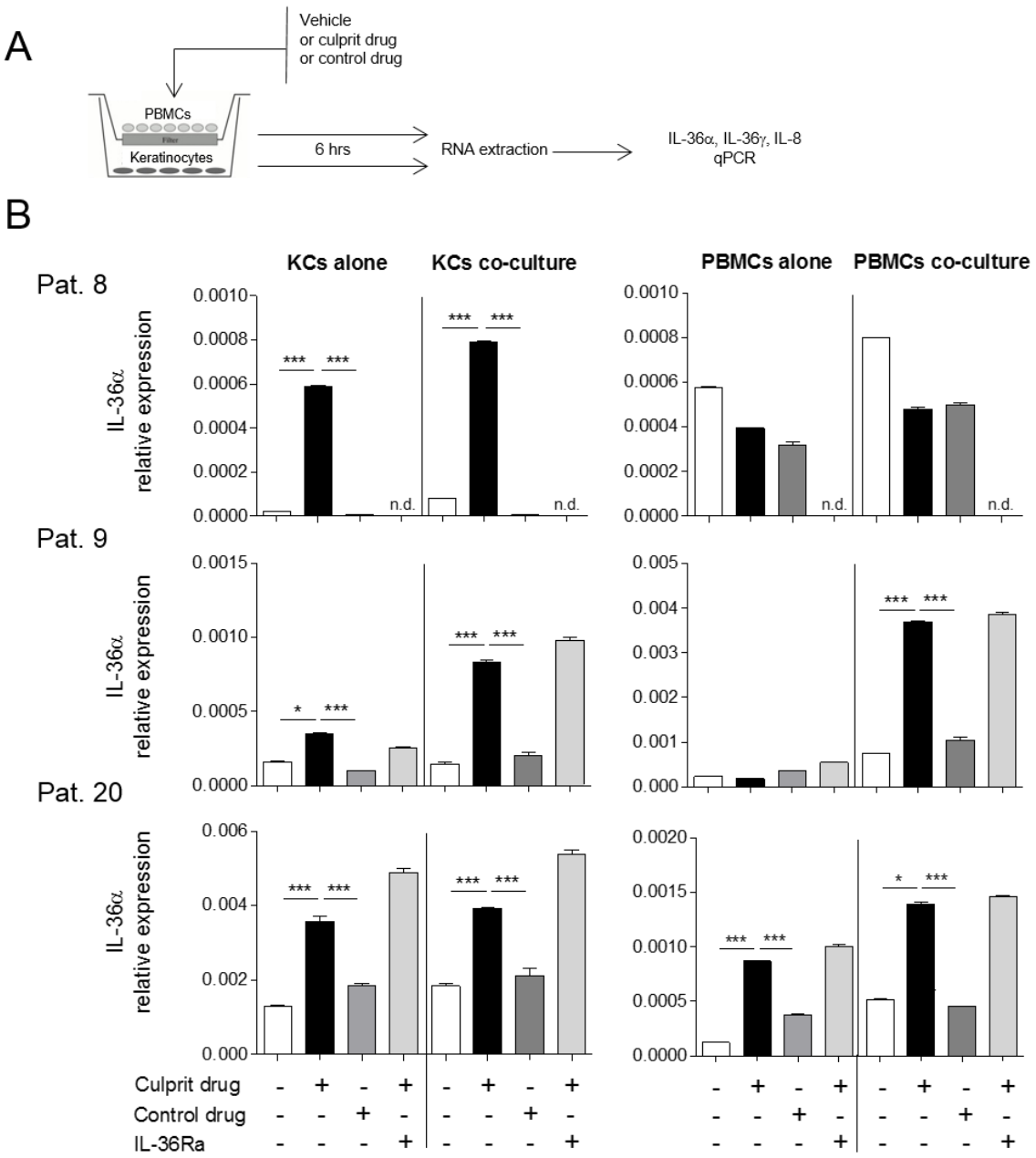

Suppl. Fig. 2. Culprit drugs induce IL-36a in PBMC and keratinocytes co-culture system. *PBMC and autologous keratinocytes (KC) from patients having experienced AGEP but in remission at the time of blood and hair collection were cultured either alone or together in a transwell system allowing for soluble factor-mediated interactions (A). Patients' cells were exposed to the culprit drug (Amoxicillin 1mg/ml, patient 8; Letrozole 100nM, patient 9; Vancomycin 500 µg/ml, patient 20) or a control drug (Metamizole 100µg/ml, patient 8; Carbamazepine 10mg/ml, patient 9; Amoxicillin 1mg/ml, patient 20) in presence or absence of IL-36RA (1µg/ml). After 6 hrs of culture, RNA was extracted from keratinocytes (left panels) and PBMC (right panels) to measure IL-36a transcripts (B). Relative IL-36a expression in KC and PBMC cultured either alone or in coculture as indicated and exposed to the culprit drug or a control drug in presence or absence of IL-36Ra is shown for each tested patient. Expression is expressed as* $2^{-\Delta CT}$*, which represents the target gene expression relative to the reference gene (RPL27). Mean±SD of replicates are shown. *p<0.05; **p<0.01; ***p<0.001.*

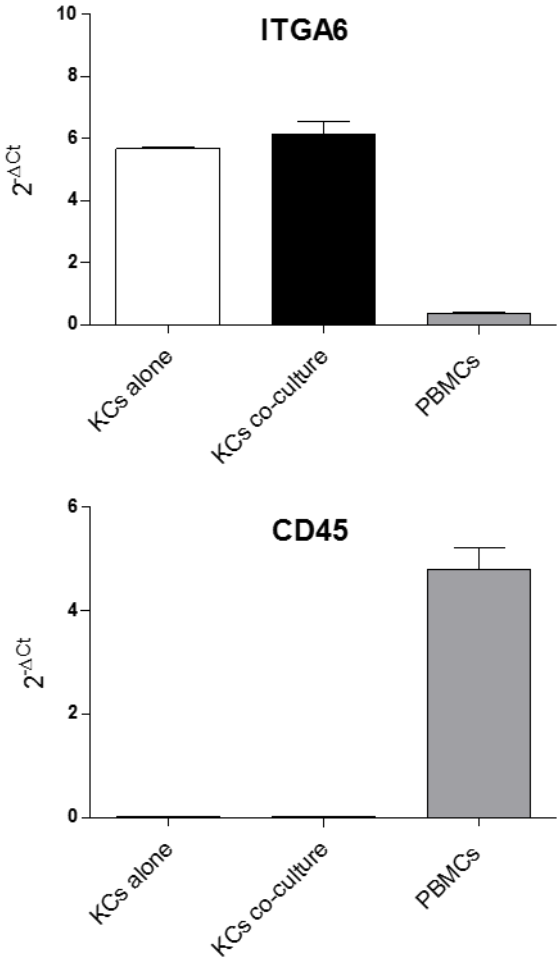

Suppl. Fig 3. Purity of PBMC and keratinocyte fraction in coculture. *After 6 hrs of coculture, RNA were extracted from PBMC and autologous keratinocytes using primers to CD45 (PBMC marker) and ITGA6 (keratinocyte marker). Expression is expressed as* $2^{-\Delta CT}$*, which represents the target gene expression relative to the reference gene (RPL27). Mean±SD of replicates are shown.*

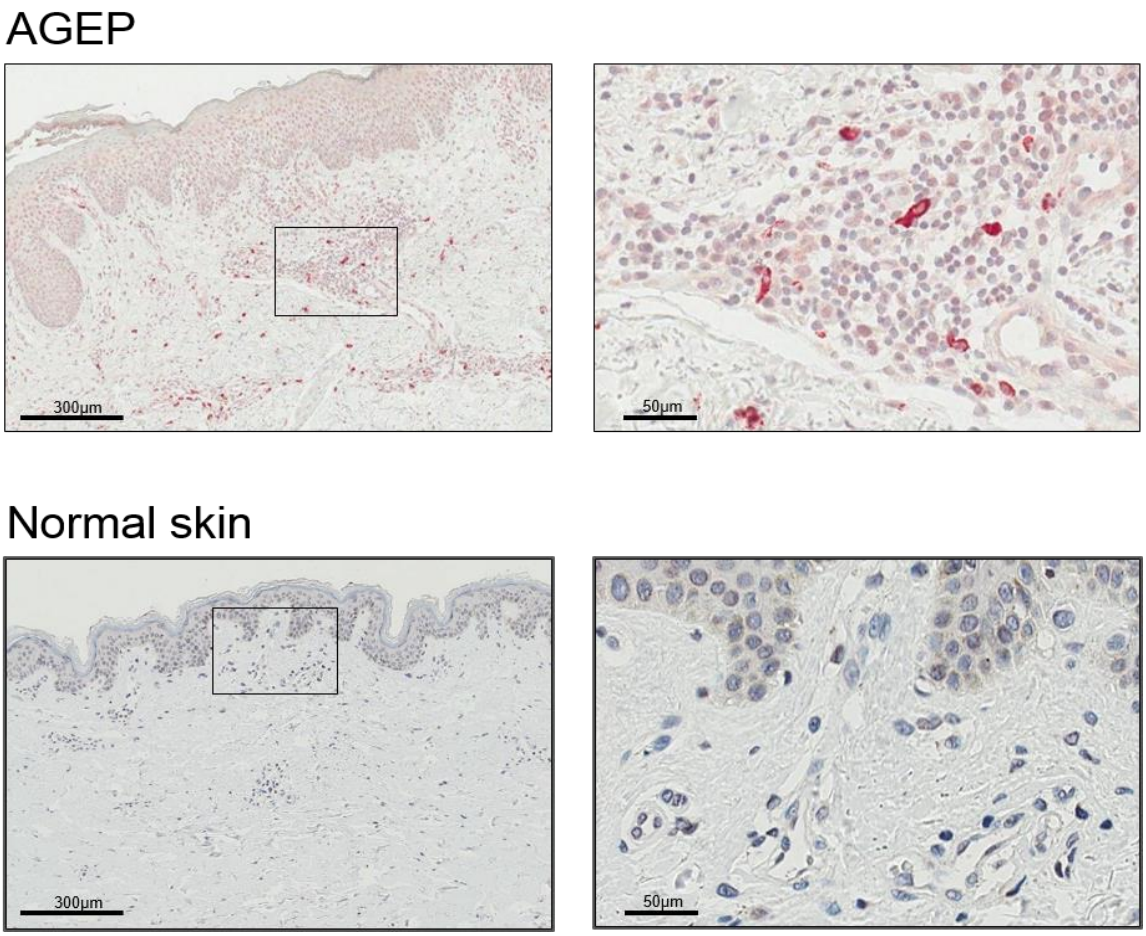

Suppl. Fig 4. IL-8 is expressed in pustular regions of lesional skin biopsies from patients suffering from AGEP. *Immunohistochemical analysis of lesional skin biopsies revealed that IL-8 is expressed at the site of pustules in AGEP in dermal immune cells but not by keratinocytes. Representative picture of 18 AGEP cases is shown (upper panels). IL-8 was not detectable in normal skin from healthy donors (lower panels).*

2. Supplementary tables

Suppl. Table 1. AGEP patients' characteristics and biological data.

Nr.	age	sex	CRP	Leukocytes	Neutrophils	Eosinophils	Body temperature
1	32	F	91	10,44	6,68	0,47	36,7
2	16	M	7,3	24,38	18,31	0,68	36,5
3	71	M	17	12,45	11,49	0,02	36,5
4	54	F	35	11,3	7,88	1,18	37,5
5	58	M	81	11,35	N.A.	N.A.	N.A.
6	41	F	61	25,64	23,15	0,01	36,3
7	81	F	130	21,68	20,57	0,06	N.A.
8	**63**	**M**	**106**	**19,37**	**18,03**	**0,7**	**39,3**
9	**49**	**F**	**40**	**10,89**	**9,92**	**0,07**	**38,2**
10	**33**	**F**	**70**	**25,04**	**23,38**	**0,72**	**38,8**
11	38	M	60	24,86	22,56	0,37	37,3
12	72	M	58	19,71	17,17	0,5	N.A.
13	68	M	233	7,46	6,27	0,12	37,2
14	85	F	180	17,74	15,09	0	36,5
15	61	M	272	27,68	26,6	0	38
16	47	F	119	17	15,1	0,2	38,8
17	51	F	249	25,53	22,49	0,33	37,3
18	43	F	59	13,5	12,86	0	37,4
19	21	F	8,3	9,98	5,9	1,65	37,4
20	**76**	**F**	**308**	**24,36**	**23,23**	**0,04**	**36,1**
21	36	M	34	10,02	8,58	0,37	37,1
22	74	F	18	8.67	6.65	0.00	36.8
23	90	F	23	14.29	12.55	0.31	36.3
24	85	M	69	13.36	10.44	0.43	36.5
25	77	F	N.A.	N.A.	N.A.	N.A.	N.A.
26	56	M	54	12.99	9.72	0.91	N.A.
27	73	F	23	10.54	8.99	0.05	N.A.
28	40	F	2.4	11.45	10.83	0.08	37.1

in bold: cells from these patients have been used in experiments shown in figures 4, 5 and supplementary figure 2.

Suppl. Table 2. AGEP patients – Patch and Prick tests, LTT, culprit drugs and presence of *IL36RN* mutations

Nr.	Patch test	Prick	LTT	Drug	*IL36RN*
1	N.A.	negative	negative	Amoxicillin	n.d.
2	N.A.	N.A.	N.A.	Terbinafin	n.d.
3	negative	negative	negative	Metformin	No mutation
4	negative	negative	N.A.	unknown	No mutation
5	positiv	positive	negative	unknown	n.d.
6	negative	negative	negative	Lonsoprazol / Clarithromycin	n.d.
7	N.A.	N.A.	N.A.	unknown	n.d.
8	**N.A.**	**N.A.**	**positive**	**Amoxicillin**	**No mutation**
9	**N.A.**	**N.A.**	**positive**	**Letrozole**	**n.d.**
10	**positive**	**positive**	**positive**	**Amoxicillin**	**No mutation**
11	N.A.	N.A.	N.A.	Amoxicillin	n.d.
12	N.A.	N.A.	N.A.	Floxapen	n.d.
13	negative	negative	N.A.	Ceftriaxon	n.d.
14	N.A.	N.A.	N.A.	Ciprofloxacin / Metamizol / Paracetamol	n.d.
15	N.A.	N.A.	N.A.	Amoxicillin	n.d.
16	positive	positive	negative	Novalgin	n.d.
17	negative	negative	N.A.	Ibuprofen / Pure Life Cleanse	No mutation
18	N.A.	N.A.	N.A.	Terbinafin	n.d.
19	positive	positive	positive	unknown	n.d.
20	**N.A.**	**N.A.**	**N.A.**	**Vancomycin**	**n.d.**
21	N.A.	N.A.	positive	Fluconazole	n.d.
22	N.A.	N.A.	N.A.	Unknown	n.d.
23	N.A.	N.A.	N.A.	unknown	n.d.
24	N.A.	N.A.	N.A.	Amoxicillin	n.d.
25	N.A.	N.A.	N.A.	Amoxicillin	n.d.
26	N.A.	N.A.	positive	Acetazolamide	n.d.
27	N.A.	N.A.	N.A.	Cotrimoxazole	n.d.
28	Positive	Positive	negative	Cotrimoxazole / Codein / Paracetamol	n.d.

n.d.: not determined; in bold: cells from these patients have been used in experiments shown in figures 4, 5 and supplementary figure 2.

Suppl. Table 3. Genes with significantly different expression as compared to normal skin

Unique for AGEP	Common	Unique for MPR
SERPINA1	*ALDH1A1*	*CCL27*
ASPN	*APOC1*	*CXCL11*
CD163	*DPT*	*CXCL9*
S100A9	*FADS2*	*CA2*
S100A12	*FABP9*	*COL14A1*
S100A8	*GAL*	*ELOVL5*
S100A9	*ITGBL1*	*GSDMC*
CA6	*LCE3D*	*HERC6*
EIF1AX	*LPHN3*	*INSIG1*
PI3	*MGST1*	*CXCL10*
FGFR1	*NR4A2*	*IGHG1*
FLG2	*PTN*	*IGKC*
FLG	*THRSP*	*KRT79*
HEPHL1	*SFRP2*	*LUM*
IL1F6	*SOAT1*	*PLA2G12A*
IL1F9	*STMN2*	*PLA2G2A*
IGKC	*TCHH*	*PRDX6*
IGHA1	*EIF1AX*	*PLA2G7*
IGHA2	*EIF1AY*	*IFIT3*
IGKC		*SPRR4*
IL-8		
IGHG2		
IGHG4		
KRT16		
KRT2		
KRT6A		
KRT6C		
LTF		
LOR		
MSMB		
POSTN		
ROPN1B		
S100A7A		
SAA1		
SAA2		
SERPINB3		
SERPINB4		
SERPINB13		
SLC6A14		
SPRR2B		
DCT		
TCN1		
EIF1AX		

Suppl. Table 4. Top 50 upregulated genes in AGEP biopsies (n=8) as compared to normal skin (n=7). Affymetrix Human Exon 1.0 ST Array analysis

Identifier	Gene name	log2(ratio)	ratio	p value
ENSG00000057149	*SERPINB3*	3.627	12.36	6.34E-06
ENSG00000163221	*S100A12*	3.264	9.609	0.0001602
ENSG00000196805	*SPRR2B*	2.507	5.685	2.98E-05
ENSG00000184330	*S100A7A*	2.464	5.518	9.88E-05
ENSG00000124102	*PI3*	2.462	5.508	9.02E-05
ENSG00000012223	*LTF*	2.452	5.474	3.85E-05
ENSG00000181333	*HEPHL1*	2.367	5.159	0.0001375
ENSG00000206073	*SERPINB4*	2.328	5.022	0.000815
ENSG00000163220	*S100A9*	2.245	4.741	0.0002109
ENSG00000087916	*SLC6A14*	2.142	4.413	0.000105
ENSG00000134827	*TCN1*	1.921	3.788	0.01886
ENSG00000177575	*CD163*	1.657	3.153	0.004581
ENSG00000134339	*SAA2*	1.623	3.079	0.003722
ENSG00000136688	***IL1F9***	**1.616**	**3.064**	**0.0006775**
ENSG00000163202	*LCE3D*	1.601	3.033	0.02765
ENSG00000170465	*KRT6C*	1.574	2.977	0.04494
ENSG00000197641	*SERPINB13*	1.56	2.949	0.0004119
ENSG00000186832	*KRT16*	1.515	2.858	0.001006
ENSG00000148346	*LCN2*	1.453	2.737	0.001458
ENSG00000198553	*KCNRG*	1.371	2.587	0.0001009
ENSG00000143556	*S100A7*	1.363	2.572	0.0006319
ENSG00000129226	*CD68*	1.358	2.563	0.006454
ENSG00000189057	*FAM111B*	1.358	2.562	0.0006161
ENSG00000110077	*MS4A6A*	1.351	2.552	0.006225
ENSG00000147697	*GSDMC*	1.332	2.517	4.18E-05
ENSG00000165168	*CYBB*	1.321	2.499	0.04744
ENSG00000124107	*SLPI*	1.321	2.498	0.006837
ENSG00000155659	*VSIG4*	1.317	2.492	0.02365
ENSG00000124491	*F13A1*	1.31	2.48	0.005231
ENSG00000185966	*LCE3E*	1.302	2.465	0.0675
ENSG00000214787	*MS4A4E*	1.279	2.427	0.001563
ENSG00000199004	*MIR21*	1.26	2.395	0.001729
ENSG00000165474	*GJB2*	1.256	2.389	0.0002327
ENSG00000137462	*TLR2*	1.253	2.384	0.001919
ENSG00000006074	*CCL18*	1.239	2.36	0.1121
ENSG00000213927	*CCL27*	1.227	2.341	0.03032
ENSG00000166535	*A2ML1*	1.223	2.334	0.012
ENSG00000198074	*AKR1B10*	1.217	2.325	0.06558
ENSG00000149968	*MMP3*	1.196	2.291	0.1771
ENSG00000092295	*TGM1*	1.156	2.228	0.001027
ENSG00000169429	***IL8***	**1.153**	**2.225**	**0.0103**
ENSG00000170688	*OR5E1P*	1.151	2.221	0.03809
ENSG00000179477	*ALOX12B*	1.133	2.193	3.23E-05
ENSG00000127954	*STEAP4*	1.132	2.192	0.004494
ENSG00000062038	*CDH3*	1.121	2.175	0.002682
ENSG00000125780	*TGM3*	1.102	2.147	0.008916

ENSG00000205420	*KRT6A*	1.092	2.132	0.002187
ENSG00000105427	*CNFN*	1.09	2.128	0.004554
ENSG00000149573	*MPZL2*	1.076	2.108	0.0002388
ENSG00000134757	*DSG3*	1.072	2.102	0.00123

Suppl. Table 5. Top 50 upregulated genes in AGEP biopsies (n=8) as compared to MPR skin (n=6). Affymetrix Human Exon 1.0 ST Array analysis

Identifier	Gene name	log2(ratio)	ratio	p-value
ENSG00000057149	*SERPINB3*	2.798	6.95	0.0009307
ENSG00000206073	*SERPINB4*	2.694	6.47	0.001229
ENSG00000163221	*S100A12*	2.642	6.24	0.0005447
ENSG00000012223	*LTF*	2.497	5.65	0.0003801
ENSG00000134827	*TCN1*	2.31	4.96	0.002876
ENSG00000184330	*S100A7A*	1.989	3.97	0.004018
ENSG00000087916	*SLC6A14*	1.949	3.86	0.0008485
ENSG00000134339	*SAA2*	1.907	3.75	0.0223
ENSG00000153802	*TMPRSS11D*	1.831	3.56	0.001073
ENSG00000149968	*MMP3*	1.588	3.01	0.03996
ENSG00000196805	*SPRR2B*	1.56	2.95	0.003465
ENSG00000148346	*LCN2*	1.547	2.92	0.002194
ENSG00000181333	*HEPHL1*	1.533	2.89	0.009847
ENSG00000202042	*SNORD49B*	1.522	2.87	0.003253
ENSG00000163220	*S100A9*	1.466	2.76	0.005031
ENSG00000167755	*KLK6*	1.421	2.68	0.007998
ENSG00000167759	*KLK13*	1.378	2.60	0.007276
ENSG00000136688	***IL1F9***	**1.346**	**2.54**	**0.005832**
ENSG00000075673	*ATP12A*	1.3	2.46	0.01231
ENSG00000177575	*CD163*	1.27	2.41	0.05099
ENSG00000090382	*LYZ*	1.266	2.40	0.007701
ENSG00000124491	*F13A1*	1.264	2.40	0.03593
ENSG00000165474	*GJB2*	1.254	2.39	0.002016
ENSG00000185275	*CD24L4*	1.234	2.35	3.24E-05
ENSG00000139329	*LUM*	1.224	2.34	0.01131
ENSG00000105835	*PBEF1*	1.192	2.28	0.0006817
ENSG00000176171	*BNIP3*	1.189	2.28	0.01314
ENSG00000165168	*CYBB*	1.167	2.25	0.07221
ENSG00000169429	***IL8***	**1.161**	**2.24**	**0.008632**
ENSG00000169084	*DHRSX*	1.159	2.23	0.004618
ENSG00000110077	*MS4A6A*	1.143	2.21	0.05424
ENSG00000006074	*CCL18*	1.129	2.19	0.08582
ENSG00000173432	*SAA1*	1.106	2.15	0.05391
ENSG00000137462	*TLR2*	1.103	2.15	0.01375
ENSG00000110079	*MS4A4A*	1.094	2.13	0.06057
ENSG00000081041	*CXCL2*	1.089	2.13	0.0001574
ENSG00000124102	*PI3*	1.048	2.07	0.004655
ENSG00000143556	*S100A7*	1.03	2.04	0.002713
ENSG00000121742	*GJB6*	1.025	2.03	0.0006617
ENSG00000199004	*MIR21*	1.017	2.02	0.03609
ENSG00000087086	*FTL*	0.986	1.98	0.07913
ENSG00000129226	*CD68*	0.971	1.96	0.0579
ENSG00000129538	*RNASE1*	0.970	1.96	0.09199
ENSG00000154175	*ABI3BP*	0.942	1.92	0.01506
ENSG00000204020	*LIPN*	0.933	1.91	0.05536
ENSG00000166535	*A2ML1*	0.908	1.88	0.04812
ENSG00000160593	*AMICA1*	0.895	1.86	0.04174

ENSG00000197930	*ERO1L*	0.885	1.85	0.01465
ENSG00000164647	*STEAP1*	0.879	1.84	0.08395
ENSG00000214787	*MS4A4E*	0.879	1.84	0.03828

Curriculum vitae

Name	Meier Barbara
Academic title	Dr. med.
Date of birth	18.04.1985
City of birth	Munich, Germany
Nationality	German
Position	MD PhD student / Resident physician
Address	Schulhausstrasse 35 8706 Meilen Switzerland
E-Mail	barbara.meier2@usz.ch

Education

05/2013 – present	**MD PhD** MD PhD program of the University of Zurich PhD program in Microbiology&Immunology of the University of Zurich and the Swiss Federal Institute of Technology Zurich Research group Prof. Dr. Lars E. French
05/2013 – present	**Master of Science** Medical Biology, University of Zurich
06/2011	**Medical state examination**
02/2010 - 01/2011	**Practical year of medical studies** University Hospital Ulm, University Hospital Zurich
02/2009-04/2015	**MD thesis** Department of Dermatology, University Hospital Ulm Research group Prof. Dr. K. Scharffetter-Kochanek Scholarship: Experimental Medicine, International Graduate School in Molecular Medicine Ulm
09/2007 - 06/2008	**Medical studies** Faculty of Medicine, University of Franche-Comté Besançon, France Scholarship: Erasmus program
10/2006	**Preliminary medical examination**
10/2004 - 02/2011	**Medical studies** Faculty of Medicine, University of Ulm
09/1995 - 06/2004	**Abitur** Ludwigsgymnasium Munich

Professional Experience

05/2013 - present	**MD PhD student / Resident physician** Department of Dermatology, University Hospital Zurich Research group Prof. Dr. L.E. French
03/2012 - 02/2013	**Resident physician** Clinic for Thoracic Surgery, University Hospital Zurich

Scientific publications

2017 *Culprit drug specific IL-36 overexpression in Acute Generalized Exanthematous Pustulosis.* **Meier B**, Feldmeyer L, Jankovic D, Satoh TK, Mellett M, Yerly D, Navarini A, Abe R, Yawalkar N, Chung WH, Contassot E, French LE. Manuscript in preparation.

10/2016 *Pyoderma gangrenosum and Sweet's syndrome: Cutaneous manifestations of autoinflammatory disorders.* **Meier B**, Maul JT & French L.E. Hautarzt 2016. doi:10.1007/s00105-016-3888

07/2016 *In Situ Mapping of Innate Lymphoid Cells in Human Skin: Evidence for Remarkable Differences between Normal and Inflamed Skin.* Brüggen MC, Bauer WM, Reininger B, Clim E, Captarencu C, Steiner GE, Brunner PM, **Meier B**, French LE, Stingl G. J Invest Dermatol. 2016 Jul 22. pii: S0022-202X(16)32126-1. doi: 10.1016/j.jid.2016.07.017.

07/2016 *Tumor hypoxia promotes melanoma growth and metastasis via High Mobility Group Box-1 and M2-like macrophages.* Huber R*, **Meier B***, Otsuka A*, Fenini G, Satoh T, Gehrke S, Widmer D, Levesque MP, …, Kabashima K, Nonomura Y, Dummer R, Contassot E, and French LE. Sci Rep 2016 Jul 18;6:29914 doi: 10.1038/srep29914. *These authors contributed equally.

03/2016 *Cytotoxic cutaneous adverse drug reactions during anti-PD-1 therapy.* Goldinger SM, Stieger P, **Meier B**, Micaletto S, Contassot E, French LE, Dummer R.; Clin Cancer Res. 2016 Mar 8. pii: clincanres.2872.2015.

11/2015 *Canakinumab in adults with steroid-refractory pyoderma gangrenosum.* Kolios AG*, Maul JT*, **Meier B***, Kerl K, Traidl-Hoffmann C, Hertl M, Zillikens D, Röcken M, Ring J, Facchiano A, Mondino C, Yawalkar N, Contassot E, Navarini AA, French LE. Br J Dermatol. 2015 Nov;173(5):1216-23. doi: 10.1111/bjd.14037 *These authors contributed equally.

09/2015 *ABCB5 Identifies Immunoregulatory Dermal Cells.* Schatton T, Yang J, Kleffel S, Uehara M, Barthel SR, Schlapbach C, Zhan Q, Dudeney S, Mueller H, Lee N, de Vries JC, **Meier B**, Vander Beken S, …, Scharffetter-Kochanek K, Murphy GF, Kupper TS, Frank NY, Frank MH. Cell Rep. 2015 Sep 8;12(10):1564-74. doi: 10.1016/j.celrep.2015.08.010.

03/2015 *Severe Sweet's Syndrome with Elevated Cutaneous Interleukin-1β after Azathioprine Exposure: Case Report and Review of the Literature.* Imhof L, **Meier B**, Frei P, Kamarachev J, Rogler G, Kolios A, Navarini AA, Contassot E, French LE. Dermatology. 2015;230(4):293-8. doi: 10.1159/000371879.

01/2015 *Propionibacterium acnes promotes Th17 and Th17/Th1 responses in acne patients.* Kistowska M, **Meier B**, Proust T, Feldmeyer L, Cozzio A, Kuendig T, Contassot E, French LE. J Invest Dermatol. 2015 Jan;135(1):110-8. doi: 10.1038/ jid.2014.290.

07/2014 *Autoinflammatory syndromes-cutaneous manifestations.* **Meier B**, French LE Dtsch Med Wochenschr. 2014 Jul;139(28-29):1468-72. doi: 10.1055/s-0034-1370159.

01/2014 *Metastatic melanoma cell lines do not secrete IL-1β but promote IL-1β production from macrophages.* Gehrke S, Otsuka A, Huber R, **Meier B**, Kistowska M, Fenini G, Cheng P, Dummer R, Kerl K, Contassot E, French LE. J Dermatol Sci. 2014 May;74(2):167-9. doi: 10.1016/ j.jdermsci.2014.01.006.

Acknowledgements

First of all, I thank Prof. Dr. Lars French for giving me the opportunity to work with him and to achieve my PhD in his laboratory. I am very thankful for all your scientific and personal support, for constructive discussions on Monday morning and for all the knowledge you shared with me. I am really inspired by your enthusiasm about research and I am happy that I am able to continue working with you in the future.

A special thank you goes to Dr. Emmanuel Contassot who was always the first contact person for all my concerns. You helped me a lot with the design of experiments, the interpretation of my results and the overall understanding of scientific topics. Also, you taught me very well how to write scientific manuscripts and you were always helping me to improve by giving me constructive feedback. I really enjoyed working with you on adverse drug reactions and I am looking forward to continue working on it.

I thank the members of my thesis committee, Prof. Dr. Onur Boyman, Prof. Dr. Maries van den Broek, Prof. Dr. Annette Oxenius, and Prof. Dr. Thomas Kündig, for their support, for important scientific input to help improving my project, and for inspiring discussions during the thesis committee meetings.

Moreover, I thank my group members Gabriele Fenini, Takashi Satoh, Deepa Mohanan and Mark Mellett for great discussions in our lab meetings and for always helping out – everyone of you is expert in their own field and I am very thankful to be able to exchange our knowledge.

A special thanks goes to Mark Mellett who has been great help with my new project concerning TLR4. I thank you for sharing your knowledge with me and for never getting tired to answer all my questions. You are a very good person and a great colleague, thank you!

I thank my former lab member Magdalena Kistowska for introducing me to all the important research techniques when I started in the lab four years ago. Moerover, I thank Dragana Jankovic for isolating the first set of RNA for the Affymetrix assay which was the basis for the start of my project. Also, I want to thank Laurence Feldmeyer for collecting samples of adverse drug reactions during many years and for helping to start our project. I further thank my former lab member Roman Huber

for great teamwork and involving me in his melanoma project which I enjoyed very much.

Another thanks goes to the members of Hans-Dietmar Beer's research group, Jenny, Martha, Serena and Gerhard, with who I have shared the benches for many years. Thank you for your input in our Friday meetings and for all the good „procrastination times" in our office.

I thank Alexander Navarini for his support and for giving me insight in his whole exome sequencing data. Without you it would have been much more difficult to identify genetic changes in AGEP patients. Thank you!

I want to thank Alaz Özcan Özge for her great help with measuring IL-1β in the blood of AGEP patients. A great thanks goes also to her supervisor Dr. Antonios Kolios who is always willing to help and to collaborate.

I want to thank Karin Schnyder for your help with experiments and for being a very good colleague with a very good heart. I am happy that you did not give up and that we were able to establish the LTT in our Department.

I thank my parents for always being there for me. You are feeling with me since my first day of medical studies and you had to go through even much more in times when I worked for my MD thesis title. The cherry of the cake was certainly my decision to do a PhD and it was probably not always easy to watch me going through times of no sleep and frustration. But you always had an open ear and showed me that you are proud of me. Thank you for being wonderful parents!

I want to thank my sister Stefanie for being a great example in life. I always admired your strong personality, your intelligence, your humour and your big heart and I couldn't be any happier to have such great sister!

Finally, I want to thank my fiancé Oliver for being who he is. You went with me through all my moments of happiness, of sadness and frustration. In moments of doubts, you cheered me up and convinced me to stand up and continue. I am really grateful for all your support and to have you by my side.

Appendix

TITLE

Culprit drug specific IL-36 overexpression in Acute Generalized Exanthematous Pustulosis

Barbara Meier, MD [a], Laurence Feldmeyer, MD, PhD [b], Dragana Jankovic, PhD [a], Takashi K. Satoh, MD, PhD [a], Mark Mellett, PhD [a], Daniel Yerly, PhD [c], Alexander Navarini, MD, PhD [a], Riichiro Abe, MD, PhD [d], Nikhil Yawalkar, MD [b], Chung Wen-Hung [e], Emmanuel Contassot, PhD [a,#], Lars E. French, MD [a,#]

[a] Department of Dermatology, University Hospital, Zürich, Switzerland

[b] Department of Dermatology, Inselspital, Bern University Hospital, University of Bern, Switzerland

[c] Department of Rheumatology, Clinical Immunology and Allergology, Inselspital, Bern University Hospital, University of Bern, Switzerland

[d] Division of Dermatology, Niigata University Graduate School of Medical and Dental Sciences, Niigata, Japan

[e] Department of Dermatology, Drug Hypersensitivity Clinical and Research Center, Chang Gung Memorial Hospital, Taipei and Linkou, Taiwan

[#] Co-senior authors

Correspondence:
Lars E. French, Dermatology Department, University Hospital, Gloriastrasse 31, Zürich, Switzerland. Phone: + 41 44-255 25 50; e-mail: lars.french@usz.ch or Emmanuel Contassot, Dermatology Department, University Hospital, Gloriastrasse 31, Zürich, Switzerland. Phone: + 41 44-255 99 52; e-mail: emmanuel.contassot@usz.ch

ABSTRACT

Background

Acute generalized exanthematous pustulosis (AGEP) is a severe adverse cutaneous drug reaction. Although an involvement of drug-specific T cells has been reported, the physiopathology of AGEP and mechanism of neutrophilic skin inflammation remains incompletely understood. Recently, mutations in *IL-36RN*, the gene encoding the IL-36 receptor antagonist, have been reported to be more frequent in AGEP patients and pustular psoriasis.

Methods

Gene expression profiling, quantitative RT-PCR and immunohistochemistry in skin lesions from patients suffering from AGEP were compared to that of patients with maculo-papular rash (MPR), a benign adverse cutaneous reaction to drugs and healthy skin. The nature of cells secreting upregulated proinflammatory cytokines in AGEP patients' skin was assessed using immunofluorescence. The ability of the causative drug to trigger proinflammatory cytokine production in AGEP patients' peripheral blood mononuclear cells and keratinocytes was assessed using single cell-type cultures or co-culture experiments and subsequent analysis of cytokine production by ELISPOT or quantitative RT-PCR.

Results

An unbiased approach revealed significant IL-36 α and γ upregulation in lesional skin of AGEP patients when compared to MPR. Keratinocytes and macrophages were found to be the source of IL-36γ in AGEP patients. *In vitro*, the causative drug specifically induced IL-36γ release either directly by peripheral blood monocytes, or indirectly in presence of autologous peripheral blood mononuclear cells by keratinocytes of patients with AGEP. Such culprit drug induction of IL-36γ secretion *in vitro* was specific for AGEP and was not observed for MPR.

Conclusions

Our results demonstrate that IL-36γ secretion by monocytes/macrophages and keratinocytes in response to culprit drug exposure likely plays a key role in the pathogenesis of AGEP.

CAPSULE SUMMARY

- IL-36 is overexpressed in lesional skin of patients with acute generalized exanthematous pustulosis (AGEP) and not in patients with a moderate form of drug reaction.
- Culprit drugs selectively induce IL-36 secretion in AGEP patients' monocytes and keratinocytes.
- IL-36 produced by monocytes and keratinocytes from AGEP patients induce the secretion of the neutrophil chemoattractant IL-8

KEYWORDS

Acute generalized exanthematous pustulosis; IL-36; IL-8; culprit drug; monocytes; keratinocytes

ABBREVIATIONS

AGEP: Acute generalized exanthematous pustulosis; MPR: maculo-papular rash; ADR: adverse drug reaction; IL: interleukin; PBMC: Peripheral blood mononuclear cells.

INTRODUCTION

Acute generalized exanthematous pustulosis (AGEP) is a severe adverse cutaneous drug reaction (ADR) caused mainly by antibiotics, antimalarials, and antifungals [1]. Clinically, AGEP is characterized by a disseminated eruption of sterile nonfollicular pustules on the background of a widespread erythematous skin eruption, accompanied with fever and peripheral blood neutrophilia. The pathophysiology of AGEP remains unclear. However, AGEP is currently considered as a T cell-mediated disease [2]. Indeed, drug-specific T cells are suspected to play a central role in AGEP as evidenced by the high levels of T cell stimulation induced by causative (culprit) drugs as measured by the lymphocyte transformation test (LTT) [3]. Furthermore, drug-specific $CD4^+$ and $CD8^+$ T cells have been derived *in vitro* from AGEP patients' peripheral blood. Most of these drug-specific T cells [4] produce IL-8 [5, 6], a powerful neutrophil chemoattractant. IL-8-producing T cells are therefore, considered to be the cause of neutrophil survival and recruitment to the skin [7]. It has also been suggested that Th17 effector cytokines, namely IL-17 and IL-22, stimulate keratinocytes to produce IL-8, and that keratinocyte-derived IL-8 also contributes to neutrophil accumulation in AGEP patients' skin [8]. Hence, T cell- and keratinocyte-derived IL-8 has been proposed to be responsible for the recruitment of neutrophils to the intraepithelial pustules.

AGEP shares certain clinical and histological features with pustular psoriasis. Recently, genetic studies identified mutations in the IL-36 receptor antagonist gene (IL-36RN) in patients with general pustular psoriasis [9-12]. Interestingly, mutations in *IL-36RN* have also been reported in AGEP [13], suggesting that IL-36 signaling dysregulation is involved in the physiopathology of both diseases. IL-36 receptor antagonist (IL-36Ra) inhibits the binding of IL-36α, β and γ to their receptor. A mutation in *IL-36RN* may therefore result in exacerbated IL-36 signaling leading to the production of IL-1, IL-6 and IL-8 and subsequent neutrophilic skin infiltration with pustule formation.

IL-36 cytokines have emerged as important cytokines mediating inflammatory responses in the skin. Indeed, several reports have shown that all IL-36 isoforms are overexpressed in psoriatic skin [14-17]. In keratinocytes, production of IL-36 family members can be induced by TNF, IL-17 and IL-22, cytokines known to be involved in psoriasis which further supports an important role for IL-36 in this disease [18]. Recently, it has been reported that antigen-presenting cells located in human skin, express high levels of IL-36R and are responsive to IL-36 cytokines [19], an observation that further supports an important role of IL-36 in skin biology.

Here, we provide evidence that drugs causing AGEP can specifically trigger IL-36 cytokine production by peripheral blood monocytes and keratinocytes from AGEP patients and subsequently induce IL-8 by peripheral blood mononuclear cells in an IL-36-dependent manner. These observations are supportive of a drug-specific dysregulation of IL-36 signaling

as an important potential driver of AGEP pathogenesis, and identify myeloid cells and keratinocytes as new important players in AGEP.

METHODS

Patients

The characteristics of all studied AGEP patients from the Dermatology Department of the University Hospital of Zürich are presented in Tables 1 and 2. All human samples were collected after informed written patient consent with approval of Local Ethics Committees and according to the Declaration of Helsinki Principles.

Skin biopsy

Skin biopsies were taken from lesional skin of patients in the acute phase of the ADR (4-6mm punch biopsies). Healthy skin samples were obtained from the Department of Plastic Surgery, University Hospital of Zürich. For paraffinization, skin samples were fixed in formalin 4% overnight. For RNA isolation, samples were snap-frozen in liquid nitrogen and stored at -80°C.

Collection of peripheral blood mononuclear cells

Peripheral blood from patients was taken both in the acute phase of the disease and under healthy conditions (at least 6 months after the ADR). Healthy controls were obtained from the Blood Donation Center (Schlieren, Switzerland). Peripheral blood mononuclear cells (PBMC) were isolated using a density gradient (Ficoll-Paque, Pharmacia, Glattbrugg, Switzerland).

Monocyte and T cell purification

Where indicated, $CD14^+$ monocytes were sorted from PBMC by positive selection using magnetic beads (Miltenyi Biotech, Bergisch Gladbach, Germany). $CD3^+$ cells were sorted from the $CD14^-$ fraction by negative selection using a Pan T Cell Isolation Kit (Miltenyi Biotech) according to the manufacturer's instructions. Purity was assessed by flow cytometry (Facscanto A, Becton-Dickinson) using mouse anti-human CD45-PeCy7 (Biolegend, San Diego, CA), mouse anti-human CD3-APC (Biolegend) and mouse anti-human CD14-FITC (Becton-Dickinson, Franklin Lakes, NJ).

Primary keratinocyte culture

Hair follicles were collected from patients at least 6 months after resolution of the ADR. Hair follicle extremities containing outer root sheath were cut, washed in complete keratinocyte medium [20] and incubated for 3 minutes in 1mg/ml Dispase II, followed by three washing steps in medium. The hair was then plated on J2 feeder cells in complete medium and cultured until small colonies of keratinocytes become visible. Cells were splitted at 80% confluence and passaged three times before being used for experiments.

Gene expression array

Sample processing

Gene expression profiling was performed using Human Exon 1.0 ST Affymetrix chips. Raw fluorescence intensity values were analyzed using the R packages Affy [21] and Limma of Bioconductor [22]. Data analysis consisted in the following steps: 1. between-array normalization, 2. probe summary with the rma algorithm, 3. fitting the data to a linear model and 4. detection of differential gene expression. Quantile-normalization was applied to the log2-transformed intensity values as a method for between-array normalization, to ensure that the intensities had similar distributions across arrays [23]. To find genes with significant expression changes between groups, empirical Bayes statistics were applied by moderating the standard errors of the estimated values. P-values were obtained from the moderated t-statistic and corrected for multiple testing with the Benjamini–Hochberg method [24]. The P-value adjustment guarantees a smaller number of false positive findings by controlling the false discovery rate (fdr).

Data analysis

Quality control and gene expression analysis was done using R/Bioconductor software (Fred Hutchinson Cancer Research Center, Seattle, WA) [22]; signal intensity files were summarized using the robust multi array average (RMA) [23] for processing and quantile normalization. A modified t-test using *limma* software (part of the Bioconductor project) [25] was performed to compare the experimental conditions. P-values and the Benjamini-Hochberg False Discovery Rate (FDR) are reported.

RNA-sequencing

Library preparation

RNA quantity and quality were determined with a Qubit® (1.0) Fluorometer (Life Technologies, California, USA) and a Bioanalyzer 2100 (Agilent, Waldbronn, Germany). The TruSeq Stranded mRNA Sample Prep Kit (Illumina, Inc, California, USA) was used in the subsequent steps. Total RNA (1µg) were ribosome depleted and reverse-transcribed into double-stranded cDNA with Actinomycin added during first-strand synthesis. cDNA samples were fragmented, end-repaired and polyadenylated before ligation of TruSeq adapters. Adapters contain the index for multiplexing. Fragments containing TruSeq adapters on both ends were enriched by PCR. Quality and quantity of the enriched libraries were validated using a Qubit® (1.0) Fluorometer and the Bioanalyzer 2100. Libraries were normalized to 10nM in Tris-Cl 10mM, pH8.5 with 0.1% Tween 20.

Cluster Generation and RNA Sequencing

The TruSeq PE Cluster Kit v3-cBot-HS (Illumina, Inc., CA) was used for cluster generation using 8pM of pooled normalized libraries on the cBOT. RNA sequencing was performed on an Illumina HiSeq with a 2500 paired end approach at 2 X126 bp using the TruSeq SBS Kit v3-HS (Illumina, Inc.).

Data analysis

Bioinformatic analysis was performed using SUSHI [26]. In detail, the raw reads were quality checked using Fastqc (http://www.bioinformatics.babraham.ac.uk/projects/fastqc/) and FastQ Screen (http://www.bioinformatics.babraham.ac.uk/projects/fastq_screen/). Quality controlled reads (first five bases trimmed, minimum average quality Q20, minimum tail quality Q10) were aligned to the reference transcriptome (Ensembl GRCh38, not patched) for transcript abundance estimation using RSEM [27]. Differential expression analysis was performed using edgeR [28]. Gene ontology (GO) enrichment analysis was performed using the Bioconductor packages goseq [29] and GOStats [30], and visualized using ReViGo [31]. Enrichment analysis of other gene sets was performed using Enrichr [32].

RNA isolation and Real-Time quantitative PCR

Total RNAs were isolated from AGEP, MPR and healthy skin biopsies, as well as from keratinocytes and PBMC using the RNeasy Mini Kit (Qiagen, Hilden, Germany) according to manufacturer's instructions, followed by cDNA synthesis by reverse-transcription using the RevertAid First Strand cDNA Synthesis Kit (Thermo Scientific, Watham, MA). Real-Time quantitative PCR was performed using a LightCycler® 96 (Roche). The primer sequences were obtained from http://pga.mgh.harvard.edu/primerbank/:

hRPL27 F	5`-ATC GCC AAG AGA TCA AAG ATA A-3'
hRPL27 R	5`-TCT GAA GAC ATC CTT ATT GAC G-3'
hIL36a F	5`-CCA GAC GCT CAT AGC AGT CC-3'
hIL36a R	5`-AGA TGG GGT TCC CTC TGT CTT-3'
hIL36b F	5`-ATG AAC CCA CAA CGG GAG G-3`
hIL36b R	5`-TAA TGC TGC GGC TAA GAG GAG-3`
hIL-36g F	5`-AGG AAG GGC CGT CTA TCA ATC-3'
hIL-36g R	5`-CAC TGT CAC TTC GTG GAA CTG-3'
hIL-36R F	5`-CCG AGG TGT TGG AGA GAC AAT G-3'
hIL-36R R	5`-GGA CCA CAA TGA CAA TCA GCC TC-3'
hIL36RN F	5`-ACT CGG CAT TGA AGG TGC TTT-3'

hIL36RN R	5`-GGG ACC ACG CTG ATC TCT T-3'
hIL-8 F	5`-TTT TGC CAA GGA GTG CTA AAG A-3'
hIL-8 R	5`-AAC CCT CTG CAC CCA GTT TTC-3'
hCD45 F	5'-ACA GCC AGC ACC TTT CCT AC-3'
hCD45 R	5'-GTG CAG GTA AGG CAG CAG A-3'
ITGA6 F	5'-TCA TGG ATC TGC AAA TGG AA-3'
ITGA6 R	5'-AGG GAA CCA ACA GCA ACA TC-3'

Real-time quantitative PCR included an initial denaturation at 95°C for 10 min, followed by 40 cycles at 95°C for 30 s, 55°C for 1 min, 72°C for 1 min, and one cycle at 95°C for 1 min, 55°C for 30 s, 95°C for 30 s. RPL27 was used as a housekeeping gene.

Immunohistochemistry

Five µm paraffin-embedded AGEP, MPR, PP and healthy skin sections were deparaffinized and rehydrated. Antigen demasking was performed using pressure cooker heating for 25 min in Target Retrieval solution (DAKO, Glostrup, Denmark). After permeabilization (0.03% Triton X for 10 minutes), sections were blocked using 5% BSA in PBS for one hour at room temperature and washed.

For immunohistochemistry, sections were stained overnight at 4 °C with 0.5µg/ml goat anti-human IL-36α or 0.5µg/ml goat anti-human IL-36γ (both from R&D, Minneapolis, MN), or 2µg/ml rabbit anti-human IL-8 (LSBio, Seattle, WA). A goat IgG isotype antibody (R&D Systems, Minneapolis, MN) and a rabbit IgG isotype antibody (Abcam, Cambridge, United Kingdom) at corresponding concentrations were used as controls. Slides were washed with PBS and a donkey anti-goat secondary antibody (Abcam) for IL-36α and γ and a goat anti-rabbit (Southern Biotech, Birmingham, USA) for IL-8 was added and incubated for 1 hour at room temperature. Slides were washed with PBS and mounted with an Avidin-Biotin-complex (Vector Laboratories, Peterborough, UK). After 45 min, slides were washed with PBS and AEC - HRP substrate (Vector Laboratories) was added. After washing, slides were counterstained with hematoxylin. Sections were mounted in mounting medium (DAKO) and imaged by using an Aperio ScanScope (Leica Biosystems, Wetzlar, Germany).

For immunofluorescence, sections were then stained overnight at 4 °C with a) 0.5µg/ml goat anti-human IL-36α (R&D Systems), together with either 20µg/ml mouse anti-human CD3 (Dako), 20µg/ml mouse anti-human CD68 (Dako) or 20µg/ml rabbit anti-human MPO (DAKO), or b) with 0.5µg/ml goat anti-human IL-36γ (R&D Systems), together with either 20µg/ml mouse anti-human CD3 (Dako), 20µg/ml mouse anti-human CD68 (Dako) or rabbit anti-human MPO (DAKO). Goat IgG isotype (R&D Systems), mouse IgG isotype (Abcam) and rabbit IgG

isotype (Abcam) antibodies at corresponding concentrations were used as isotype-specific controls. After washing with PBS, samples were incubated for 60 min at room temperature with conjugated secondary antibodies as follows: Alexa Fluor® 488 Goat Anti-Mouse IgG or Alexa Fluor® 488 Donkey Anti-Rabbit and Alexa Fluor® 647 Donkey Anti-Goat IgG (Life Technologies, Carlsbad, CA). Nuclear staining was performed using 4',6-diamidino-2-phenylindole (DAPI, Thermo Fisher Scientific, Carlsbad, CA). Slides were mounted with Fluorescence Mounting Medium (DAKO) and analyzed with a Widefield BX61 fluorescence microscope (Olympus, Tokyo, Japan) using the Analysis Pro software (Soft Imaging Systems, Münster, Germany).

ELISPOT

To perform Elispot analysis, PVDF-plates (Merck Millipore, Billerica, MA) were pre-wetted by 70% ethanol for 2 minutes. After washing, plates were coated with 2µg/ml rabbit anti-human IL-36γ (Peprotech, Rocky Hill, NJ) per well overnight. After removing excess antibody and washing, a blocking step was performed using RPMI medium containing 10% FBS. After one hour, medium was removed and 200.000 cells ± culprit drug (Amoxicillin 1mg/ml; Letrozole 100nM) or control drug (Metamizole 100µg/ml; Carbamazepine 10µg/ml) or a vehicle (RPMI medium containing 10% FBS) were added and incubated at 37°C for the indicated time. After washing, 2µg/ml rabbit anti-human biotinylated IL-36γ antibody (Peprotech) was added to the wells and incubated for 2 hours at room temperature, followed by one-hour incubation with Streptavidin-ALP (Mabtech, Nacka Strand, Sweden). For detection of the protein, BCIP/NBT substrate (Promega, Dübendorf, Switzerland) was added and developed until distinct spots emerged. Data was analyzed using the AID Elispot Reader (AID GmbH, Strassberg, Germany).

Co-culture experiments

PBMC and keratinocytes used in these experiments were collected at least 6 months after resolution of the ADR. 70.000 AGEP hair follicle keratinocytes were plated on a 12mm transwell plate with 0.4µm pore polycarbonate membrane inserts (Corning, NY, USA) overnight to allow them to adhere. The following day, keratinocyte medium was replaced by Gibco Opti-MEM medium (Thermo Scientific) and $1x10^6$ PBMC were added inside the inserts, followed by addition of culprit drug (Amoxicillin 1mg/ml; Letrozole 100nM; Vancomycin 500µg/ml) or control drug (Metamizole 100µg/ml; Carbamazepine 10µg/ml; Amoxicillin, 1mg/ml) or vehicle (RPMI medium containing 10% FBS) in both compartments at the same concentration. After 6 hours, cells were harvested and RNA was isolated for quantitative RT-PCR analysis.

293

294 **Statistical analysis**

295 Differences between groups were assessed using one-way Anova followed by Turkey's post-
296 test. Differences were considered significant when: *p≤0.05, ** p≤0.01 and *** p≤0.001 and
297 **** p≤0.0001.

298

RESULTS

Enhanced IL36γ and IL-8 gene expression in lesional skin of AGEP patients

First, we performed gene expression profiling using Affymetrix Human Exon 1.0 ST chips. Total RNA were extracted from lesional skin from patients with AGEP (n=8) or maculo-papular rash (MPR, n=6), and from skin from healthy individuals (n=7). The hierarchical clustering of genes differentially expressed in AGEP, MPR and healthy skin revealed a perfect segregation of these three conditions based on the gene expression profile of individual samples and the magnitude of change in gene expression (Fig.1A and Table E1 in the Online Repository). IL-8 has been previously reported to be produced by drug-specific T cells in AGEP patients [6] and in accordance with this, *IL-8* expression was significantly upregulated in AGEP skin when compared to healthy skin (ratio=2.25, p=0.01; Table E2 in the Online Repository) but also when compared to MPR (ratio=2.24, p=0.008; Table E3 in the Online Repository). Interestingly, the IL-36γ gene (*IL1F9*) was also found to be overexpressed in AGEP skin when compared to healthy skin (ratio=3.06, p=0.0006; Table E2 in the Online Repository) and MPR (ratio=2.54, p=0.005; Table E3 in the Online Repository). RNAseq analysis of an independent series of AGEP (n=9) and MPR (n=8) patient lesional skin confirmed the overexpression of *IL-36γ* gene (ratio=3.12; p=0.02) in AGEP (Fig.1B). Although not reaching statistical significance (p=0.12), RNAseq analysis also revealed an overexpression of *IL-8* (ratio=2.31) in AGEP skin.

We then confirmed the observed upregulation of *IL-36* and *IL-8* by quantitative PCR in AGEP (n=16) and MPR (n=16) skin biopsies. In accordance with the gene expression array and RNAseq data, expression of *IL-36γ* was found to be upregulated in AGEP skin when compared to MPR (32-fold, p<0.001) and normal skin (3-fold, p<0.001) (Fig. 1C). In addition to *IL-36γ*, *IL-36α* expression was also upregulated in AGEP skin when compared to MPR (15-fold, p<0.001) and normal skin (7-fold, p<0.001). Similarly, *IL-36β* was upregulated in AGEP when compared to MPR (28-fold, p<0.001) and normal skin (1.35-fold, p<0.05). The expression of *IL-36RN* was found to be higher (4.5-fold, p<0.001) in AGEP skin as compared to MPR whereas it was not different to that found in normal skin. *IL-36R* was similarly expressed in both diseases. As previously reported, levels of IL-8 mRNA were higher in the skin of AGEP patients than in MPR patients (127-fold, p<0.001) and normal skin (34-fold, p<0.01).

IL-36α and IL-36γ cytokines are highly expressed in AGEP skin lesions

Unlike IL-36β, IL-36α and γ were found to be unique for AGEP (Table E1 in the Online Repository). To further analyze their expression and tissue distribution, we labeled AGEP and MPR lesional skin biopsies with antibodies to both cytokines. IL-36α and γ were found to be highly expressed in pustular and peri-pustular regions of AGEP skin (Fig.2A). Both

keratinocytes and dermal immune cells infiltrating pustular areas were found to produce IL-36α and γ (Fig. 2B). In contrast, IL-36γ was weakly expressed in MPR skin biopsies and IL-36α was barely detectable (Fig. 2A). In AGEP lesional skin, IL-36γ was predominantly expressed by keratinocytes in the epidermis and by immune cells infiltrating the dermis in pustular areas (Fig. 2B). Also, IL-36γ staining was particularly intense in non-pustular epidermis surrounding the pustules in AGEP. As previously reported [33], IL-36 was also expressed in pustules from patients suffering from pustular psoriasis (PP) and, like in AGEP biopsies, IL-36γ was the predominant form in the epidermis (Fig. 2B). To identify which cell types release IL-36α and γ in AGEP skin, we co-labeled AGEP biopsy sections with antibodies to IL-36α and γ and antibodies to CD68 to identify macrophages, and to CD3 to identify T-cells (Fig. 3). IL-36α was predominantly expressed by $CD68^+$ macrophages (41.17%±4.71 of positively labeled cells) and to a lesser extent by keratinocytes and $CD3^+$ T cells (27.33%±2.17 and 22.33%±2.39 of positively labeled cells, respectively). IL-36γ was predominantly expressed by keratinocytes and $CD68^+$ macrophages (44.08%±4.47 and 43.17%±3.31 of positively labeled cells, respectively) and to a lesser extent by $CD3^+$ T cells (15.17%±1.26 of positively labeled cells). In contrast, IL-36α and IL-36γ were not expressed by neutrophils present in pustular areas (Fig. E1 in the Online Repository).

Culprit drugs specifically induce rapid monocyte IL-36γ secretion in AGEP

Since our immunofluorescence analyses of AGEP biopsies suggested that, in addition to keratinocytes, immune cells may also represent an important source of IL-36γ in the skin, we assessed whether peripheral blood mononuclear cells (PBMC) taken from AGEP patients 8, 9 and 20 more than 6 months after the ADR - when in complete remission - were still able to respond directly to the causative drug. To this end, PBMC from patients having experienced AGEP or MPR were exposed to the culprit drug or an irrelevant control drug in ELISPOT plates. The number of IL-36γ^+ spots were counted after 1, 2, 4, 6 and 8 hrs. IL-36γ release was detected in PBMC from AGEP patients already after 1 hr of culprit drug exposure (1.7-fold more spots than control drug, $p<0.001$) and reached a plateau after 4 hrs (2.7-fold more spots than control drug, $p<0.001$; Fig. 4A, left panel), whereas no increase in IL-36γ production was observed with an irrelevant control drug (Fig. 4A, right panel). In contrast, the culprit drug did not induce IL-36γ secretion in MPR. Similarly, none of the drugs used was able to induce IL-36γ secretion in PBMC from healthy blood donors (Fig 4A). Since immunofluorescence analyses of AGEP skin lesions revealed that macrophages and, to a lesser extent, T cells are possible sources of IL-36, we sorted $CD14^+$ (monocytes) and $CD3^+$ cells (T cells) from patients' PBMC and exposed them to culprit or control drug to evaluate IL-36γ secretion by ELISPOT

(Fig. 4B). Whereas the control drug did not induce IL-36γ secretion in PBMC or in $CD14^+$ and $CD3^+$ cells, the culprit drug was able to induce IL-36γ secretion in $CD14^+$ cells at levels similar to those observed with total PBMC. In contrast, the culprit drug was not able to induce IL-36γ secretion in $CD3^+$ PBMC. These results suggest that PBMC from patients having experienced AGEP are able to respond directly and specifically to the causative drug and that monocytes/macrophages are an important source of IL-36 production in response to culprit drug exposure.

IL-36 can be induced by culprit drugs in keratinocytes and PBMC from patients having experienced AGEP

By immunolabeling both keratinocytes and macrophages were positively labeled for IL-36α and γ in pustular areas of AGEP biopsies. To assess a possible cross-talk between macrophages and keratinocytes, and the relative contribution of each cell type to drug-induced IL-36 secretion, we performed co-culture experiments using autologous hair follicle-derived keratinocytes and PBMC from three patients having experienced AGEP but in remission at the time of blood and hair collection (at least 6 months after disappearance of symptoms, patients 8, 9 and 20). Keratinocytes and PBMC were cultured either alone or together using a transwell culture system (Figure E2A in the Online Repository). To formally exclude the contamination of one cell type by the other, we performed qPCR using primers to CD45 (PBMC marker) and ITGA6 (keratinocyte marker) on both PBMC and keratinocytes after a 6hr-coculture (Fig. E3 in the Online Repository). When keratinocytes and PBMC were each cultured alone, only PBMC showed elevated IL-36γ mRNA levels after exposure to the culprit drug. Interestingly, both keratinocytes and PBMC showed culprit drug-specific IL-36γ gene expression when cultured together. In contrast, keratinocytes exposed alone to the culprit drug exhibited increased IL-36α gene expression (Fig. E2 in the Online Repository). This increase was further augmented in keratinocytes co-cultured with PBMC but remained modest when compared to IL-36γ (about 10-fold less). The addition of soluble IL-36Ra did not reduce IL-36 expression, suggesting that, at the analyzed time point, there was no auto- or paracrine amplification and/or induction of IL-36 gene expression by IL-36 released by PBMC or keratinocytes. Taken together, these results indicate that, in culprit drug-induced responses of patient-derived keratinocytes and monocytes, IL-36γ is the predominant form of IL-36 induced. Furthermore, in response to culprit drug exposure IL-36 is expressed directly by PBMC and indirectly by keratinocytes.

IL-8 is selectively produced by patients' PBMC and induced by IL-36

IL-8 has previously been reported to be a key chemokine in AGEP physiopathology and has been shown to be inducible by IL-36 [19, 34]. Immunohistochemistry analysis confirmed that IL-8

406 was expressed by cells of the infiltrate in pustular regions of AGEP skin (Fig. E4 in the Online
407 Repository). Using the keratinocyte/PBMC co-culture model described above, we assessed
408 whether IL-36 could promote IL-8 gene expression, and if so, which cell type could produce
409 IL-8 in response to IL-36. We observed that high levels of IL-8 gene expression (4.6-fold
410 increase over control-drug exposure, $p<0.05$) occurred exclusively in patients' PBMC co-
411 cultured with autologous keratinocytes selectively in response to culprit drug (Fig. 5B).
412 Interestingly, upregulation of IL-8 gene expression in AGEP patients PBMC was abrogated by
413 IL-36Ra. IL-8 gene expression was weakly induced by culprit drugs in isolated PBMC cultures,
414 and barely detectable in isolated keratinocyte cultures. These results indicate that PBMC are
415 the main source of drug-induced IL-8 production, and that IL-8 gene expression is dependent
416 on PBMC- and/or keratinocyte-derived IL-36.
417

DISCUSSION

T cells and neutrophils are considered to be major players in AGEP [6, 35]. It has been proposed that drugs causing AGEP elicit drug-specific T cell responses, and that these T cells secrete IL-8 [6]. Recently mutations in the IL-36RN gene have been reported in AGEP [13], suggesting that a deregulation in IL-36 signaling may contribute to the physiopathology of AGEP. Our data is supportive of this hypothesis, showing that culprit drugs can directly induce IL-36 secretion in AGEP patients' monocytes, and indirectly in patients' keratinocytes *in vitro*. Analysis of IL-36 gene and protein expression *ex vivo* is also supportive of the above, revealing that macrophages and keratinocytes are the main producers of IL-36 in the pustular areas of AGEP skin. IL-36γ was found to be the predominant form of IL-36 expressed in AGEP skin biopsies, and also the predominant form induced by the culprit drug in monocytes and keratinocytes *in vitro*. Interestingly, causative drugs were able to induce IL-36 and subsequent IL-8 production in PBMC taken from patients months to years after AGEP resolution whereas these cytokines could not be induced by drugs in healthy control donors who had never experienced an adverse drug reaction. This observation suggests that there is a memory of drug sensitization within AGEP patients' PBMC and/or that genetic or epigenetic factors rendering AGEP patients susceptible to drug-induced IL-36 production were already present at the time of first drug intake.

Keratinocytes are a major source of IL-36 cytokines in cutaneous inflammation, particularly in psoriasis [18]. Our data suggests that keratinocytes are also an important source of IL-36 in the skin in AGEP. However, co-culture experiments revealed that keratinocytes exposed to culprit drugs were only able to produce little amounts of IL-36α and IL-36γ when cultured alone but, interestingly, produced high amounts of IL-36γ when cultured in presence of autologous monocytes and culprit drug. This observation suggests that, when exposed to the causative drug, patients' monocytes release a soluble factor that further stimulates IL-36γ production by keratinocytes. This factor remains to be identified but our results using IL-36Ra suggest that it is very likely not IL-36 itself. Indeed, unlike what has been reported in psoriasis [18], we could not observe any IL-36 induction by IL-36 itself in AGEP patients' keratinocytes as evidenced by the lack of effect of IL-36Ra. Like in other inflammatory diseases such as psoriasis [36], contact hypersensitivity [37] or sunburn [38], keratinocytes may actively participate in the pathogenesis of AGEP by secreting IL-36α and IL-36γ, which could contribute to the herein observed and previously reported induction of IL-8 gene expression by macrophages. The latter likely contributes to the observed neutrophil recruitment to the epidermis in AGEP. As previously reported in AGEP, IL-8 may also originate from drug-specific T cells [6]. Indeed, AGEP is currently seen a delayed type hypersensitivity reaction with T cell involvement. However, the mechanisms leading to drug-specific T cell priming and recruitment to the skin

in AGEP have not been elucidated to date. Unlike murine T cells, human T cells do not express IL-36R [39]. In AGEP, IL-36 may nevertheless contribute to T cell-mediated immune responses through its strong stimulatory effects on antigen-presenting cells [40]. Our findings that IL-36 can be induced by a drug very early in innate immune cells do not exclude a delayed drug-specific T cell response but whether the induction of IL-36 in monocytes by culprit drugs and the activation of drug-specific T cells are dependent events in AGEP pathogenesis or not remains to be investigated.

Th17 cells may also be involved in AGEP as revealed by their previously reported increased frequencies and elevated IL-22 blood levels in AGEP patients [8]. IL-17 is known to increase IL-8 secretion by keratinocytes[41] in allergic contact dermatitis [42] and in psoriasis [43]. Our *in vitro* data revealed however that in response to IL-36, the major source of IL-8 was patients' monocytes consistently with the previously reported elevated expression of IL-36R and potential strong responsiveness to IL-36 by dermal myeloid cells [19]. Although keratinocytes also express high levels of IL-36R [19], IL-8 production by keratinocytes was marginal as confirmed by qPCR in co-culture experiments and immunohistochemistry where IL-8 was only detected in the peri-pustular immune infiltrate (Fig. E3 in the Online Repository).

Although mutations in the *IL-36RN* gene have been identified in AGEP patients, no other marker(s) of genetic predisposition have been formally identified for AGEP to date. Noteworthy, our data shows that a deregulation of the IL-36-IL-8 axis can occur independently of *IL-36RN* mutations in AGEP, suggesting that other factors influencing the susceptibility to an IL-36-mediated proinflammatory response to culprit drugs are at play in AGEP patients.

Overall, we provide evidence that IL-36 is involved in AGEP pathogenesis, and identify monocytes and keratinocytes as potential key producers of IL-36 in AGEP. Given that monocytes/PBMC of all AGEP patients tested have an enhanced propensity to produce IL-36 upon culprit drug exposure, the identification of predictive genetic markers that would help identify patients prone to pathological IL-36 production upon exposure to certain medications may be achievable.

ACKOWLEDGMENTS

This work was supported by grants from the Zurich Center for Integrative Human Physiology (ZIHP), the Promedica Stiftung, and the Swiss National Science Foundation (grant 310030-156384) to LEF, the OPO-Stiftung, EMDO-Stiftung and Forschungskredit der Universität Zürich to LF and the Hartmann Müller Stiftung to EC.

References

1. Sidoroff A, Halevy S, Bavinck JN, Vaillant L, Roujeau JC. Acute generalized exanthematous pustulosis (AGEP)--a clinical reaction pattern. J Cutan Pathol 2001; 28:113-9.
2. Pichler WJ. Delayed drug hypersensitivity reactions. Ann Intern Med 2003; 139:683-93.
3. Anliker MD, Wuthrich B. Acute generalized exanthematous pustulosis due to sulfamethoxazol with positive lymphocyte transformation test (LTT). J Investig Allergol Clin Immunol 2003; 13:66-8.
4. Nishio D, Izu K, Kabashima K, Tokura Y. T cell populations propagating in the peripheral blood of patients with drug eruptions. J Dermatol Sci 2007; 48:25-33.
5. Britschgi M, Pichler WJ. Acute generalized exanthematous pustulosis, a clue to neutrophil-mediated inflammatory processes orchestrated by T cells. Curr Opin Allergy Clin Immunol 2002; 2:325-31.
6. Britschgi M, Steiner UC, Schmid S, Depta JP, Senti G, Bircher A, et al. T-cell involvement in drug-induced acute generalized exanthematous pustulosis. J Clin Invest 2001; 107:1433-41.
7. Schaerli P, Britschgi M, Keller M, Steiner UC, Steinmann LS, Moser B, et al. Characterization of human T cells that regulate neutrophilic skin inflammation. J Immunol 2004; 173:2151-8.
8. Kabashima R, Sugita K, Sawada Y, Hino R, Nakamura M, Tokura Y. Increased circulating Th17 frequencies and serum IL-22 levels in patients with acute generalized exanthematous pustulosis. J Eur Acad Dermatol Venereol 2011; 25:485-8.
9. Sugiura K, Takeichi T, Kono M, Ogawa Y, Shimoyama Y, Muro Y, et al. A novel IL36RN/IL1F5 homozygous nonsense mutation, p.Arg10X, in a Japanese patient with adult-onset generalized pustular psoriasis. Br J Dermatol 2012; 167:699-701.
10. Onoufriadis A, Simpson MA, Pink AE, Di Meglio P, Smith CH, Pullabhatla V, et al. Mutations in IL36RN/IL1F5 are associated with the severe episodic inflammatory skin disease known as generalized pustular psoriasis. Am J Hum Genet 2011; 89:432-7.
11. Marrakchi S, Guigue P, Renshaw BR, Puel A, Pei XY, Fraitag S, et al. Interleukin-36-receptor antagonist deficiency and generalized pustular psoriasis. N Engl J Med 2011; 365:620-8.
12. Kanazawa N, Nakamura T, Mikita N, Furukawa F. Novel IL36RN mutation in a Japanese case of early onset generalized pustular psoriasis. J Dermatol 2013; 40:749-51.
13. Navarini AA, Valeyrie-Allanore L, Setta-Kaffetzi N, Barker JN, Capon F, Creamer D, et al. Rare variations in IL36RN in severe adverse drug reactions manifesting as acute generalized exanthematous pustulosis. J Invest Dermatol 2013; 133:1904-7.
14. Johnston A, Xing X, Guzman AM, Riblett M, Loyd CM, Ward NL, et al. IL-1F5, -F6, -F8, and -F9: a novel IL-1 family signaling system that is active in psoriasis and promotes keratinocyte antimicrobial peptide expression. J Immunol 2011; 186:2613-22.
15. He Q, Chen HX, Li W, Wu Y, Chen SJ, Yue Q, et al. IL-36 cytokine expression and its relationship with p38 MAPK and NF-kappaB pathways in psoriasis vulgaris skin lesions. J Huazhong Univ Sci Technolog Med Sci 2013; 33:594-9.
16. Gresnigt MS, van de Veerdonk FL. Biology of IL-36 cytokines and their role in disease. Semin Immunol 2013; 25:458-65.
17. Debets R, Timans JC, Homey B, Zurawski S, Sana TR, Lo S, et al. Two novel IL-1 family members, IL-1 delta and IL-1 epsilon, function as an antagonist and agonist of NF-kappa B activation through the orphan IL-1 receptor-related protein 2. J Immunol 2001; 167:1440-6.
18. Carrier Y, Ma HL, Ramon HE, Napierata L, Small C, O'Toole M, et al. Inter-regulation of Th17 cytokines and the IL-36 cytokines in vitro and in vivo: implications in psoriasis pathogenesis. J Invest Dermatol 2011; 131:2428-37.
19. Dietrich D, Martin P, Flacher V, Sun Y, Jarrossay D, Brembilla N, et al. Interleukin-36 potently stimulates human M2 macrophages, Langerhans cells and keratinocytes to produce pro-inflammatory cytokines. Cytokine 2016; 84:88-98.
20. Strittmatter GE, Garstkiewicz M, Sand J, Grossi S, Beer HD. Human Primary Keratinocytes as a Tool for the Analysis of Caspase-1-Dependent Unconventional Protein Secretion. Methods Mol Biol 2016; 1459:135-47.
21. Gautier L, Cope L, Bolstad BM, Irizarry RA. affy--analysis of Affymetrix GeneChip data at the probe level. Bioinformatics 2004; 20:307-15.
22. Gentleman RC, Carey VJ, Bates DM, Bolstad B, Dettling M, Dudoit S, et al. Bioconductor: open software development for computational biology and bioinformatics. Genome Biol 2004; 5:R80.

23. Irizarry RA, Hobbs B, Collin F, Beazer-Barclay YD, Antonellis KJ, Scherf U, et al. Exploration, normalization, and summaries of high density oligonucleotide array probe level data. Biostatistics 2003; 4:249-64.
24. Klipper-Aurbach Y, Wasserman M, Braunspiegel-Weintrob N, Borstein D, Peleg S, Assa S, et al. Mathematical formulae for the prediction of the residual beta cell function during the first two years of disease in children and adolescents with insulin-dependent diabetes mellitus. Med Hypotheses 1995; 45:486-90.
25. Smyth GK. Linear models and empirical bayes methods for assessing differential expression in microarray experiments. Stat Appl Genet Mol Biol 2004; 3:Article3.
26. Hatakeyama M, Opitz L, Russo G, Qi W, Schlapbach R, Rehrauer H. SUSHI: an exquisite recipe for fully documented, reproducible and reusable NGS data analysis. BMC Bioinformatics 2016; 17:228.
27. Li B, Dewey CN. RSEM: accurate transcript quantification from RNA-Seq data with or without a reference genome. BMC Bioinformatics 2011; 12:323.
28. Robinson MD, McCarthy DJ, Smyth GK. edgeR: a Bioconductor package for differential expression analysis of digital gene expression data. Bioinformatics 2010; 26:139-40.
29. Young MD, Wakefield MJ, Smyth GK, Oshlack A. Gene ontology analysis for RNA-seq: accounting for selection bias. Genome Biol 2010; 11:R14.
30. Falcon S, Gentleman R. Using GOstats to test gene lists for GO term association. Bioinformatics 2007; 23:257-8.
31. Supek F, Bosnjak M, Skunca N, Smuc T. REVIGO summarizes and visualizes long lists of gene ontology terms. PLoS One 2011; 6:e21800.
32. Chen EY, Tan CM, Kou Y, Duan Q, Wang Z, Meirelles GV, et al. Enrichr: interactive and collaborative HTML5 gene list enrichment analysis tool. BMC Bioinformatics 2013; 14:128.
33. Song HS, Kim SJ, Park TI, Jang YH, Lee ES. Immunohistochemical Comparison of IL-36 and the IL-23/Th17 Axis of Generalized Pustular Psoriasis and Acute Generalized Exanthematous Pustulosis. Ann Dermatol 2016; 28:451-6.
34. van de Veerdonk FL, Stoeckman AK, Wu G, Boeckermann AN, Azam T, Netea MG, et al. IL-38 binds to the IL-36 receptor and has biological effects on immune cells similar to IL-36 receptor antagonist. Proc Natl Acad Sci U S A 2012; 109:3001-5.
35. Feldmeyer L, Heidemeyer K, Yawalkar N. Acute Generalized Exanthematous Pustulosis: Pathogenesis, Genetic Background, Clinical Variants and Therapy. Int J Mol Sci 2016; 17.
36. Nickoloff BJ. Keratinocytes regain momentum as instigators of cutaneous inflammation. Trends Mol Med 2006; 12:102-6.
37. Watanabe H, Gaide O, Petrilli V, Martinon F, Contassot E, Roques S, et al. Activation of the IL-1beta-processing inflammasome is involved in contact hypersensitivity. J Invest Dermatol 2007; 127:1956-63.
38. Feldmeyer L, Keller M, Niklaus G, Hohl D, Werner S, Beer HD. The inflammasome mediates UVB-induced activation and secretion of interleukin-1beta by keratinocytes. Curr Biol 2007; 17:1140-5.
39. Foster AM, Baliwag J, Chen CS, Guzman AM, Stoll SW, Gudjonsson JE, et al. IL-36 promotes myeloid cell infiltration, activation, and inflammatory activity in skin. J Immunol 2014; 192:6053-61.
40. Vigne S, Palmer G, Lamacchia C, Martin P, Talabot-Ayer D, Rodriguez E, et al. IL-36R ligands are potent regulators of dendritic and T cells. Blood 2011; 118:5813-23.
41. Pennino D, Eyerich K, Scarponi C, Carbone T, Eyerich S, Nasorri F, et al. IL-17 amplifies human contact hypersensitivity by licensing hapten nonspecific Th1 cells to kill autologous keratinocytes. J Immunol 2010; 184:4880-8.
42. Albanesi C, Cavani A, Girolomoni G. IL-17 is produced by nickel-specific T lymphocytes and regulates ICAM-1 expression and chemokine production in human keratinocytes: synergistic or antagonist effects with IFN-gamma and TNF-alpha. J Immunol 1999; 162:494-502.
43. Chiricozzi A, Guttman-Yassky E, Suarez-Farinas M, Nograles KE, Tian S, Cardinale I, et al. Integrative responses to IL-17 and TNF-alpha in human keratinocytes account for key inflammatory pathogenic circuits in psoriasis. J Invest Dermatol 2011; 131:677-87.

Figure legends

FIG 1. *IL-36* and *IL-8* gene overexpression in AGEP lesional skin.
Gene expression hierarchical clustering in lesional skin biopsies from patients suffering from AGEP and MPR analyzed using (A) Affymetrix Human Exon 1.0 ST chips or (B) RNAseq technology. (C) Quantitative RT-PCR analysis of IL-36α, IL-36β, IL-36γ, IL-36R, IL-36RN and IL-8 in lesional skin biopsies of patients suffering from AGEP (n=16), MPR (n=16) and normal skin (NS; n=5). **** $p<0.0001$. The patient cohorts studied in (A), (B) and (C) were independent and all recruited in the Dermatology Department of the University Hospital of Zürich (patients no. 1-19).

FIG 2. IL-36α and IL-36γ are overexpressed in pustular regions of AGEP lesional skin biopsies. (A) Immunohistochemical analysis of lesional skin biopsies revealed that IL-36α and IL-36γ are overexpressed at the site of pustules in AGEP and PP controls while, in MPR, IL-36α and IL-36γ were weakly expressed. Representative pictures of 18 AGEP, 10 PP and 18 MPR cases are shown. Neither IL-36α, nor IL-36γ were detectable in normal skin (NS) from healthy donors. (B) Semi-quantitative evaluation of IL-36α and IL-36γ labeling by immunohistochemistry in the pustular epidermis, non-pustular epidermis, and dermis of lesional skin biopsies from patients with AGEP (n=18; patients no. 5, 6, 8, 10, 11, 13-17, and 21-28), PP (n=10), MPR (n=18) and normal skin (NS) from healthy donors (n=5). Expression levels were qualified as very strong (++++), strong (+++), moderate (++), weak (+) or absent (0). *$p<0.05$; **$p<0.01$; *** $p<0.001$; **** $p<0.0001$.

FIG 3. IL-36γ is expressed by keratinocytes and immune cells in AGEP skin.
Pustule-containing sections of AGEP skin samples were co-labeled with antibodies to CD68 (green), CD3 (green) and IL-36α (red) (A) or IL-36γ (red) (B). The percentage of epidermal cells (keratinocytes), CD68 and CD3-labeled cells among the IL-36α or IL-36γ-labeled cells was determined (C). Cell nuclei appear in blue (DAPI). The mean±SD of 12 examined patients is shown (patients no. 8-10 and 20-28).

FIG 4. PBMC and monocytes taken from AGEP patients more than 6 months after the ADR selectively secrete IL-36γ in response to culprit drug exposure. (A) PBMC from AGEP or MPR patients as well as healthy donors were cultured in IL-36γ ELISPOT plates for 8 hrs in presence of the culprit drug (left panel) or a control drug (right panel). The number of spots was counted 1, 2, 4, 6 and 8 hrs after drug exposure. The means±SD of 3 different AGEP patients (no. 8,

10 and 21), 3 MPR patients and 3 healthy blood donors are shown. ***p<0.001. (B) $CD14^+$ monocytes and $CD3^+$ T cells were isolated from AGEP blood with a purity of >96% and were cultured in IL-36γ ELISPOT plates in presence of the culprit drug or a control drug and compared to total PBMC. The number of spots was counted 8 hrs after drug exposure. The mean±SD of 3 different patients (patient no. 8, 9 and 10) is shown. *p<0.05.

FIG 5. Culprit drugs specifically induce IL-36 in PBMC and keratinocytes and IL-8 in PBMC in a co-culture system. Autologous PBMC and keratinocytes (KC) from patients having experienced AGEP but in remission at the time of blood and hair collection were cultured either alone or together in a transwell system allowing for soluble factor-mediated interactions. Patients' cells were exposed to the culprit drug (Amoxicillin 1mg/ml, patient 8; Letrozole 100nM, patient 9; Vancomycin 500µg/ml, patient 20) or a control drug (Metamizole 100µg/ml, patient 8; Carbamazepine 10µg/ml, patient 9; Amoxicillin 1mg/ml, patient 20) in presence or absence of IL-36RA (1µg/ml). After 6 hrs of culture, RNA was extracted from KC (left panels) and PBMC (right panels) to measure IL-36γ mRNA levels (A). Relative *IL-36γ* expression in KC and PBMC cultured either alone or in co-culture as indicated and exposed to the culprit drug or a control drug in presence or absence of IL-36Ra are shown for each tested patient. Means±SD of 3 replicates are shown. (B) Quantitative PCR analysis of IL-8 gene expression in PBMC (upper panels) and KC (lower panels) cultured either alone or in co-culture as indicated and exposed to the culprit drug or a control drug in the presence or absence of IL-36Ra. Gene expression reported as $2^{-\Delta CT}$, which represents the target gene expression relative to the reference gene (RPL27). Mean±SD of the 3 tested patients is shown. The figure illustrates a representative experiment that was repeated 3 times for each patient. *p<0.05; **p<0.01; ***p<0.001.

SCIENTIFIC REPORTS

OPEN

Tumour hypoxia promotes melanoma growth and metastasis via High Mobility Group Box-1 and M2-like macrophages

Received: 16 July 2015
Accepted: 24 June 2016
Published: 18 July 2016

Roman Huber[1,*], Barbara Meier[1,*], Atsushi Otsuka[1,*], Gabriele Fenini[1], Takashi Satoh[1], Samuel Gehrke[1], Daniel Widmer[1], Mitchell P. Levesque[1], Joanna Mangana[1], Katrin Kerl[1], Christoffer Gebhardt[2,3], Hiroko Fujii[4], Chisa Nakashima[4], Yumi Nonomura[4], Kenji Kabashima[4], Reinhard Dummer[1], Emmanuel Contassot[1,#] & Lars E. French[1,#]

Hypoxia is a hallmark of cancer that is strongly associated with invasion, metastasis, resistance to therapy and poor clinical outcome. Tumour hypoxia affects immune responses and promotes the accumulation of macrophages in the tumour microenvironment. However, the signals linking tumour hypoxia to tumour-associated macrophage recruitment and tumour promotion are incompletely understood. Here we show that the damage-associated molecular pattern High-Mobility Group Box 1 protein (HMGB1) is released by melanoma tumour cells as a consequence of hypoxia and promotes M2-like tumour-associated macrophage accumulation and an IL-10 rich milieu within the tumour. Furthermore, we demonstrate that HMGB1 drives IL-10 production in M2-like macrophages by selectively signalling through the Receptor for Advanced Glycation End products (RAGE). Finally, we show that HMGB1 has an important role in murine B16 melanoma growth and metastasis, whereas in humans its serum concentration is significantly increased in metastatic melanoma. Collectively, our findings identify a mechanism by which hypoxia affects tumour growth and metastasis in melanoma and depict HMGB1 as a potential therapeutic target.

Hypoxia is a hallmark of a wide range of advanced solid tumours[1] and is often associated with poor prognosis in cancer patients[2]. Up to 60% of advanced solid tumours exhibit large hypoxic areas as a result of an imbalance between their oxygen supply and consumption[3]. A hypoxic environment, as frequently observed in solid tumours, results in focal areas of tumour cell necrosis and the release of damage associated molecular patterns (DAMPs) and alarmins, a group of endogenous molecules including hyaluronan fragments, S100 molecules and heat shock proteins, amyloid-β, uric acid, IL-1, IL-33 and high-mobility group box 1 protein (HMGB1)[4].

The non-histone nuclear protein HMGB1, a highly conserved DNA-binding protein with 98.5% sequence homology across mammals[5,6], can be actively secreted by immune cells including macrophages or passively released upon cell damage. HMGB1 has been shown to engage several different receptors including members of the Toll-like receptor (TLR) family[7] and the Receptor for Advanced Glycation End products (RAGE), thereby inducing an inflammatory response[8,9]. HMGB1 has been reported to be overexpressed in various solid tumours, shown to be released by mesothelial cells exposed to asbestos and erionite and implicated in malignant mesothelioma development in an autocrine manner[10–12]. HMGB1 has also been implicated in the development of hepatocellular carcinoma[13] and both colon and inflammation-related skin cancers[14,15].

Tumour hypoxia has a major impact on the tumour microenvironment and the subsequent immune response. Areas of hypoxia in tumours have been reported to be associated with advanced stage malignancy and resistance to therapy[16]. Paradoxically, tumour hypoxia promotes the recruitment of leukocytes, which can promote

[1]Department of Dermatology, University Hospital Zürich, Zürich 8091, Switzerland. [2]Skin cancer Unit, German Cancer Research Centre (DKFZ), Heidelberg, Germany. [3]Department of Dermatology, Venereology and Allergology, University Medical Centre Mannheim, Ruprecht-Karl University of Heidelberg, Mannheim, Germany. [4]Department of Dermatology, Kyoto University Graduate School of Medicine, Kyoto, Japan. *These authors contributed equally to this work. #These authors jointly supervised this work. Correspondence and requests for materials should be addressed to E.C. (email: emmanuel.contassot@usz.ch) or L.E.F. (email: lars.french@uzh.ch)

tumour cell proliferation, angiogenesis and metastasis[17,18]. Among the diverse immune cell populations present in the tumour microenvironment, macrophages are the most abundant[19] and are referred as Tumour-Associated Macrophages (TAMs). Macrophages differentiate or polarize in response to inflammatory stimuli and secrete a distinctive set of cytokines and amongst the different types of polarized macrophages described to date, the so-called M1-like or M2-like macrophages appear to have opposing effects on tumour progression[20]. M1-like macrophages are associated with type 1 T-cell responses and anti-tumour immune responses, while M2-like macrophages are reported to display tumour-promoting properties including the production of proteolytic enzymes, the suppression of anti-tumour immune responses and the promotion of angiogenesis[21]. Finally, in advanced tumours, TAMs have been reported to be preferentially skewed towards an M2-like phenotype[22–24].

Given the strong association between tumour hypoxia, tumour progression and poor clinical outcome, deciphering the precise molecular mechanisms by which hypoxia regulates tumour behaviour is of great interest and relevance. Here, we show that hypoxic melanoma cells release the alarmin HMGB1, which promotes tumour growth and metastasis through the accumulation, within tumours, of TAMS bearing an M2-like phenotype.

Results

Serum HMGB1 levels are elevated in metastatic melanoma patients. We first determined whether levels of HMBG1 are altered in cancer patients. To this end, we analysed HMGB1 levels in the serum of patients with primary melanoma, metastatic melanoma and in age-matched healthy volunteers. Significantly, increased levels of HMGB1 were found in the serum of patients with metastatic melanoma when compared to patients with primary melanoma and to healthy donors (Fig. 1a). This observation suggests that the extent of HMGB1 release correlates with the stage of the disease.

Tumour cell hypoxia drives HMGB1 release *in vitro* and *in vivo*. Hypoxia in the context of liver ischemia and hepatocellular carcinoma has been previously reported to induce HMGB1 release[13,25]. To determine if metastatic melanoma cells release HMGB1 in response to hypoxia, we analysed metastatic melanoma cell-lines grown in hypoxic versus normoxic conditions *in vitro*. When compared to their counterparts grown in normoxic conditions, all tested melanoma cell-lines ($n = 7$) released enhanced levels of HMGB1 when grown in hypoxic conditions in which increased expression of the hypoxia target gene VEGF-A was also observed[26] (Fig. 1b,c). Notably, under the hypoxic conditions tested no increase in cell mortality was observed as revealed by the consistently low levels of LDH release. The induction of HMGB1 expression by hypoxia in melanoma cells in culture was only significantly induced after 72 hours of hypoxia, but not at shorter exposure times to hypoxia.

Under physiologic conditions, HMGB1 is known to be sequestered in the nucleus, whereas cytoplasmic relocalization of HMGB1 has been reported to occur prior to active secretion or passive HMGB1 release[11]. First, we observed that melanoma metastasis cell lines expressed both cytosolic and nuclear HIF1α when cultured under low oxygen conditions, whereas HIF1α was not detectable when cells were kept in normoxic conditions. The co-labelling with an anti-HMGB1 antibody revealed that HMGB1 is located in the cytosol of HIF1α-positive cells in hypoxic conditions whereas HMGB1 was confined to the nucleus of cells kept in normoxic conditions (Fig. S1). When the intracellular localization of HMGB1 was assessed in tissue sections of nevi, primary melanoma (superficial spreading melanoma) and melanoma metastases, nuclear HMGB1 staining was observed in nevi and primary melanomas, whereas in melanoma metastases large areas of the tumour were composed of cells with cytoplasmic HMGB1 staining (Fig. 2a). Interestingly, the latter areas were also Hif1α-positive indicating that HMGB1 is released within hypoxic areas of metastatic melanomas (Fig. 2a). Co-labelling with an anti-melanosome antibody (clone HMB-45) showed that, in metastasis, HMGB1 is released by HMB-45$^+$ melanoma cells in contrast to primary tumours where HMGB1 was exclusively found in the nucleus of HMB-45$^+$ melanoma cells (Fig. 2b). These observations indicate that HMGB1 is released by hypoxic tumour cells within metastases in melanoma patients.

HMGB1 release is partly dependent on HIF1α in cells in hypoxic condition. To assess whether HMGB1 release under hypoxic culture condition was dependent on HIF1α or not, we knocked HIF1α down using siRNA in two human melanoma cell lines. After seventy-two hours under low oxygen conditions, increased levels of stabilized HIF1α were detected in both cell lines, either unmodified or transfected with a control siRNA (and Fig. 3a). In contrast, little or no expression of HIF1α was detected in both cell lines transfected with 2 independent HIF1α sequences (Fig. 3a). Interestingly, a reduced HMGB1 secretion under hypoxia was observed in both cell lines transfected with both HIF1α-siRNA as measure by ELISA (Fig. 3b,c). Under the hypoxic conditions tested, no increase in cell mortality was observed as revealed by the consistently low levels of LDH release and VEGFA was always found to be upregulated (Fig. 3b). Notably, HMGB1 secretion decrease was of only 50%, suggesting that mechanisms, other than HIF1α, are involved (Fig. 3b,c). By inhibiting oxygen-sensitive prolyl hydroxylases (PHDs) with DMOG, we observed that the resulting increased stabilization of HIF1α (Fig. 3d) was associated with a higher HMGB1 release in melanoma cell lines (Fig. 3e). DMOG exposure of siRNA-transfected melanoma cells did not result in significant increase of HMGB1 release (Fig. 3e), therefore reinforcing the role of the hypoxia/HIF1α axis in HMGB1 secretion.

HMGB1 promotes melanoma growth and metastasis. To assess whether HMGB1 plays a functional role in melanoma progression, we diminished HMGB1 expression in B16 melanoma cells using shRNA technology. Four HMGB1-specific shRNA sequences and 2 lamin-specific shRNA sequences were transduced into B16 cells. B16 cells showing the highest downregulation of HMGB1 expression (shRNA sequence 5, Fig. S2a, top panel) were subsequently cloned by limiting dilution and expanded under selection pressure (puromycin). B16 cells transduced with shRNA to lamin showing no variation in HMGB1 expression when compared to wild-type B16 cells (shRNA sequence 2 to lamin, Fig. S2a, top panel) were chosen as controls and were also cloned by limiting

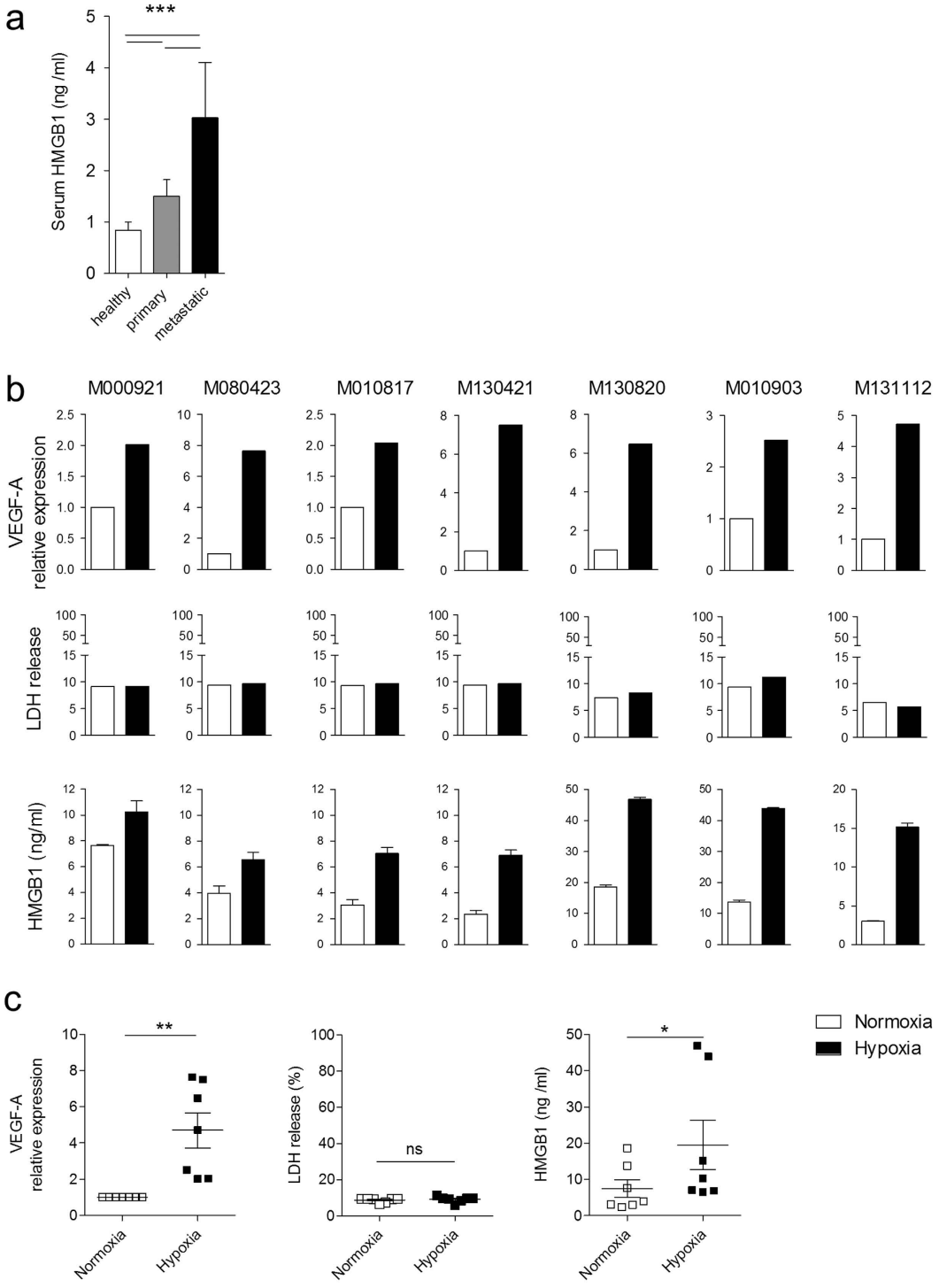

Figure 1. HMGB1 is increased in the serum of patients with metastatic melanoma and released by melanoma cells under hypoxic conditions. (**a**) HMGB1 was measured by ELISA in the serum of healthy individuals (n = 10), and patients with primary (n = 9) or metastatic melanoma (n = 11). Data are expressed as the mean +/− SEM are presented. ***$P < 0.001$ using ANOVA followed by Turkey test. (**b**) Cell-lines derived from human melanoma metastases were cultured under normoxic or hypoxic conditions for 72 h. As a marker of hypoxia, VEGF-A expression was assessed by qPCR (top panels). Cell viability was assessed in cell culture supernatants with an LDH release assay (middle panels) and HMGB1 release measured by ELISA (bottom panels). (**c**) Statistical representation and analysis of the data presented in (**b**). Data expressed as the mean +/− SEM are presented. A paired Student t-test was performed. *$P < 0.05$, **$P < 0.01$.

dilution and expanded under selection pressure. The silencing of HMGB1 was highly stable during *in vitro* expansion (Fig. S2b) and after 13 days of *in vivo* growth (Fig. S2c). The B16 clones transduced with HMGB1-specific

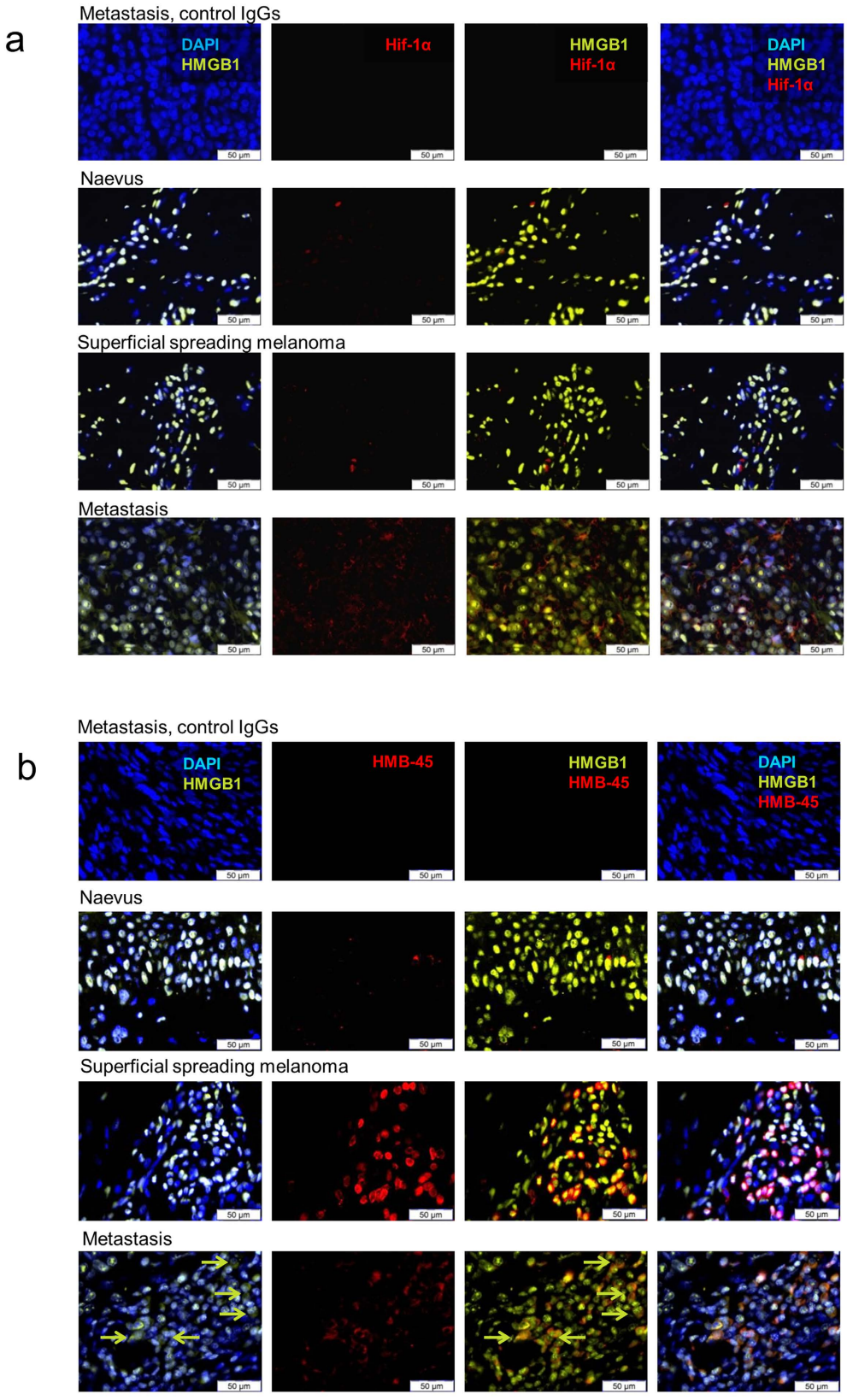

Figure 2. HMGB1 is released by tumour cells in hypoxic tumour areas of human metastatic melanoma. (**a**) Immunofluorescence labelling, using antibodies to HIF1α (red) and HMGB1 (green), was performed on healthy skin, nevi, primary cutaneous melanoma and metastases as indicated (n = 5/group; representative pictures are presented). (**b**) Immunofluorescence labelling using antibodies to human melanosome (clone HMB-45, red) and HMGB1 (green) was performed on healthy skin, nevi, primary cutaneous melanoma and metastases as indicated (n = 5/group; representative pictures are presented).

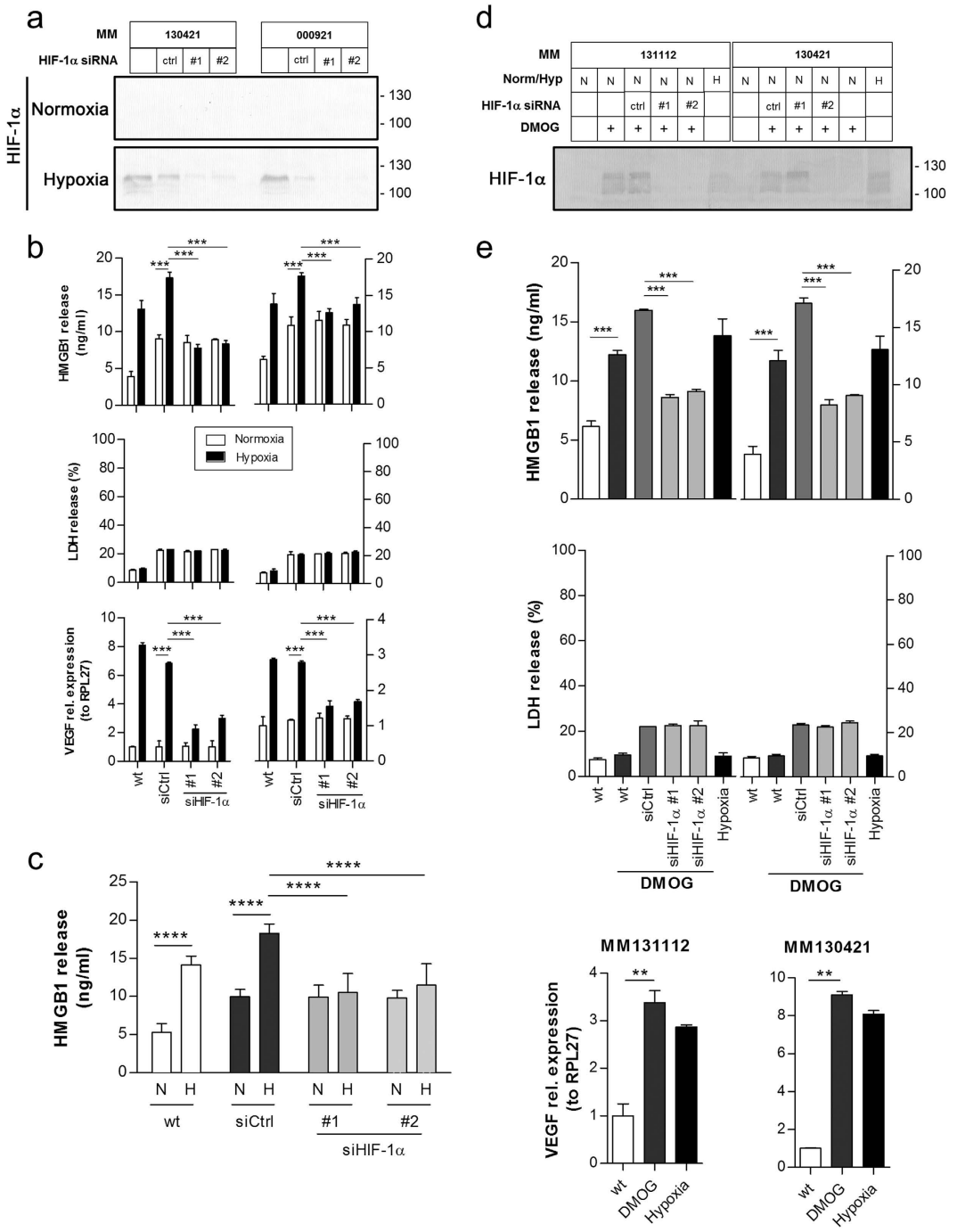

Figure 3. HMGB1 release is dependent on HIF1α. (**a**) HIF1α expression was assess by Western blotting in two human metastatic melanoma cell lines (MM130421 and MM000921) transfected with 2 sequences of siRNA to HIF1α and incubated for 72 hrs in normoxic or hypoxic conditions. (**b**) MM130421 and MM000921 were cultured under normoxic or hypoxic conditions for 72 hrs. As an hypoxia target gene, VEGF-A expression was assessed by qPCR (bottom panels). Cell viability was assessed in cell culture supernatants with an LDH release assay (middle panels) and HMGB1 release measured by ELISA (top panel). (**c**) HMGB1 release summary and statistical analysis of the data presented for individual cell lines in (**b**). Data expressed as the mean +/− SEM are presented. A paired Student t-test was performed. ****$P < 0.0001$. (**d**) HIF1α expression was assessed by Western blotting in two human metastatic melanoma cell lines (MM130421 and MM131112) transfected with 2 sequences of siRNA to HIF1α and exposed to DMOG or incubated for 72 hrs in normoxic (Nor, N) or hypoxic conditions (Hyp, H). (**e**) HMGB1 release was measured by ELISA (top panels). Cell viability was assessed in cell culture supernatants with an LDH release assay (middle panels) and VEGF-A expression was assessed by qPCR (bottom panels).

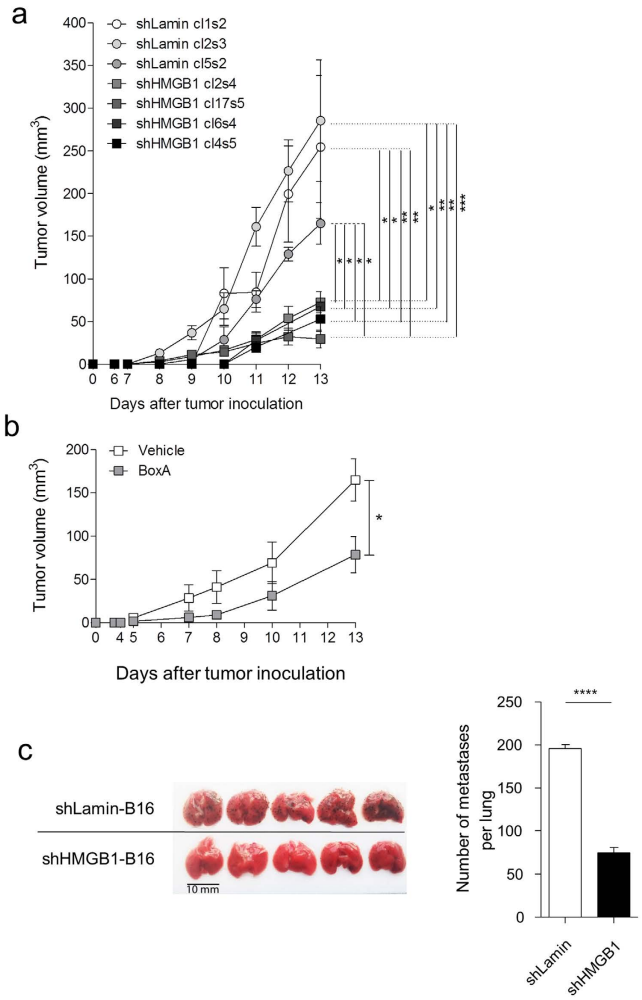

Figure 4. HMGB1 promotes tumour growth and metastasis, and is released by hypoxic tumour cells *in vivo*. (**a**) Tumour growth in C57BL/6 mice subcutaneously injected with 1×10^5 B16 clones transduced with shRNAs specific to HMGB1 or lamin and (**b**) tumour growth in C57BL/6 mice subcutaneously injected with 1×10^5 B16 cells transduced with lamin-shRNA (cl1s2: clone 1, shRNA sequence 2) and treated i.p. every 3 days from day 0 with 50 μg a recombinant HMGB1 inhibitor (BoxA). (**c**) 1×10^5 B16 cells transduced with HMGB1- or lamin-shRNA were injected i.v. to C57BL/6 mice and lung metastases were counted after 13 days. A macroscopic view of 5 representative lungs from each group and the numeration of metastases in the lungs (n = 9) are shown. Results are expressed as the mean +/− SEM. *P < 0.05, **P < 0.01, ***P < 0.001, ****P < 0.0001.

shRNA exhibiting the highest HMGB1 knockdown (Fig. S2a, bottom panel) and the clones transduced with lamin-shRNA showing similar HMGB1 expression when compared to wild-type B16 were then injected s.c. in C57BL/6 mice. Following sub-cutaneous injection, mice implanted with HMGB1-shRNA-transduced B16 clones exhibited significantly reduced tumour growth when compared to mice implanted with the same number of lamin-shRNA-transduced B16 clones (Fig. 4a). Importantly, the transduction of lamin-shRNA did not alter the *in vivo* growth kinetics of B16 tumours when compared to wild-type B16 cells (Fig. S3). Since such a reduced growth was reproducibly obtained irrespective of the shRNA sequence and clonal selection of B16 cells, all experiments described below were performed with one B16 clone transduced with HMGB1-specific shRNA and one B16 clone transduced with lamin-specific shRNA (HMGB1 clone 17 (sequence 5) and lamin clone 1 (sequence 2), respectively). This growth delay was neither due to an intrinsic effect of shRNA transduction or HMGB1 knockdown on growth or apoptosis as revealed by the identical *in vitro* growth and apoptosis of HMGB1- and lamin-shRNA-transduced B16 cells (Fig. S4). To further validate the above observation and assess the contribution of released extracellular HMGB1 on tumour growth, we next treated mice implanted subcutaneously with lamin-shRNA-transduced B16 cells with either a recombinant HMGB1 inhibitor (BoxA, 50 μg i.p. every 3 days) or vehicle (PBS) in an independent set of *in vivo* experiments. In accordance with results observed with HMGB1 silencing using shRNA, systemic treatment of tumour-bearing mice with the HMGB1 inhibitor BoxA also resulted in significantly delayed tumour growth compared to mice exposed to vehicle alone (Fig. 4b).

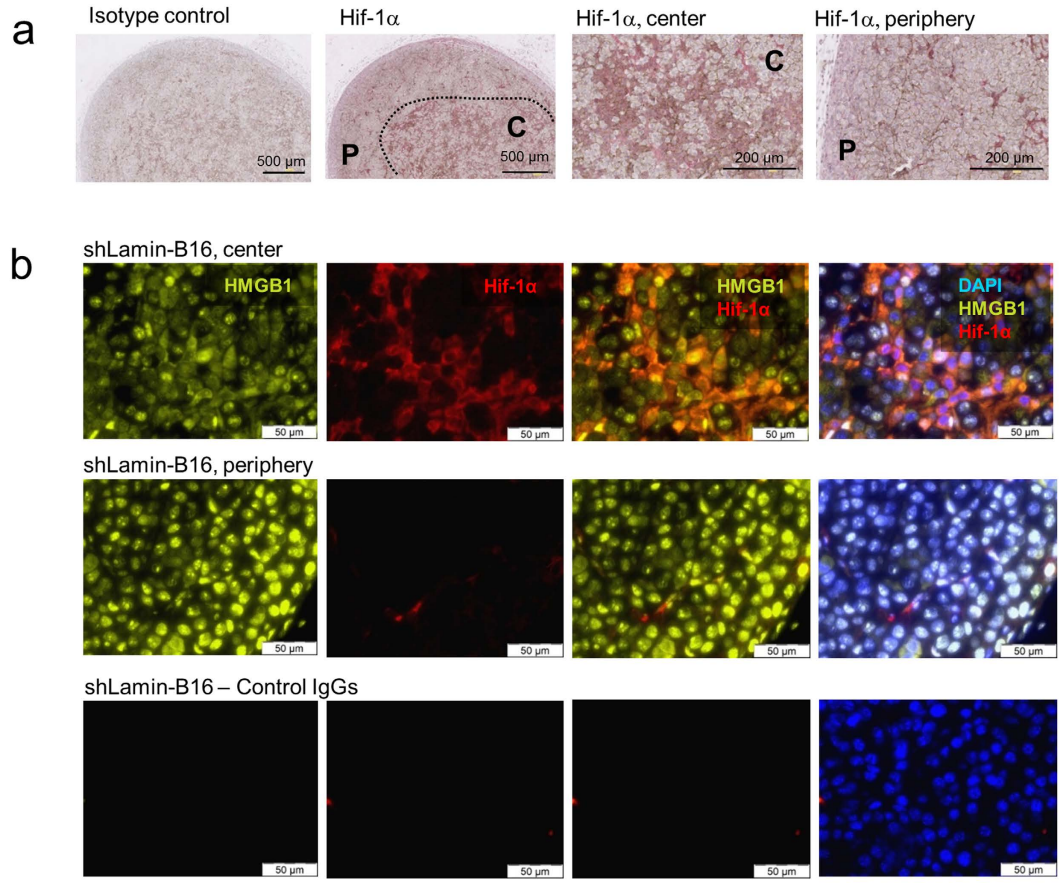

Figure 5. HMGB1 is released in hypoxic regions of B16 tumours. (**a**) Immunohistochemistry using a HIF1α$^-$ specific antibody was performed on 200 mm^3 tumours and revealed large HIF1α$^+$ hypoxic areas in the center (C) and HIF1α$^-$ normoxic areas in the periphery (P). Representative pictures of 10 tumours are presented. (**b**) Immunofluorescence analysis of B16 tumours transduced with lamin-shRNA using antibodies to HIF1α (red) and HMGB1 (green) showed nuclear HMGB1 localization in normoxic (HIF1α$^-$) areas and cytoplasmic HMGB1 localization in hypoxic (HIF1α$^+$) areas. Representative pictures of 10 tumours are presented.

We next evaluated the role of HMGB1 in metastasis by injecting either HMGB1-shRNA-transduced B16 cells or lamin-shRNA-transduced B16 cells i.v. into wild type mice. After 13 days, mice injected with HMGB1-shRNA-transduced B16 cells also exhibited significantly less lung metastases when compared to mice injected with lamin-shRNA-transduced control cells (Fig. 4c).

To determine whether HMGB1 release in this mouse model of melanoma was reminiscent of what was observed in human melanoma metastases, we assessed the intra-cellular localization of HMGB1 in tumours of mice implanted s.c. with lamin-shRNA-transduced B16 cells. Large areas where HIF was stabilized were found mainly in the centre of B16 tumours, as revealed by immunocytochemistry using a HIF1α antibody (Fig. 5a). Within HIF1α-positive tumour areas, large numbers of tumour cells displaying cytoplasmic HMGB1 expression were observed and double-labelling experiments identified numerous cells co-expressing HMGB1 and HIF1α (Fig. 5b). In contrast, nuclear HMGB1 localisation was predominantly observed in HIF-1α-negative areas of the tumour, and no evident co-labelling of anti-HMGB1 and HIF1α antibodies was observed in such areas. These observations are in line with data from human melanomas. Altogether, these results suggest that HMGB1 released by hypoxic tumour cells promotes melanoma growth and metastasis.

HMGB1 promotes the accumulation of tumour-associated M2-like macrophages. To further investigate the tumour-promoting effects of HMGB1 release, as a consequence of tumour hypoxia and given the absence of evidence for a direct effect of HMGB1 on tumour cell growth or apoptosis *in vitro*, we analysed the immune cell infiltrate within the tumour microenvironment. Analysis of dissociated tumours by flow-cytometry revealed a significant increase in the total number of TAMs and a slight but significant decrease in the total number of neutrophils in HMGB1-shRNA-transduced B16 tumours (Fig. 6a). To assess the phenotype of these TAMs, we analysed the *in vivo* expression of markers discriminating M1-like and M2-like macrophage subpopulations[27]. Quantitative PCR of macrophages accumulating at the tumour site revealed that the downregulation of HMGB1 in B16 cells was associated with a significant induction of the expression of the M1 macrophage marker *CD80*[28], whereas lamin-shRNA-transduced B16 tumours were associated with a significant upregulation of the

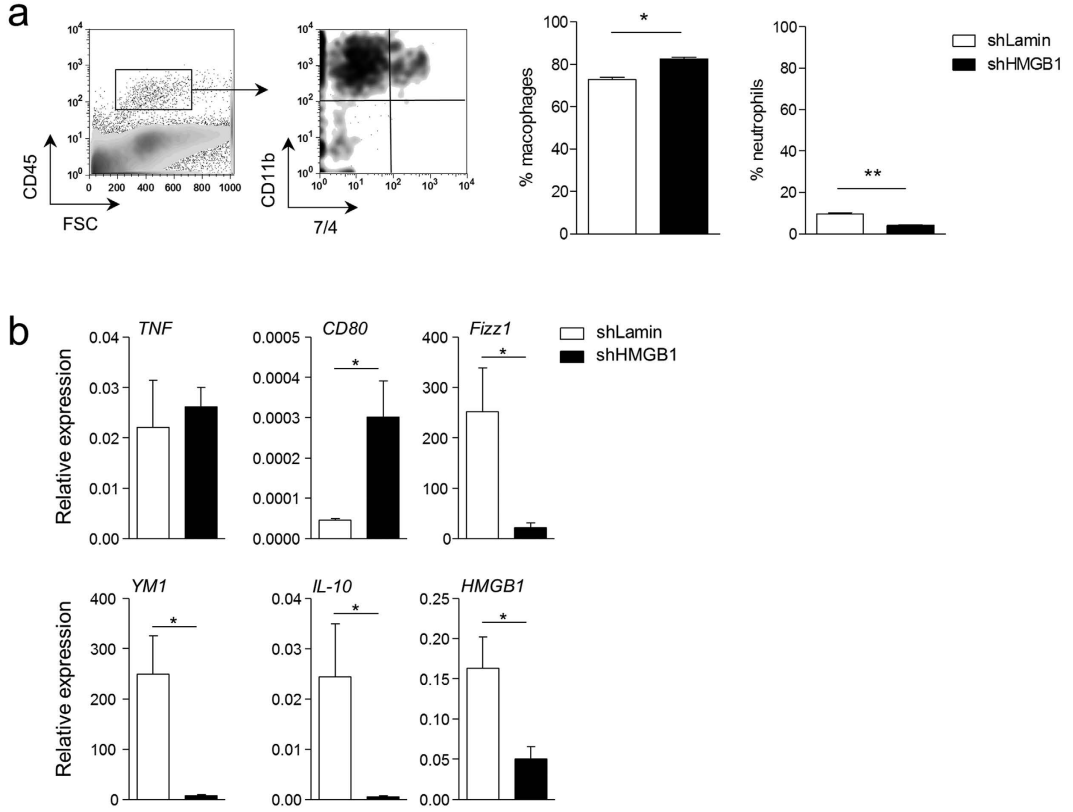

Figure 6. Tumour-derived HMGB1 induces the accumulation of macrophages harbouring an M2-like phenotype. (**a**) Macrophage and neutrophil infiltrates were quantified in 200 mm^3 tumours. Representative flow cytometry pictures (left panels) and quantification (right panels) of total macrophages and neutrophils in tumours of mice implanted with B16 cells transduced with lamin- (n = 6) or HMGB1-shRNA (n = 6). (**b**) Quantification of M1- and M2-specific gene expression by qPCR in size-matched (200 mm^3) primary tumours from mice implanted with B16 cells transduced with HMGB1- (shHMGB1, n = 5) or lamin-shRNA (shLamin, n = 5). Results are presented as the mean +/− SEM. *P < 0.05, **P < 0.01.

M2 markers *YM1, Fizz1, and IL-10* (Fig. 6b). These results suggest that HMGB1 expression and release within tumours favours the accumulation of M2-like macrophages in the microenvironment.

HMGB1 induces IL-10 in M2-like macrophages through RAGE. Given the reported role of the cytokine milieu of the tumour microenvironment on tumour progression[29,30], we evaluated the effect of HMGB1 on TAM cytokine expression. While HMGB1 had no effect on IL-6, TNF or IL-1β expression, it significantly increased IL-10 expression in bone marrow-derived M2-like macrophages (BMM2, Fig. 7a). Furthermore, HMGB1-induced upregulation of IL-10 expression was not observed in BMM2 from $RAGE^{-/-}$ mice while it was retained in TLR2- and TLR4-deficient BMM2 (Fig. 7b), suggesting that HMGB1 induces IL-10 in TAMs through RAGE-dependent signalling. To assess the effect of IL-10 on tumour development in the model used herein, mice implanted with lamin-shRNA transduced B16 tumours were treated with an anti-IL-10 neutralizing antibody. Similar to mice in which tumour expression of HMGB1 was silenced or inhibited with recombinant BoxA, mice treated with anti-IL-10 exhibited significantly delayed tumour growth compared to controls, whereas anti-IL-10 did not significantly affect the growth of HMGB1-shRNA-transduced B16 tumours (Fig. 7c). Collectively, these results indicate that HMGB1-dependent production of IL-10 by tumour-associated M2-like macrophages contributes to tumour progression in our mouse melanoma model. In further support for a potential role of TAMs and IL-10 in melanoma is the presence of IL-10-producing TAMs in human melanoma metastases as revealed by the presence of $CD163^+$ $IL\text{-}10^+$ cells infiltrating human metastases in areas with high cytoplasmic HMGB1 expression (Fig. 7d). In contrast, lower expression and nuclear localisation of HMGB1 in nevi was associated with a very discrete presence of $CD163^+$ cells and an absence of IL-10 production. Taken together, these results are supportive of a tumour-promoting role for HMGB1 dependent on its ability to induce IL-10 secretion by M2-like macrophages in a RAGE-dependent manner.

Discussion

Tumour-associated macrophages (TAMs) have emerged as key components of the tumour microenvironment with a crucial role in tumour progression[31]. TAMs are reported to be associated with poor prognosis in several types of cancer[32–35], and it has been proposed that monocytes, which continuously infiltrate tumours, once polarized to M2-like macrophages preferentially accumulate in hypoxic tumour areas[36–40]. By promoting angiogenesis

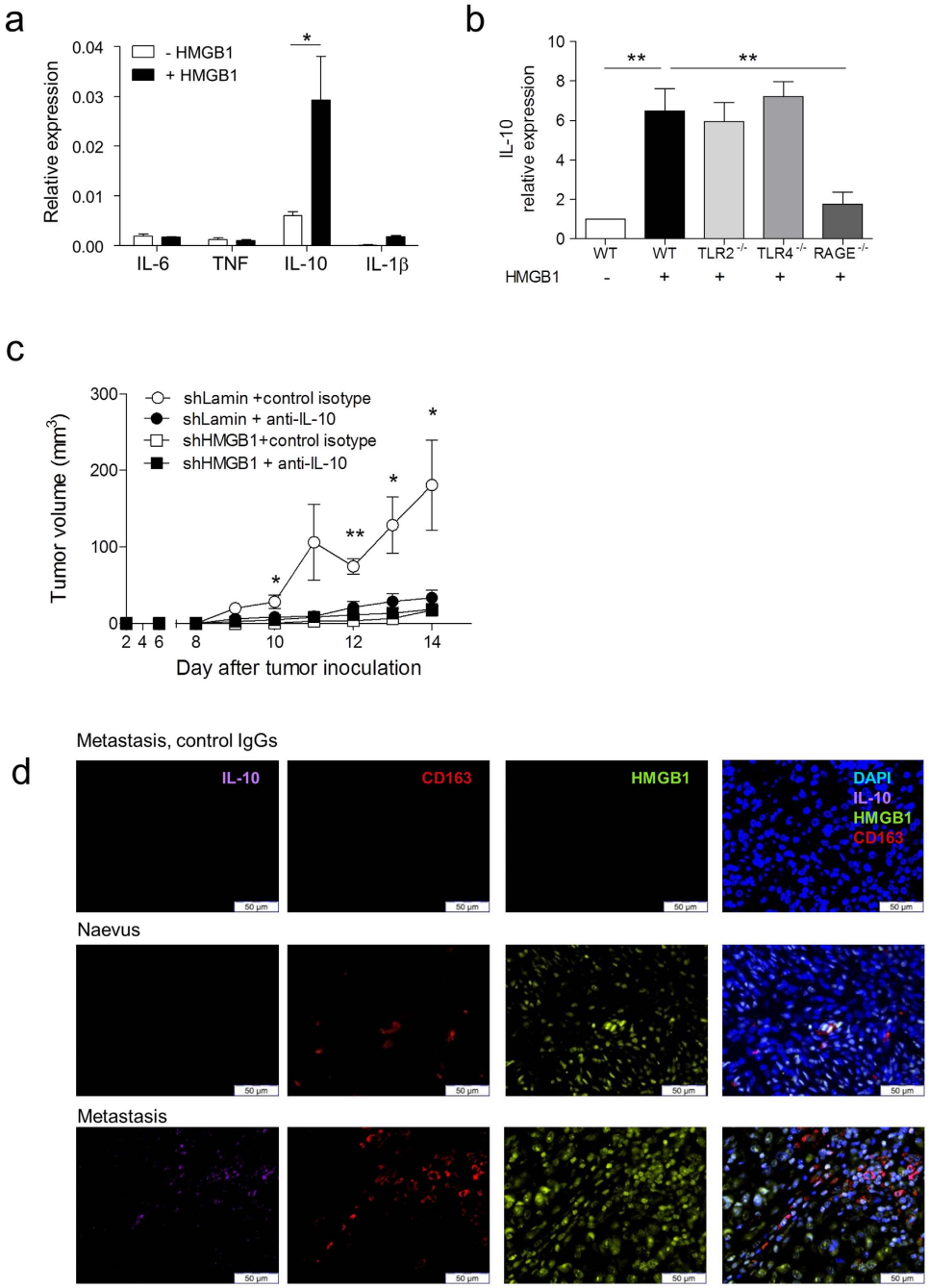

Figure 7. HMGB1 and RAGE-dependent IL-10 production by TAMs favour melanoma growth. (**a**) *IL-6*, *TNF*, *IL-10* and *IL-1β* mRNA expression, relative to housekeeper *RPL27*, in *in vitro*-generated murine M2-like macrophages in the presence or absence of recombinant HMGB1. (**b**) *IL-10* mRNA expression in *in vitro*-differentiated M2-like macrophages from wild-type (WT), *Tlr2*$^{-/-}$, *Tlr4*$^{-/-}$ and *Rage*$^{-/-}$ mice stimulated with recombinant HMGB1. Expression is relative to untreated WT M2-like macrophages. (**c**) Tumour growth in C57BL/6 mice having received 1×10^5 B16 cells transduced with either HMGB1- or lamin-shRNA and treated with an anti-IL-10 blocking antibody or a control isotype (n = 7 mice/group). (**d**) Immunofluorescence analysis of human biopsies of nevi and melanoma metastases using anti-CD163, anti-HMGB1 and anti-IL-10 antibodies (n = 5/group) revealing IL-10 secretion by TAMs in regions with cytoplasmic (secreted) HMGB1. Representative pictures are shown.

and metastasis, M2-polarized TAMs can "assist" the tumour in overcoming a hostile hypoxic environment and thus sustain its progression[24,41]. Therapeutic targeting of this process in cancer is currently limited by an inadequate understanding of factors released by hypoxic cells that may be associated with M2-like macrophage accumulation in the tumour microenvironment. Here, we show that the alarmin HMGB1, which is released from

tumour cells under hypoxic conditions, plays a critical role in promoting tumour progression by triggering the accumulation of M2-like TAMs. We demonstrate that HMGB1 released by hypoxic tumour cells favours the accumulation of M2-like macrophages at the tumour site and their secretion of IL-10. The relevance of the *in vitro* and *in vivo* data generated in this mouse model of melanoma is substantiated by the observation that HMGB1 release also occurs in human melanoma cell-lines under hypoxic conditions *in vitro*, particularly in Hif-1α-positive areas within human melanoma metastases and by the fact that melanoma metastases but not benign melanocytic nevi are infiltrated by $CD163^+$ IL-10^+ TAMs.

Areas of hypoxia in tumours have been reported to be associated with advanced stage malignancy and resistance to therapy[16]. Whether hypoxia and its by-products directly induce an M2-like phenotype in TAMs remains unclear. Our data suggest that, although HMGB1 clearly contributes to the accumulation of M2-like macrophages within tumours, it does not appear to be directly involved in M2 polarization. Indeed, and in line with a previous report showing that hypoxia is not a driver of the differentiation of TAMs[37], we were not able to differentiate macrophages towards an M2-like phenotype *in vitro* using recombinant HMGB1 alone. However, a recent study showed that lactic acid, produced by tumour cells as a by-product of hypoxic glycolysis, has a critical function in tumour development by inducing VEGF expression and M2-like polarization of TAMs in a HIF1α-dependent manner[42]. Furthermore, oncostatin M and eotaxin have been suggested to promote breast cancer metastasis by favouring M2 polarization and tumour infiltration[43]. Recent evidence also suggests that HMGB1 may directly act on progenitor cells to favour the induction of myeloid-derived suppressive cells[44].

Mechanistically, hypoxia-induced HMGB1 release seems to be associated with several tumour-promoting events. In advanced hepatocarcinomas, hypoxia has also been shown to be associated with the release of HMGB1[45], and it has been suggested that HMGB1, via RAGE, induces the expression of NF-κB-dependent pro-angiogenic factors including VEGF[46] and the matrix metalloproteinases MMP2 and MMP9[47]. It has also been observed that HMGB1 released from dying cells in prostate cancer induces the accumulation of tumour-infiltrating T cells and the expression of lymphotoxin-α1β2 on their surface, which in turn recruits macrophages to the tumour and supports angiogenesis[48]. Noteworthy, tumour cells or tumour-infiltrating immune cells seem not to be the sole source of HMGB1. Indeed, UVB radiation of the skin has been shown to induce HMGB1 release from epidermal keratinocytes, resulting in a neutrophilic inflammatory response that stimulate angiogenesis and promotes melanoma metastasis in mice[49].

We also observed that HMGB1 directly induced the production of IL-10 in TAMs and that blockade of IL-10 with a neutralizing antibody led to delayed tumour growth in the B16 mouse melanoma model. As we cannot, at present, technically and specifically delete IL-10 in TAMs, the relative role of HMGB1-induced IL-10 in TAMs remains incompletely elucidated in our model. It is known that regulatory T cell-mediated/IL-10-dependent suppression of $CD8^+$ T cells can be blocked by removal of tumour-derived HMGB1[50], which is consistent with our observation that HMGB1 inhibition leads to delayed tumour growth although via an alternate mechanism. It is likely that IL-10, which can also be produced by melanoma cells[51] and tumour-associated myeloid-derived suppressor cells[44] may favour immunoregulatory responses by inducing the downregulation of molecules involved in antigen presentation to $CD8^+$ T cells[52], by inducing regulatory T cells[53,54] and/or by supressing the production of pro-inflammatory cytokines including TNFα, IFN-γ and IL-2 by T cells[55]. In accordance with this, elevated IL-10 production levels in melanoma patients are associated with poor prognosis[56].

HMGB1 can signal by binding to TLR2, -4 and -9 as well as RAGE. According to our data, TLR signalling was not required for HMGB1-dependent induction of IL-10, the latter being selectively dependent on RAGE signalling. The potential importance of the HMGB1-RAGE interaction in promoting tumour progression is supported by a recent report showing that RAGE and HMGB1 are associated with the progression of prostate cancer and poor patient outcome[57]. However, since our data shows that HMGB1 downregulation or the use of a soluble inhibitor did not lead to complete inhibition of tumour growth, it is very likely that signalling by other alarmins through TLRs or RAGE also have the ability to induce a tumour-promoting microenvironment[58]. In addition, we do not exclude an incomplete inhibition of the effect of HMGB1 in our model or other HMGB1-independent mechanisms of tumourigenesis.

In conclusion, we demonstrate that HMGB1, derived from hypoxic tumour cells, significantly contributes to melanoma progression by favouring the accumulation of IL-10-secreting TAMs within the tumour. Tumour-derived HMGB1 released as a consequence of focal intra-tumoural hypoxia thus directly contributes to tumour progression and likely represents an attractive therapeutic target for tumour therapy as demonstrated here in the case of melanoma.

Methods

Biological samples from melanoma patients and healthy donors. Serum and tumour biopsies were collected from patients with primary melanoma or metastatic melanoma (stage IIIB to IV) in the Department of Dermatology of the University Hospital of Zürich. Characteristics of patients with primary and metastatic melanoma are reported in Tables 1 and 2, respectively. Serum was obtained from healthy blood donors and healthy skin was obtained as excess skin resulting from aesthetic/reconstructive procedures in the plastic surgery unit at the University Hospital of Zürich. All human biological samples were collected after written informed consent of the patient and with approval of Local Ethics Committee (Kantonale Ethikkommission Zürich, KEK-ZH authorization Nr. 2014-0425) in accordance to GCP guidelines and the Declaration of Helsinki.

Mice. Six to 8-week-old female C57BL/6 mice (Harlan, Venray, Netherlands) were used in this study. $TLR2^{-/-}$ C57BL/6 mice were kindly provided by Prof. Marc Donath (Department of Biomedicine, University Hospital Basel, Switzerland), $TLR4^{-/-}$ C57BL/6 mice were kindly provided by Prof. Markus G. Manz (Division of Haematology, University Hospital Zürich, Switzerland) and $RAGE^{-/-}$ C57BL/6 mice were kindly provided by Prof. Peter P. Nawroth (Department of Internal Medicine and Clinical Chemistry, University of Heidelberg,

Patient number	Date of Birth	Gender	Melanoma type	Localization	Breslow (mm)
1	24.04.1941	M	NMM	Right upper arm	1.6
2	19.05.1945	M	NMM	Left lower arm	3
3	13.01.1980	M	SSM	Left upper arm	0.9
3	10.08.1944	M	SSM	Left-side chest	1.42
4	12.05.1957	F	SSM	Left upper arm	1.77
5	23.09.1956	F	SSM	Right shoulder blade	1.06
6	14.10.1935	M	SSM	Right lower leg	4
7	14.09.1968	F	SSM	Right shoulder blade	0.82
8	04.03.1980	M	SSM	Abdomen	0.68
9	02.05.1946	F	SSM	Back	1.1

Table 1. Characteristics of patients with primary cutaneous melanoma. All the patients were Caucasian. (SSM: superficial spreading melanoma; NMM: nodular melanoma).

Patient number	Date of birth	Gender	Stage
1	01.05.1934	M	IV
2	02.05.1964	M	IV
3	24.11.1961	M	IV
4	17.07.1958	M	IIIB
5	09.10.1960	M	IV
6	17.04.1971	M	IIIC
7	25.10.1938	M	IV
8	30.06.1947	F	IV
9	21.11.1979	M	IV
10	09.05.1943	M	IV

Table 2. Characteristics of patients with metastatic melanoma. All the patients were Caucasian.

Germany). All experimental procedures were approved by the Veterinary Office of Zürich and the institutional animal care officer and were carried out in accordance to the approved guidelines.

Generation of HMGB1-shRNA-transduced B16. B16-F10 mouse melanoma cell-lines stably expressing shRNA specific to Lamin or HMGB1 were generated by transducing B16-F10 cells with a lentiviral vector. Briefly, specific shRNA were generated by inserting oligonucleotides targeting Lamin or HMGB1 into the pSUPER vector (Oligoengine, Seattle, WA) and subsequent cloning into the lentiviral vector pSP-93 (Oligoengine). Second-generation packaging plasmids pMD2-VSVG and psPAX2 (kindly provided by Prof. J. Tschopp, Biochemistry Institute, Lausanne, Switzerland) were used for lentivirus production and infection. For each target molecule, the procedure was performed with different shRNA sequences. ShRNA-transduced B16 cells were subsequently cloned by limiting dilution under selection pressure (puromycin). For each shRNA, one clone was chosen according to knock-down efficiency and stability as well as *in vitro* properties (Figs S1 and S3).

Generation of HIF1α-siRNA-transduced human melanoma cell lines. siRNA transfection of metastatic melanoma cells was carried out using INTERFERin transfection solution according to the manufacturer's protocol (Polyplus Transfection, Illkirch, France). Cells were transfected with 10 nM of siRNA to Hif1α two hours before hypoxia treatment for 72 hours before supernatant was harvested and RNA or protein was extracted. All-Star negative siRNA sequence (Qiagen) was used as control siRNA. The following siRNAs were used:

siHIF-1α#1: Hs_HIF1A_5 (NM_001530; S102664053, Qiagen FlexiTube).
siHIF-1α#2: Hs_HIF1A_6 (NM_001530; S102664431, Qiagen FlexiTube).

Tumour growth and metastasis experiments. Lamin-shRNA-transduced or HMGB1-shRNA-transduced B16 cells (1×10^5) were injected subcutaneously in 100 μl PBS into the flank of wild-type mice. Where indicated, mice were treated with 50 μg BoxA (HMGBiotech, Milano, Italy), one of the highly conserved DNA-binding domains of HMGB1, which antagonizes HMGB1 binding to its receptor RAGE. In independent sets of experiments, 50 μg anti-IL-10 antibody or control isotype (Biolegend, San Diego, CA) was injected intraperitoneally every 3 days in 100 μl PBS. Mice were monitored every other day and tumour size was measured using a microcaliper (Mitutoyo, Kawasaki, Japan). Tumour volume is expressed as (long diameter × shorter diameter^2) × π/6. Lung metastases were generated by tail vein intravenous injection of 1×10^5 B16 cells in 100 μl of PBS. Mice were sacrificed 13 days after tumour cell inoculation and the number of macroscopically visible melanoma metastases on the surface of the lungs was counted in a blinded manner by two different investigators.

Flow cytometry analysis of tumour-infiltrating cells. Minced tumours were incubated at 37 °C for 60 min in complete RPMI containing 1.5 mg/ml collagenase D (Roche Diagnostics, Rotkreuz, Switzerland). The resulting cell suspensions were filtered through a 40 μm cell strainer (Corning Inc., New York, NY) and stained with anti-mouse 7/4 antibody (Abcam, Cambridge, UK), anti-mouse CD11b and CD45 antibodies (Biolegend). The absolute numbers of each cell subset were calculated by flow cytometry and presented are the numbers per mm^3 of tumour. Flow-cytometry analysis was performed with a FACS Canto II (Becton-Dickinson, Franklin Lakes, NJ) and FACS DIVA software (Becton-Dickinson).

Immunohistochemistry and immunofluorescence. To analyze Hif-1α expression in immunohistochemistry, 2 μm paraffin-embedded sections were stained overnight at 4 °C with a monoclonal anti-mouse Hif-1α Ab (Abcam) or an isotype IgG control Ab (Abcam). Samples were incubated for 60 min at room temperature with biotinylated goat anti-mouse IgG (Abcam) coupled to streptavidin-alkaline phosphatase (Vector Laboratories, Burlingame, CA) for 45 min at room temperature. Alkaline phosphatase activity was revealed with the DAKO real detection system (DAKO, Glostrup, Denmark) following the manufacturers' instructions. After counter-staining with Haematoxylin solution (Sigma, Zug, Switzerland), slides were mounted with Fluorescence Mounting Medium (DAKO) and scanned with a digital slide scanner (Hamamatsu Photonics, Hamamatsu, Japan). Pictures were analysed with the ImageJ software (open source from the National Institutes of Health). For immunofluorescence analyses, 2 μm paraffin-embedded sections were stained overnight at 4 °C with 1 μg/ml rabbit polyclonal anti-mouse HMGB1 Ab (Abcam) and 10 μg/ml mouse monoclonal anti-mouse Hif-1α Ab (Abcam) or alternatively 714 μg/ml monoclonal anti-human melanosome (clone HMB-45, DAKO) or with control IgG antibodies (Abcam) at corresponding concentrations. To determine IL-10 and CD163 expression together with HMGB1sections were stained overnight at 4 °C with rabbit polyclonal anti-human IL-10 (R&D Systems), monoclonal anti-human CD163 (Leica Biosystems, Wetzlar, Germany) and HMGB1 (Abcam) or with respective control IgG antibodies. Samples were then incubated for 60 min at room temperature with conjugated secondary antibodies as follows: Alexa Fluor® 546 Goat Anti-Rabbit IgG (Life Technologies) for HMGB1 and IL-10, and DyLight® 650 Goat Anti-Mouse IgG (Abcam) for Hif-1α and CD163, and Alexa Fluor® 647 Donkey Anti-Goat IgG H&L (Abcam) for IL-10. Slides were mounted with Fluorescence Mounting Medium (DAKO) and analysed with a Widefield BX61 fluorescence microscope (Olympus, Tokyo, Japan) using the Analysis Pro software (Soft Imaging Systems, Münster, Germany).

Cell culture in hypoxic conditions and treatment with DMOG. To determine the release of HMGB1 under hypoxic conditions *in vitro*, primary cell cultures from metastatic melanoma patients were cultured under hypoxia. One million cells were cultured in 2.5 ml complete RPMI medium. After an overnight incubation in standard conditions allowing the cells to adhere, cells were incubated in a MIC-101 Modular Incubator Chamber (Billups-Rothenberg, Del Mar, CA), flushed with 20 l/min of certified pre-mixed gas composed of 1% O_2, 5% CO_2, and 94% N_2 (Carbagas, Guemligen, Switzerland). The O_2 concentration inside the chamber was measured with a disposable VTI-122 Polaro-graphic oxygen cell oxygen sensor (Vascular Technology, Nashua, NH). The hypoxia chamber was placed in an incubator at 37 °C for 72 h and samples were harvested on ice for analysis.

Alternatively, to stabilize HIF1α expression in metastatic melanoma cells, cells were treated with 1 mM Dimethyloxalylglycine (DMOG, Sigma-Aldrich, St Louis, MO) for 72 hours.

Quantitative PCR analysis and quantitative PCR array. For tumour mRNA isolation, tumours excised from mice were cut into small pieces and incubated for 60 min in lysis buffer (Qiagen, Hilden, Germany) with iron beads. RNA was isolated using an RNeasy kit (Qiagen). For mRNA isolation from *in vitro* cell cultures, supernatants were discarded and cells were washed twice with cold PBS. RNA was isolated using an RNeasy kit (Qiagen) according to the manufacturers' instructions. Total RNA was converted into cDNA with the RevertAid First Strand cDNA Synthesis Kit (Thermo Fisher Scientific, Waltham, MA). Quantitative RT-PCR was performed with a ViiA™ 7 Real-Time PCR System (Life Technologies, Carlsbad, CA) using FastStart Universal SYBR Green Master (Roche). The PCR included an initial denaturation at 95 °C for 10 min, followed by 40 cycles of 95 °C for 10 s and 58 °C for 30 s. After 15 s at 95 °C, 20 s at 60 °C and 15 s at 95 °C, samples were kept at 4 °C. Expression of mRNA (relative) was normalized to the expression of RPL27 mRNA by the change in cycling threshold (ΔC_T) method and calculated as $2^{-\Delta\Delta CT}$. The following primers were used:

Human RPL27: forward 5′-ATCGCCAAGAGATCAAAGATAA-3′, reverse 5′-TCTGAAGACATCCTTATTGACG-3′, Human VEGF-α: forward 5′-TACCTCCACCATGCCAAGTG-3′, reverse 5′-GATGATTCTGCCCTCCTCCTT-3′, Mouse CD80: forward 5′-TCAGTTGATGCAGGATACACCA-3′, reverse 5′-AAAGACGAATCAGCAGCACAA-3′, Mouse Fizz1: forward 5′-CCAATCCAGCTAACTATCCCTCC-3′, reverse 5′-ACCCAGTAGCAGTCATCCCA-3′, Mouse HMGB1: forward 5′-GGCGAGCATCCTGGCTTATC-3′, reverse 5′-GGCTGCTTGTCATCTGCTG-3′, Mouse IL-1β: forward 5′-ATCTTTTGGGGTCCGTCAACT-3′, reverse 5′-GACAGCACACATTTGCAGCTC-3′, Mouse IL-6: forward 5′-TAGTCCTTCCTACCCCAATTTCC-3′, reverse 5′-TTGGTCCTTAGCCACTCCTTC-3′, Mouse IL-10: forward 5′-GCTCTTACTGACTGGCATGAG-3′, reverse 5′-CGCAGCTCTAGGAGCATGTG-3′, Mouse RPL27: forward 5′-AAAGCCGTCATCGTGAAGAAC-3′, reverse 5′-GCTGTCACTTTCCGGGGATAG-3′, Mouse TNF-α: forward 5′-CCCTCACACTCAGATCATCTTCT-3′, reverse 5′-GCTACGACGTGGGCTACAG-3′, Mouse Ym1: forward 5′-AGAAGGGAGTTTCAAACCTGGT-3′, reverse 5′-GTCTTGCTCATGTGTGTAAGTGA-3′.

Detection of HMGB1 by ELISA. To determine the concentration of HMGB1 in the serum of healthy donors, primary melanoma patients and melanoma patients with metastasis, serum samples were analysed using the HMGB1 ELISA kit (IBL International, Hamburg, Germany) according to the manufacturers' instructions. To determine the concentration of released HMGB1 from *in vitro* cell cultures, supernatants were centrifuged at

1,500 g for 5 min at 4 °C and analysed using the HMGB1 ELISA kit (IBL International) according to the manufacturers' instructions.

***In vitro* differentiation of M1- and M2-like macrophages from bone marrow cells.** Recombinant cytokines were all from Peprotech (Rocky Hill, NJ). To generate of M1 and M2 macrophages, bone marrow cells from the tibia and fibula of C57BL/6 mice (Harlan) were cultured at 37 °C in 5% CO_2 in RPMI supplemented with 1% L-glutamine and 10% foetal bovine serum with 10 ng/ml mouse M-CSF. Medium was replaced on days 3 and 6 and cells were harvested on day 8. For M1 phenotype induction, cells were stimulated for 24 h with 10 ng/ml M-CSF and 100 ng/ml IFN-γ and for an additional 24 h with 10 ng/ml M-CSF and 20 ng/ml ultra-pure LPS (Invitrogen, Carlsbad, CA). For M2 phenotype induction, cells were stimulated twice for 24 h with 10 ng/ml M-CSF and 20 ng/ml IL-4. To determine the effect of HMGB1 on M1 and M2 macrophages, culture medium used to induce M1- or M2-like macrophages was supplemented with 1 μg/ml recombinant HMGB1 (HMGBiotech).

Statistical analyses. Unless otherwise indicated, data are presented as the means $\pm$ standard error of the mean (SEM) and are representative of three independent experiments. Statistical analyses were performed using the Prism Software (GraphPad Software, San Diego, CA). *P*-values were calculated with paired or unpaired Student's *t* test. Where indicated, statistical analyses where performed using ANOVA test followed by a Tukey test. Differences were considered significant when: *$P \leq 0.05$, **$P \leq 0.01$, ***$P \leq 0.001$ and ****$P \leq 0.0001$.

References

1. Harris, A. L. Hypoxia–a key regulatory factor in tumour growth. *Nat Rev Cancer* **2,** 38–47 (2002).
2. Vaupel, P. & Mayer, A. Hypoxia in cancer: significance and impact on clinical outcome. *Cancer Metastasis Rev* **26,** 225–239 (2007).
3. Vaupel, P., Kallinowski, F. & Okunieff, P. Blood flow, oxygen and nutrient supply, and metabolic microenvironment of human tumours: a review. *Cancer Res* **49,** 6449–6465 (1989).
4. Sims, G. P., Rowe, D. C., Rietdijk, S. T., Herbst, R. & Coyle, A. J. HMGB1 and RAGE in inflammation and cancer. *Annu Rev Immunol* **28,** 367–388 (2010).
5. Agresti, A. & Bianchi, M. E. HMGB proteins and gene expression. *Curr Opin Genet Dev* **13,** 170–178 (2003).
6. Bianchi, M. E., Beltrame, M. & Paonessa, G. Specific recognition of cruciform DNA by nuclear protein HMG1. *Science* **243,** 1056–1059 (1989).
7. Ibrahim, Z. A., Armour, C. L., Phipps, S. & Sukkar, M. B. RAGE and TLRs: relatives, friends or neighbours? *Mol Immunol* **56,** 739–744 (2013).
8. Andersson, U. & Tracey, K. J. HMGB1 is a therapeutic target for sterile inflammation and infection. *Annu Rev Immunol* **29,** 139–162 (2011).
9. Bianchi, M. E. HMGB1 loves company. *J Leukoc Biol* **86,** 573–576 (2009).
10. Carbone, M. *et al.* Erionite exposure in North Dakota and Turkish villages with mesothelioma. *Proc Natl Acad Sci USA* **108,** 13618–13623 (2011).
11. Jube, S. *et al.* Cancer cell secretion of the DAMP protein HMGB1 supports progression in malignant mesothelioma. *Cancer Res* **72,** 3290–3301 (2012).
12. Yang, H. *et al.* Programmed necrosis induced by asbestos in human mesothelial cells causes high-mobility group box 1 protein release and resultant inflammation. *Proc Natl Acad Sci USA* **107,** 12611–12616 (2010).
13. Liu, Y. *et al.* Hypoxia induced HMGB1 and mitochondrial DNA interactions mediate tumour growth in hepatocellular carcinoma through Toll Like Receptor 9. *J Hepatol* **63,** 114–121 (2015).
14. Gebhardt, C. *et al.* RAGE signalling sustains inflammation and promotes tumour development. *J Exp Med* **205,** 275–285 (2008).
15. Mittal, D. *et al.* TLR4-mediated skin carcinogenesis is dependent on immune and radioresistant cells. *Embo J* **29,** 2242–2252 (2010).
16. Hockel, M. *et al.* Association between tumour hypoxia and malignant progression in advanced cancer of the uterine cervix. *Cancer Res* **56,** 4509–4515 (1996).
17. Hanahan, D. & Weinberg, R. A. The hallmarks of cancer. *Cell* **100,** 57–70 (2000).
18. Semenza, G. L. Cancer-stromal cell interactions mediated by hypoxia-inducible factors promote angiogenesis, lymphangiogenesis, and metastasis. *Oncogene* **32,** 4057–4063 (2013).
19. Sica, A., Schioppa, T., Mantovani, A. & Allavena, P. Tumour-associated macrophages are a distinct M2 polarised population promoting tumour progression: potential targets of anti-cancer therapy. *Eur J Cancer* **42,** 717–727 (2006).
20. Mantovani, A. & Sica, A. Macrophages, innate immunity and cancer: balance, tolerance, and diversity. *Curr Opin Immunol* **22,** 231–237 (2010).
21. Talmadge, J. E., Donkor, M. & Scholar, E. Inflammatory cell infiltration of tumours: Jekyll or Hyde. *Cancer Metastasis Rev* **26,** 373–400 (2007).
22. Biswas, S. K. & Mantovani, A. Macrophage plasticity and interaction with lymphocyte subsets: cancer as a paradigm. *Nat Immunol* **11,** 889–896 (2010).
23. Ruffell, B., Affara, N. I. & Coussens, L. M. Differential macrophage programming in the tumour microenvironment. *Trends Immunol* **33,** 119–126 (2012).
24. Qian, B. Z. & Pollard, J. W. Macrophage diversity enhances tumour progression and metastasis. *Cell* **141,** 39–51 (2010).
25. Tsung, A. *et al.* HMGB1 release induced by liver ischemia involves Toll-like receptor 4 dependent reactive oxygen species production and calcium-mediated signalling. *J Exp Med* **204,** 2913–2923 (2007).
26. Rofstad, E. K. & Danielsen, T. Hypoxia-induced angiogenesis and vascular endothelial growth factor secretion in human melanoma. *Br J Cancer* **77,** 897–902 (1998).
27. Mantovani, A. *et al.* The chemokine system in diverse forms of macrophage activation and polarization. *Trends Immunol* **25,** 677–686 (2004).
28. Liu, G. *et al.* Phenotypic and functional switch of macrophages induced by regulatory CD4 + CD25+ T cells in mice. *Immunol Cell Biol* **89,** 130–142 (2011).
29. Wan, L., Pantel, K. & Kang, Y. Tumour metastasis: moving new biological insights into the clinic. *Nat Med* **19,** 1450–1464 (2013).
30. Joyce, J. A. & Pollard, J. W. Microenvironmental regulation of metastasis. *Nat Rev Cancer* **9,** 239–252 (2009).
31. Siveen, K. S. & Kuttan, G. Role of macrophages in tumour progression. *Immunol Lett* **123,** 97–102 (2009).
32. Farinha, P. *et al.* Analysis of multiple biomarkers shows that lymphoma-associated macrophage (LAM) content is an independent predictor of survival in follicular lymphoma (FL). *Blood* **106,** 2169–2174 (2005).
33. Hanada, T. *et al.* Prognostic value of tumour-associated macrophage count in human bladder cancer. *Int J Urol* **7,** 263–269 (2000).
34. Steidl, C. *et al.* Tumour-associated macrophages and survival in classic Hodgkin's lymphoma. *N Engl J Med* **362,** 875–885 (2010).
35. Zhu, X. D. *et al.* High expression of macrophage colony-stimulating factor in peritumoural liver tissue is associated with poor survival after curative resection of hepatocellular carcinoma. *J Clin Oncol* **26,** 2707–2716 (2008).

36. Chai, C. Y. *et al.* Hypoxia-inducible factor-1alpha expression correlates with focal macrophage infiltration, angiogenesis and unfavourable prognosis in urothelial carcinoma. *J Clin Pathol* **61,** 658–664 (2008).
37. Laoui, D. *et al.* Tumour hypoxia does not drive differentiation of tumour-associated macrophages but rather fine-tunes the M2-like macrophage population. *Cancer Res* **74,** 24–30 (2014).
38. Lima, L. *et al.* The predominance of M2-polarized macrophages in the stroma of low-hypoxic bladder tumours is associated with BCG immunotherapy failure. *Urol Oncol* **32,** 449–457 (2014).
39. Murdoch, C. & Lewis, C. E. Macrophage migration and gene expression in response to tumour hypoxia. *Int J Cancer* **117,** 701–708 (2005).
40. Murdoch, C., Muthana, M., Coffelt, S. B. & Lewis, C. E. The role of myeloid cells in the promotion of tumour angiogenesis. *Nat Rev Cancer* **8,** 618–631 (2008).
41. Kimura, Y. N. *et al.* Inflammatory stimuli from macrophages and cancer cells synergistically promote tumour growth and angiogenesis. *Cancer Sci* **98,** 2009–2018 (2007).
42. Colegio, O. R. *et al.* Functional polarization of tumour-associated macrophages by tumour-derived lactic acid. *Nature* (2014).
43. Tripathi, C. *et al.* Macrophages are recruited to hypoxic tumour areas and acquire a Pro-Angiogenic M2-Polarized phenotype via hypoxic cancer cell derived cytokines Oncostatin M and Eotaxin. *Oncotarget* **5,** 5350–5368 (2014).
44. Parker, K. *et al.* HMGB1 enhances immune suppression by facilitating the differentiation and suppressive activity of myeloid-derived suppressor cells. *Cancer Res* (2014).
45. Yan, W. *et al.* High-mobility group box 1 activates caspase-1 and promotes hepatocellular carcinoma invasiveness and metastases. *Hepatology* **55,** 1863–1875 (2012).
46. van Beijnum, J. R. *et al.* Tumour angiogenesis is enforced by autocrine regulation of high-mobility group box 1. *Oncogene* **32,** 363–374 (2013).
47. Taguchi, A. *et al.* Blockade of RAGE-amphoterin signalling suppresses tumour growth and metastases. *Nature* **405,** 354–360 (2000).
48. He, Y. *et al.* Tissue damage-associated "danger signals" influence T-cell responses that promote the progression of preneoplasia to cancer. *Cancer Res* **73,** 629–639 (2013).
49. Bald, T. *et al.* Ultraviolet-radiation-induced inflammation promotes angiotropism and metastasis in melanoma. *Nature* **507,** 109–113 (2014).
50. Liu, Z., Falo, L. D., Jr. & You, Z. Knockdown of HMGB1 in tumour cells attenuates their ability to induce regulatory T cells and uncovers naturally acquired CD8 T cell-dependent antitumour immunity. *J Immunol* **187,** 118–125 (2011).
51. Terai, M. *et al.* Interleukin 6 mediates production of interleukin 10 in metastatic melanoma. *Cancer Immunol Immunother* **61,** 145–155 (2012).
52. Kurte, M. *et al.* A synthetic peptide homologous to functional domain of human IL-10 down-regulates expression of MHC class I and Transporter associated with Antigen Processing 1/2 in human melanoma cells. *J Immunol* **173,** 1731–1737 (2004).
53. Carter, N. A., Rosser, E. C. & Mauri, C. Interleukin-10 produced by B cells is crucial for the suppression of Th17/Th1 responses, induction of T regulatory type 1 cells and reduction of collagen-induced arthritis. *Arthritis Res Ther* **14,** R32 (2012).
54. Carter, N. A. *et al.* Mice lacking endogenous IL-10-producing regulatory B cells develop exacerbated disease and present with an increased frequency of Th1/Th17 but a decrease in regulatory T cells. *J Immunol* **186,** 5569–5579 (2011).
55. Chen, Q., Daniel, V., Maher, D. W. & Hersey, P. Production of IL-10 by melanoma cells: examination of its role in immunosuppression mediated by melanoma. *Int J Cancer* **56,** 755–760 (1994).
56. Mahipal, A. *et al.* Tumour-derived interleukin-10 as a prognostic factor in stage III patients undergoing adjuvant treatment with an autologous melanoma cell vaccine. *Cancer Immunol Immunother: CII* **60,** 1039–1045 (2011).
57. Zhao, C. B. *et al.* Co-expression of RAGE and HMGB1 is associated with cancer progression and poor patient outcome of prostate cancer. *Am J Cancer Res* **4,** 369–377 (2014).
58. Coffelt, S. B. & Scandurro, A. B. Tumours sound the alarmin(s). *Cancer Res* **68,** 6482–6485 (2008).

Acknowledgements

This work was supported in part by the Association for International Cancer Research (AICR 09-0230 to L.E.F), the Zürich Center for Integrative Human Physiology (ZIHP to L.E.F.), by the Zürich University Research Priority Program (URPP) Translational Cancer Research, by the Swiss National Science Foundation (Sinergia Grant CRSII3-136203 to L.E.F), and by the Society for Skin Cancer Research to M.P.L. We thank Prof. Burkhard Becher for critically reviewing the manuscript. We thank Horomi Doi, Ines Kleiber-Schaaf and Tatiana Proust for technical assistance.

Author Contributions

A.O., E.C. and L.E.F. designed the research; E.C., L.E.F. and K.Ka. supervised the research; R.H., A.O., B.M., G.F., T.S., S.G., D.W., M.P.L., K.Ke., M.M., C.G., H.F., C.N. and Y.N. conducted the studies; R.D. and J.M. collected human biological samples and patients' data. A.O., B.M., E.C. and L.E.F. analysed the data; E.C. and L.E.F. prepared the manuscript. E.C. and B.M. revised the manuscript. All authors reviewed the manuscript.

Additional Information

Supplementary information accompanies this paper at http://www.nature.com/srep

Competing financial interests: The authors declare no competing financial interests.

How to cite this article: Huber, R. *et al.* Tumour hypoxia promotes melanoma growth and metastasis via High Mobility Group Box-1 and M2-like macrophages. *Sci. Rep.* **6**, 29914; doi: 10.1038/srep29914 (2016).

Propionibacterium acnes Promotes Th17 and Th17/Th1 Responses in Acne Patients

Magdalena Kistowska[1], Barbara Meier[1], Tatiana Proust[1], Laurence Feldmeyer[2], Antonio Cozzio[1], Thomas Kuendig[1], Emmanuel Contassot[1,3] and Lars E. French[1,3]

Propionibacterium acnes is a Gram-positive commensal bacterium thought to be involved in the pathogenesis of acne vulgaris. Although the ability of *P. acnes* in the initiation of pro-inflammatory responses is well documented, little is known about adaptive immune responses to this bacterium. The observation that infiltrating immune cells consist mainly of $CD4^+$ T cells in the perifollicular space of early acne lesions suggests that helper T cells may be involved in immune responses caused by the intra-follicular colonization of *P. acnes*. A recent report showing that *P. acnes* can induce IL-17 production by T cells suggests that acne might be a T helper type 17 (Th17)-mediated disease. In line with this, we show in this work that, in addition to IL-17A, both Th1 and Th17 effector cytokines, transcription factors, and chemokine receptors are strongly upregulated in acne lesions. Furthermore, we found that, in addition to Th17, *P. acnes* can promote mixed Th17/Th1 responses by inducing the concomitant secretion of IL-17A and IFN-γ from specific $CD4^+$ T cells *in vitro*. Finally, we show that both *P. acnes*-specific Th17 and Th17/Th1 cells can be found in the peripheral blood of patients suffering from acne and, at lower frequencies, in healthy individuals. We therefore identified *P. acnes*-responding Th17/Th1 cells as, to our knowledge, a previously unreported $CD4^+$ subpopulation involved in inflammatory acne.

Journal of Investigative Dermatology (2015) **135,** 110–118; doi:10.1038/jid.2014.290; published online 14 August 2014

INTRODUCTION

Propionibacterium acnes (*P. acnes*) is a Gram-positive normal skin commensal bacterium present in all individuals. The intra-follicular colonization and proliferation of *P. acnes* has been associated with the pathogenesis of acne, the most common human inflammatory skin disorder (Leeming *et al.*, 1988; Leyden *et al.*, 1998). It has been proposed that *P. acnes* contributes to the development of inflammatory lesions by releasing chemotactic substances and attracting polymorphonuclear leukocytes to the site of inflammation. Infiltrating cells are locally activated and release pro-inflammatory cytokines including IL-6, tumor necrosis factor-α, IL-12, IL-8, and IL-1β (Kim *et al.*, 2002; Kalis *et al.*, 2005; Nagy *et al.*, 2005; Kistowska *et al.*, 2013). Surprisingly, in early acne lesions, infiltrating cells consist mainly of $CD4^+$ T cells (Norris and Cunliffe, 1988; Layton *et al.*, 1998). These memory/effector $CD4^+$ T cells are detected in close proximity to macrophages and are also present in uninvolved follicles from acne patients but not in non-acne controls (Jeremy *et al.*, 2003). In addition, *P. acnes* has been shown to induce T-cell proliferation (Jappe *et al.*, 2002), and reactive *P. acnes*-specific $CD4^+$ T cells have been isolated from early inflamed acne lesions (Mouser *et al.*, 2003). These T cells have the capacity to secrete IFN-γ, but not IL-4, upon stimulation with *P. acnes* and have therefore revealed to be Th1 cells.

$CD4^+$ T helper (Th) cells have a key role in the regulation of adaptive immune responses by secreting cytokines and chemokines that activate and/or recruit effector cells. Because of the discovery of an IL-17-producing T-cell subset, known as Th17, numerous studies have revealed IL-17 as a pro-inflammatory cytokine involved in the pathogenesis of autoimmune disorders as well as in response to certain pathogens at both the barrier site and at a systemic level (O'Connor *et al.*, 2010; Miossec and Kolls, 2012). Th17 cells have a role in the protection against extracellular bacteria and fungi (Zhu and Paul, 2008; Zhu *et al.*, 2010), particularly those colonizing the respiratory and gastrointestinal tracts and the skin (Peck and Mellins, 2010). The protective effects of IL-17-producing cells have been demonstrated in patients with hyper-immunoglobulin E syndrome, who suffer from recurrent infections with *Candida albicans* (*C. albicans*) and *Staphylococcus aureus* (*S. aureus*) due to the impairment in Th17 development (Milner *et al.*, 2008; Puel *et al.*, 2011). In addition to their protective effect, Th17 have also been reported to be pathogenic. Indeed, Th17 cells are associated with many autoimmune and inflammatory disorders including Crohn's disease, colitis, psoriasis, multiple sclerosis, rheumatoid arthritis, and chronic graft-versus-host disease (Wilke *et al.*,

[1]*Department of Dermatology, University Hospital, Zürich, Switzerland and* [2]*Department of Dermatology and Venereology, Centre Hospitalier Universitaire Vaudois, Lausanne, Switzerland*

[3]*These authors contributed equally to this work.*

Correspondence: Lars E. French, Department of Dermatology, University Hospital, Gloriastrasse 31, Zürich 8006, Switzerland.
E-mail: lars.french@usz.ch

Received 28 March 2014; revised 27 May 2014; accepted 4 June 2014; accepted article preview online 10 July 2014; published online 14 August 2014

2011; McGeachy, 2013). Moreover, Th17 cells are suspected to have a role in cutaneous inflammatory disorders, including psoriasis, allergic contact dermatitis, or atopic dermatitis (Asarch *et al.*, 2008). In a recent report, Agak *et al.* (2013) showed that the secretion of IL-17 by naïve $CD4^+$ T cells can be induced by *P. acnes*, thus suggesting that both Th1 and Th17 responses may be involved in responses to this bacterium.

In this work, we show that, in addition to IL-17A, both Th1 and Th17 effector cytokines, transcription factors, and chemokine receptors are strongly upregulated in acne lesions. We also observed that, besides Th17, *P. acnes* can promote mixed Th17/Th1 responses by inducing the concomitant secretion of IL-17A and IFN-γ from specific $CD4^+$ T cells *in vitro*. Finally, we show that both *P. acnes*-reactive Th17 and Th17/Th1 cells can be found in the peripheral blood of patients suffering from acne and, at lower frequencies, in healthy individuals. Our data suggest that, in addition to Th17, Th17/Th1 T cells may have a role in acne pathogenesis.

RESULTS

T cells of Th1 and Th17 phenotypes are found in acne lesions

We first assessed the expression of Th effector cytokines in human acne biopsies. We detected significantly increased levels of *IFN-γ* and, in line with the recent report from Agak *et al.* (2013), *IL-17A* mRNA in human acne samples when compared with normal skin. IL-21, an essential cytokine for the differentiation and homeostasis of Th17 cells (Korn *et al.*, 2007; Weaver *et al.*, 2007; Wei *et al.*, 2007), was also found to be highly expressed in acne biopsies (Figure 1a). In accordance with previous studies (Mouser *et al.*, 2003; Agak *et al.*, 2013), the levels of *IL-4* mRNA were not higher in acne lesions compared with those in normal skin (Figure 1a). *IL-22* mRNA levels were also not increased in acne lesions in comparison with normal skin (Figure 1a). Noteworthy, we observed a correlation between the mRNA levels of IL-17A and IFN-γ in acne biopsies (Figure 1b). The immunohistochemical analysis of acne biopsies not only confirmed a strong expression of IL-17A but also revealed strong IFN-γ expression in the same areas of the immune cell infiltrates (Figure 1c).

Differentiation of Th subsets is tightly regulated by master transcription factors, signaling transducers, and activators of transcription (signal transducer and activator of transcriptions (STATs)). Th1 differentiation depends on STAT4 and T-bet (TBX-21), whereas Th2 cells require STAT5a and GATA3, and RAR-related orphan receptor gamma (ROR-γt) (RORC) and STAT3 are critical factors for Th17 subset differentiation (for review (Zhu *et al.*, 2010)). In acne biopsies, increased levels of Th1 and Th17 transcription factor mRNA were observed, whereas transcription factors required for Th2 cells remained unchanged when compared with normal skin (Figure 1d).

Analysis of chemokine receptors in skin biopsies revealed elevated *CXCR3*, *CCR4,* and *CCR6* mRNA levels in acne lesions when compared with normal skin (Figure 1e). These receptors are preferentially expressed in Th1 (CXCR3) or Th17 (CCR4 and CCR6) subsets (Bromley *et al.*, 2008; Brodie *et al.*, 2013). In contrast, the expression of the Th2 chemokine receptor *CRTh2* in acne lesions was not different from the one of normal skin. Our detailed analysis of $CD4^+$ T-cell subset markers further supports the presence of cells of Th1 and Th17 in inflammatory lesions of patients suffering from acne.

P. acnes triggers Th17 and mixed Th17/Th1 responses *in vitro*

To further characterize Th responses to *P. acnes*, peripheral blood mononuclear cells (PBMCs) from healthy donors were exposed to live *P. acnes*, at different multiplicities of infection (MOI). After 24 hours, we observed a strong secretion of Th1 and Th17 polarizing cytokines: namely IL-12 (Th1) and IL-1β, IL-6, and IL-23 (Th17) (Supplementary Figure S1a online). Moreover, we could confirm that, after 6 days of incubation, a robust release of Th1 and Th17 effector cytokines, namely IFN-γ and IL-17A, respectively, could be detected, whereas *P. acnes* failed to induce the secretion of IL-4 and IL-22 from PBMCs (Supplementary Figure S1b online). However, using intracellular stainings and flow-cytometric analysis, we observed that IL-17A was secreted by two distinct cell populations upon *P. acnes* exposure. In accordance with the recent report from Agak *et al.* (2013), we also found a first population secreting IL-17A alone. Interestingly, we identified a second cell population secreting IL-17A and IFN-γ concomitantly (Figure 2a). In line with ELISA data, we did not detect cells producing IL-4 or IL-22 upon stimulation with *P. acnes*. The induction of *P. acnes*-reactive $IL\text{-}17A^+$ $IFN\text{-}\gamma^-$ and $IL\text{-}17A^+$ $IFN\text{-}\gamma^+$ cells was significant in 100% of the tested healthy donors (Figure 2b). In contrast, induction of $IL\text{-}17A^-$ $IFN\text{-}\gamma^+$ cells was observed in only 40% of the tested donors (Figure 2b). Nearly 100% of the *P. acnes*-induced $IL\text{-}17A^+$ cells were $CD4^+$ (Figure 2c). Taken together, these data show that *P. acnes* not only induces Th17 ($IL\text{-}17A^+$ $IFN\text{-}\gamma^-$) but also Th17/Th1 ($IL\text{-}17A^+$ $IFN\text{-}\gamma^+$) responses.

P. acnes-exposed monocytes activate $CD4^+$ T cells in an major histocompatibility complex II-dependent manner

These findings prompted us to further characterize the $CD4^+$ T-cell response to *P. acnes.* Therefore we isolated $CD4^+$ T cells from PBMCs from healthy donors and stimulated them with live bacteria in the presence of autologous monocytes. After 6 days, we assessed the production of IL-17A and IFN-γ by intracellular staining. Flow-cytometric analysis showed that both $IL\text{-}17A^+$ $IFN\text{-}\gamma^-$ and $IL\text{-}17A^+$ $IFN\text{-}\gamma^+$ $CD4^+$ cells are strongly induced in response to *P. acnes* (Figure 3a and b). In about 50% of tested donors also $IL\text{-}17A^-$ $IFN\text{-}\gamma^+$ T cells were increased upon *P. acnes* exposure (Figure 3b). It has been previously shown that human leukocyte antigen-DR (HLA-DR) is upregulated in acne lesions and that HLA-DR-expressing cells are present in close association with $CD4^+$ T cells surrounding the lesions (Layton *et al.*, 1998). We addressed the role of major histocompatibility complex (MHC) class II in the induction of T-cell response upon *P. acnes* exposure by blocking its function with a neutralizing antibody. Treatment with an anti-HLA-DR antibody, but not with an irrelevant control antibody, led to a significant decrease in IL-17A single producers as well as IL-17A and IFN-γ double producers in all analyzed donors (Figure 3c and d). Anti-HLA-DR also led to a decrease in the number of T cells producing

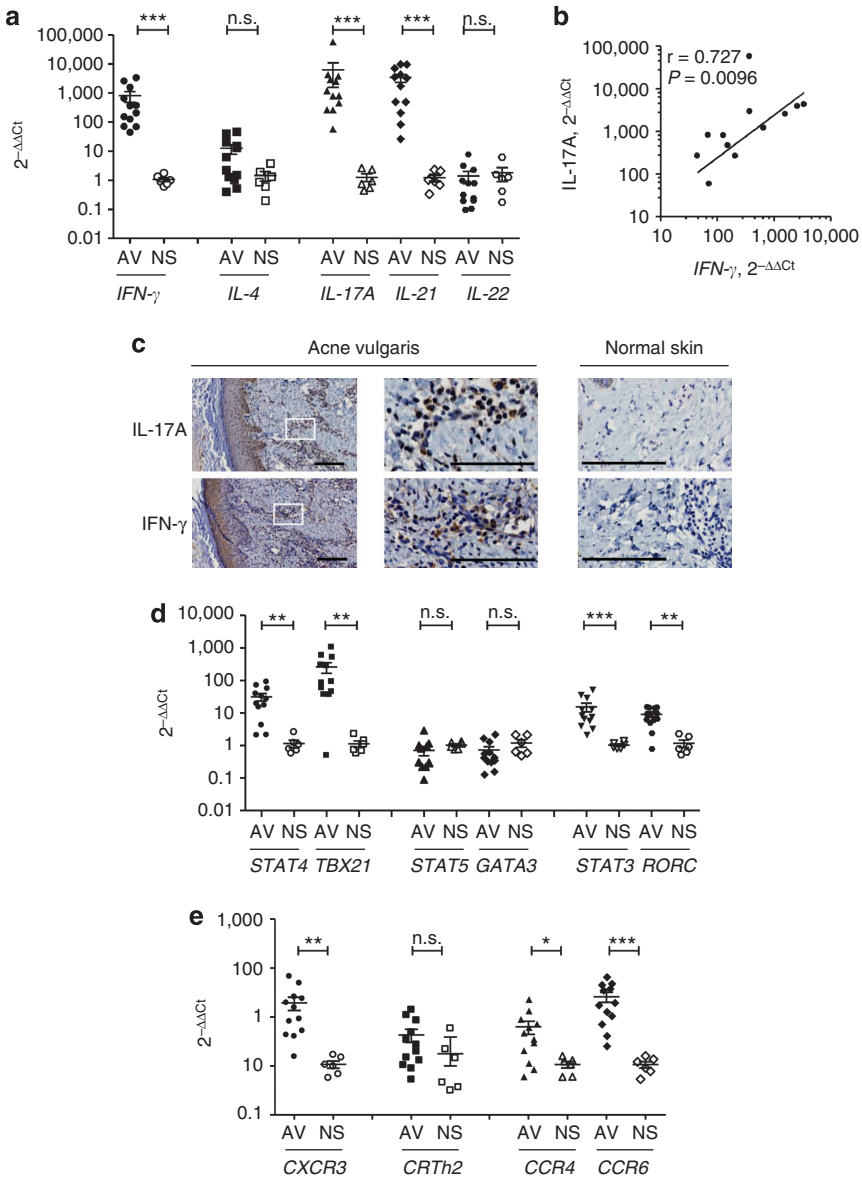

Figure 1. Cells with T helper type 1 (Th1) and Th17 profile are found in acne lesions. (**a**) Th cell effector cytokine gene expression in acne lesions (AV, $n=12$) and normal skin (NS, $n=6$) measured by quantitative reverse transcriptase in real time (qPCR). (**b**) Scatter plot showing the correlation (Spearman's rank correlation) between IL-17A and IFN-γ mRNA expression in human acne biopsies. (**c**) Immunohistochemical analysis of IL-17 and IFN-γ in an acne lesion compared with healthy skin (scale bar = 500 μm). (**d**) Transcription factors and (**e**) chemokine receptor gene expression in acne lesions (AV, $n=12$) and normal skin (NS, $n=6$) measured by qPCR. The relative mRNA abundance of indicated genes against ribosomal protein L27 (RPL27) mRNA levels was analyzed and normalized with the average of normal skin. *$P\leqslant0.01$, **$P\leqslant0.001$, and ***$P\leqslant0.0001$ by the Mann–Whitney two-tailed test for acne lesions compared with normal skin. Presented are mean and SEM.

only IFN-γ in about 80% of the donors, as shown in Figure 3d. However, for unknown reasons, the extent of this reduction was not as strong as the one obtained in IL-17A single producer or IL-17A and IFN-γ double-producer reduction and was not statistically significant. Moreover, the blockade of MHC II resulted in a strong reduction of T-cell proliferation upon *P. acnes* exposure (Figure 3e). These data demonstrate that proliferation and cytokine secretion by $CD4^+$ T cells upon *P. acnes* exposure are dependent on MHC II.

IL-1β and IL-12/IL-23 modulate the T-cell response to *P. acnes*

The IL-1 family cytokines and STAT activators are able to influence effector cytokine production from differentiated Th subsets. IL-12 activates STAT4 and, together with IL-18, induces IFN-γ production from Th1 cells (Guo *et al.*, 2009). Secretion of IL-17A from Th17 cells can be promoted by IL-1 and STAT3 activators, including IL-6, IL-21, and IL-23 (Chung *et al.*, 2009; Guo *et al.*, 2009). The observation that IL-1β, IL-12, and IL-23 are secreted by PBMCs upon *P. acnes*

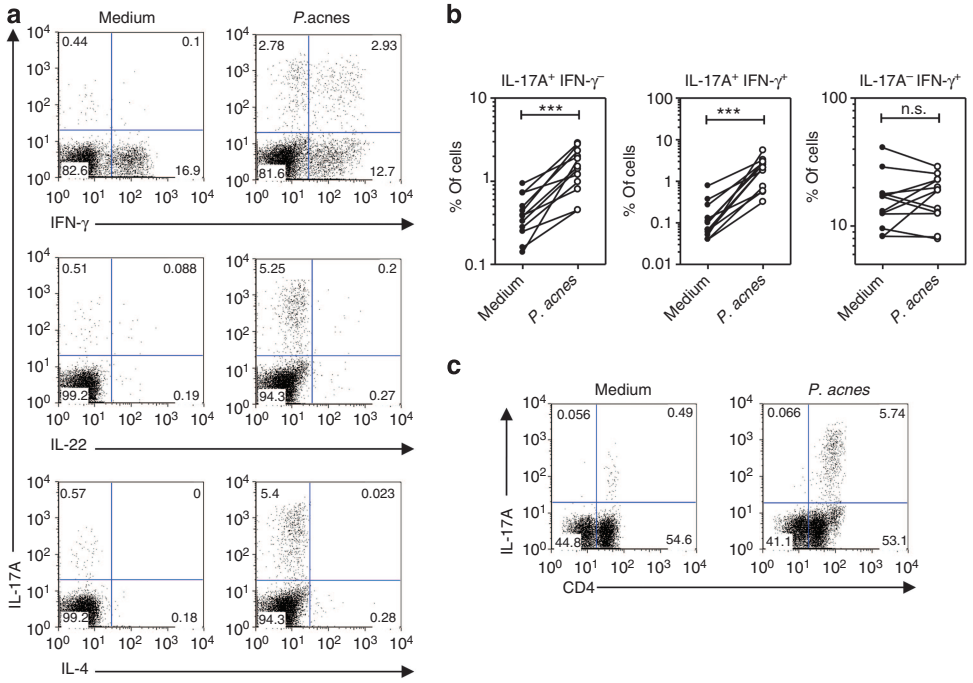

Figure 2. *P. acnes* induces production of IL-17A and IFN-γ by CD4$^+$ T cells. Peripheral blood mononuclear cells (PBMCs) were exposed to *P. acnes* (multiplicity of infection (MOI) = 3) or incubated with medium. On day 6, cells were stimulated for 4.5 hours with phorbol 12-myristate 13-acetate (PMA) and ionomycin, fixed, permeabilized, and stained with antibodies against CD4, IL-17A, and IFN-γ or IL-22 or IL-4. (**a**) Representative flow-cytometric analysis. (**b**) Percentages of IL-17A$^+$IFN-γ$^-$, IL-17A$^+$IFN-γ$^+$, and IL-17A$^-$IFN-γ$^+$ detected in PBMCs from healthy donors untreated (●) or stimulated with *P. acnes* (○) ($n = 12$). Each symbol represents a unique donor. ***$P \leqslant 0.0001$ and ****$P \leqslant 0.00001$ by two-tailed paired Student's *t*-test for *P. acnes*-exposed PBMCs compared with medium-exposed PBMCs. (**c**) Representative flow-cytometric analysis of CD4 expression among IL-17A$^+$ PBMCs stimulated with *P. acnes*.

exposure (Supplementary Figure S1a online) prompted us to investigate whether these cytokines may have a role in shaping T-cell responses. Sorted CD4$^+$ T cells were stimulated with live *P. acnes* in the presence of various neutralizing mAb. The inhibition of IL-1β resulted in a reduction in IL-17A$^+$ IFN-γ$^-$ and IL-17A$^+$ IFN-γ$^+$ T cells, whereas the neutralization of the IL-12/23-p40 common subunit alone reduced the response of IL-17A$^+$ IFN-γ$^+$ cells but did not affect IL-17A$^+$ IFN-γ$^-$ T cells unless used together with anti-IL-1β (Figure 4). The effect of anti-IL-12/23 blocking mAb on IL-17A$^+$ IFN-γ$^+$ T cells was further enhanced when used in combination with anti-IL-1β mAb. In contrast, tumor necrosis factor-α inhibition did not significantly affect the T-cell response to *P. acnes*. These results suggest that the stimulation of *P. acnes*-induced Th17 and Th17/Th1 T cells can be efficiently prevented by blocking IL-12/23-p40 and IL-1β, whereas the responses of IL-17A$^-$ IFN-γ$^+$ cells are less susceptible to the blockade of these cytokines.

Acne patients exhibit stronger Th17 and Th17/Th1 responses to *P. acnes*

The presence of *P. acnes*-reactive T cells in the blood of healthy individuals raised the question whether these cells could be detected at higher frequencies in acne patients. To address this question and assess the specificity of responding CD4$^+$ T cells, the ability of *P. acnes* to induce Th17 and Th17/Th1 responses was compared with *Staphylococcus aureus* (*S. aureus*). As *S. aureus* could not be used in its live form, cells were stimulated with bacterial lysates. *P. acnes* lysates induced comparable number of IL-17A$^+$IFN-γ$^-$ as well as IL-17A$^+$IFN-γ$^+$ cells as live bacteria (Supplementary Figure S2 online). Then, we compared the response to *P. acnes* and *S. aureus* in healthy donors and in acne patients. In healthy donors, both *P. acnes* and *S. aureus* induced, at a similar extent, a discrete increase of IL-17A$^+$ IFN-γ$^-$ as well as IL-17A$^+$IFN-γ$^+$ CD4$^+$ cells (Figure 5). In contrast, *P. acnes* was able to induce a dramatic increase in both IL-17A$^+$IFN-γ$^-$ and IL-17A$^+$IFN-γ$^+$ CD4$^+$ cells, whereas the induction of both CD4$^+$ subsets remained discrete and comparable with that of healthy donors upon exposure to *S. aureus* lysates (Figure 5). Neither *P. acnes* nor *S. aureus* was able to induce IL-17A$^-$IFN-γ$^+$ cells in both healthy individuals' and acne patients' cells. Altogether, these data show that acne patients have increased frequencies of circulating *P. acnes*-specific Th17 and Th17/Th1 cells.

DISCUSSION

In the present study, we have investigated the adaptive immune response to the skin commensal bacterium *P. acnes*. Previous studies have shown that *P. acnes*-specific Th1 are cells present in early inflamed acne lesions (Mouser *et al.*, 2003). In addition to IFN-γ, we have found significantly increased levels of IL-17A but not IL-4 or IL-22 in acne

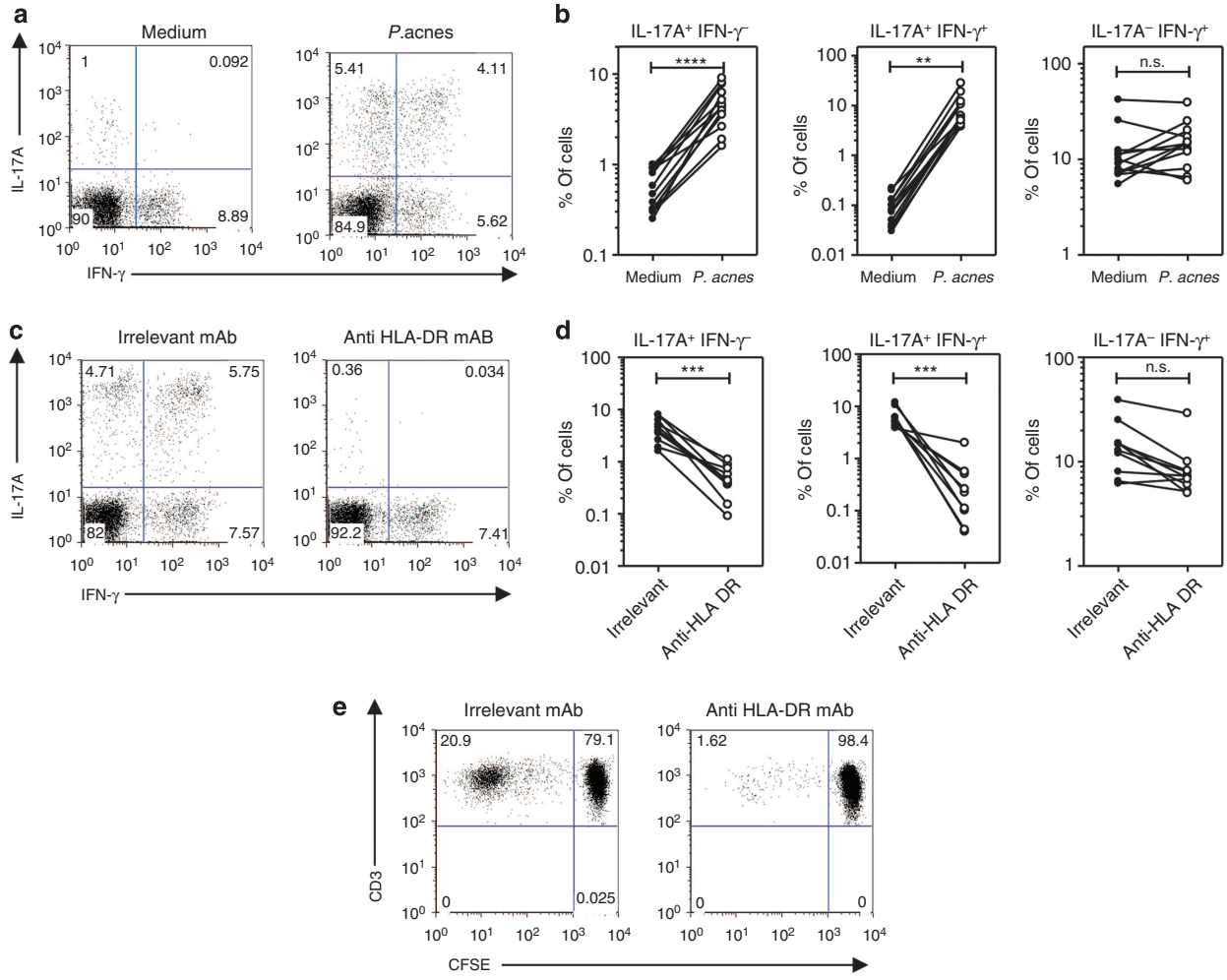

Figure 3. Major histocompatibility complex II (MHC II)-dependent response of CD4$^+$ T cells to *P. acnes* infection. (**a**, **b**) Freshly isolated CD4$^+$ T cells from healthy donors were left untreated or exposed to *P. acnes* in the presence of autologous monocytes. On day 6, cells were stimulated with P/I and stained with antibodies against CD4, IL-17A, and IFN-γ. (**a**) Representative flow-cytometric analysis. (**b**) Percentages of IL-17A$^+$IFN-γ$^-$, IL-17A$^+$IFN-γ$^+$, and IL-17A$^-$IFN-γ$^+$ within CD4$^+$ T cells untreated (●) or stimulated with *P. acnes* (○) ($n=12$). (**c**, **d**) IL-17A and INF-γ production by CD4$^+$ T cells stimulated with *P. acnes* in the presence of irrelevant or anti-HLA-DR-neutralizing mAb determined by intracellular staining following P/I stimulation on day 6. (**c**) Representative flow-cytometric analysis. (**d**) Percentages of IL-17A$^+$IFN-γ$^-$, IL-17A$^+$IFN-γ$^+$, and IL-17A$^-$IFN-γ$^+$ within CD4$^+$ T cells stimulated with *P. acnes* in the presence of irrelevant mAb (●) or anti-HLA-DR mAb (○) ($n=10$). (**e**) Carboxyfluorescein succinimidyl ester (CFSE) profile of CD4$^+$ T cells stimulated with autologous monocytes exposed to *P. acnes* in the presence of irrelevant mAb or anti-HLA-DR mAb. Data are representative of at least three different experiments. (**b**, **d**) Each symbol represents an individual donor. ***$P\leqslant0.0001$ and ****$P\leqslant0.00001$ by two-tailed paired Student's *t*-test. HLA-DR, human leukocyte antigen-DR; P/I, phorbol 12-myristate 13-acetate (PMA)/ionomycin.

biopsies. *In vitro,* we demonstrated that *P. acnes* has the ability to induce the secretion of IL-17A and IFN-γ, therefore confirming the recent observation by Agak *et al.* (2013) that *P. acnes* induces Th17 differentiation. However, in contrast to the data reported in the same study, we show that IL-17A is produced by two distinct subsets of T cells producing either IL-17A alone or in conjunction with IFN-γ. We also observed that Th1 cells could be induced in only 40% of the tested donors, whereas Th17 and Th17/Th1 cells could be induced by *P. acnes* in 100% of them. This is also in apparent contradiction with the recent study by Agak *et al.* (2013), who concluded that both Th17 and Th1 cells could be induced in 100% of the tested PBMC donors. In fact, we show here that, in addition to Th17 and Th1 cells, a third subset secreting both IL-17A and IFN-γ may be involved in the inflammatory response to *P. acnes*. Interestingly, our data suggest that the use of anti-IL-1β and anti-IL-12/IL-23 may represent an efficient strategy for the targeting of Th17/Th1 cells. While anti-IL-1β had a discrete but significant effect on the induction of IL-17A$^+$/IFN-γ$^-$ cells, an anti-IL-12/IL-23-p40 antibody alone did not impact the response of these cells, suggesting that, in this setting, the induction of Th17 cells by *P. acnes* does not require IL-23, as previously reported (Agak *et al.*, 2013). In contrast, anti-IL-1β and anti-IL-12/IL-23-p40 had pronounced additive inhibitory effects on cells producing both IL-17 and IFN-γ, suggesting that IL-1β and IL-12 or/and IL-23 are key cytokines in the differentiation of these cells. We also found elevated levels of IL-21 mRNA in acne lesions, whereas, surprisingly, IL-22 mRNA levels were similar to those found in healthy skin.

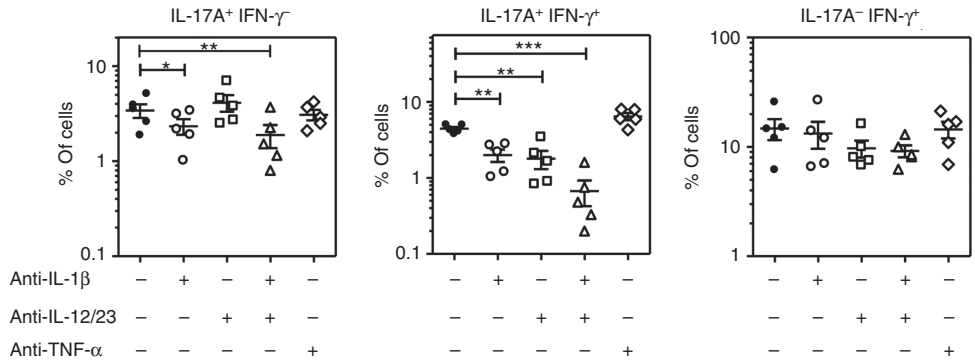

Figure 4. T helper type 17 (Th17) and Th17/Th1 responses are prevented by blocking differentiation cytokines. Freshly isolated CD4$^+$ T cells from healthy donors ($n=5$) were left untreated or exposed to *P. acnes* in the presence of autologous monocytes. On day 6, cells were stimulated with phorbol 12-myristate 13-acetate (PMA) and ionomycin and stained with antibodies to CD4, IL-17A, and IFN-γ. Percentages of IL-17A$^+$IFN-γ$^-$, IL-17A$^+$IFN-γ$^+$, and IL-17A$^-$IFN-γ$^+$ within CD4$^+$ T cells stimulated with *P. acnes* in the absence or presence of the indicated blocking antibodies. $^{**}P\leqslant0.001$ and $^{***}P\leqslant0.0001$ by two-tailed paired Student's *t*-test. Results are presented as mean and SEM.

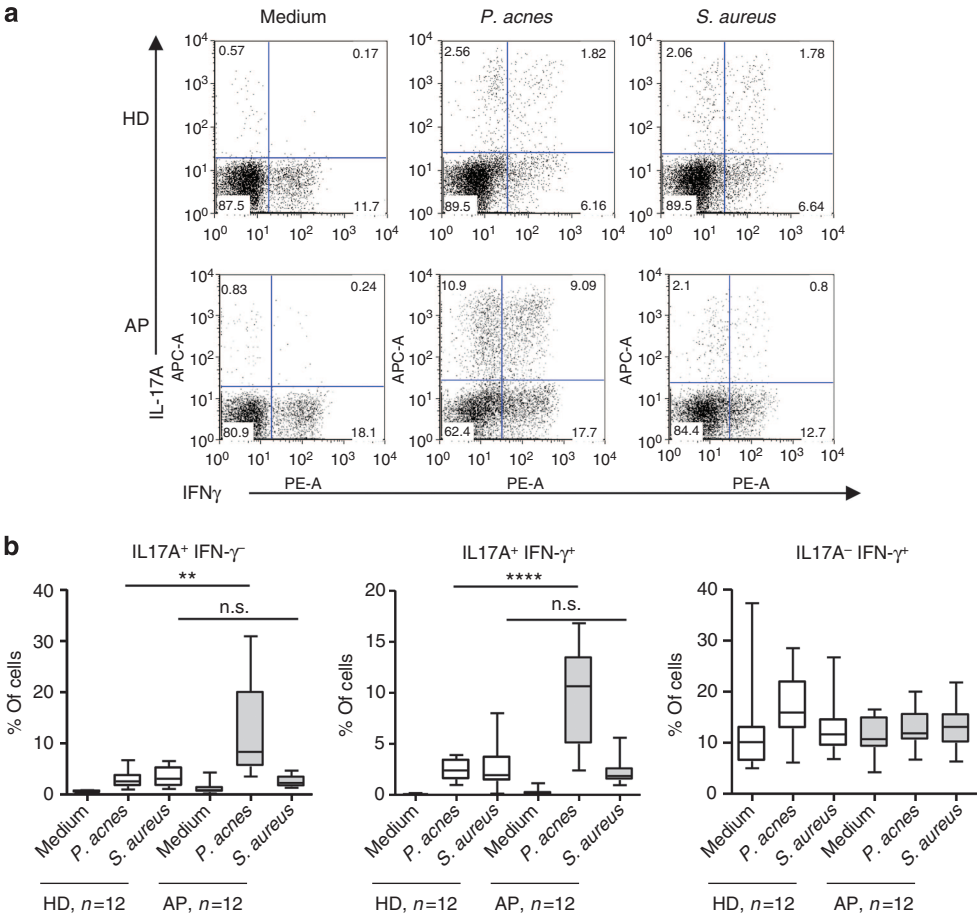

Figure 5. Acne patients have enhanced T-cell responses to *P. acnes*. Freshly isolated peripheral blood mononuclear cells (PBMCs) from healthy donors (HD, $n=12$) and acne patients (AP, $n=12$) were exposed to bacterial lysates from *P. acnes* or *S. aureus* or incubated with medium. On day 6, cells, after 4.5 hours stimulation with phorbol 12-myristate 13-acetate (PMA) and ionomycin, were subjected to intracellular staining with antibodies against CD4, IL-17A, and IFN-γ. (**a**) Representative flow-cytometric analysis. (**b**) Percentages IL-17A$^+$IFN-γ$^-$, IL-17A$^+$IFN-γ$^+$, and IL-17A$^-$IFN-γ$^+$ detected among CD4$^+$ cells from healthy donors and acne patients untreated or stimulated with *P. acnes* or *S. aureus*. $^{**}P\leqslant0.001$ and $^{****}P\leqslant0.00001$ by two-tailed unpaired Student's *t*-test for HD-PBMCs compared with AP-PBMCs exposed to indicated bacteria.

Th17 effector cytokines, IL-17 and IL-22, have the capacity to stimulate the production of various antimicrobial peptides (Peck and Mellins, 2010). Moreover, IL-17 induces the production of neutrophil-recruiting chemokines such as IL-8 (CXCL8) in epithelial cells (Laan *et al.*, 1999; Ye *et al.*, 2001; Annunziato *et al.*, 2012). It has been previously shown that neutrophils infiltrate late-stage acne lesions (Norris and Cunliffe, 1988) and that the expression levels of IL-8 in acne biopsies are elevated (Trivedi *et al.*, 2006). In addition to its ability to induce pro-inflammatory cytokine secretion in the perifollicular area, *P. acnes* is thought to produce low-molecular weight chemotactic factors, resulting in the accumulation of neutrophils at the site of acne comedones. Our observation that IL-17A is found in acne lesions and that *P. acnes* has the ability to induce IL-17-secreting $CD4^+$ T cells supports an additional T-cell–dependent role of this bacterium in the recruitment of neutrophils at the site of acne lesions.

The coproduction of IFN-γ and IL-17 has been previously observed in memory T cells residing in the gut of patients with Crohn's disease (Annunziato *et al.*, 2007) and in T cells responding to the mycobacterial antigen purified protein derivative (Acosta-Rodriguez *et al.*, 2007). Moreover, it has been shown that *Candida albicans*-specific T cells have the capacity to produce IL-17A in combination with IFN-γ and co-express ROR-γt and T-bet (Zielinski *et al.*, 2012). These cells with a mixed Th17/Th1cytokine profile most likely derive from Th17 subsets exhibiting a certain plasticity and can acquire functional characteristics of Th1 cells (Muranski and Restifo, 2013).

Alhough Th17 cells have been extensively studied, the precise role of Th17/Th1 cells in host defense and diseases remains to be investigated. The development of these mixed T-cell subset depends on the cytokine microenvironment (Zielinski *et al.*, 2012) but also might be induced by chronic stimulation of Th17 cells (Dileepan *et al.*, 2011).

In the present work, we also demonstrate that recall responses could be elicited by *P. acnes* and that such responses are mainly mediated by Th17 and Th17/Th1 cells. Interestingly, the Th17- and Th17/Th1-mediated recall responses could be observed in all the healthy donors tested ($n = 12$), suggesting that such a pool of memory cells is present in a majority of healthy individuals. The increased responses of IL-17A- and IL-17A/IFN-γ-producing $CD4^+$ cells found in individuals with an active disease revealed higher frequencies of circulating *P. acnes*-specific T cells in acne patients. In contrast, responses to *S. aureus* were not enhanced in PBMCs from patients with acne when compared with healthy individuals.

Altogether, our data suggest that $CD4^+$ T cells harboring a Th17 and Th17/Th1 cytokine profile may be involved in the inflammatory response associated with acne. The targeting of effector cytokines—namely, IL-17 and IFN-γ—or differentiation cytokines—namely, IL-1β and IL-23—may represent a new therapeutic approach for the treatment of acne. However, a better knowledge of the precise contribution of these T-cell subsets in the pathogenesis of this common skin disease remains to be further investigated.

MATERIALS AND METHODS

Human samples

All human skin biopsies and peripheral blood samples were collected with informed written consent upon approval from Local Ethical Committees and were conducted according to the Declaration of Helsinki Principles. All acne patients included in this study had a moderate form of acne vulgaris. All of them were 19–25-year-old men who were not treated at the time of biopsy.

Cell sorting

PBMCs were isolated from buffy coats (obtained from healthy donors, Blood Donation Center, Schlieren, Switzerland) and from peripheral blood from acne patients using a density gradient (Ficoll-Paque, Pharmacia, Glattbrugg, Switzerland). $CD4^+$ T cells were sorted from PBMCs by negative selection using magnetic beads ($CD4^+$ T Cell Isolation Kit II, MACS, Miltenyi Biotech, Bergisch Gladbach, Germany) with a purity of 97% (determined by staining with CD3 and CD4 antibodies and flow-cytometric analysis). Monocytes were sorted with anti-CD14-labeled magnetic beads according to the manufacturer's instructions (MACS, Miltenyi Biotech). The purity was over 96% as determined by CD14 staining and flow-cytometric analysis.

Bacteria

P. acnes (DSM 1897, DMSZ, Braunschweig, Germany) was cultured under anaerobic conditions as previously described (Kistowska *et al.*, 2013). Bacteria were harvested by centrifugation at 5,000 r.p.m. for 10 minutes, washed, and suspended in phosphate-buffered saline (PBS) or medium for experiments. To prepare bacterial lysates, bacterial pellets were resuspended in PBS and heat inactivated for 1 hour at 65 °C and then subjected to five freeze–thaw cycles followed by two rounds of sonication (5 minutes each). Protein concentration was measured using the bicinchoninic acid assay (BCA Protein Assay Reagent, Pierce, Rockford, IL) according to the manufacturer's instructions.

T-cell–stimulation assays

Cells were cultured in RPMI 1640 medium (Invitrogen, Basel, Switzerland), supplemented with 5% human serum (Blood Donation Center, Schlieren, Switzerland), 1% Antibiotic-Antimycotic (Invitrogen, Life Technologies, Zug, Switzerland), 1 mM sodium pyruvate (Invitrogen), and 2 mM GlutaMAX solution (Invitrogen). PBMCs from healthy donors and patients were exposed to live *P. acnes* at the indicated MOI or to bacterial lysates (2.5 μg ml^{-1}) for 6 days. Sorted $CD4^+$ T cells were cocultured for 6 days with autologous monocytes (ratio 2:1) pre-exposed to live *P. acnes* at the indicated MOI. In some experiments, T-cell activation was performed in the presence of the following neutralizing antibodies (all at 10 μg ml^{-1}): anti-human leukocyte antigen HLA-DR (L243, kindly provided by Prof G. De Libero, Basel, Switzerland), irrelevant mouse IgG2a (MG2a-53, Biolegend, San Diego, CA), anti-IL-1β (Canakinumab, Novartis, Basel, Switzerland), anti-IL-12/IL-23 (Ustekinumab, Janssen Biotech, Zug, Switzerland), and tumor necrosis factor-α inhibitor (5 μg ml^{-1} Etanercept, Pfizer, Zürich, Switzerland).

Cytokine analysis

Cell culture supernatants were collected at indicated time points, and the following cytokines were measured by ELISA: IL-1β IL-6, IL-17A, IFN-γ IL-22 (R&D Systems, Minneapolis, MN), IL-4, IL-12p70 (Biolegend), and IL-23 (eBioscience, San Diego, CA). All ELISAs were

performed according to the manufacturer's instructions. For intracellular cytokine stainings, cells were stimulated at indicated time points for 4.5 hours with phorbol-12-myristate-13-acetate (50 ng ml^{-1}, Sigma-Aldrich, Buchs, Switzerland) and ionomycin (500 ng ml^{-1}, Sigma-Aldrich) in the presence of brefeldin A (5 μg ml^{-1}, Sigma-Aldrich). Cells were fixed with paraformaldehyde (2%, Sigma-Aldrich), permeabilized with saponin (0.1%, Sigma-Aldrich), and stained with anti-IL-17A (BL168), anti-IFN-γ (B27), anti-IL-4 (MP4-25D2), and anti-IL-22 (BG/IL-22) (all from Biolegend) and were analyzed by flow cytometry (FacsCanto A, Becton-Dickinson, Basel, Switzerland). Flow-cytometric data were analyzed by FlowJo (Tree Star, Ashland, OR).

Gene expression analysis

Total RNA was isolated from human skin samples obtained from healthy donors ($n=6$) or from acne patients ($n=12$) using the RNeasy Fibrous Tissue Kit (Qiagen, Basel, Switzerland) according to the manufacturer's instructions. RNA was converted into cDNA by standard reverse transcription with the RevertAid First Strand cDNA Synthesis Kit (Thermo Scientific, Life Technologies, Carlsbad, CA). Quantitative PCR was performed using Power SYBR Green PCR Master Mix (Applied Biosystems, Life Technologies). The following primers were used:

RPL27: forward 5′-ATCGCCAAGAGATCAAAGATAA-3′, reverse 5′-TCTGAAGACATCCTTATTGACG-3′

IFN-γ: forward 5′-TCGGTAACTGACTTGAATGTCCA-3′, reverse 5′-TCGCTTCCCTGTTTTAGCTGC-3′

IL-4: forward 5′-CCGTAACAGACATCTTTGCTGCG-3′, reverse 5′-GAGTGTCCTTCTCATGGTGGCT-3′

IL-17A: forward 5′-CAATCCCACGAAATCCAGGATG-3′, reverse 5′-GGTGGAGATTCCAAGGTGAGG-3′

IL-21: forward 5′-CCAAGGTCAAGATCGCCACATG-3′, reverse 5′-TGGAGCTGGCAGAAATTCAGGG-3′

IL-22: forward 5′-GCTTGACAAGTCCAACTTCCA-3′, reverse 5′-GCTCACTCATACTGACTCCGTG-3′

STAT3: forward 5′-CTTTGAGACCGAGGTGTATCACC-3′, reverse 5′-GGTCAGCATGTTGTACCACAGG-3′

STAT4: forward 5′-CAGTGAAAGCCATCTCGGAGGA-3′, reverse 5′-TGTAGTCTCGCAGGATGTCAGC-3′

STAT5a: forward 5′-GTTCAGTGTTGGCAGCAATGAGC-3′, reverse 5′-AGCACAGTAGCCGTGGCATTGT-3′

RORC: forward 5′-GAGGAAGTGACTGGCTACCAGA-3′, reverse 5′-GCACAATCTGGTCATTCTGGCAG-3′

TBX-21: forward 5′-ATTGCCGTGACTGCCTACCAGA-3′, reverse 5′-GGAATTGACAGTTGGGTCCAGG-3′

GATA3: forward 5′-ACCACAACCACACTCTGGAGGA-3′, reverse 5′-TCGGTTTCTGGTCTGGATGCCT-3′

CXCR3: forward 5′-ACGAGAGTGACTCGTGCTGTAC-3′, reverse 5′-GCAGAAAGAGGAGGCTGTAGAG-3′

CRTh2: forward 5′-TGGAGTCATCCTCTTCGTGGTG-3′, reverse 5′-AGTAGGTGAAGAAGGGCAGGGA-3′

CCR4: forward 5′-CTCTGGCTTTTGTTCACTGCTGC-3′, reverse 5′-AGCCCACAGTATTGGCAGAGCA-3′

CCR6: forward 5′-CTGAACCCTGTGCTCTACGCTT-3′, reverse 5′-CACAGGAGAAGCCTGAGGACTT-3′

The real-time PCR included an initial denaturation at 95 °C for 10 minutes, followed by 40 cycles of 95 °C for 30 seconds, 55 °C for 1 minute, and 72 °C for 1 minute, and one cycle of 95 °C for 1 minute, 55 °C for 30 seconds, and 95 °C for 30 seconds.

Immunohistochemistry

Human acne skin samples ($n=12$) and normal skin samples ($n=3$) from distinct individuals were cross-sectioned, and immunohistochemistry stainings were performed. After deparaffinization by heat and ascending alcohol series, the slides were stored in Retrieval Solution (DAKO, Agilent Technologies, Santa Clara, CA) and heated under pressure in a pressure cooker for 25 minutes for antigen demasking. Unspecific binding sites were blocked by incubation in 5% (wt/v) BSA and 5% (v/v) normal goat serum (DAKO) in PBS for 1 hour. Antibodies against IFN-γ (Abcam, Cambridge, UK) and Interleukin-17 (Abcam) were diluted in antibody diluent (DAKO S0809), and an appropriate isotype control antibody was substituted for every primary antibody on a separate section. Slides were washed with PBS, and secondary antibody goat anti-rabbit (Southern Biotech, Birmingham, AL) was added and incubated for 1 hour at room temperature. Slides were again washed with PBS and mounted with an Avidin–Biotin complex (Vectastain, Vector Laboratories, Burlingame, CA). After 45 minutes, incubation slides were washed with PBS and mounted with (3,3′-diaminobenzidine) HRP substrate (Vectastain) to produce a brown reaction product. After the washing steps, a counterstain with hematoxylin was performed. The sections were mounted in mounting medium (DAKO) and imaged using Aperio ScanScope (Leica, Nussloch, Germany).

Statistics

The statistical analysis for quantitative reverse transcriptase in real time on human samples was performed using the Mann–Whitney two-tailed test. Data obtained from *in vitro* experiments were subjected to two-tailed paired or unpaired Student's *t*-test as indicated. Differences were considered significant when $*P \leqslant 0.05$, $**P \leqslant 0.001$, $***P \leqslant 0.0001$, and $****P \leqslant 0.00001$. All statistical analyses were performed using GraphPad Prism software (La Jolla, CA).

CONFLICT OF INTEREST

The authors state no conflict of interest.

ACKNOWLEDGMENTS

We thank Prof Onur Boyman for helpful discussions, and the medical staff from the Dermatology Department of the University Hospital of Zürich for their help in collecting biological samples from patients suffering from acne. This work was supported by grants from the Swiss National Science Foundation (grants 31003A-120400 and 31003A-135465 to LEF).

SUPPLEMENTARY MATERIAL

Supplementary material is linked to the online version of the paper at http://www.nature.com/jid

REFERENCES

Acosta-Rodriguez EV, Rivino L, Geginat J *et al.* (2007) Surface phenotype and antigenic specificity of human interleukin 17-producing T helper memory cells. *Nat Immunol* 8:639–46

Agak GW, Qin M, Nobe J *et al.* (2013) *Propionibacterium acnes* induces an IL-17 response in acne vulgaris that is regulated by vitamin A and vitamin D. *J Invest Dermatol* 134:366–73

Annunziato F, Cosmi L, Liotta F *et al.* (2012) Defining the human T helper 17 cell phenotype. *Trends Immunol* 33:505–12

Annunziato F, Cosmi L, Santarlasci V *et al.* (2007) Phenotypic and functional features of human Th17 cells. *J Exp Med* 204:1849–61

Asarch A, Barak O, Loo DS *et al.* (2008) Th17 cells: a new paradigm for cutaneous inflammation. *J Dermatol Treat* 19:259–66

Brodie T, Brenna E, Sallusto F (2013) OMIP-018: chemokine receptor expression on human T helper cells. *Cytometry A* 83:530–2

Bromley SK, Mempel TR, Luster AD (2008) Orchestrating the orchestrators: chemokines in control of T cell traffic. *Nat Immunol* 9:970–80

Chung Y, Chang SH, Martinez GJ *et al.* (2009) Critical regulation of early Th17 cell differentiation by interleukin-1 signaling. *Immunity* 30:576–87

Dileepan T, Linehan JL, Moon JJ *et al.* (2011) Robust antigen specific th17 T cell response to group A *Streptococcus* is dependent on IL-6 and intranasal route of infection. *PLoS Pathog* 7:e1002252

Guo L, Wei G, Zhu J *et al.* (2009) IL-1 family members and STAT activators induce cytokine production by Th2, Th17, and Th1 cells. *Proc Natl Acad Sci USA* 106:13463–8

Jappe U, Ingham E, Henwood J *et al.* (2002) *Propionibacterium acnes* and inflammation in acne; *P. acnes* has T-cell mitogenic activity. *Br J Dermatol* 146:202–9

Jeremy AH, Holland DB, Roberts SG *et al.* (2003) Inflammatory events are involved in acne lesion initiation. *J Invest Dermatol* 121:20–7

Kalis C, Gumenscheimer M, Freudenberg N *et al.* (2005) Requirement for TLR9 in the immunomodulatory activity of *Propionibacterium acnes*. *J Immunol* 174:4295–300

Kim J, Ochoa MT, Krutzik SR *et al.* (2002) Activation of toll-like receptor 2 in acne triggers inflammatory cytokine responses. *J Immunol* 169:1535–41

Kistowska M, Gehrke S, Jankovic D *et al.* (2013) IL-1β drives inflammatory responses to *Propionibacterium acnes in vitro* and *in vivo*. *J Invest Dermatol* 134:677–85

Korn T, Bettelli E, Gao W *et al.* (2007) IL-21 initiates an alternative pathway to induce proinflammatory T(H)17 cells. *Nature* 448:484–7

Laan M, Cui ZH, Hoshino H *et al.* (1999) Neutrophil recruitment by human IL-17 via C-X-C chemokine release in the airways. *J Immunol* 162: 2347–52

Layton AM, Morris C, Cunliffe WJ *et al.* (1998) Immunohistochemical investigation of evolving inflammation in lesions of acne vulgaris. *Exp Dermatol* 7:191–7

Leeming JP, Holland KT, Cuncliffe WJ (1988) The microbial colonization of inflamed acne vulgaris lesions. *Br J Dermatol* 118:203–8

Leyden JJ, McGinley KJ, Vowels B (1998) *Propionibacterium acnes* colonization in acne and nonacne. *Dermatology* 196:55–8

McGeachy MJ (2013) Th17 memory cells: live long and proliferate. *J Leukoc Biol* 94:921–6

Milner JD, Brenchley JM, Laurence A *et al.* (2008) Impaired T(H)17 cell differentiation in subjects with autosomal dominant hyper-IgE syndrome. *Nature* 452:773–6

Miossec P, Kolls JK (2012) Targeting IL-17 and TH17 cells in chronic inflammation. *Nat Rev Drug Discov* 11:763–76

Mouser PE, Baker BS, Seaton ED *et al.* (2003) *Propionibacterium acnes*-reactive T helper-1 cells in the skin of patients with acne vulgaris. *J Invest Dermatol* 121:1226–8

Muranski P, Restifo NP (2013) Essentials of Th17 cell commitment and plasticity. *Blood* 121:2402–14

Nagy I, Pivarcsi A, Koreck A *et al.* (2005) Distinct strains of *Propionibacterium acnes* induce selective human beta-defensin-2 and interleukin-8 expression in human keratinocytes through toll-like receptors. *J Invest Dermatol* 124:931–8

Norris JF, Cunliffe WJ (1988) A histological and immunocytochemical study of early acne lesions. *Br J Dermatol* 118:651–9

O'Connor W Jr., Zenewicz LA, Flavell RA (2010) The dual nature of T(H)17 cells: shifting the focus to function. *Nat Immunol* 11:471–6

Peck A, Mellins ED (2010) Precarious balance: Th17 cells in host defense. *Infect Immun* 78:32–8

Puel A, Cypowyj S, Bustamante J *et al.* (2011) Chronic mucocutaneous candidiasis in humans with inborn errors of interleukin-17 immunity. *Science* 332:65–8

Trivedi NR, Gilliland KL, Zhao W *et al.* (2006) Gene array expression profiling in acne lesions reveals marked upregulation of genes involved in inflammation and matrix remodeling. *J Invest Dermatol* 126:1071–9

Weaver CT, Hatton RD, Mangan PR *et al.* (2007) IL-17 family cytokines and the expanding diversity of effector T cell lineages. *Annu Rev Immunol* 25:821–52

Wei L, Laurence A, Elias KM *et al.* (2007) IL-21 is produced by Th17 cells and drives IL-17 production in a STAT3-dependent manner. *J Biol Chem* 282:34605–10

Wilke CM, Bishop K, Fox D *et al.* (2011) Deciphering the role of Th17 cells in human disease. *Trends Immunol* 32:603–11

Ye P, Rodriguez FH, Kanaly S *et al.* (2001) Requirement of interleukin 17 receptor signaling for lung CXC chemokine and granulocyte colony-stimulating factor expression, neutrophil recruitment, and host defense. *J Exp Med* 194:519–27

Zhu J, Paul WE (2008) CD4 T cells: fates, functions, and faults. *Blood* 112:1557–69

Zhu J, Yamane H, Paul WE (2010) Differentiation of effector CD4 T cell populations (*). *Annu Rev Immunol* 28:445–89

Zielinski CE, Mele F, Aschenbrenner D *et al.* (2012) Pathogen-induced human TH17 cells produce IFN-gamma or IL-10 and are regulated by IL-1beta. *Nature* 484:514–8

In Situ Mapping of Innate Lymphoid Cells in Human Skin: Evidence for Remarkable Differences between Normal and Inflamed Skin

Marie-Charlotte Brüggen[1,2,6], Wolfgang M. Bauer[1,6], Bärbel Reininger[1], Eduard Clim[3], Catalin Captarencu[4], Georg E. Steiner[5], Patrick M. Brunner[1], Barbara Meier[2], Lars E. French[2] and Georg Stingl[1]

Although innate lymphoid cells (ILCs) have recently been identified also in skin, their role in this organ remains poorly understood. In this study, we aimed at developing a technique to assess ILCs in situ and to determine their topographical distribution in human skin. We collected lesional skin biopsies from patients with atopic dermatitis and psoriasis (both n = 13) and normal human skin from healthy controls. After establishing immunofluorescence ILC in situ stainings, we developed an analysis approach (gating combined with manual validation) to reliably identify ILCs. Topographical mapping was obtained by automated calculations of the distances between ILCs and different cellular/structural elements of the skin. Whereas normal human skin harbored a very scarce ILC population (mostly ILC1s and *AHR*$^+$ILC3s), atopic dermatitis and psoriasis skin was infiltrated by clearly visible ILC subsets. We observed atopic dermatitis skin to contain not only ILC2s but also a prominent AHR$^+$ILC3 population. Conversely, we encountered almost equal proportions of ILC1s and RORC$^+$ILC3s in psoriasis skin. Distance calculations revealed ILCs to reside near the epidermis and in close proximity to T lymphocytes. ILC mapping in situ will provide valuable information about their likely communication partners in normal and diseased skin and forms the basis for the appropriate mechanistic studies.

Journal of Investigative Dermatology (2016) **136,** 2396–2405; doi:10.1016/j.jid.2016.07.017

INTRODUCTION

The skin is a barrier organ directly exposed to the outside world. As such, it often faces environmental challenges ranging from immunogenic haptens to invading microbes. Protection from such danger signals is provided by a highly complex cutaneous immune network consisting of both innate and adaptive components (Modlin et al., 2012). Among the latter, a population of skin-resident T cells has been recognized as an important player (Clark, 2015). A novel subset of innate immune cells has more recently entered the stage of immune defense (Kim, 2015), namely innate lymphoid cells (ILCs). These leukocytes require IL-7 for their development and, thus, uniformly express the IL-7 receptor alpha chain CD127. They do not express any lineage (Lin) markers of other leukocyte populations and lack a recombinant antigen recognition receptor (Spits and Cupedo, 2012). What they do share with T-cell subsets, however, are striking similarities regarding their transcription factor (TF) and, hence, cytokine profiles. Based on the latter, three groups of noncytotoxic human ILCs can be defined (De Obaldia and Bhandoola, 2015; Eberl et al., 2015). Group 1 ILCs depend on the TF TBET, and generate IFN-γ and tumor necrosis factor-α, but no cytotoxic molecules. Group 2 ILCs express high levels of the GATA3 and produce T helper type 2 (Th2) cytokines (IL-4, IL-5, and IL-13). Group 3 ILCs constitute a group of cells displaying heterogeneous expression of the TFs' nuclear receptor gamma (RORC), the AHR, and TBET (Serafini et al., 2015). Functionally, ILC3s produce variable amounts of IFN-γ, IL-22, and IL-17 (Eberl and Littman, 2004). This apparent heterogeneity of ILC3s, rather than being indicative of their multifocal origin, seems to be a sign of their plasticity imposed by different types of stimuli in their environment.

All ILCs have in common the capacity of immediately responding to different, often epithelial cell-derived mediators, mostly by cytokine production (Sonnenberg and Artis,

[1]Department of Dermatology, Division of Immunology, Allergy and Infectious Diseases, Medical University of Vienna, Vienna, Austria; [2]Department of Dermatology, Zurich University Hospital, Zurich, Switzerland; [3]Department of Application Support and Image Processing, TissueGnostics srl, Iasi, Romania; [4]Department of Product Development, TissueGnostics srl, Iasi, Romania; and [5]TissueGnostics GmbH, Vienna, Austria

[6]These authors contributed equally to this work.

Correspondence: Georg Stingl, Department of Dermatology, Division of Immunology, Allergy and Infectious Diseases, Medical University of Vienna, Waehringer Guertel 18-20, 1090 Vienna, Austria. E-mail: georg.stingl@meduniwien.ac.at

Abbreviations: AD, atopic dermatitis; IF, immunofluorescence; ILC, innate lymphoid cell; Lin, lineage; NHS, normal human skin; Pso, psoriasis; TF, transcription factor; Th, T helper

Received 8 April 2016; revised 28 June 2016; accepted 14 July 2016; accepted manuscript published online 22 July 2016; corrected proof published online 9 September 2016

2015). This innate response is not only biologically important by itself, but can also initiate and orchestrate adaptive immune responses (Eberl et al., 2015; Sonnenberg and Artis, 2015). Dependent on the type of ILC subset involved, the complex functional interplay of ILCs with other leukocyte populations may either result in inflammation or in the downregulation of inflammatory events. In addition, ILCs play an important role in tissue repair and, as described for a special subset of ILC3s, in the histogenesis of secondary lymphoid tissues (Eberl and Littman, 2004; Yoshida et al., 1999).

It is not entirely clear whether and, if so, how ILCs are embedded in the cutaneous immune network. Most data currently available on the occurrence of ILCs in skin are derived from the murine system. These point to the existence of a small ILC population in normal skin and suggest an involvement of ILC2s (Imai et al., 2013; Kim et al., 2013; Roediger et al., 2013; Salimi et al., 2013) and ILC3s (Pantelyushin et al., 2012) in mouse models of atopic dermatitis (AD) and psoriasis (Pso), respectively. Our knowledge about cutaneous ILCs in humans is currently limited to a few studies conducted on single cell suspensions isolated from skin (Dyring-Andersen et al., 2014; Salimi et al., 2013; Teunissen et al., 2014; Villanova et al., 2014).

In this study, we sought to develop an in situ approach allowing to detect and quantify ILCs in the skin, and, importantly, to obtain a detailed topographic description of these cells in the cutaneous microenvironment. By doing so, we hoped to gain new insights into the role of ILCs in skin biology under physiologic (normal human skin [NHS]) and pathologic conditions (AD and Pso).

RESULTS

In situ identification of ILCs in human skin by a newly developed two-step validation algorithm

Our first aim was to establish multicolor immunofluorescence (IF) in situ stainings for ILC subsets in human skin. We used a microscope equipped with four filters capable of discriminating DAPI, green fluorescent protein, Cy3, and Cy5 fluorescence.

A major requirement for the identification of ILCs is to reliably exclude the expression of markers for any other leukocyte population (Eberl et al., 2015), especially T cells. We implemented this by including the relevant Lin markers (i.e., for natural killer cells [CD16, CD94], Th cells (CD3, CD4), B cells (CD20), Langerhans cells (CD1a), myeloid dendritic cells (CD11c), monocytes (CD14), stem/endothelial cells (CD34), neutrophils (CD15), plasmacytoid dendritic cells (CD123), and mast cells (CD203c); Supplementary Figure S1a online) in a single fluorescence channel. Another channel was used for the identification of TFs that are known to be a prerequisite for the development and functional specialization of, on the one hand, different ILC subpopulations (TBET for ILC1, GATA3 for ILC2, RORC, and AHR for ILC3), and, on the other, Th-cell subtypes (Shih et al., 2014). TF stainings were established using differentiated, sorted Th-cell subsets (Supplementary Figure S1b and c). GATA3 expression in keratinocytes (Kaufman et al., 2003) served as an additional positive validation. We then followed either of two staining strategies to unequivocally identify ILCs in situ (Supplementary Table S1 online). In staining protocol A, we deliberately counterstained with CD3 for the precise exclusion of T cells and also for comparison of Th cell and ILC subtypes. In staining protocol B, we included CD3 in the lineage cocktail and used the third and remaining channel for the depiction of CD45 or of prototypic ILC markers (CD127, CD161, chemoattractant receptor-homologous molecule expressed on T helper type 2, CD117, NKp44, and NKp46).

When examining tissue sections of NHS stained in this way by conventional (i.e., eye based) epiluminescence microscopy, we were able to occasionally identify Lin^- TF^+ cells classified as ILCs but could not grasp the complete picture. The paucity of ILCs and small field of views were the main limiting factors. To overcome this problem, we scanned and recorded the entire skin sections. We then used analysis software (TissueFAXS) to apply an automated algorithm on the scanned images measuring the mean IF intensities of the stained markers in cells (identified with DAPI). Software analysis allowed graphical depiction of the cells as events in dot plots, allowing for gating strategies similar to conventional FACS data assessment. Concerned that the slightest "contamination" of the ILC gate with falsely positive cells would bias results, we implemented a manual validation step in our software. This algorithm cropped out all cells automatically identified as ILCs on a single-cell basis (Figure 1a, Supplementary Figure S2 online) allowing for the manual reassessment of the different fluorescence channels and the cells' morphologic shape. Each cell was manually confirmed or rejected by two observers (Figure 1a).

Using these measurements, we reliably identified a very small population of Lin^-CD3^- cells expressing one of the ILC-associated TFs (Figure 1a). Similar numbers of Lin^-TF^+ cells were encountered when we used staining protocol B, in which we assessed the expression of phenotypic ILC markers in the $Lin^-CD3^-TF^+$ cell population (Figure 1b). We were thereby able to show that these cells are indeed ILCs, as evidenced by their positive expression of CD45, CD127, CD161, or CRTH2 in the case of $GATA3^+$ILC2s (Figure 1b–h and Supplementary Figure S3a–c online).

NHS harbors a sparse dermal ILC population

In a first set of experiments, we searched for ILCs residing in epidermal, upper dermal, and hypodermal areas of NHS. This analysis revealed a very sparse ILC population in the upper dermis (Figure 2a), whereas hypodermal areas as well as the epidermis were essentially devoid of $CD45^+Lin^-$ cells expressing ILC TFs (data not shown). Approximately half of upper dermal ILCs belonged to the group 1 subset ($TBET^+$). AHR-expressing ILC3s accounted for the second most prominent subgroup in NHS followed by $RORC^+$ILC3s, whereas hardly any $GATA3^+$ILC2s were identified. With the exception of ILC2, this composition of ILC subpopulations corresponds to what we and others observed using FACS analysis of dermal cell suspensions (Supplementary Figure S4 online).

Next, we sought to assess the spatial arrangement of ILCs within the skin, especially their topographical distribution with regard to the epidermis and to vascular structures. Therefore, we developed and applied an algorithm calculating the distance of each validated ILC to the epidermis as well as to the nearest blood vessel. These measurements (Figure 2b)

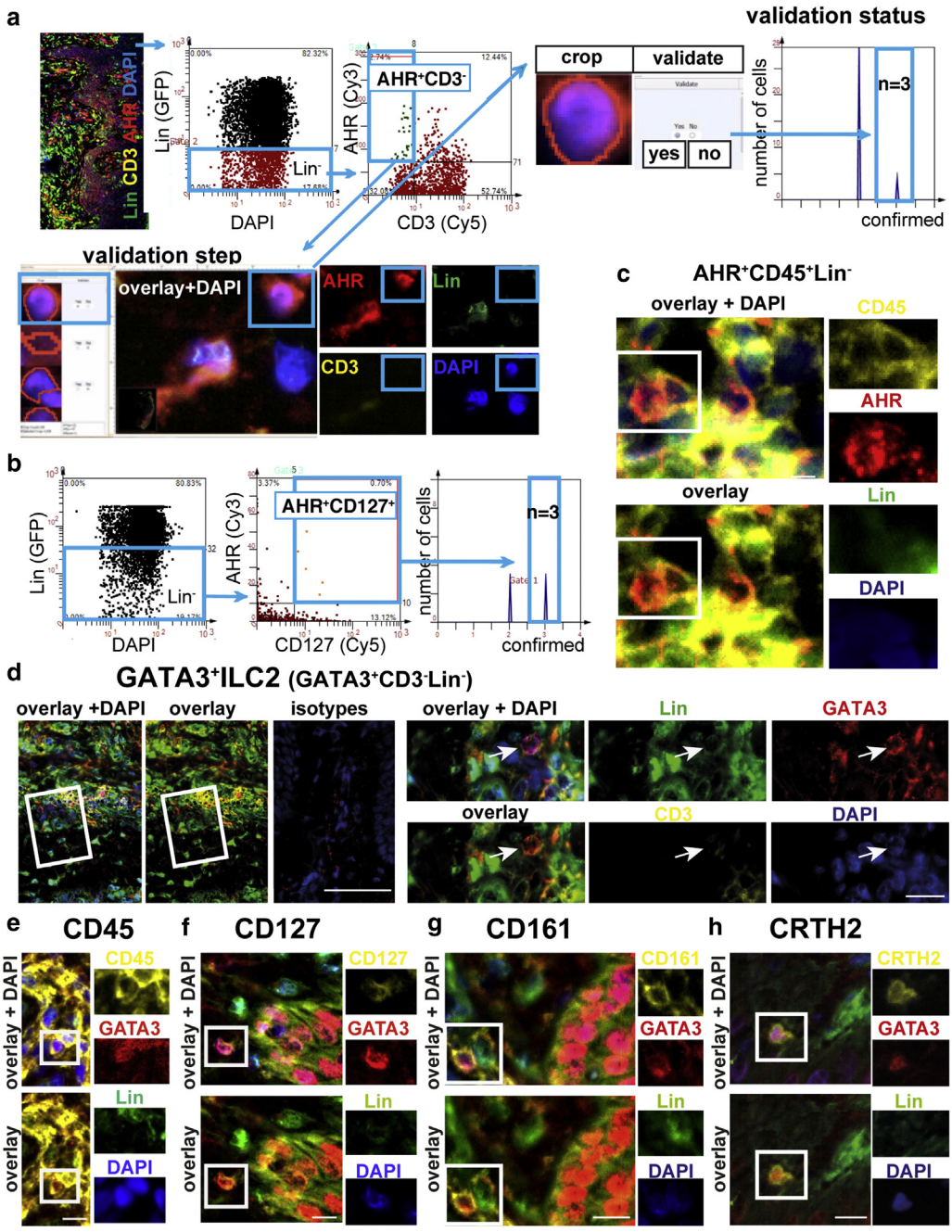

Figure 1. In situ identification of ILCs. (**a**) Illustration of the gating strategy and validation algorithm. The ILC gating strategy was based on mean fluorescence measurements. Lin^- cells were gated for $CD3^-AHR^+$ cells. In the implemented validation step, each cell in the target gate (e.g., $Lin^-CD3^-AHR^+$) was automatically cropped out and back-gated in the section, allowing a manual validation. Validated cells (n = 3) were displayed in a "confirmation gate." (**b**) Alternative gating strategy (of the same sample, consecutive section) for $Lin^-CD127^+AHR^+$ cells yielding the same number of confirmed ILCs. (**c**–**h**) Representative image of IF multicolor stainings. The following marker combinations are displayed (all with DAPI): (**c**) CD45/AHR/Lin, scale bar = 5 μm, (**d**) CD3/GATA3/Lin, scale bars = 100 μm and 20 μm, (**e**) CD45/GATA3/Lin, (**f**) CD127/GATA3/Lin, (**g**) CD161/GATA3/Lin, and (**h**) CRTH2/GATA3/Lin, scale bar = 10 μm. CRTH2, chemoattractant receptor-homologous molecule expressed on T helper type 2; IF, immunofluorescence; ILC, innate lymphoid cell; Lin, lineage.

revealed all ILCs to reside in a close (<30 μm) distance to the epidermis. In contrast, ILCs did not occupy the perivascular areas of the dermis (Figure 2c).

Diverse ILC subsets infiltrate cutaneous AD versus Pso lesions

We next asked which changes in number and composition the cutaneous ILC population would undergo in AD and Pso, both inflammatory skin diseases driven by distinct T-cell subsets (Nograles et al., 2009). When compared with NHS, we found considerably increased numbers of ILCs (Figures 2d–g and 3a) in both AD and Pso skin lesions (both n = 13). In AD, this numerical increment mainly affected $GATA3^+$ILC2s and AHR^+ILC3s (Figures 2g and 3a). AHR^+ILC3s even represented the most prominent ILC subset in AD. In Pso skin, by contrast, we observed an expansion of

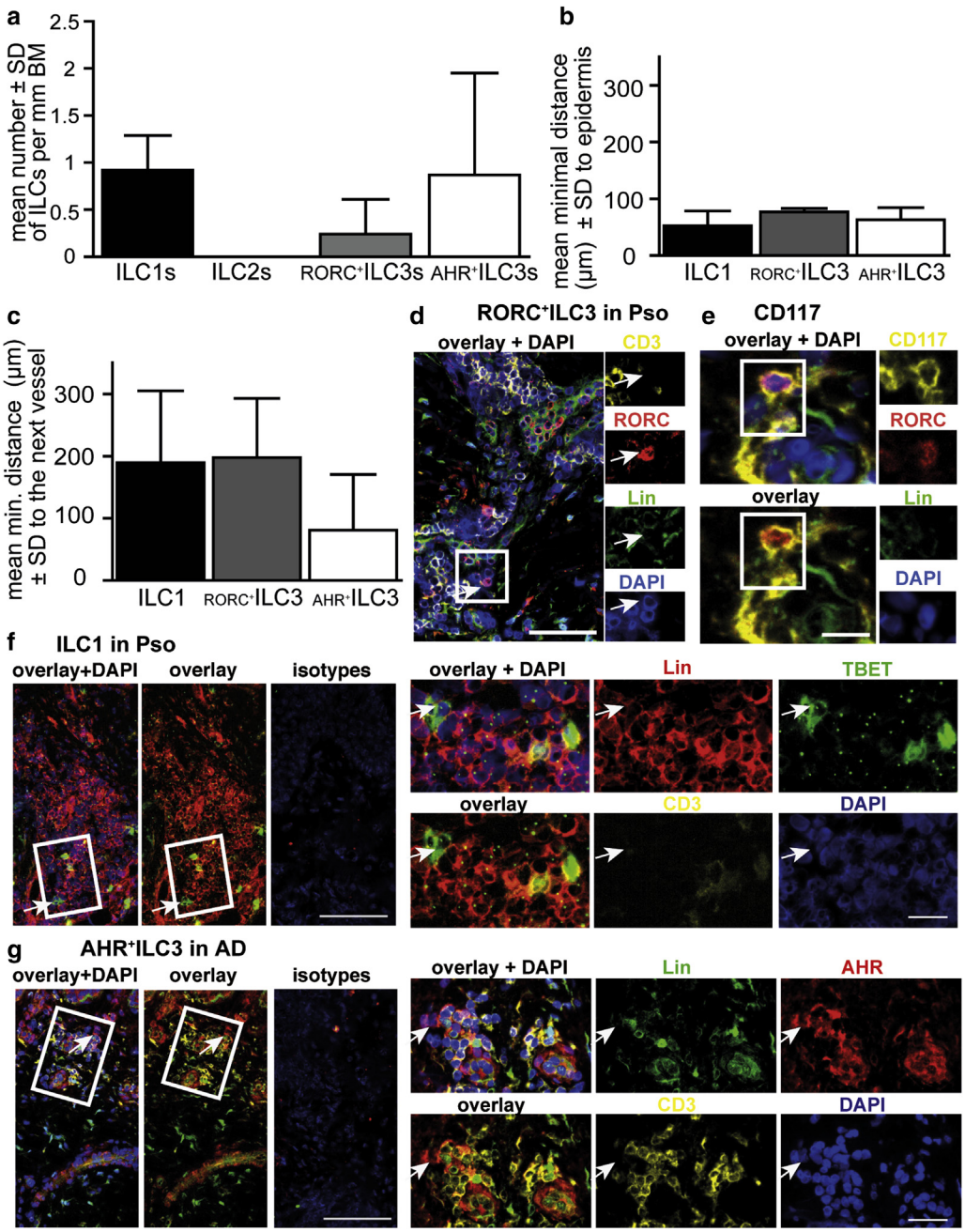

Figure 2. Distinct ILC infiltrates in NHS, AD, and Pso. (**a**) Results from the automated and validated quantitative in situ analysis of ILCs in the upper dermis of abdominal NHS (n = 10). Data are displayed as mean absolute numbers of cells ± SD per mm basement membrane (BM). (**b, c**) Distance measurements in NHS (n = 10) of ILC subsets to (**b**) the epidermis and to (**c**) BVs. Data are shown as mean minimal distance (µm) ± SD. (**d**–**g**) Representative images of IF multicolor stainings. The framed areas are displayed in a higher magnification in the lower panel of the respective images. (**d**) ILC3 ($Lin^-CD3^-RORC^+$) in Pso, scale bar = 100 µm, (**e**) CD117 expression in $RORC^+$ILC3s, scale bar = 10 µm, (**f**) ILC1s ($Lin^-CD3^-TBET^+$) in Pso, (**g**) AHR^+ILC3s ($Lin^-CD3^-AHR^+$) in AD, scale bars = 100 µm and 20 µm. AD, atopic dermatitis; AHR, aryl hydrocarbon receptor; BV, blood vessel; IF, immunofluorescence; ILC, innate lymphoid cell; Lin, lineage; NHS, normal human skin; Pso, psoriasis.

both ILC1s and ILC3s (Figures 2d–f and 3a), but hardly of ILC2s.

When determining the topographical relationship between ILCs and the skin's structural components, in AD and Pso lesions, we found an almost random distribution of these cells within the upper dermis with no signs of perivascular clustering (Figure 3b and c). In fact, none of the subsets was located in a close distance (Figure 3f) from blood vessels but rather far (≥80 µm) or very far (≥150 µm) away from them (Figure 3d). As far as their topographic relationship to the epidermis is concerned, ILC subsets in AD and Pso were found to reside at an intermediate distance (50–60 µm; Figure 3e and f, Supplementary Figure S5 online) from the basal cell layer. With the exception of $RORC^+$ILC3s, this distribution was similar to that observed in NHS.

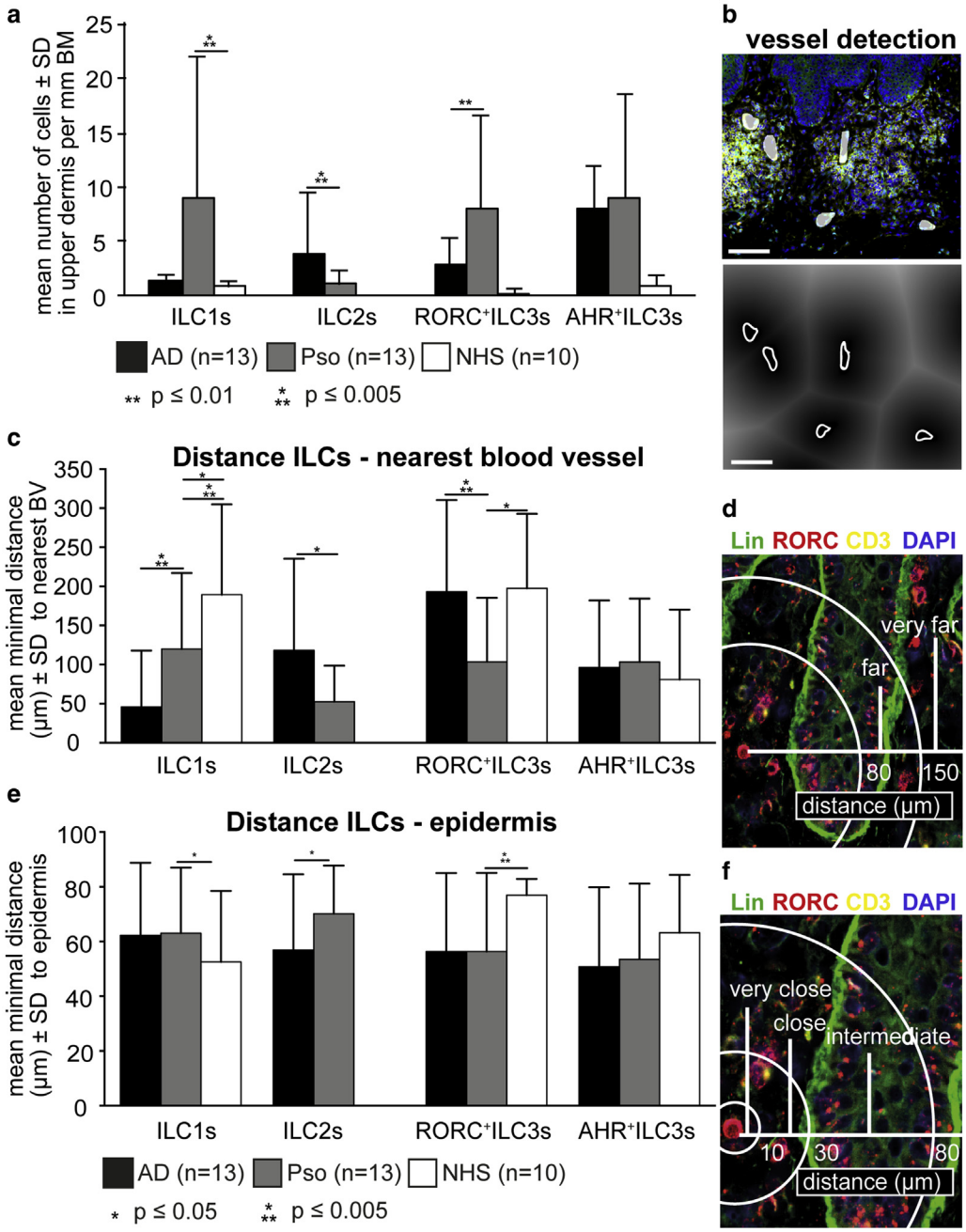

Figure 3. No perivascular ILC clustering in Pso and AD lesions. (**a**) Results from the in situ analysis of ILCs in AD and Pso skin lesions (both n = 13) as well as in abdominal NHS (n = 10). (**b**) Illustration of the vessel detection algorithm used: detected vessels (white areas, upper row) and "screening" (color gradient, lower row) of their surroundings for ILCs, scale bars = 100 µm. (**c**) Distances between ILCs and the nearest BV in AD, Pso (both n = 13) and NHS (n = 10). (**d, f**) Scheme showing a distance scale as well as the terms used in the text to describe/interpret distance measurements. (**e**) Distances between ILCs and the epidermis in AD, Pso (both n = 13) and NHS (n = 10). *$P < 0.05$, **$P < 0.01$, ***$P < 0.001$. AD, atopic dermatitis; BV, blood vessel; ILC, innate lymphoid cell; NHS, normal human skin; Pso, psoriasis.

ILCs are in intimate contact with T cells

On the basis of the observation that murine ILCs engage in a biologically relevant functional interaction with T lymphocytes (Halim et al., 2014), we studied the localization of human skin ILCs vis-à-vis their T-cell counterparts.

Strikingly, our analyses revealed a close proximity (maximal distance: 30 µm) between ILCs and T cells in both AD and Pso (Figure 4a and b, Supplementary Figure S6a–c online). Even in NHS, ILCs were found not further than 70–80 µm away from T cells (Figure 4b). A particularly intimate relationship (<10 µm) was observed between ILC1s and T cells in Pso lesions.

We next investigated the contribution of T cells to the closest cellular environment of ILCs. We developed an analysis algorithm for this purpose, in which the whole cellular content of the upper dermal area was screened to calculate the percentage of T cells in a defined radius around validated ILCs (Figure 4c). Direct cell-cell contact

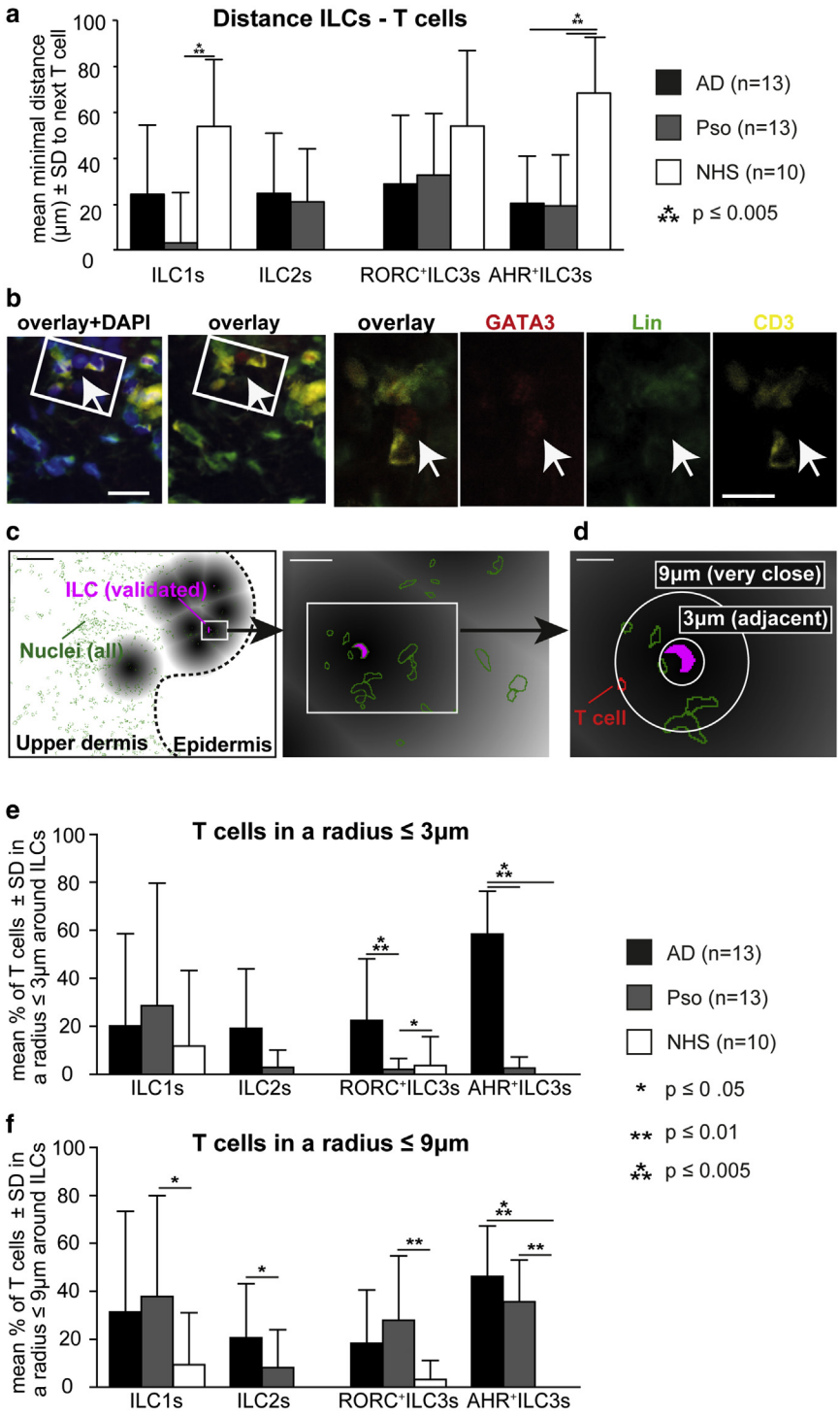

Figure 4. Close proximity between ILCs and T cells. (**a**) Distance measurements between the different ILC subsets and T cells in AD, Pso (both n = 13) and NHS (n = 10). (**b**) ILC2 ($Lin^{-}CD3^{-}GATA3^{+}$) surrounded by two T cells ($CD3^{+}$), scale bar = 20 µm. (**c**) Scheme of the applied software algorithm layer assessing the cellular environment of ILCs. The entire cellular content of the upper dermis was screened and assessed as to its distance to validated ILCs. Scale bars = 50 µm and 10 µm. (**d**) The cellular environment was assessed in a radius of 3 µm (direct cell-cell contact) and 9 µm (closest cellular environment), scale bar = 5 µm. (**e, f**) Percentage of T cells among total cells in an environmental radius of (**e**) 3 µm or (**f**) 9 µm around validated ILCs for AD, Pso (both n = 13) and NHS (n = 10). $^{*}P < 0.05$, $^{**}P < 0.01$, $^{***}P < 0.001$. AD, atopic dermatitis; GATA3, trans-acting T-cell-specific transcription factor GATA-3; ILC, innate lymphoid cell; Lin, lineage; NHS, normal human skin; Pso, psoriasis.

corresponded to an analysis radius of 3 µm. The "inner circle" of the ILC microenvironment was arbitrarily defined with a 9 µm radius (Figure 4d). The percentage of T cells directly adjacent to all ILCs ranged between 3% and 30%, with the notable exception of AHR^{+}ILC3s of AD skin, which were surrounded by a dense mantle of T cells (Figure 4e, Supplementary Figure S6d–f). We ensured that our results were not biased by overlapping cells; the analysis of a 3 µm and a 5 µm (corresponding to our section thickness) radius yielded essentially the same results (data not shown). The proportion of T cells within the radius of 9 µm ranged between 15% and 50% and did not differ greatly between the various ILC subsets (Figure 4f).

ILC and Th-cell patterns in AD and Pso are similar but not identical

The close vicinity between ILCs and T cells prompted us to ask whether the TF-based composition of ILCs mirrored the one of their Th cell counterparts in AD and Pso. The

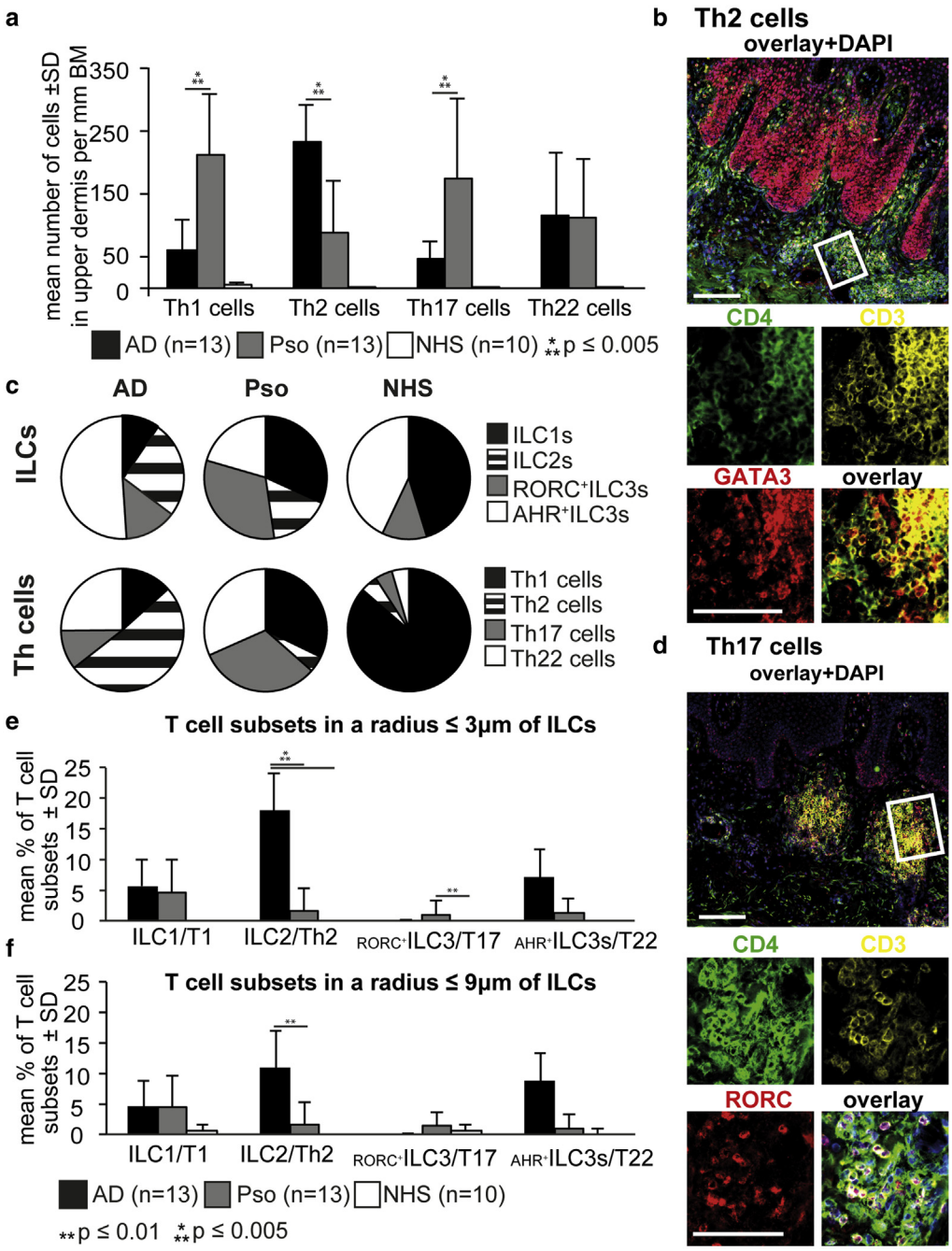

Figure 5. Characteristic Th-cell infiltrates in AD versus Pso skin lesions. (**a**) Automated quantitative in situ analysis of the Th-cell infiltrate in AD and Pso skin lesions as well as in NHS. (**b**) Representative image of a multicolor IF staining of Th2 cells in AD ($CD3^+CD4^+GATA3^+$), scale bars = 100 µm and 50 µm. (**c**) Pie charts displaying the relative composition of ILC and Th-cell populations in AD, Pso and NHS, respectively. (**d**) Representative image of a multicolor IF staining Th17 cells in Pso ($CD3^+CD4^+RORC^+$), scale bars = 100 µm and 50 µm. (**e, f**) Percentage of the respective T-cell subsets among total cells in an environmental radius of 3 µm or 9 µm around validated ILCs for AD, Pso (both n = 13) and NHS (n = 10). $^{**}P < 0.01$, $^{***}P < 0.001$. AD, atopic dermatitis; GATA3, trans-acting T-cell-specific transcription factor GATA-3; IF, immunofluorescence; ILC, innate lymphoid cell; NHS, normal human skin; Pso, psoriasis; Th, T helper.

analysis of IF stainings for Th-cell subsets (Figure 5a) revealed $GATA3^+$Th2 cells to clearly predominate the $CD3^+CD4^+$ T-cell infiltrate in AD (see also Figure 5b). AHR^+, putative Th22 cells were the second most prominent subset in AD, followed by $TBET^+$Th1 and $RORC^+$Th17 cells. Pso lesions, on the other hand (Figure 5a, c, and d), contained considerable numbers of Th1 as well as Th17 cells.

A comparison of the relative ILC and Th-cell subset composition in NHS, AD, and Pso skin (Figure 5c) showed no absolute correlation between TF-defined ILC and Th-cell lineages. In AD, Th2 cells and AHR^+ILC3s predominated within the Th-cell and ILC infiltrate, respectively. In Pso, we found an $RORC^+/AHR^+$ILC3 predominance among ILCs juxtaposed to a Th17 pattern among $CD4^+$ T lymphocytes. TBET expression was prevailing in both ILCs and T cells of NHS. A sizable proportion of AHR-positive cells were only found in the ILC, but not the Th-cell fraction of NHS.

Next, we were interested in whether T cells in close proximity (≤9 µm and ≤3 µm) to ILCs belong to the respective "mirror" subsets. Overall, this was surprisingly not the case (Figure 5e and f, Supplementary Figure S6). Only 3–5% of the cells surrounding ILCs belonged to their respective adaptive T-cell counterparts. Exceptions to this were Th2 cells/ILC2s in AD; in both a 3 µm and 9 µm radius, we found them to make up for 10–20% of all neighboring cells.

DISCUSSION

Although previous human studies have used flow cytometric approaches to identify ILCs in peripheral organs, our aim was to provide an in situ characterization of ILCs in skin under homeostatic (NHS) and inflammatory conditions (AD and Pso). We established an IF staining panel for ILCs and developed a computed analysis algorithm allowing enumeration and topographic assessment of ILCs on a single-cell basis. Our analysis of ILC subpopulations was based on the fact that the expression of certain TFs is a prerequisite for the differentiation of ILCs into distinct lineages (Eberl et al., 2015). The same TFs are responsible for the polarization of Th-cell subsets (Shih et al., 2014), allowing us to subsequently compare these two lymphocyte populations in situ. A limiting factor in choosing this approach is the known plasticity of ILCs and in part overlapping TF expression. GATA3, for example, is not only expressed by ILC2 and Th2 cells but is also required early during ILC lineage specification and ILC3 homeostasis (De Obaldia and Bhandoola, 2015; Yagi et al., 2014). RORC$^+$/AHR$^+$ILC3s can differentiate into TBET$^+$ILC1s under special conditions (Bernink et al., 2013). In addition, some controversy as to the assignment of ILC3 to a distinct lineage still exists (Hughes et al., 2014). These caveats should be kept in mind when snap-shot analyzing ILC subsets either by FACS or IF.

Our investigations revealed a very sparse ILC population in NHS consisting almost exclusively of TBET$^+$ILC1s and AHR$^+$ILC3s. In contrast, inflamed skin harbored much larger numbers of ILCs. AD was found to mainly host AHR$^+$ILC3s and GATA3$^+$ILC2s. In Pso lesions, TBET$^+$ILC1s and ILC3s predominated, whereas GATA3$^+$ILC2s were almost absent. Topographically, ILCs were mainly clustered beneath the dermoepidermal junction and exhibited a very close spatial relationship to T lymphocytes.

Some of our data on NHS, that is, the presence of ILC3s and ILC1s, correspond to those obtained by Teunissen et al. and Villanova et al. in flow cytometric studies. In contrast, these authors as well as our own group (Supplementary Figure S4a) identified approximately 10% of all ILCs in dermal cell suspensions as ILC2s by FACS analysis, but we hardly found any GATA3$^+$ILC2s in tissue sections by IF. Kim et al. (2013), in contrast, were not able to demonstrate CRTH2 expression on ILC2s in NHS or patients with AD by FACS. The reasons for this discrepancy are not entirely understood and may include: (i) differences in ILC density in different body locations, as it has been reported for T cells (Foster et al., 1990); (ii) phenotypic alterations during isolation and purification procedures; (iii) differences in the sensitivity of the staining and detection method. The high threshold of detection applied in our study together with lower mean fluorescence intensities measured by IF in comparison to FACS and the paucity of ILCs in NHS may have led to a slight underestimation of the actual number of ILCs in NHS.

The role of ILCs in NHS escapes us at the present time. Intriguingly, certain ILC3s are involved in fetal development of secondary lymphoid tissues (Yoshida et al., 1999). One could speculate that ILCs, in addition to forming a first line of antimicrobial defense (Klose et al., 2014), contribute to skin histogenesis/organogenesis. This raises questions about the time point at which ILCs start populating this organ and whether in adults ILCs are permanently residing/renewing in skin or transiting from the blood. The previously described expression of cutaneous lymphocyte-associated antigen on circulating ILCs suggests their entry from blood (Teunissen et al., 2014; Villanova et al., 2014). Further studies are needed to investigate the time of entry of ILCs into the skin and their possible role in antimicrobial defense or as promoters of tissue remodeling/repair (Dudakov et al., 2015).

As opposed to the rare occurrence of ILCs in NHS, we found AD lesions to be prominently populated by AHR$^+$ILC3s and GATA3$^+$ILC2s. Their adaptive Th-cell counterparts consisted mostly of Th2, and, to a lesser extent, of Th22 cells.

Concerning ILC2s, our results are in keeping with observations by other investigators demonstrating this leukocyte subset in cell suspensions isolated from human AD lesions and murine AD-like skin (Bonefeld and Geisler, 2016). Concerning the latter, mostly keratinocyte-derived cytokines (e.g., thymic stromal lymphopoietin) activate ILC2s. Their main effector function in AD seems to be the release of cytokines further accentuating epidermal barrier breaching (Salimi et al., 2013). Particularly striking regarding the potential role of ILCs in AD was our observation that among T cells directly adjacent to ILC2s, the majority belonged to the Th2 subset. This may indicate that ILC2s modulate the Th2 response in AD. Studies in murine allergic asthma models support a Th2-promoting role of ILC2s (Halim et al., 2014, 2016).

An unexpected finding of our investigations was the identification of substantial amounts of AHR$^+$ILC3s in AD skin. The TF AHR is known to be not only an important modulator of IL-22 production of ILC3s but is also necessary for their development and maintenance (Cella and Colonna, 2015; Hughes et al., 2014; Mjosberg et al., 2012). In analogy to the role of Th22 cells in AD (Czarnowicki et al., 2015; Nograles et al., 2009), IL-22 producing ILC3 could be coresponsible not only for inflammation but also for lichenification of the skin, a hallmark of AD (Zheng et al., 2007).

The question whether AHR$^+$ILC3s and ILC2s act in concert with their Th-cell counterparts and thus, to which extent they contribute to the pathogenic process in a given situation, remains to be elucidated. Because cytokine release by ILCs occurs in an antigen-independent fashion, one may hypothesize that ILCs play an important role especially in the intrinsic form of AD, which, as opposed to the extrinsic one, is not associated with allergen sensitization and/or elevated IgE levels (Weidinger and Novak, 2016).

When compared with NHS, Pso skin sections were found to harbor substantially increased numbers of ILC1s as well as of ILC3s. ILC2s, in contrast, were only rarely encountered. Again, all ILCs showed a preferential topographic distribution near the epidermis. Strikingly, all ILC subsets were found to reside close to T lymphocytes, which, as reported by others, consisted mainly of Th1 and Th17 cells (Kryczek et al., 2008; Lowes et al., 2008).

As far as the ILC3 subset is concerned, our in situ data are complementary to FACS studies published previously (Dyring-Andersen et al., 2014; Teunissen et al., 2014; Villanova et al., 2014) pointing to the existence of an ILC3

population in Pso skin. In contrast to findings by others (Teunissen et al., 2014), we observed an abundance of TBET$^+$ILC1s in cutaneous Pso lesions. Although we cannot exclude the possibility that these cells directly originate from the common ILC precursor, we should not forget that ILC3s can downregulate RORC and, reciprocally, increase the expression of TBET. Concurrent with these changes, the cells acquire the capacity to produce IFN-γ and tumor necrosis factor-α at the expense of IL-17 and IL-22 secretion (Serafini et al., 2015). It is currently unknown whether TBET$^+$ILC1s play a disease-promoting role in Pso. A possible argument against this possibility is the recently published finding that neutralization of IL-17A is even more efficient in the treatment of moderate-to-severe plaque Pso than the blockade of IL-12/IL-23p40 (Thaci et al., 2015). Whether TBET$^+$ILC1s may have perhaps a dampening effect on their neighboring Th17 populations remains to be determined.

In summary, we have developed an algorithm-based in situ analysis technique enabling us to reliably quantify and, importantly, topographically characterize ILCs in human skin. As opposed to flow cytometric studies conducted so far, our approach additionally allows us to accurately describe the structural and cellular environment of ILCs on a single-cell basis. Deeper insights into the nature of cutaneous ILC subpopulations and their surroundings in human skin will constitute a solid basis for future analyses of the functional relationship between ILCs and other constituents of the cutaneous immunological microcosmos.

MATERIALS AND METHODS

Study design, skin sampling, and processing

We collected lesional biopsies from patients with Pso (n = 13) and AD (n = 13) treated at Division of Immunology, Allergy and Infectious Diseases, Dermatology Department of Vienna's Medical University, or at the Dermatology Department of the University Hospital Zurich between 2009 and 2015. NHS (n = 10) was obtained as tissue discarded from abdominoplasties. Patient characteristics are displayed in Supplementary Table S2 online. Details of skin sampling and processing are given in the Supplementary Material and Methods online.

The study was approved by the Ethics Committees of the Medical University of Vienna (EK700/2009) and of the University of Zurich (EK 647/2006) and conducted according to the Declaration of Helsinki. All study subjects participated voluntarily and gave written informed consent.

IF stainings, section scanning

A complete list of antibodies used in this study is shown in Supplementary Table S3 online. Details of the performed multicolor IF stainings and the scanning of sections are given in the Supplementary Material and Methods.

Images displayed in the figures were taken with Zeiss LD Plan-Neofluar objectives (primary objective ×20/0.4, ocular objective ×10) using a PC pixelfly camera (Carl Zeiss Inc, Jena, Germany) and exported from the StrataQuest software as TIFF images. Some images were processed in Adobe Photoshop CS6 (Adobe Systems, San Jose, CA).

Automated analysis of IF stainings, validation step

The computed analysis of skin sections was performed using StrataQuest V64 (TissueGnostics GmbH, Vienna, Austria). A detailed description of the created algorithms and analysis layers is given in the Supplementary Material and Methods and Supplementary Figure S2. Briefly, a first set of analysis layers was applied to automatically differentiate between epidermal, upper dermal, and hypodermal areas and detected regions manually validated. ILCs were gated based on the IF mean intensity of the respective channels; cutoffs were adapted to isotype controls.

A specific tool was developed to manually validate/reject all events (ILCs) on a single cell basis in the gates of interest regarding their staining as well as the cell shape. The validation step was performed by two independent observers.

Topographic analyses

Two additional analysis layers were created in the program to explore the topographic distribution of manually validated cells. In the first topography layer, the shortest distance of each ILC nucleus in the dermal area to (i) the epidermis and to (ii) other cells of interest was calculated (precision: 0.31 μm). The second topography layer calculated the distance between validated ILCs and the closest blood vessel. Blood vessel detection was based on their morphological shape (i.e., endothelial-shaped cells surrounding a lumen) and the mean intensity of green fluorescent protein expression (CD34 included in the lineage cocktail) followed by manual corrections.

Proximity analysis

This algorithm layer was created to more precisely assess the cellular environment of validated ILCs by screening the complete cellular content of the upper dermis with regard to its distance to every validated ILC. The percentage of T cells in a defined radius (3 μm and 9 μm) of validated ILCs was calculated.

Statistical analysis

All statistical analyses were performed using GraphPad Prism software (Graphpad, San Diego, CA). For comparison of means between more than two groups (NHS, AD, and Pso), one-way analysis of variance with the Tukey post-test was used for all experiments. A P value <0.05 was considered statistically significant.

CONFLICT OF INTEREST

The authors state no conflict of interest.

ACKNOWLEDGMENTS

We thank Robin Ristl from the Department of Statistics of the Medical University of Vienna for his statistical advice. This work was supported, in part, by the Austrian Science Fund (DK W1248-B13) and the Medical University of Vienna.

SUPPLEMENTARY MATERIAL

Supplementary material is linked to the online version of the paper at www.jidonline.org, and at http://dx.doi.org/10.1016/j.jid.2016.07.017.

REFERENCES

Bernink JH, Peters CP, Munneke M, te Velde AA, Meijer SL, Weijer K, et al. Human type 1 innate lymphoid cells accumulate in inflamed mucosal tissues. Nat Immunol 2013;14:221–9.

Bonefeld CM, Geisler C. The role of innate lymphoid cells in healthy and inflamed skin. Immunol Lett 2016. http://dx.doi.org/10.1016/j.imlet.2016.01.005.

Cella M, Colonna M. Aryl hydrocarbon receptor: linking environment to immunity. Semin Immunol 2015;27:310–4.

Clark RA. Resident memory T cells in human health and disease. Sci Transl Med 2015;7:269rv261.

Czarnowicki T, Gonzalez J, Shemer A, Malajian D, Xu H, Zheng X, et al. Severe atopic dermatitis is characterized by selective expansion of circulating TH2/TC2 and TH22/TC22, but not TH17/TC17, cells within the

skin-homing T-cell population. J Allergy Clin Immunol 2015;136:104–115.e107.

De Obaldia ME, Bhandoola A. Transcriptional regulation of innate and adaptive lymphocyte lineages. Annu Rev Immunol 2015;33:607–42.

Dudakov JA, Hanash AM, van den Brink MR. Interleukin-22: immunobiology and pathology. Annu Rev Immunol 2015;33:747–85.

Dyring-Andersen B, Geisler C, Agerbeck C, Lauritsen JP, Gudjonsdottir SD, Skov L, et al. Increased number and frequency of group 3 innate lymphoid cells in nonlesional psoriatic skin. Br J Dermatol 2014;170:609–16.

Eberl G, Colonna M, Di Santo JP, McKenzie AN. Innate lymphoid cells. Innate lymphoid cells: a new paradigm in immunology. Science 2015;348:aaa6566.

Eberl G, Littman DR. Thymic origin of intestinal alphabeta T cells revealed by fate mapping of RORgammat+ cells. Science 2004;305:248–51.

Foster CA, Yokozeki H, Rappersberger K, Koning F, Volc-Platzer B, Rieger A, et al. Human epidermal T cells predominantly belong to the lineage expressing alpha/beta T cell receptor. J Exp Med 1990;171:997–1013.

Halim TY, Hwang YY, Scanlon ST, Zaghouani H, Garbi N, Fallon PG, et al. Group 2 innate lymphoid cells license dendritic cells to potentiate memory TH2 cell responses. Nat Immunol 2016;17:57–64.

Halim TY, Steer CA, Matha L, Gold MJ, Martinez-Gonzalez I, McNagny KM, et al. Group 2 innate lymphoid cells are critical for the initiation of adaptive T helper 2 cell-mediated allergic lung inflammation. Immunity 2014;40:425–35.

Hughes T, Briercheck EL, Freud AG, Trotta R, McClory S, Scoville SD, et al. The transcription factor AHR prevents the differentiation of a stage 3 innate lymphoid cell subset to natural killer cells. Cell Rep 2014;8:150–62.

Imai Y, Yasuda K, Sakaguchi Y, Haneda T, Mizutani H, Yoshimoto T, et al. Skin-specific expression of IL-33 activates group 2 innate lymphoid cells and elicits atopic dermatitis-like inflammation in mice. Proc Natl Acad Sci USA 2013;110:13921–6.

Kaufman CK, Zhou P, Pasolli HA, Rendl M, Bolotin D, Lim KC, et al. GATA-3: an unexpected regulator of cell lineage determination in skin. Genes Dev 2003;17:2108–22.

Kim BS. Innate lymphoid cells in the skin. J Invest Dermatol 2015;135:673–8.

Kim BS, Siracusa MC, Saenz SA, Noti M, Monticelli LA, Sonnenberg GF, et al. TSLP elicits IL-33-independent innate lymphoid cell responses to promote skin inflammation. Sci Transl Med 2013;5:170ra116.

Klose CS, Flach M, Mohle L, Rogell L, Hoyler T, Ebert K, et al. Differentiation of type 1 ILCs from a common progenitor to all helper-like innate lymphoid cell lineages. Cell 2014;157:340–56.

Kryczek I, Bruce AT, Gudjonsson JE, Johnston A, Aphale A, Vatan L, et al. Induction of IL-17+ T cell trafficking and development by IFN-gamma: mechanism and pathological relevance in psoriasis. J Immunol 2008;181:4733–41.

Lowes MA, Kikuchi T, Fuentes-Duculan J, Cardinale I, Zaba LC, Haider AS, et al. Psoriasis vulgaris lesions contain discrete populations of Th1 and Th17 T cells. J Invest Dermatol 2008;128:1207–11.

Mjosberg J, Bernink J, Peters C, Spits H. Transcriptional control of innate lymphoid cells. Eur J Immunol 2012;42:1916–23.

Modlin RL, Miller LS, Bangert C, Stingl G. Innate and adaptive immunity in the skin. In: Goldsmith L, Katz S, Gilchrest B, Paller A, Leffell D, Wolff K, editors. Fitzpatrick's dermatology in general medicine, 8th ed., vol. 1. McGraw-Hill Education; 2012. p. 105.

Nograles KE, Zaba LC, Shemer A, Fuentes-Duculan J, Cardinale I, Kikuchi T, et al. IL-22-producing "T22" T cells account for upregulated IL-22 in atopic dermatitis despite reduced IL-17-producing TH17 T cells. J Allergy Clin Immunol 2009;123:1244–1252.e1242.

Pantelyushin S, Haak S, Ingold B, Kulig P, Heppner FL, Navarini AA, et al. Rorgammat+ innate lymphocytes and gammadelta T cells initiate psoriasiform plaque formation in mice. J Clin Invest 2012;122:2252–6.

Roediger B, Kyle R, Yip KH, Sumaria N, Guy TV, Kim BS, et al. Cutaneous immunosurveillance and regulation of inflammation by group 2 innate lymphoid cells. Nature Immunol 2013;14:564–73.

Salimi M, Barlow JL, Saunders SP, Xue L, Gutowska-Owsiak D, Wang X, et al. A role for IL-25 and IL-33-driven type-2 innate lymphoid cells in atopic dermatitis. J Exp Med 2013;210:2939–50.

Serafini N, Vosshenrich CA, Di Santo JP. Transcriptional regulation of innate lymphoid cell fate. Nat Rev Immunol 2015;15:415–28.

Shih HY, Sciume G, Poholek AC, Vahedi G, Hirahara K, Villarino AV, et al. Transcriptional and epigenetic networks of helper T and innate lymphoid cells. Immunol Rev 2014;261:23–49.

Sonnenberg GF, Artis D. Innate lymphoid cells in the initiation, regulation and resolution of inflammation. Nat Med 2015;21:698–708.

Spits H, Cupedo T. Innate lymphoid cells: emerging insights in development, lineage relationships, and function. Annu Rev Immunol 2012;30:647–75.

Teunissen MB, Munneke JM, Bernink JH, Spuls PI, Res PC, Te Velde A, et al. Composition of innate lymphoid cell subsets in the human skin: enrichment of NCR(+) ILC3 in lesional skin and blood of psoriasis patients. J Invest Dermatol 2014;134:2351–60.

Thaci D, Blauvelt A, Reich K, Tsai TF, Vanaclocha F, Kingo K, et al. Secukinumab is superior to ustekinumab in clearing skin of subjects with moderate to severe plaque psoriasis: CLEAR, a randomized controlled trial. J Am Acad Dermatol 2015;73:400–9.

Villanova F, Flutter B, Tosi I, Grys K, Sreeneebus H, Perera GK, et al. Characterization of innate lymphoid cells in human skin and blood demonstrates increase of NKp44+ ILC3 in psoriasis. J Invest Dermatol 2014;134:984–91.

Weidinger S, Novak N. Atopic dermatitis. Lancet 2016;387:1109–22.

Yagi R, Zhong C, Northrup DL, Yu F, Bouladoux N, Spencer S, et al. The transcription factor GATA3 is critical for the development of all IL-7Ralpha-expressing innate lymphoid cells. Immunity 2014;40:378–88.

Yoshida H, Honda K, Shinkura R, Adachi S, Nishikawa S, Maki K, et al. IL-7 receptor alpha+ CD3(−) cells in the embryonic intestine induces the organizing center of Peyer's patches. Int Immunol 1999;11:643–55.

Zheng Y, Danilenko DM, Valdez P, Kasman I, Eastham-Anderson J, Wu J, et al. Interleukin-22, a T(H)17 cytokine, mediates IL-23-induced dermal inflammation and acanthosis. Nature 2007;445:648–51.

Published OnlineFirst March 8, 2016; DOI: 10.1158/1078-0432.CCR-15-2872

Cancer Therapy: Clinical

Clinical Cancer Research

Cytotoxic Cutaneous Adverse Drug Reactions during Anti-PD-1 Therapy

Simone M. Goldinger, Pascale Stieger, Barbara Meier, Sara Micaletto, Emmanuel Contassot, Lars E. French, and Reinhard Dummer

Abstract

Purpose: Immunotherapy has experienced impressive progress in cancer treatment. Antibodies against PD-1 improved survival in different types of cancer including melanoma. They are generally well tolerated. However, skin toxicities including pruritus, rashes, and vitiligo are reported. Although frequent, they have not been characterized further yet. In this analysis, we aimed to systematically assess and characterize the adverse cutaneous reactions observed in patients with melanoma treated with anti-PD-1 antibodies.

Experimental Design: Patients with melanoma were treated with anti-PD-1 antibodies within clinical trials and an early-access program. Adverse cutaneous eruptions that emerged in our melanoma patient cohort were systematically investigated and classified using histology and gene expression profiling in comparison with maculopapular drug rash, cutaneous GVHD, and the severe drug eruption toxic epidermal necrolysis (TEN).

Results: Between February 2013 and September 2015, 68 patients with stage IV melanoma were treated at the University Hospital Zurich (Zurich, Switzerland); 15 patients (22%) developed cutaneous reactions and 10 (15%) vitiligo. The cutaneous reactions ranged from small erythematous papules with mild pruritus to disseminated erythematous maculopapular rashes (MPR) without signs of epidermal involvement to severe MPRs, including epidermal detachment and mucosal involvement. Although skin involvement varied from mild rash to bullous drug eruptions, gene expression profiling pathogenically classified all investigated cases as TEN-like reactions.

Conclusions: As predicted by the PD-1 knockout mouse, anti-PD-1 antibodies frequently cause adverse cutaneous reactions. Gene expression profiling reminds in all cases of a TEN-like pattern, suggesting that PD-1/PD-L1 interaction is required to preserve epidermal integrity during inflammatory skin reactions.
Clin Cancer Res; 22(16); 4023–9. ©2016 AACR.

Introduction

Antibodies against PD-1, a checkpoint in the effector phase of cytotoxic T cells, have been successfully used in cancer immunotherapy (1–3). Through the binding to PD-1, its ligands, namely PD-L1 and PD-L2, inhibit T-cell–mediated immune responses. By preventing the binding of PD-L to PD-1, the FDA-approved antibodies, pembrolizumab and nivolumab, promote T-cell–mediated cytotoxic responses, which result in tumor regression in a variety of cancers (2). In several randomized pivotal studies, pembrolizumab and nivolumab demonstrated improved overall response rates and progression-free survival compared with chemotherapy or the anti-CTLA-4 antibody ipilimumab (4–7).

Besides efficacy, the introduction of anti-PD-1 antibodies led to a new benchmark for treatment tolerability in cancer being a treatment with very few adverse events. Adverse cutaneous reactions have however been reported. These include skin exanthemas with a frequency of 10% to 25% and vitiligo in 9% to 11% of the treated patients (2, 4, 5). Hua and colleagues hypothesize that vitiligo is associated with a favorable outcome of anti-PD-1 therapy (8). Moreover, one case of bullous pemphigoid in association with pembrolizumab (9) and one case of psoriasiform exanthema under nivolumab (10) have been published. The adverse cutaneous reactions observed under the treatment with anti-PD-1 antibodies have not been characterized in detail so far.

Stevens–Johnson syndrome (SJS) and toxic epidermal necrolysis (TEN) are severe cutaneous drug eruptions characterized by widespread macules, papules, and/or targetoid lesions with varying degrees of epidermal necrolysis clinically presenting as skin detachment and/or bullous skin lesions with mucosal erosions (11). Common drugs inducing SJS/TEN include allopurinol, trimethoprim–sulfamethoxazole, carbamazepin, lamotrigine, nevirapine, NSAIDs, phenobarbital, and phenytoin (12). The molecular events that cause potentially fatal SJS and TEN are only partially understood, although "drug"-specific adaptive immune responses in the effector phase of TEN are well documented (13). In the skin, T-cell–mediated immune responses occurring during SJS/TEN result in a massive keratinocyte apoptosis mediated by cytolytic molecules, including FasL (14), perforin/granzyme B (15), annexin A1 (16), and granulysin (17). Histologically, SJS and TEN are characterized by full-thickness epidermal necrolysis due to extensive keratinocyte apoptosis associated with varying degrees of inflammation and epidermal infiltration by $CD8^+$ lymphocytes.

In this study, we aimed to systematically assess and characterize the adverse cutaneous reactions observed in patients with

Department of Dermatology, University Hospital Zurich, Zurich, Switzerland.

L.E. French and R. Dummer contributed equally to this article.

Corresponding Author: Reinhard Dummer, University Hospital of Zurich, Gloriastrasse 31, Zurich 8091, Switzerland. Phone: 0041-4425-52507; Fax: 0041-4425-58988; E-mail: reinhard.dummer@usz.ch

doi: 10.1158/1078-0432.CCR-15-2872

Published OnlineFirst March 8, 2016; DOI: 10.1158/1078-0432.CCR-15-2872

Translational Relevance

Antibodies against PD-1 have revolutionized cancer immunotherapy. This article describes relevant skin toxicities emerging upon treatment with antibodies against PD-1, such as nivolumab and pembrolizumab. Skin toxicities were classified using histology and gene expression profiling in comparison with mild maculopapular drug rashes and severe drug eruptions, such as toxic epidermal necrolysis (TEN). Although the clinical picture was variable, ranging from mild to severe, gene expression profiling resembled in all cases to severe cytotoxic SJS/TEN–like patterns. This suggests that the PD-1/PD-L1 interaction is involved in the preservation of epidermal integrity during inflammatory skin reactions. We advocate a careful examination of the skin of patients treated with immunotherapy in the near future, as these adverse cutaneous reactions can imply a loss of epidermal integrity.

advanced melanoma treated with anti-PD-1 antibodies using gene expression profiling and compared the data with other clinical types of drug eruptions.

Patients and Methods

Patients with advanced melanoma were treated with either the anti-PD-1 antibody pembrolizumab (2 or 10 mg/kg) or with nivolumab (3 mg/kg) within clinical trials (clinicaltrials.gov NCT01704287, NCT01721746, and NCT02156804; refs. 4, 7) and an early-access program. The first 68 patients with melanoma treated with pembrolizumab or nivolumab at the University of Zurich (Zurich, Switzerland) were systematically investigated for adverse skin reactions by board-certified dermatologists experienced in immunotherapy and familiar with associated adverse events (S.M. Goldinger and/or R. Dummer).

Complete and accurate skin examinations were performed before and during immunotherapy. Previously selected untreated skin eruptions of eight patients emerging during therapy were biopsied and analyzed by histology. The decision to take a biopsy was based on whether the lesion was new (i.e., not apparent prior treatment start), on the severity (grade 2 or greater), on the localization and distribution (favoring multiple and disseminated lesions), and on the clinical characteristics (palpable or scaling presentation). In general, the most infiltrated lesion was chosen and biopsied provided patient's consent and that the lesion was in a region of the body that allowed proper wound healing. Expression of PD-1 on skin-infiltrating T cells (eBioscience) and PD-L1 (Immunobiology Yale, Yale University, New Haven, CT) on keratinocytes at the foci of lymphocytic epidermal infiltration was assessed by IHC.

Gene expression analyses of five of these eight skin biopsies during anti-PD-1 therapy with pembrolizumab were in addition analyzed and compared with expression profiles of skin biopsies from patients with maculopapular rashes (MPR; $n = 8$), SJS/TEN ($n = 5$), and cutaneous GVHD ($n = 9$). RNA was isolated from patients' skin ($n = 5$) and from healthy control skin ($n = 4$) using a Qiagen RNeasy Kit (Qiagen) following the manufacturer's instructions, and total RNA was converted into cDNA by standard reverse transcription using a RevertAid RT Reverse Transcription Kit (Thermo Scientific). Quantitative PCR was performed using Power SYBR Green PCR Master Mix (Applied Biosystems). Primer sequences were obtained from http://pga.mgh.harvard.edu/primerbank/. The real-time PCR included an initial denaturation at 95°C for 10 minutes, followed by 40 cycles of 95°C for 30 seconds, 56°C for 1 minute, and 72°C for 1 minute and one cycle of 95°C for 1 minute, 56°C for 30 seconds, and 95°C for 30 seconds. Moreover, we performed gene expression arrays (Affymetrix) on the skin of patients with MPR ($n = 8$), patients with SJS/TEN ($n = 5$), patients with GVHD ($n = 9$), and healthy donors ($n = 8$) as controls. Healthy skin was obtained from healthy individuals undergoing plastic surgery. All human skin biopsies were collected with informed written consent upon the approval of local ethical committees and were conducted according to the Declaration of Helsinki Principles (KEK nr. 647). On the basis of the results of the gene expression arrays, we selected a set of genes that could be used as a specific signature for TEN as opposed to MPR and GVHD (Fig. 2A). Using quantitative RT-PCR, we determined the expression levels of the gene set specific for SJS/TEN in the skin of patients with an adverse cutaneous reaction occurring during anti-PD-1 therapy.

Results

Between February 2013 and September 2015, 68 patients were treated with either pembrolizumab (2 and 10 mg/kg; every 3 weeks) or nivolumab (3 mg/kg; every 2 weeks) in different clinical trials (clinicaltrials.gov NCT01704287, NCT01721746, and NCT02156804; refs. 4, 7) and an early-access program. Of the first 68 patients with stage IV melanoma treated with pembrolizumab ($n = 54$) or nivolumab ($n = 14$) at the University Hospital of Zurich (Zurich, Switzerland), 15 patients (22%) developed a cutaneous inflammatory reaction, and 10 (15%) developed vitiligo. Clinically, the adverse cutaneous reactions ranged from small erythematous papules with mild pruritus to disseminated erythematous MPRs without major clinical signs of epidermal involvement to severe MPRs, including epidermal detachment and mucosal involvement (Table 1). Histology performed on selected lesional skin biopsies of eight patients at the onset of the adverse cutaneous reaction revealed different manifestation grades of apoptotic keratinocytes and even focal full-thickness necrosis of the epidermis in two cases in the histology (Table 1). In particular, a 77-year-old patient presented with a generalized unspecific MPR predominantly affecting the trunk with focal areas of epidermal detachment a few days after the first pembrolizumab infusion (Fig. 1A, <10% of the body surface area). Histology showed epidermal damage with apoptotic keratinocytes, subepidermal lymphocytic infiltrates, and dermo-epidermal cleavage (Fig. 1B). One week later, mucosal involvement and genital ulcerations developed. Taken together, these features led to a diagnosis of SJS, and pembrolizumab therapy was discontinued.

Skin biopsies from six patients were also analyzed by IHC and revealed in all cases an accumulation of $CD8^+$ cells at the dermo-epidermal junction and some $CD8^+$ exocytosis within the epidermis, as well as keratinocyte apoptosis suggestive of a cytotoxic etiology. Expression of PD-1 on skin-infiltrating T cells and keratinocytes at the foci of lymphocytic epidermal infiltration was also assessed by IHC (Fig. 1C and D). Despite topical steroids, the lesions of this patient subsequently evolved into persistent polygonal flat erythematous papules, clinically suggestive of

Published OnlineFirst March 8, 2016; DOI: 10.1158/1078-0432.CCR-15-2872

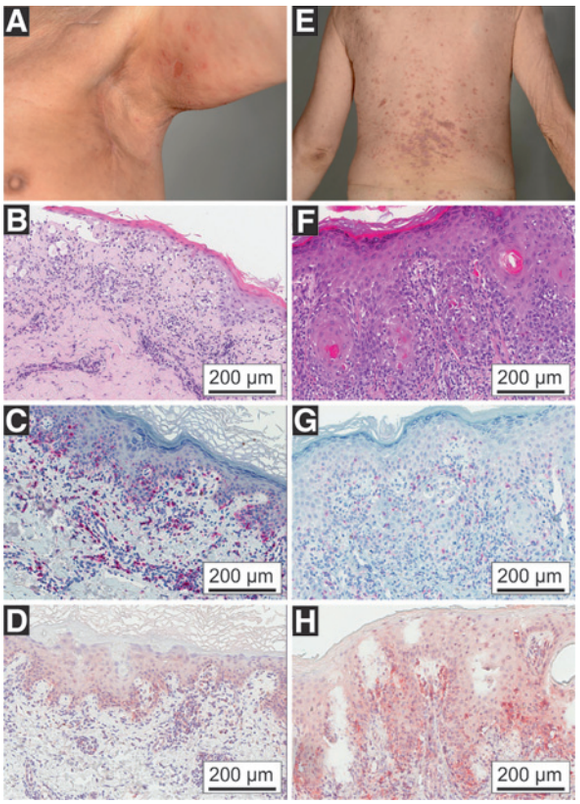

Figure 1.
Clinical and histologic presentation of a patient with metastatic melanoma developing a severe adverse cutaneous reaction (ACR) upon treatment with pembrolizumab. **A–D,** SJS. **E–H,** lichen planus. **A,** clinical features of SJS. **B,** histology of SJS (hematoxylin–eosin stain). **C,** PD-1 stain of SJS. **D,** PD-L1 stain of SJS. **E,** clinical features of lichen planus. **F,** histology of lichen planus. **G,** PD-1 stain of lichen planus. **H,** PD-L1 stain of lichen planus.

lichen planus (Fig. 1E). Accumulation of cytotoxic $CD8^+$ lymphocytes in the junction zone and in the epidermis, causing apoptotic cell death of keratinocytes, classical for lichen planus, was confirmed by histology (Fig. 1F). PD-L1 expression on keratinocytes was clearly detectable by IHC in the proximity of T cells (Fig. 1G and H).

In all cases, none of the concomitant medications taken by patients had been recently started or were known to cause SJS/TEN (Table 1). Furthermore, lymphocyte transformation tests to the concomitant medication taken by patient 1 did not provide evidence for a "drug"-specific immune response (data not shown; Table 1).

Treatment included systemic steroids (prednisone 1 mg/kg, tapered for 4 weeks), systemic steroids (over a course of 4 weeks), disinfectant agents when necessary, and rehydration of the skin. Treatment with pembrolizumab could be continued in six of eight cases and did not further affect the skin.

Gene expression profiling of RNA extracted from lesional skin of validated cases of MPR (eight cases), SJS/TEN (five cases), and cutaneous GVHD (nine cases) enabled us to identify a set of 18 genes for which the expression levels enable differentiation among the three diagnostic categories (Fig. 2A). Analysis of the level of expression of these 18 genes was performed in the lesional skin biopsies of five patients and revealed a gene expression profile reminiscent of SJS/TEN (Fig. 2B). Both SJS/TEN skin ($n = 5$) and skin of five patients presenting an adverse cutaneous reaction upon anti-PD-1 therapy had significant upregulation of *PI3*, *SPRR2B*, *GZMB*, *CXCL9*, *CXCL10*, and *CXCL11;* whereas expression of *DSC3*, *LOR*, *FLG*, and *KRT1* were similar to those in healthy skin. Differences were seen in the expression levels of *CCL27*, *NURR1*, *GNLY*, *FASLG*, and *PRF1*, which were all upregulated in the skin of the five anti-PD-1 patients, but not in SJS/TEN skin (Fig. 2B).

Taken together, our clinical, histologic, immunohistologic, and gene expression analyses provide evidence that the adverse cutaneous reactions observed in patients treated with anti-PD-1 antibodies are reminiscent of SJS/TEN and point to a role for PD-1 in regulating cytotoxic T-cell responses in the skin.

Discussion

The cross-talk between cancer cells and immune cells of the tumor microenvironment is crucial for the outcome of antitumor immune responses and immunotherapy. In various cancers, these interactions often result in a local immunosuppression, resulting in the escape of tumor cells from immunosurveillance. The use of checkpoint inhibitors, such as antibodies to PD-1, leads to significant clinical benefits by inducing advanced and metastatic tumor regression. Although anti-PD-1 antibody therapy is safe and well tolerated in patients with melanoma (2, 18–20), adverse cutaneous reactions have been reported (2, 4, 9, 10, 21). Here, we report and describe adverse cutaneous reactions during anti-PD-1 immunotherapy with pembrolizumab. In 22% of the patients, which is more than reported in clinical trials (4, 7, 21), we observed inflammatory skin lesions ranging from mild MPRs, typically associated with scaling and/or lichenoid lesions to very severe SJS-like skin lesions that slowly improved and resulted in a chronic lichen planus.

Clinical and histologic features of the lesions strikingly resemble the findings reported in mice with a disrupted PD-1 gene (22). These mice develop a lupus-like inflammatory syndrome with proliferative glomerulonephritis, arthritis with sometimes granulomatous inflammation and skin lesions, reported as "dermatitis-like lesions, necrotic lesions, and erythema" (22). The histologies of the skin of these mice present features compatible with lichen planus, including acanthosis, hypergranulosis, and apoptotic keratinocytes, together with a lymphocytic infiltrate of the grenz zone of the basal membrane resulting in a vacuolization and, sometimes, split formation (22).

The histologic analysis of these human adverse cutaneous reaction cases demonstrated signs of a cytotoxic skin eruption characterized by an accumulation of $CD8^+$ T cells at the dermo-epidermal junction and $CD8^+$ T-cell exocytosis into the epidermis with apoptotic keratinocytes. These features can also be observed in severe immune-mediated skin diseases, such as acute GVHD and SJS/TEN. Gene expression analysis of lesional skin from anti-PD-1–treated patients revealed a gene expression profile resembling SJS/TEN with an upregulation of major inflammatory chemokines, such as *CXCL9*, *CXCL10*, and *CXCL11*, of cytotoxic mediators such as *PRF1* and *GZMB* and the pro-apoptotic molecule *FASLG*, as well as an upregulation of PD-L1, which was confirmed by IHC in three cases. In contrast, the expression pattern of selected genes in the skin lesions of anti-PD-1–treated patients was different from that seen in acute GVHD and MPR. Therefore, clinical, histologic, immunohistologic, and gene

Published OnlineFirst March 8, 2016; DOI: 10.1158/1078-0432.CCR-15-2872

Table 1. Patients' characteristics, clinical presentation, and histology of the adverse cutaneous reactions

	Characteristics [M/F; age (y)]	Onset (weeks after starting anti-PD-1 Abs)	Clinical presentation	Histology	Concomitant medication	Other possibly treatment related adverse reactions	Discontinuation of pembrolizumab (yes/no)	Treatment of the adverse cutaneous drug reaction
Patient 1	M; 76	1 (after 1 infusion)	MPR evolving into subepidermal blister formation including mucosal involvement with pain and pruritus, evolving into lichen planus	Four biopsies over time: 1. Lichenoid dermatitis with accumulation of $CD8^+$ cells at the dermo-epidermal junction and $CD8^+$ exocytosis and focal keratinocytic apoptosis 2. Lichenoid inflammation with vacuolization of junction zone and keratinocytic apoptosis 3. Lichenoid accumulation of cytotoxic $CD8^+$ lymphocytes in the junction zone and in the epidermis with apoptotic keratinocytes 4. Lichenoid inflammation with hyperkeratosis resembling lichen verrucosus	Phenprocoumon; spironolactone; acetylsalicylic acid; bisoprolol; metamizole[a]; rabeprazole; mirtazapine; lorazepam; torasemide, ramipril; oxycodone[a]; dalteparin[b]	None	Yes	Systemic prednisone 1 mg/kg (tapering for 4 weeks); topical steroids, including oral application for 4 weeks; topical disinfectants (panthenol, hyaluronate sodium with silver sulfadiazine; chlorhexidine) skin hydration
Patient 2	M; 66	6 (after 3 infusions)	Disseminated MPR with moderate pruritus	Lichenoid drug reaction with follicular accentuation focal spongiosis and $CD8^+$ exocytosis	Fluticasone/salmeterol; salbutamol	Vitiligo	No	Topical steroids for 4 weeks; skin hydration
Patient 3	M; 50	5 (after 3 infusions)	Disseminated MPR with main focus on the trunc and neck. No pruritus	Lichenoid dermatitis with vacuolization of junction zone and focal keratinocyte apoptosis	Pantoprazole[c]; bisoprolol[c]	Anemia (hemolysis)	Yes (due to anemia)	Topical steroids for 4 weeks; skin hydration
Patient 4	M; 82	1 (after 1 infusion)	Small erythematous papules with moderate pruritus	Lichenoid dermatitis with $CD8^+$ cells in the dermo-epidermal junction and focal full thickness necrosis	Phenprocoumon	None	No	Skin hydration
Patient 5	M; 72	51 (after 17 infusions)	Psoriasiform disseminated skin lesions predominantly on the lower extremities both sides. Mild pruritus	Two biopsies over time: 1. Focal acanthosis and spongiosis and some apoptotic keratino cytes with lichenoid aspect 2. Lymphocytic infiltration of the adnexa	Simvastatin; losartan; chondroitin sulfate	Vitiligo	No	Topical steroids for 4 weeks; skin hydratation
Patient 6	M; 78	21 (after 7 infusions)	Focal erythematous plaques on the trunk and on the neck with mild pruritus	Lichenoid drug reaction with lymphocytic infiltrate and few eosinophils	Candesartan; acetylsalicylic acid; atorvastatin	Vitiligo	No	Systemic prednisone 1 mg/kg (tapering over 2 weeks); topical steroids for 4 weeks; skin hydration
Patient 7	M; 58	9 (after 3 infusions)	Focal erythematous plaques on the lower leg with mild pruritus	Lymphocytic perivascular sleeve-like inilftrates and lichenoid inflammation with spongiosis	Lisinopril; ibuprofen; xylometazoline	Vitiligo	No	Topical steroids for 2 weeks; skin hydration
Patient 8	F; 66	60 (after 21 infusions)	Focal erythematous papule with moderate pruritus on the back	Acanthosis, papillomatosis, and lichenoid inflammation	Losartan	None	No	Skin hydration

[a]Start 8 weeks before onset.
[b]Start 1 week before onset.
[c]Start 4 weeks before onset.

Published OnlineFirst March 8, 2016; DOI: 10.1158/1078-0432.CCR-15-2872

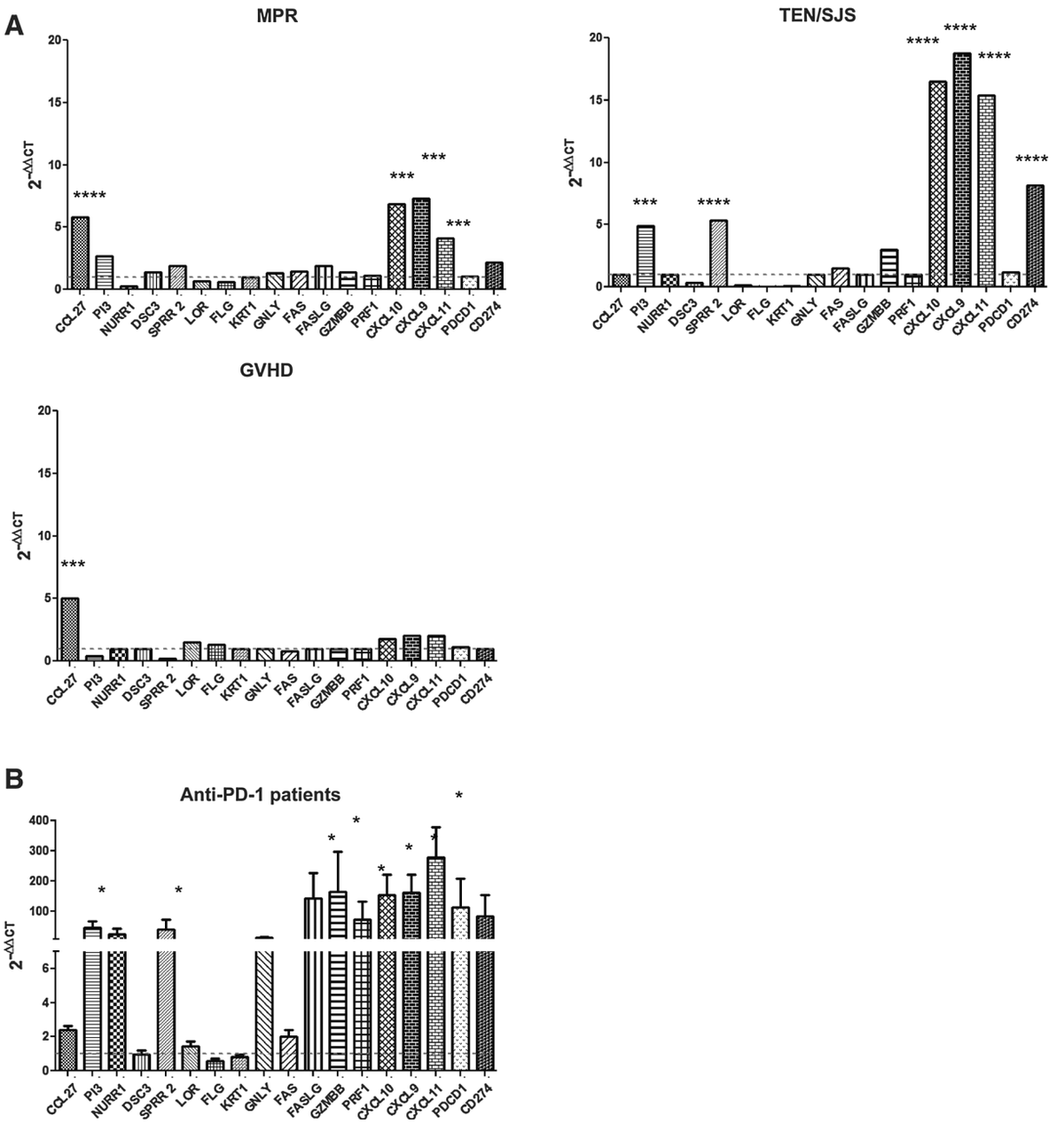

Figure 2.

Gene expression profiling. **A,** the mRNA expression levels of 6,564 different genes were measured in lesional skin of MPR; $n = 8$), TEN/SJS ($n = 5$), and GVHD ($n = 9$) patients and skin of healthy donors ($n = 8$) using the Affymetrix Human Transcriptome Array 2.0. The relative expression levels were normalized to healthy skin and indicated as fold change ($2^{-\Delta\Delta C_t}$). **B,** the mRNA expression levels of selected genes were measured in lesional skin of patients developing a skin drug eruption under anti-PD-1 therapy ($n = 5$). The relative expression levels were normalized to healthy skin ($n = 4$) and indicated as fold change ($2^{-\Delta\Delta C_t}$). Statistical analyses were performed using the Student t test. *, $P \leq 0.05$; **, $P \leq 0.01$; ***, $P \leq 0.001$; ****, $P \leq 0.0001$.

expression analyses strongly suggest that, at least in some patients, anti-PD-1 antibody can induce SJS/TEN–like adverse cutaneous reactions.

The intensity of the immune-mediated tissue damage varies and is interindividual, a possible explanation could be the genetic predisposition and variation based on SNPs in genes related to immune functions. These genetic background alterations can cause differences in the susceptibility to develop cutaneous drug reactions.

The exact pathomechanism of the adverse cutaneous reactions occurring upon pembrolizumab and nivolumab therapy remains to be elucidated. Although vitiligo can be considered as a successful (re)-activation of T cells with a repertoire specific to melanocyte antigens, the induction of a cytotoxic response to

Published OnlineFirst March 8, 2016; DOI: 10.1158/1078-0432.CCR-15-2872

keratinocytes was not expected and is indicative of the activation of T cells with non-melanoma–derived self-antigen specificity (ies). Interestingly, both vitiligo and/or cutaneous reactions emerging during nivolumab treatment in patients with melanoma have recently been reported to be associated with overall survival (23). As a consequence, cutaneous reactions during anti-PD-1 treatment could potentially be used as biomarkers in the therapy. Although larger prospective analyses are still needed to validate this association, detection and diagnosis of cutaneous reactions during anti-PD-1 therapy gain further importance in this context. By inhibiting T-cell activation and sustaining Tregs (24), the PD-1/PD-L pathway plays a major role in peripheral tolerance, including transplant (25) and feto-maternal tolerance (26). The concept of a tolerogenic role for PD-1/PD-1L has emerged from observations that PD-1–deficient mice develop autoimmune pathologies (27), including lichenoid reactions (22). One could hypothesize that, at the steady state, PD-1/PD-L interactions are crucial for the homeostasis of T cells in the skin and for preventing severe skin-directed inflammatory reactions from occurring. In line with this, it has been recently reported that in a mouse model that PD-L1 expressed on keratinocytes presenting self-antigens, regulates autoreactive $CD8^+$ T-cell activity and prevents the development of cutaneous autoimmune disease (28). The reason for which cutaneous adverse events in anti-PD-1–treated patients can vary from vitiligo to SJS-like reactions remains unknown, and larger series of subjects would be required to assess this. A detailed characterization of the T cells causing damage to healthy tissues in patients treated with anti-PD-1 antibodies, as well as complementary skin investigations in patients without adverse skin reactions, would be of interest for a better understanding and, ultimately, the prevention of such severe forms of adverse cutaneous reactions.

Disclosure of Potential Conflicts of Interest

S.M. Goldinger is a consultant/advisory board member for Bristol-Myers Squibb, MSD, Novartis, and Roche. No potential conflicts of interest were disclosed by the other authors.

Authors' Contributions

Conception and design: S.M. Goldinge, L.E. French, R. Dummer
Development of methodology: S.M. Goldinger, R. Dummer
Acquisition of data (provided animals, acquired and managed patients, provided facilities, etc.): S.M. Goldinger, P. Stieger, S. Micaletto, E. Contassot, R. Dummer
Analysis and interpretation of data (e.g., statistical analysis, biostatistics, computational analysis): S.M. Goldinger, B. Meier, E. Contassot, L.E. French, R. Dummer
Writing, review, and/or revision of the manuscript: S.M. Goldinger, B. Meier, L.E. French, R. Dummer
Administrative, technical, or material support (i.e., reporting or organizing data, constructing databases): S.M. Goldinger, P. Stieger, L.E. French, R. Dummer
Study supervision: S.M. Goldinger
Other (laboratory experiments): B. Meier

Grant Support

This study was supported by the University of Zurich (Zurich, Switzerland).

Received November 25, 2015; revised February 17, 2016; accepted February 20, 2016; published OnlineFirst March 8, 2016.

References

1. Topalian SL, Hodi FS, Brahmer JR, Gettinger SN, Smith DC, McDermott DF, et al. Safety, activity, and immune correlates of anti-PD-1 antibody in cancer. N Engl J Med 2012;366:2443–54.
2. Hamid O, Robert C, Daud A, Hodi FS, Hwu WJ, Kefford R, et al. Safety and tumor responses with lambrolizumab (anti-PD-1) in melanoma. N Engl J Med 2013;369:134–44.
3. Wolchok JD, Kluger H, Callahan MK, Postow MA, Rizvi NA, Lesokhin AM, et al. Nivolumab plus ipilimumab in advanced melanoma. N Engl J Med 2013;369:122–33.
4. Ribas A, Puzanov I, Dummer R, Schadendorf D, Hamid O, Robert C, et al. Pembrolizumab versus investigator-choice chemotherapy for ipilimumab-refractory melanoma (KEYNOTE-002): a randomised, controlled, phase 2 trial. Lancet Oncol 2015;16:908–18.
5. Robert C, Schachter J, Long GV, Arance A, Grob JJ, Mortier L, et al. Pembrolizumab versus ipilimumab in advanced melanoma. N Engl J Med 2015;372:2521–32.
6. Robert C, Long GV, Brady B, Dutriaux C, Maio M, Mortier L, et al. Nivolumab in previously untreated melanoma without BRAF mutation. N Engl J Med 2015;372:320–30.
7. Weber JS, D'Angelo SP, Minor D, Hodi FS, Gutzmer R, Neyns B, et al. Nivolumab versus chemotherapy in patients with advanced melanoma who progressed after anti-CTLA-4 treatment (CheckMate 037): a randomised, controlled, open-label, phase 3 trial. Lancet Oncol 2015;16:375–84.
8. Hua C, Boussemart L, Mateus C, Routier E, Boutros C, Cazenave H, et al. Association of vitiligo with tumor response in patients with metastatic melanoma treated with pembrolizumab. JAMA Dermatol 2015;152:45–51.
9. Carlos G, Anforth R, Chou S, Clements A, Fernandez-Penas P. A case of bullous pemphigoid in a patient with metastatic melanoma treated with pembrolizumab. Melanoma Res 2015;25:265–8.
10. Ohtsuka M, Miura T, Mori T, Ishikawa M, Yamamoto T. Occurrence of psoriasiform eruption during nivolumab therapy for primary oral mucosal melanoma. JAMA Dermatol 2015;151:797–9.
11. Harr T, French LE. Toxic epidermal necrolysis and Stevens-Johnson syndrome. Orphanet J Rare Dis 2010;5:39.
12. Mockenhaupt M, Viboud C, Dunant A, Naldi L, Halevy S, Bouwes Bavinck JN, et al. Stevens-Johnson syndrome and toxic epidermal necrolysis: assessment of medication risks with emphasis on recently marketed drugs. The EuroSCAR-study. J Invest Dermatol 2008;128:35–44.
13. Pichler WJ, Naisbitt DJ, Park BK. Immune pathomechanism of drug hypersensitivity reactions. J Allergy Clin Immunol 2011;127:S74–81.
14. Viard I, Wehrli P, Bullani R, Schneider P, Holler N, Salomon D, et al. Inhibition of toxic epidermal necrolysis by blockade of CD95 with human intravenous immunoglobulin. Science 1998;282:490–3.
15. Nassif A, Bensussan A, Dorothee G, Mami-Chouaib F, Bachot N, Bagot M, et al. Drug specific cytotoxic T-cells in the skin lesions of a patient with toxic epidermal necrolysis. J Invest Dermatol 2002;118:728–33.
16. Saito N, Qiao H, Yanagi T, Shinkuma S, Nishimura K, Suto A, et al. An annexin A1-FPR1 interaction contributes to necroptosis of keratinocytes in severe cutaneous adverse drug reactions. Sci Transl Med 2014;6:245ra95.
17. Chung WH, Hung SI, Yang JY, Su SC, Huang SP, Wei CY, et al. Granulysin is a key mediator for disseminated keratinocyte death in Stevens-Johnson syndrome and toxic epidermal necrolysis. Nat Med 2008;14:1343–50.
18. Topalian SL, Sznol M, McDermott DF, Kluger HM, Carvajal RD, Sharfman WH, et al. Survival, durable tumor remission, and long-term safety in patients with advanced melanoma receiving nivolumab. J Clin Oncol 2014;32:1020–30.
19. Robert C, Ribas A, Wolchok JD, Hodi FS, Hamid O, Kefford R, et al. Anti-programmed-death-receptor-1 treatment with pembrolizumab in ipilimumab-refractory advanced melanoma: a randomised dose-comparison cohort of a phase 1 trial. Lancet 2014;384:1109–17.
20. Rizvi NA, Mazieres J, Planchard D, Stinchcombe TE, Dy GK, Antonia SJ, et al. Activity and safety of nivolumab, an anti-PD-1 immune checkpoint inhibitor, for patients with advanced, refractory squamous non-small-cell lung cancer (CheckMate 063): a phase 2, single-arm trial. Lancet Oncol 2015;16:257–65.

Published OnlineFirst March 8, 2016; DOI: 10.1158/1078-0432.CCR-15-2872

21. Robert C, Schachter J, Long GV, Arance A, Grob JJ, Mortier L, et al. Pembrolizumab versus ipilimumab in advanced melanoma. N Engl J Med 2015;372:2521–32.
22. Nishimura H, Nose M, Hiai H, Minato N, Honjo T. Development of lupus-like autoimmune diseases by disruption of the PD-1 gene encoding an ITIM motif-carrying immunoreceptor. Immunity 1999;11: 141–51.
23. Freeman-Keller M, Kim Y, Cronin H, Richards A, Gibney G, Weber JS. Nivolumab in resected and unresectable metastatic melanoma: characteristics of immune-related adverse events and association with outcomes. Clin Cancer Res 2016;22:886–94.
24. Francisco LM, Salinas VH, Brown KE, Vanguri VK, Freeman GJ, Kuchroo VK, et al. PD-L1 regulates the development, maintenance, and function of induced regulatory T cells. J Exp Med 2009;206: 3015–29.
25. McGrath MM, Najafian N. The role of coinhibitory signaling pathways in transplantation and tolerance. Front Immunol 2012;3:47.
26. Zhang YH, Tian M, Tang MX, Liu ZZ, Liao AH. Recent insight into the role of the PD-1/PD-L1 pathway in feto-maternal tolerance and pregnancy. Am J Reprod Immunol 2015;74:201–8.
27. Nishimura H, Okazaki T, Tanaka Y, Nakatani K, Hara M, Matsumori A, et al. Autoimmune dilated cardiomyopathy in PD-1 receptor-deficient mice. Science 2001;291:319–22.
28. Okiyama N, Katz SI. Programmed cell death 1 (PD-1) regulates the effector function of CD8 T cells via PD-L1expressed on target keratinocytes. J Autoimmun 2014;53:1–9.

Published OnlineFirst March 8, 2016; DOI: 10.1158/1078-0432.CCR-15-2872

AACR American Association for Cancer Research

Clinical Cancer Research

Cytotoxic Cutaneous Adverse Drug Reactions during Anti-PD-1 Therapy

Simone M. Goldinger, Pascale Stieger, Barbara Meier, et al.

Clin Cancer Res 2016;22:4023-4029. Published OnlineFirst March 8, 2016.

Case and Review

Dermatology

Dermatology 2015;230:293–298
DOI: 10.1159/000371879

Received: October 6, 2014
Accepted after revision: January 2, 2015
Published online: March 14, 2015

Severe Sweet's Syndrome with Elevated Cutaneous Interleukin-1β after Azathioprine Exposure: Case Report and Review of the Literature

Laurence Imhof[a] Barbara Meier[a] Pascal Frei[b] Jivko Kamarachev[a] Gerhard Rogler[b]
Antonios Kolios[a] Alexander A. Navarini[a] Emmanuel Contassot[a] Lars E. French[a]

[a]Department of Dermatology and [b]Division of Gastroenterology and Hepatology, University Hospital, Zurich, Switzerland

Key Words
Azathioprine · Inflammatory bowel disease · Neutrophilic dermatosis · Sweet's syndrome · Interleukin-1β

Abstract
Sweet's syndrome (SS) is a dermatosis with systemic symptoms characterized by tender, red nodules or papules, occasionally covered with vesicles, pustules or bullae, usually affecting the upper limbs, face and neck. SS is frequently observed in patients with leukemia or connective tissue diseases, while it is rather seldom in patients with inflammatory bowel disease. The exact pathogenesis of SS is only partially understood. We report the case of a 50-year-old patient with indeterminate colitis, presenting with a febrile diffuse papulopustular and necrotizing skin eruption that healed with significant scarring and appeared 14 days after onset of treatment with azathioprine. Histological examination revealed the presence of features typical of SS, gene expression analysis very high levels of interleukin-1β (IL-1β) mRNA in lesional skin, and immunohistochemistry high levels of IL-1β at the protein level. SS associated with azathioprine is being increasingly reported and is reviewed herein.

Introduction

Sweet's syndrome (SS), or acute febrile neutrophilic dermatosis, belongs to the group of the so-called neutrophilic dermatoses and was first described in 1964 by Robert Douglas Sweet [1]. The cutaneous lesions of SS typically appear as tender, red or purple-red papules or nodules. They most frequently occur on the upper extremities, face and neck [2]. Less commonly SS can present as a pustular dermatosis [3]. Affected patients may appear dramatically ill. Fever and leukocytosis usually accompany the skin eruption. Several clinical conditions have been linked to SS. A probable association between the occurrence of the following conditions and the development of SS is considered likely: cancer (hematologic malignancies and solid tumors), infections (most commonly of the upper respiratory tract and the gastrointestinal tract), inflammatory bowel disease (IBD) (includes Crohn's disease and ulcerative colitis), medications (granulocyte colony-stimulating factor [G-CSF] as the most commonly reported medication), and pregnancy [2].

Various medications have been reported to induce SS, including G-CSF, antibiotics, retinoids, antiepileptics and antihypertensives. More recently azathioprine (AZA), the nitroimidazole of 6-mercaptopurine, which is widely used as a corticosteroid-sparing agent in a variety of autoimmune inflammatory diseases, has been increasingly reported as a potential cause of SS [4–14]. Here we report a severe case of SS associated with AZA therapy, review the literature concerning similar cases reported to date and analyze the expression of the proinflammatory cytokine interleukin-1β (IL-1β) in our patient's skin lesions.

Case Description

A 50-year-old male smoker was emergently referred to our department for an impressive febrile diffuse pustular and necrotizing skin eruption. He had a background history of a IBD, namely indeterminate colitis affecting the sigmoid colon that had first been diagnosed 5 months previously. Oral sulfasalazine therapy had been ineffective. Approximately 5 weeks prior to presentation, he had experienced a flare of his colitis managed with an oral medication of 50 mg prednisone daily. 14 days prior to presentation, AZA had been introduced at a dose of 50 mg once daily.

The patient's current illness began about 4 days prior to his transfer to our department. He initially developed a mac-

1018–8665/15/2304–0293$39.50/0

E-Mail karger@karger.com
www.karger.com/drm

Laurence Imhof, MD
Department of Dermatology, University Hospital
Gloriastrasse 31
CH–8091 Zurich (Switzerland)
E-Mail laurence.imhof@usz.ch

Color version available online

Fig. 1. Florid cutaneous eruption of the upper torso, face and neck consisting of erythematous papulopustular lesions 2–10 mm in diameter, many of them with a central depression and/or erosion (**a**, **c**), evolving over time to central crusting (**b**).

Color version available online

Fig. 2. Large aphthous lesions with a fibrinous base on the hard palate.

ulopapular rash predominantly on the trunk, accompanied by high fever and fatigue. In the following days he developed a painful cutaneous eruption that was most marked over the upper back, shoulders, neck and face. This was accompanied by loose, partially bloody diarrhea with more than twenty bowel movements per day. There were no relevant symptoms pertaining to other organ systems. Upon arrival he was febrile (39.6°C), tachycardic (129 beats/min) and had a blood pressure of 116/84 mm Hg. Examination of the patient's skin revealed a florid eruption consisting of scattered well-delimited nummular erythematous papulopustular lesions 2–10 mm in diameter, many of which were depressed in the center (fig. 1). Fresh lesions were infiltrated erythematous plaques with a central pustule; older lesions were infiltrated erythematous plaques with a brown-colored central crust. The cutaneous eruption was mostly confined to the upper torso, face and neck, but the mucosa was also affected, with aphthous lesions 5–10 mm in diameter and a fibrinous base (fig. 2).

Laboratory results showed a strongly elevated white cell count with pronounced neutrophilia and markedly raised C-reactive protein (table 1). Swabs were taken from the pustular skin lesions for culture, and two sets of blood cultures were collected. An incisional skin biopsy was taken from a pustular plaque on the right upper back for histopathology.

Pending the results of the above investigations, a provisional diagnosis of neutrophilic dermatosis (most closely resembling SS) was made, and the patient's daily prednisone 50 mg dose was substituted by intravenous hydrocortisone 400 mg daily. The condition was considered to be likely associated with the patient's underlying colitis, and since AZA-induced SS had been reported in a handful of previously published cases, therapy with AZA was interrupted. The patient responded well to intravenous steroids with flattening of his skin lesions, disappearance of the pustules and appearance of crusts covering the lesions. Simultaneously his body temperature normalized. Histopathological examination of the skin biopsy taken at onset (fig. 3) revealed marked superficial edema with florid neutrophilic infiltration in the whole dermal thickness, consistent with SS syndrome. Cultures taken prior to antibiotic therapy from blood and skin swabs were all sterile. Complete healing of skin lesions with residual hypopigmented scars occurred within 3 weeks. Given the patient's active colitis and the impossibility to further treat with AZA as a steroid-sparing agent, we decided to start infliximab on the ninth day of hospitalization both for induction and maintenance therapy. According to a telephone follow-up 1 year later, there were no recurrences of his symptoms, and his colitis was well controlled by therapy with infliximab and mesalazine.

A very recent review of the literature up to the 30th of May 2014 identified 16 reported cases of AZA-induced SS (table 2) [4–8, 10–17]. Analysis of these 16 reported cases shows an age distribution upon onset ranging from 9 to 89 years, an association of AZA-induced SS with IBD in 13 of 16 cases (81%), and an onset within the first month of AZA therapy (with an average time to onset of 33 days, range 7–330) in 15 of 16 patients (94%) (table 2). In the seven case reports in which the thiopurine methyltransferase (TPMT) levels were indicated, no deficiency in TPMT existed, making a defect in AZA methylation and metabolism unlikely, and the latter an unlikely cause of the observed neutrophilic dermatosis. Rechallenge with AZA was tested in 6 of the reported cases and was positive in

all of them, thus indicating direct causality of AZA in these cases of SS.

The pathogenesis of SS is incompletely understood. The association with underlying diseases and drugs suggests a hypersensitivity reaction, and it has been suggested that a dysregulation of cytokine release including IL-1, granulocyte-macrophage colony-stimulating factor (GM-CSF), G-CSF and interferon-γ may be involved [18, 19]. Based on reports linking IL-1β to diseases associated with neutrophilic infiltration of the skin, such as the rare genetic autoinflammatory syndrome associating pyogenic arthritis, pyoderma gangrenosum and acne, named PAPA syndrome [20], and the cryopyrin-associated periodic syndromes (CAPS) [21], we analyzed IL-1β expression levels in the skin lesions of the reported patient. As shown in figure 4, mRNA levels for IL-1β in our patient's skin biopsy assessed by quantitative RT-PCR with cDNA primers for the housekeeping gene RPL27 (forward 5′-ATC GCC AAG AGA TCA AAG ATA A-3′, reverse 5′-TCT GAA GAC ATC CTT ATT GAC G-3′) and IL-1β (forward 5′-CAC GAT GCA CCT GTA CGA TCA-3′, reverse 5′-GTT GCT CCA TAT CCT GTC CCT-3′) were over 250-fold higher than those observed in normal skin, and this was associated with enhanced expression of the mature active form of IL-1β in inflammatory cells – mainly neutrophils – of the dermal infiltrate as identified by immunohistochemistry.

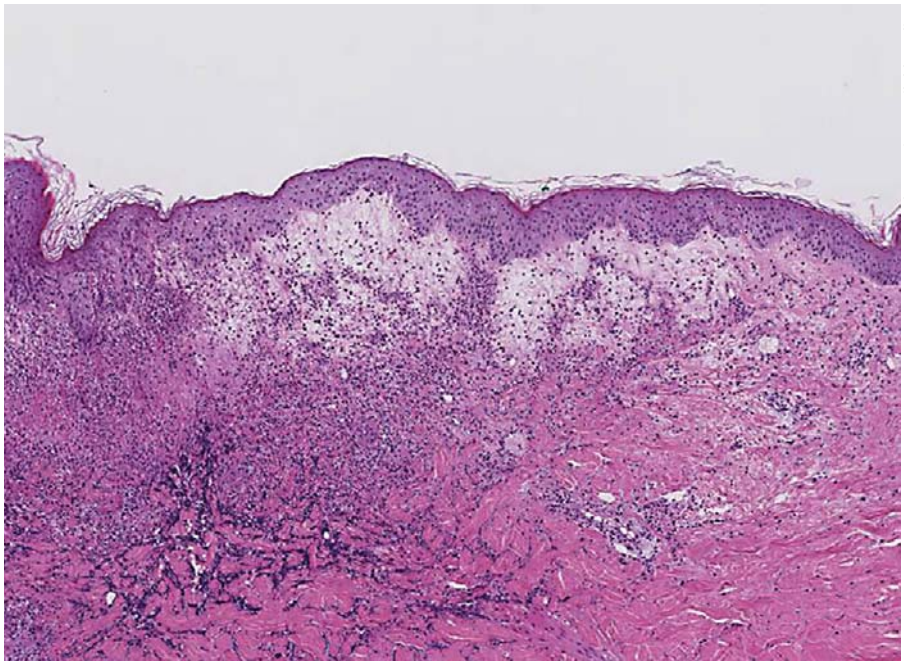

Color version available online

Fig. 3. Skin biopsy taken on the upper back showing marked superficial edema with florid neutrophilic infiltration of the whole dermal thickness. Hematoxylin and eosin, ×100.

Table 1. Summary of laboratory investigation findings

Test	Result	Normal range
Hemoglobin, g/dl	9.1	13.4–17.0
White cell count, $\times 10^3$/μl	22.4	3.0–9.6
Neutrophils, $\times 10^3$/μl	20.16	1.4–8.0
Platelets, $\times 10^3$/μl	602	143–400
Sodium, mmol/l	134	136–145
Potassium, mmol/l	3.9	3.3–4.5
Urea, mmol/l	6.6	2.14–7.14
Creatinine, μmol/l	94	62–106
Albumin, g/l	27	40–49
C-reactive protein, mg/l	193	<5

Discussion

Acute febrile neutrophilic dermatosis or SS is a prototypic neutrophilic dermatosis first described in 1964 by Dr. Robert Douglas Sweet [1]. The characteristic clinical manifestations of this disorder include acute eruption of tender, red or purple-red papules, nodules or plaques, occasionally associated with pustules, bullae or ulcers, and constant systemic symptoms (pyrexia, fatigue). Together with cutaneous manifestation SS can nearly involve any organ system. Inflammation in some of these organs can cause serious long-term quality of life impairment. The sight-threatening ocular manifestations merit particular mention [22]. Cutaneous biopsies reveal an inflammatory infiltrate consisting mainly of mature neutrophils in the upper dermis.

The pathogenesis of SS is unknown. The association of the disorder with infections, IBD, drugs, autoimmune diseases and malignancies, as well as the higher incidence in women, suggest a hypersensitivity reaction [23]. One current attractive hypothesis regarding the pathogenesis of SS is a local or systemic dysregulation of cytokine secretion. Among the potentially responsible cytokines are IL-1, IL-3, IL-6, IL-8, G-CSF, GM-CSF and interferon-γ [18]. Elevated serum levels of IL-1, IL-2 and interferon-γ, but not IL-4, suggest that the expression of Th1 cytokines may be involved in the pathogenesis of this syndrome [18].

SS does fulfill the current criteria for classification as an autoinflammatory disease [24]. Autoinflammatory diseases are a relatively new category of diseases distinct from allergic and autoimmune diseases and characterized by seemingly unprovoked recurrent inflammation in the absence of evidence of circulating autoantibodies or an antigen-specific T cell response [25]. Genetic mutations affecting proteins of the inflammasome complex or proteins that regulate the function of the inflammasome have been found in several of the autoinflammatory syndromes. In-

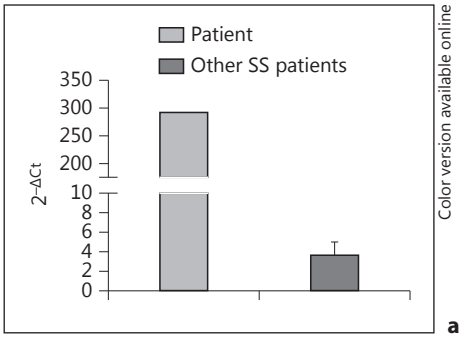

Fig. 4. a Analysis of IL-1β mRNA levels by quantitative RT-PCR in the patient's skin biopsy and healthy control skin. **b** Immunohistochemical stainings with an anti-IL-1β antibody and with an appropriate isotype control antibody were performed on the patient's skin biopsy and compared to anti-IL-1β antibody staining in healthy control skin.

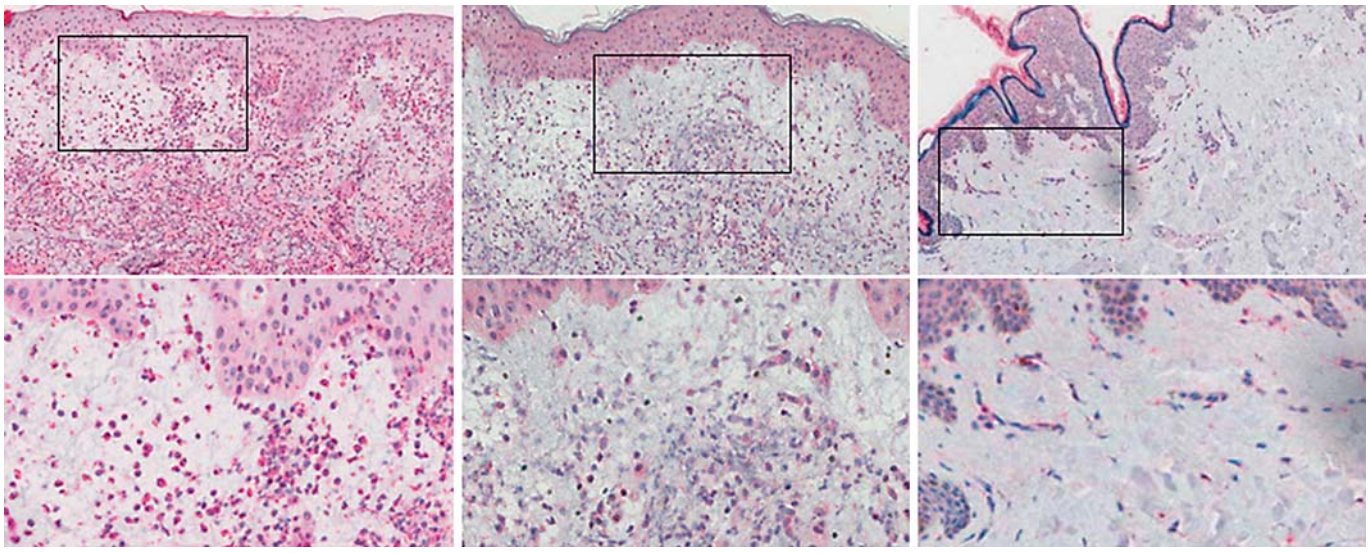

Patient skin, anti-IL-1β Ab | Patient skin, isotype control Ab | Healthy control skin, anti-IL-1β Ab

Table 2. Reported cases of AZA-induced SS

Case No. [ref.]	Age, years/ sex	Underlying disease	Time of onset after starting AZA	Recurrence with rechallenge	TPMT level	Concurrent steroid use
1 [8]	9/F	ulcerative colitis	10 days	no rechallenge	N	yes
2 [4]	39/F	Crohn's disease	28 days	yes	N	yes
3 [4]	33/M	systemic lupus erythematosus	14 days	no rechallenge	N	yes
4 [14]	46/M	ulcerative colitis	14 days	yes	NR	yes
5 [6]	49/M	ulcerative colitis	11 months	yes	NR	yes
6 [7]	32/M	Crohn's disease	7 days	yes	above ref. range	yes
7 [7]	68/M	myasthenia gravis	10 days	no rechallenge	above ref. range	yes
8 [7]	42/M	ulcerative colitis	14 days	no rechallenge	NR	yes
9 [13]	89/F	bullous pemphigoid	18 days	no rechallenge	N	yes
10 [11]	45/M	Crohn's disease	14 days	yes	NR	yes
11 [12]	55/M	Crohn's disease	7 days	yes	NR	yes
12 [10]	53/M	ulcerative colitis	7 days	no rechallenge	NR	yes
13 [15]	50/M	indeterminate colitis	14 days	no rechallenge	NR	yes
14 [17]	75/M	Crohn's disease	14 days	no rechallenge	NR	no
15 [5]	81/F	Crohn's disease	14 days	no rechallenge	NR	yes
16 [16]	51/M	Crohn's disease	10 days	no rechallenge	N	yes

F = Female; M = male; N = normal; NR = not reported.

flammasomes are a group of protein complexes that recognize a diverse set of pathogen- and/or danger-associated inflammation-inducing stimuli and that control the production of important proinflammatory cytokines such as IL-1β and IL-18 [26]. Mutations in inflammasome components may result in overactivity of the inflammasome or failure to limit IL-1-mediated inflammation, as is the case in CAPS such as Muckle-Wells syndrome that are due to activating mutations of the inflammasome component NLRP3. In a large number of autoinflammatory diseases, systemic corticosteroids have only modest effect. Biologic agents such as anakinra (Kineret®), a recombinant IL-1R antagonist, can result in a dramatic and consistent improvement in those syndromes where a clear link to IL-1 has been shown [27]. Likewise therapy with canakinumab, a human monoclonal antibody targeted at IL-1β, has been shown to induce rapid, durable and complete clinical responses in 97% of CAPS patients studied [28]. Our data showing very high levels of IL-1β mRNA and protein in the skin lesions of our patient are supportive of the above notion that SS is an autoinflammatory disease, and suggest that IL-1β may contribute to the neutrophilic infiltration of the skin and fever that characterize SS. According to the recently updated classification of autoinflammatory disease, our case is a type 1, complex/acquired autoinflammatory disease [25].

Prednisone or prednisolone at an initial dose of 0.5–1.5 mg/kg body weight/day, with gradual tapering over 2–4 weeks, represents the standard first-line treatment for SS. In recurrent disease, therapy with colchicine, potassium iodide, dapsone, doxycycline, non-steroidal anti-inflammatory agents and cyclosporine has been described, with mixed results [29]. A few case reports mention successful use of infliximab (5 mg/kg) on a compassionate use basis in refractory SS. Evidence for any of these therapeutic regimens is however limited as based on case reports and small case series. Recently very encouraging responses to Kineret have been reported in patients with refractory SS, further suggesting that IL-1α or IL-1β play a significant role in the pathophysiology of this disease [30, 31].

One of the more frequently reported diseases associated with classical SS is IBD. Benton et al. [32] described its association with ulcerative colitis for the first time in 1985. Since then, a large number of case reports have confirmed this association [32–46]. The association of SS with Crohn's disease is less common, with fewer than 40 cases described in the literature. SS associated with IBD tends to be more common in women (87%) and is usually associated with active disease [47]. The presence of extraintestinal symptoms, such as joint symptoms and other skin manifestations, is frequent in patients with IBD-associated SS [48]. As mentioned earlier, SS may be also associated with medications [2], the administration of G-CSF being responsible for the majority of drug-induced cases of SS. Many patients with IBD are treated with AZA as a corticosteroid-sparing agent. When SS occurs in such patients, IBD is the first suspected cause of the syndrome, given the well-reported association [10, 15]. However, in the last few years several papers reporting a possible association between AZA and SS have been published (table 2) [4–8, 10–17]. Interestingly, two of the cases reporting AZA-associated SS had an underlying disease other than IBD, and rechallenge of patients with AZA reproduced SS lesions in all 6 cases rechallenged, both facts providing support for a potential role of AZA as a trigger/co-factor in certain cases of SS [4, 7].

The AZA hypersensitivity syndrome, which typically occurs within the first 4 weeks of initiation of AZA therapy [9] and is characterized by systemic symptoms identical to those of SS (fever, leukocytosis, malaise, arthralgia), was considered to be the cause in many of these cases (table 2). A review of the English language literature by Bidinger et al. [4] showed that about 50% of patients with a hypersensitivity reaction to AZA had cutaneous manifestations. The majority thereof had biopsy or clinical features consistent with a neutrophilic dermatosis. Interestingly, withdrawal of AZA and rechallenge with the drug indicated that at least in some of the abovementioned cases [4, 6, 7, 11, 12, 14], a direct association between AZA and SS existed. In another case, on the other hand, the AZA dose was increased and the rash eventually resolved [41]. As the systemic manifestations described for AZA hypersensitivity syndrome have all also been reported to occur with varying frequencies in SS, it is presumed that both denominations refer to variants of the same disease [49, 50].

Our patient with SS developing 14 days after initiation of AZA therapy for active IBD meets all of the diagnostic criteria for drug-induced SS as presented by Walker and Cohen in 1996 [51]. Especially the localization and the clinical outcome arguments against the presence of an AZA hypersensitivity syndrome. The latter tends to favor the lower extremities and most cases resolve within 2–3 days after withdrawal of the medication and may not necessitate an increase in corticosteroid dose. In view of the impressive clinical presentation resulting in permanent skin scarring, rechallenge with AZA as a proof of causality was not performed. Full resolution of clinical symptoms occurred upon therapy with systemic steroids and infliximab. Our data showing involvement of IL-1β in SS, taken together with reports of successful therapy of SS with the IL-1 receptor antagonist anakinra, suggest that IL-1 plays a role in the pathogenesis of SS, and the latter therapy may be optimal in steroid-refractory cases of SS. However, anakinra was not shown to be effective in IBD. For that reason a different strategy was chosen in the patient discussed here.

Disclosure Statement

The authors have no conflict of interest to declare. There was no funding source.

References

1 Sweet RD: An acute febrile neutrophilic dermatosis. Br J Dermatol 1964;76:349–356.
2 Cohen PR, Kurzrock R: Sweet's syndrome revisited: a review of disease concepts. Int J Dermatol 2003;42:761–778.
3 Sommer S, Wilkinson SM, Merchant WJ, Goulden V: Sweet's syndrome presenting as palmoplantar pustulosis. J Am Acad Dermatol 2000;42:332–334.
4 Bidinger JJ, Sky K, Battafarano DF, Henning JS: The cutaneous and systemic manifestations of azathioprine hypersensitivity syndrome. J Am Acad Dermatol 2011;65:184–191.
5 Cyrus N, Stavert R, Mason AR, Ko CJ, Choi JN: Neutrophilic dermatosis after azathioprine exposure. JAMA Dermatol 2013;149:592–597.
6 Decisier M, Duhalde V, Faure P, Ammoury A, Gony M, Moreau J, Montastruc JL, Bagheri H: Rapid-onset febrile dermatosis. Gut 2009;58:67, 125.

7 El-Azhary RA, Brunner KL, Gibson LE: Sweet syndrome as a manifestation of azathioprine hypersensitivity. Mayo Clin Proc 2008;83:1026–1030.
8 Kim MJ, Jang KT, Choe YH: Azathioprine hypersensitivity presenting as Sweet syndrome in a child with ulcerative colitis. Indian Pediatr 2011;48:969–971.
9 Knowles SR, Gupta AK, Shear NH, Sauder D: Azathioprine hypersensitivity-like reactions – a case report and a review of the literature. Clin Exp Dermatol 1995;20:353–356.
10 Paoluzi OA, Crispino P, Amantea A, Pica R, Iacopini F, Consolazio A, Di Palma V, Rivera M, Paoluzi P: Diffuse febrile dermatosis in a patient with active ulcerative colitis under treatment with steroids and azathioprine: a case of Sweet's syndrome. Case report and review of literature. Dig Liver Dis 2004;36:361–366.
11 Stapleton M, Panaccione R: Azathioprine induced Sweet's syndrome in a patient with Crohn's disease: a case report. Can J Gastroenterol 2003;17(suppl A):abstract 255.
12 Treton X, Joly F, Alves A, Panis Y, Bouhnik Y: Azathioprine-induced Sweet's syndrome in Crohn's disease. Inflamm Bowel Dis 2008;14:1757–1758.
13 Valentine MC, Walsh JS: Neutrophilic dermatosis caused by azathioprine. Skinmed 2011;9:386–388.
14 Yiasemides E, Thom G: Azathioprine hypersensitivity presenting as a neutrophilic dermatosis in a man with ulcerative colitis. Australas J Dermatol 2009;50:48–51.
15 Burrows NP: Sweet's syndrome in association with Crohn's disease. Clin Exp Dermatol 1995;20:279–280.
16 Fenaux S, Tintillier M, Cuvelier C, Migali G, Pochet JM: Azathioprine hypersensitivity syndrome: a case report. Acta Clin Belg 2013;68:223–224.
17 Grelle JL, Halloush RA, Khasawneh FA: Azathioprine-induced acute febrile neutrophilic dermatosis (Sweet's syndrome). BMJ Case Rep 2013:2013.
18 Cohen PR: Sweet's syndrome – a comprehensive review of an acute febrile neutrophilic dermatosis. Orphanet J Rare Dis 2007;2:34.
19 Giasuddin AS, El-Orfi AH, Ziu MM, El-Barnawi NY: Sweet's syndrome: is the pathogenesis mediated by helper T cell type 1 cytokines? J Am Acad Dermatol 1998;39:940–943.
20 Wise CA, Gillum JD, Seidman CE, Lindor NM, Veile R, Bashiardes S, Lovett M: Mutations in CD2BP1 disrupt binding to PTP PEST and are responsible for PAPA syndrome, an autoinflammatory disorder. Hum Mol Genet 2002;11:961–969.
21 Sanchez GA, de Jesus AA, Goldbach-Mansky R: Monogenic autoinflammatory diseases: disorders of amplified danger sensing and cytokine dysregulation. Rheum Dis Clin North Am 2013;39:701–734.
22 Baartman B, Kosari P, Warren CC, Ali S, Jorizzo JL, Sato M, Kurup SK: Sight-threatening ocular manifestations of acute febrile neutrophilic dermatosis (Sweet's syndrome). Dermatology 2014;228:193–197.
23 Saavedra AP, Kovacs SC, Moschella SL: Neutrophilic dermatoses. Clin Dermatol 2006;24:470–481.
24 Grateau G, Hentgen V, Stojanovic KS, Jeru I, Amselem S, Steichen O: How should we approach classification of autoinflammatory diseases? Nat Rev Rheumatol 2013;9:624–629.
25 Masters SL, Simon A, Aksentijevich I, Kastner DL: Horror autoinflammaticus: the molecular pathophysiology of autoinflammatory disease (*). Annu Rev Immunol 2009;27:621–668.
26 Beer HD, Contassot E, French LE: The inflammasomes in autoinflammatory diseases with skin involvement. J Invest Dermatol 2014;134:1805–1810.
27 Hawkins PN, Lachmann HJ, McDermott MF: Interleukin-1-receptor antagonist in the Muckle-Wells syndrome. N Engl J Med 2003;348:2583–2584.
28 Lachmann HJ, Kone-Paut I, Kuemmerle-Deschner JB, Leslie KS, Hachulla E, Quartier P, Gitton X, Widmer A, Patel N, Hawkins PN: Use of canakinumab in the cryopyrin-associated periodic syndrome. N Engl J Med 2009;360:2416–2425.
29 Waltz KM, Long D, Marks JG Jr, Billingsley EM: Sweet's syndrome and erythema nodosum: the simultaneous occurrence of 2 reactive dermatoses. Arch Dermatol 1999;135:62–66.
30 Delluc A, Limal N, Puechal X, Frances C, Piette JC, Cacoub P: Efficacy of anakinra, an IL1 receptor antagonist, in refractory Sweet syndrome. Ann Rheum Dis 2008;67:278–279.
31 Kluger N, Gil-Bistes D, Guillot B, Bessis D: Efficacy of anti-interleukin-1 receptor antagonist anakinra (Kineret®) in a case of refractory Sweet's syndrome. Dermatology 2011;222:123–127.
32 Benton EC, Rutherford D, Hunter JA: Sweet's syndrome and pyoderma gangrenosum associated with ulcerative colitis. Acta Derm Venereol 1985;65:77–80.
33 Ali M, Duerksen DR: Ulcerative colitis and Sweet's syndrome: a case report and review of the literature. Can J Gastroenterol 2008;22:296–298.
34 Baba Y, Honma T, Takei S, Suzuki K, Arai F, Kobayashi M, Sugimura K, Narisawa R, Takahashi T, Asakura H, Tomiyama K, Ajioka Y: A case of ulcerative colitis with Sweet's syndrome (in Japanese). Nihon Shokakibyo Gakkai Zasshi 2001;98:1278–1282.
35 Castro-Fernandez M, Sanchez-Munoz D, Ruiz-Granados E, Merchante N, Corzo J: Coexistence of pyoderma gangrenosum and Sweet's syndrome in a patient with ulcerative colitis. Am J Gastroenterol 2007;102:2865–2866.
36 Diaz-Peromingo JA, Garcia-Suarez F, Sanchez-Leira J, Saborido-Frojan J: Sweet's syndrome in a patient with acute ulcerative colitis: presentation of a case and review of the literature. Yale J Biol Med 2001;74:165–168.
37 Fellermann K, Rudolph B, Witthoft T, Herrlinger KR, Tronnier M, Ludwig D, Stange EF: Sweet syndrome and erythema nodosum in ulcerative colitis, refractory to steroids: successful treatment with tacrolimus (in German). Med Klin (Munich) 2001;96:105–108.
38 Goikoetxea U, Eguiluz A, Lobo C, Cosme A, Ojeda E, Bujanda L: Sweet's syndrome and arthritis in a patient with ulcerative colitis (in Spanish). Gastroenterol Hepatol 2007;30:506–507.
39 Kang W, Hao C, Nie Q: Clinical challenges and images in GI. Sweet syndrome in association with ulcerative colitis. Gastroenterology 2009;136:1507, 1846.
40 Lacey BW, You D, Speziale A: Pustular skin eruption in a patient with ulcerative colitis. Clin Gastroenterol Hepatol 2011;9:e43–e44.
41 Malheiros AP, Teixeira MG, Takahashi MD, de Almeida MG, Kiss DR, Cecconello I: Sweet syndrome associated with ulcerative colitis. Inflamm Bowel Dis 2007;13:1583–1584.
42 Marco Lattur MD, Garcia Gasalla M, Nadal Llado C, Terrasa Sagrista F: Sweet syndrome in a patient with ulcerous colitis (in Spanish). Med Clin (Barc) 2009;133:568.
43 Molina Boix M, Ortega Gonzalez G, Perez Garcia B, Perez Gracia A: Sweet syndrome and ulcerative colitis (in Spanish). Rev Esp Enferm Apar Dig 1988;74:493–494.
44 Natour M, Chowers Y, Solomon M, Khaikin M, Barshack I, Ayalon A, Zmora O: Sweet's syndrome in association with ulcerative colitis and dyserythropoietic anemia. Digestion 2007;75:142–143.
45 Vazquez J, Almagro M, del Pozo J, Fonseca E: Neutrophilic pustulosis and ulcerative colitis. J Eur Acad Dermatol Venereol 2003;17:77–79.
46 Villanueva C, Mones J, Pujol R, Puig L, Such J, Sancho FJ: Vesiculopustular eruption and Sweet syndrome associated with 2 exacerbations of ulcerous colitis in a 76-year-old woman (in Spanish). Med Clin (Barc) 1989;93:298–300.
47 Ytting H, Vind I, Bang D, Munkholm P: Sweet's syndrome – an extraintestinal manifestation in inflammatory bowel disease. Digestion 2005;72:195–200.
48 Travis S, Innes N, Davies MG, Daneshmend T, Hughes S: Sweet's syndrome: an unusual cutaneous feature of Crohn's disease or ulcerative colitis. The South West Gastroenterology Group. Eur J Gastroenterol Hepatol 1997;9:715–720.
49 Fett DL, Gibson LE, Su WP: Sweet's syndrome: systemic signs and symptoms and associated disorders. Mayo Clin Proc 1995;70:234–240.
50 von den Driesch P: Sweet's syndrome (acute febrile neutrophilic dermatosis). J Am Acad Dermatol 1994;31:535–556.
51 Walker DC, Cohen PR: Trimethoprim-sulfamethoxazole-associated acute febrile neutrophilic dermatosis: case report and review of drug-induced Sweet's syndrome. J Am Acad Dermatol 1996;34:918–923.

amplification in the molecular diagnosis of XLI patients; and initial screening of exons 7-10 of the *STS* for point mutations by DNA sequencing for those patients who are already excluded for complete or partial gene deletions.

Acknowledgements

We are grateful to the patients and their family members for participation in the study. The study was conducted by grant received from Higher Education Commission (HEC) of Pakistan. SH is supported by HEC's indigenous PhD fellowship.

References

[1] Fernandes NF, Janniger CK, Schwartz RA. X-linked ichthyosis: an oculocutaneous genodermatosis. J Am Acad Dermatol 2010;62:480–5.
[2] Al-Zayir AA, Al-Alakloby OMA. Clinico-epidemiological features of primary hereditary ichthyoses in the Eastern province of Saudi Arabia. Int J Dermatol 2006;45:257–64.
[3] Kharfi M, El Fekih N, Ammar D, Khaled A, Fazaa B, Ridha Kamoun M. Hereditary ichthyosis in Tunisia: epidemiological study of 60 cases. Tunis Med 2008; 86:983–6.
[4] Cañueto J, Ciria S, Hernández-Martın A, Unamuno P, González-Sarmiento R. Analysis of the STS gene in 40 patients with X-linked ichthyosis: a high frequency of partial deletions in a Spanish population. J Eur Acad Dermatol Venereol 2010;24:1226–9.
[5] Alperin ES, Shapiro LJ. Characterization of point mutations in patients with X-linked ichthyosis. Effects on the structure and function of the steroid sulfatase protein. J Biol Chem 1997;272:20756–63.
[6] Oyama N, Satoh M, Iwatsuki K, Kaneko F. Novel point mutations in the steroid sulfatase gene in patients with X-linked ichthyosis: transfection analysis using the mutated genes. J Invest Dermatol 2000;114:1195–9.
[7] Ramesh R, Chen H, Kukula A, Wakeling EL, Rustin MHA, Irwin McLean WH. Exacerbation of X-linked ichthyosis phenotype in a female by inheritance of filaggrin and steroid sulfatase mutations. J Dermatol Sci 2011;64:159–62.
[8] Nagtzaam IF, Stegmann APA, Steijlen PM, Herbergs J, Van Lent-Albrechts JA, Van Geel M, et al. Clinically manifest X-linked recessive ichthyosis in a female due to a homozygous interstitial 1.6-Mb deletion of Xp22.31. Br J Dermatol 2012;166: 905–7.

Ghulam Murtaza, Sumaira Siddiq, Suliman Khan, Sofia Hussain, Muhammad Naeem*
Department of Biotechnology, Quaid-i-Azam University, Islamabad, Pakistan

*Corresponding author. Tel.: +92 5190644122; fax: +92 5190644110
E-mail address: mnaeemqau@gmail.com (M. Naeem).

Received 22 July 2013

http://dx.doi.org/10.1016/j.jdermsci.2013.12.012

Letter to the Editor

Metastatic melanoma cell lines do not secrete IL-1β but promote IL-1β production from macrophages

Keywords:
Melanoma; IL-1β; Inflammasome; Macrophage

To the Editor

Tumors secrete pro-inflammatory cytokines, chemokines, and other soluble factors in the microenvironment. Interleukin-1β (IL-1β) is a pleiotropic pro-inflammatory cytokine involved in cell growth, differentiation, and regulation of immune responses [1]. IL-1β is often detected in human cancer tissues including breast cancer, pancreatic cancer, and glioblastoma [2]. It has been reported that the expression levels of the IL-1β gene or protein are associated with the invasiveness and metastasis of cancers [3]. On the other hand, IL-1β production from tumor cells may be considered as a threat by the host's immune system. In this aspect, it has been reported that IL-1β-producing melanoma cells induce reduced tumor growth by recruiting immune cells [4]. Therefore, melanoma cells must have a precise mechanism of IL-1β regulation but it remains largely unknown.

IL-1β is first synthesized as a biologically inactive precursor (pro-IL-1β). Pro-IL-1β is then cleaved by caspase-1 to biologically active mature IL-1β, resulting in its release into the extracellular space [1]. Therefore, we first analyzed IL-1β production from melanoma cell lines. THP-1 macrophages and melanoma cells were primed or not with phorbol-12-myristate-13-acetate (PMA, 500 nM) and exposed to the IL-1β inducer ionomycin (1.5 mM). Under these conditions and in contrast to THP-1 monocytic cells, 13 metastatic melanoma cell lines were not able to secrete IL-1β (Fig. 1a). Inflammasomes are a multi-protein complexes whose assembly and activation are responsible for the processing of caspases-1 and -5 [1]. The NOD-like receptor pyrin domain containing-3 (NLRP3) inflammasome has been the most studied inflammasome to date. This high molecular weight complex is composed of NLRP3, apoptosis-associated speck-like protein containing a CARD domain (ASC) adaptor protein, and the cysteine protease caspase-1 [1]. Assembly of the NLRP3 inflammasome activates caspase-1, which mediates maturation of proinflammatory cytokines such as IL-1β and IL-18.

To address the expression levels of inflammasome components in metastatic melanoma cells, we performed reverse transcription polymerase chain reaction (RT-PCR) analyses. In contrast to THP-1 cells, one or several inflammasome components were not expressed in A375, Me191, and Me290 metastatic melanoma cell lines [5,6] (Fig. 1b). In addition, pro-IL-1β and pro-IL-18 transcripts were not detected in Me191 and Me290 cells (Fig. 1b). To further determine the expression pattern of inflammasome components in melanoma cells, we used 6 primary and 21 metastatic melanoma cell lines as reported previously (Supplemental Tables 1 and 2) [5,6]. One hundred percent of cell lines derived from primary melanomas expressed *ASC*. In contrast, only 19 percent of cell lines derived from metastatic melanomas expressed *ASC* (Fig. 1c). Also, caspase-1, NLRP3, IL-1β, and AIM2 were expressed in a lower proportion of metastatic melanoma cell lines when compared to cell lines derived from primary melanoma cell lines (Fig. 1c). In tumors, ASC expression is inversely correlated with the methylation status of the *ASC* promoter region [7]. Analysis of the methylation profile of ASC by MeDIP [8] revealed that 2 out of 4 tested cell lines had a methylated *ASC*-promoter (Fig. 1d). M000921 and M010817 [5,6] were found to have DNA methylation in the promoter region of *ASC* but not M990115 and M010119 [5,6]. ASC expression was then assessed by qRT-PCR and showed to inversely correlate with *ASC* methylation (data not shown). Consistently with this observation, a treatment with the demethylating agent 5-azacythitidine (AZA, 2.5 μM) induced the restoration of ASC expression as observed by RT-PCR (Fig. 1e) and western blotting (Fig. 1 f). These results suggest that most of metastatic melanoma cell lines did not secrete IL-1β

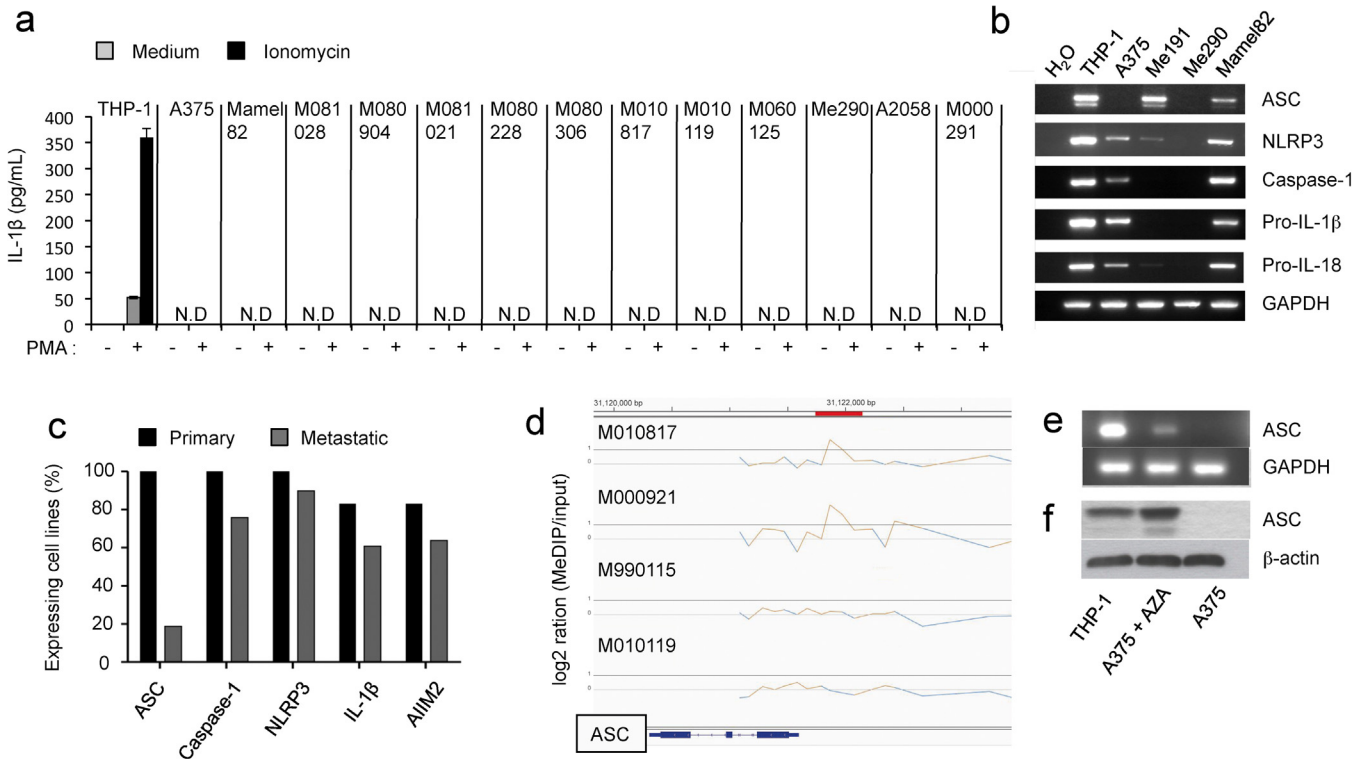

Fig. 1. Metastatic melanoma cells are not able to secrete IL-1β. (a) IL-1β secretion by THP-1 macrophages and A375 and Mamel82 metastatic human melanoma cell lines by analyzing supernatants from their culture by ELISA (R&D Systems, Minneapolis, MN). N.D., not detected. (b) mRNA expression of ASC, NLRP3, caspase-1, pro-IL-1β, pro-IL-18, and GAPDH in THP-1 and metastatic melanoma cell lines. Total RNA from THP-1 cells and metastatic melanoma cell lines (A375, Me191, Me290, and MaMel82) was isolated with an RNeasy Mini Kit (QIAGEN, Hilden Germany). RT-PCR was performed with a thermal cycler (Biometra, Gottingen, German). (c) Evaluation of the expression of inflammasome components and IL-1β in primary ($n = 6$) and metastatic ($n = 21$) melanoma cell lines by RT-PCR. (d) MeDIP analysis of four melanoma cell cultures. Two melanoma cell cultures, M010817 and M000921 were significantly methylated in the promoter region of ASC having a log 2 ratio >1 of methylated DNA compared to input. The other two-melanoma cell cultures, M990115 and M010119, were not significantly methylated in the promoter region of ASC. (e) A375 human metastatic melanoma cells were treated with 2.5 mM AZA for 24 h and ASC expression was assessed by RT-PCR and (f) Western blotting. All data are presented as mean ± SD and are representative of two experiments. *P*-values were calculated with Wilcoxon singled-rank test. $^*p < 0.05$.

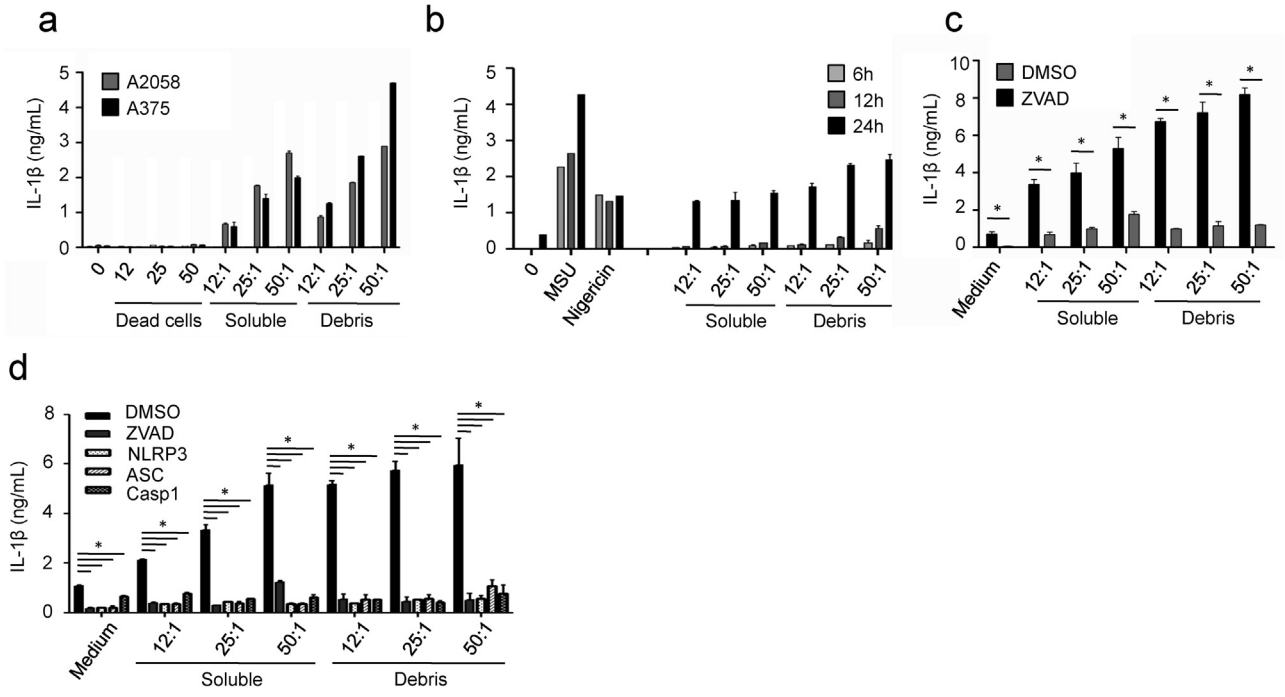

Fig. 2. Necrotic melanoma cells promote IL-1β secretion from macrophages. (a) Human primary monocytes were exposed to different proportions of necrotic cells (A2059/A375 human metastatic melanoma) per for 24 h and IL-1β secretion was measured in the supernatant with ELISA. Necrotic products of cells were separated between soluble and debris fraction. (b) THP-1 macrophages were treated with inflammasome activators (MSU, 150 μg/ml and Nigericin, 5 μM), or necrotic (debris or supernatant?) A375 metastatic human melanoma cell line for 6, 12, and 24 h and IL-1β secretion was measured in the culture supernatant with ELISA. (c) THP-1 cells pre-treated with ZVAD for 30 min were incubated with necrotic A375 for 24 h and IL-1β secretion was measured in the supernatant with ELISA. (d) NLRP3, ASC and caspase-1 knock down THP-1 were incubated with necrotic soluble of A375 for 24 h and IL-1β secretion was measured in the supernatants with ELISA and compared to the one of lamin knock down exposed to DMSO (vehicle) or ZVAD. All IL-1β ELISA data are presented as mean ± SD and are representative of two experiments. P-values were calculated with Wilcoxon singled-rank test. $^*p < 0.05$.

because of the lack of one or more inflammasome components, and DNA methylation is one of the mechanisms that can silence the expression of these components.

Macrophages are potent producers of IL-1β and reported to be present in the melanoma skin lesion [9]. Necrotic melanoma cells are often found in cutaneous melanomas of patients with progressive disease [10] and may be a source of danger-associated molecular patterns sensed by NLRs [1]. Therefore, we next analyzed whether necrotic melanoma cells promote IL-1β production from macrophages. The soluble fraction and debris from necrotic A2058, and A375 melanoma cell lines promoted IL-1β production from human primary monocytes in a dose-dependent manner (Fig. 2a). We also show that IL-1β production from THP-1 macrophages was detected after adding soluble fraction or debris from necrotic melanoma cells (Fig. 2b). A pre-treatment of THP-1 cells with the caspase inhibitor Z-VAD-fmk (Z-VAD) (5 μM) prior to exposure to the soluble fraction or debris from necrotic A375 melanoma cells significantly suppressed IL-1β production (Fig. 2c), suggesting a caspase-dependent mechanism. To further confirm that IL-1β production from THP-1 cells depends on inflammasome activation, we generated ASC, caspase-1, and NLRP3 knock-down THP-1 macrophages. All THP-1 cells transduced with either ASC-shRNA, NLRP3-shRNA or caspase-1-shRNAs showed a dramatic decrease of IL-1β production compared to control lamin-shRNA THP-1 (Fig. 2d), demonstrating that IL-1β release upon exposure to products of necrotic melanoma cells depends on the NLRP3 inflammasome. Finally, we examined IL-1β expression in naevus, superficially spreading melanomas (SSM), nodular melanomas (NM), and skin metastases of melanoma by immunohistochemistry. IL-1β positive cells were not detected in naevus and SSM, whilst they were in NM and skin metastasis of melanoma (Fig. 2e). Consistent with *in vitro* experiments, these IL-1β positive cells were melanophages but not melanoma cells.

In summary, we demonstrate that the inability of metastatic melanoma cells to secrete IL-1β is due to the lack of expression of one or more inflammasome components. On the other hand, one or more factors originating from necrotic melanoma cells can promote IL-1β production by macrophages. Taken together, metastatic melanoma cells seem to have lost the ability for IL-1β production whereas macrophages of the microenvironment secrete high amounts of IL-1β in response to putative danger signals released by necrotic tumor cells. It has been reported that the expression levels of the IL-1β protein are associated with the invasiveness and metastasis of cancers. In this respect, IL-1β is an important factor for the expansion of metastatic melanoma. However, the cellular source of IL-1β in tumors is not clear. Here, we demonstrate that IL-1β is produced by macrophages upon stimulation with danger signals from necrotic melanoma cells. Although not being able to produce IL-1β themselves, tumor cells may benefit from IL-1β release by macrophages present in the micro-environment. A better understanding of the mechanisms and consequences of IL-1β production by infiltrating macrophages may be of interest for the development of IL-1β targeted therapy, such as anti-IL-1β antibody (Canakinumab), of metastatic melanoma.

Acknowledgements

This work was supported in part by the Association for International Cancer Research, AICR 09-0230 to L.E.F., and Oncosuisse. We thank Marianne Spalinger and Tatiana Proust for technical assistance.

Appendix A. Supplementary data

Supplementary data associated with this article can be found, in the online version, at http://dx.doi.org/10.1016/j.jdermsci.2014.01.006.

References

[1] Gross O, Thomas CJ, Guarda G, Tschopp J. The inflammasome: an integrated view. Immunol Rev 2011;243:136–51.
[2] Arlt A, Vorndamm J, Muerkoster S, Yu H, Schmidt WE, Folsch UR, et al. Autocrine production of interleukin 1beta confers constitutive nuclear factor kappaB activity and chemoresistance in pancreatic carcinoma cell lines. Cancer Res 2002;62:910–6.
[3] Elaraj DM, Weinreich DM, Varghese S, Puhlmann M, Hewitt SM, Carroll NM, et al. The role of interleukin 1 in growth and metastasis of human cancer xenografts. Clin Cancer Res 2006;12:1088–96.
[4] Bjorkdahl O, Wingren AG, Hedhund G, Ohlsson L, Dohlsten M. Gene transfer of a hybrid interleukin-1 beta gene to B16 mouse melanoma recruits leucocyte subsets and reduces tumour growth in vivo. Cancer Immunol Immunother 1997;44:273–81.
[5] Zipser MC, Eichhoff OM, Widmer DS, Schlegel NC, Schoenewolf NL, Stuart D, et al. A proliferative melanoma cell phenotype is responsive to RAF/MEK inhibition independent of BRAF mutation status. Pigment Cell Melanoma Res 2011;24:326–33.
[6] Hoek KS, Schlegel NC, Brafford P, Sucker A, Ugurel S, Kumar R, et al. Metastatic potential of melanomas defined by specific gene expression profiles with no BRAF signature. Pigment Cell Res 2006;19:290–302.
[7] Yokoyama T, Sagara J, Guan X, Masumoto J, Takeoka M, Komiyama Y, et al. Methylation of ASC/TMS1, a proapoptotic gene responsible for activating procaspase-1, in human colorectal cancer. Cancer Lett 2003;202:101–8.
[8] Weber M, Davies JJ, Wittig D, Oakeley EJ, Haase M, Lam WL, et al. Chromosome-wide and promoter-specific analyses identify sites of differential DNA methylation in normal and transformed human cells. Nat Genet 2005;37:853–62.
[9] Torisu H, Ono M, Kiryu H, Furue M, Ohmoto Y, Nakayama J, et al. Macrophage infiltration correlates with tumor stage and angiogenesis in human malignant melanoma: possible involvement of TNFalpha and IL-1alpha. Int J Cancer 2000;85:182–8.
[10] Boni R, Boni RA, Steinert H, Burg G, Buck A, Marincek B, et al. Staging of metastatic melanoma by whole-body positron emission tomography using 2-fluorine-18-fluoro-2-deoxy-D-glucose. Br J Dermatol 1995;132:556–62.

Samuel Gehrke[1], Atsushi Otsuka[1], Roman Huber[1], Barbara Meier, Magdalena Kistowska, Gabriele Fenini, Phil Cheng, Reinhard Dummer, Katrin Kerl, Emmanuel Contassot*, Lars E. French*

Department of Dermatology, University Hospital Zurich, Zurich 8091, Switzerland

*Corresponding authors at: Department of Dermatology, University Hospital Zurich, Gloriastrasse 31, Zurich 8091, Switzerland.
Tel.: +41 44 255 2550; fax: +41 44 255 4403

E-mail address: emmanuel.contassot@usz.ch (E. Contassot).

[1]These authors contributed equally to this work.

Received 8 October 2013

http://dx.doi.org/10.1016/j.jdermsci.2014.01.006